DOKUZ EYLÜL UNIVERSITY

GRADUATE SCHOOL OF NATURAL AND APPLIED

SCIENCES

A STUDY OF SEMI-VOLATILE TOXIC ORGANIC AIR POLLUTANTS IN ALİAĞA HEAVY INDUSTRIAL REGION

by
Ayşe BOZLAKER

July, 2008
İZMİR

A STUDY OF SEMI-VOLATILE TOXIC ORGANIC AIR POLLUTANTS IN ALİAĞA HEAVY INDUSTRIAL REGION

A Thesis Submitted to the

Graduate School of Natural and Applied Sciences of Dokuz Eylül University
In Partial Fulfillment of the Requirements for the Degree of Doctor of
Philosophy in Environmental Engineering, Environmental Technology Program

by

Ayşe BOZLAKER

July, 2008
İZMİR

Ph.D. THESIS EXAMINATION RESULT FORM

We have read the thesis entitled **"A STUDY OF SEMI-VOLATILE TOXIC ORGANIC AIR POLLUTANTS IN ALİAĞA HEAVY INDUSTRIAL REGION"** completed by **AYŞE BOZLAKER** under supervision of **PROF. DR. AYSEN MÜEZZİNOĞLU** and we certify that in our opinion it is fully adequate, in scope and in quality, as a thesis for the degree of Doctor of Philosophy.

Prof. Dr. Aysen MÜEZZİNOĞLU

Supervisor

Assoc. Prof. Dr. Mustafa ODABAŞI

Thesis Committee Member

Assoc. Prof. Dr. Aysun SOFUOĞLU

Thesis Committee Member

Prof. Dr. Gülen GÜLLÜ

Examining Committee Member

Prof. Dr. Abdurrahman BAYRAM

Examining Committee Member

Prof. Dr. Cahit HELVACI
Director
Graduate School of Natural and Applied Sciences

ACKNOWLEDGMENTS

A STUDY OF SEMI-VOLATILE TOXIC ORGANIC AIR POLLUTANTS IN ALİAĞA HEAVY INDUSTRIAL REGION

ABSTRACT

Ambient air, dry deposition, and soil samples were collected during the summer and winter periods at a sampling site close to the Aliaga industrial region in Izmir, Turkey. Soil samples were also taken from additional 48 different sites around the study area. All samples were investigated for SOCs (PAHs, PCBs, and OCPs). Atmospheric PAH concentrations were higher in winter than in summer, indicating that wintertime concentrations were affected by residential heating emissions. On the contrary, increased atmospheric PCBs and OCP levels were observed in summer, probably due to increased volatilization at higher temperatures and seasonal agricultural applications of in-use pesticides. Low molecular weight PAHs (phenanthrene, fluorene, fluoranthene) and PCBs (tri-, tetra-, penta-CBs) were the most abundant compounds in air for both seasons. For OCPs, they were endosulfan-I, endosulfan-II and chlorpyrifos in summer, and chlorpyrifos, α-HCH, and endosulfan-I in winter, respectively. In contrast to PCBs, particulate fluxes of PAHs and OCPs were generally higher in summer than in winter. Overall average deposition velocities calculated for SOCs agree well with the literature values. Calculated net gas fluxes at the soil-air interface indicated that the contaminated soil is a secondary source to the atmosphere for lighter PAHs and PCBs and as a sink for heavier ones. OCPs tending to volatilize were chlordane related compounds and p,p'-DDT in summer, and in winter, they were α-CHL, γ-CHL, t-nonachlor, endosulfan sulfate, and p,p'-DDT. All mechanisms were comparable for the studied compounds, but their input was generally dominated by gas absorption, followed by dry and wet deposition.

Keywords: Polycyclic aromatic hydrocarbons (PAHs), polychlorinated biphenyls (PCBs), organochlorine pesticides (OCPs), ambient air concentrations, gas-particle partitioning, dry deposition, deposition velocity, soil-air exchange.

ALİAĞA AĞIR SANAYİ BÖLGESİNDE YARI UÇUCU TOKSİK ORGANİK HAVA KİRLETİCİLERİ ÜZERİNE BİR ÇALIŞMA

ÖZ

Dış hava, kuru çökelme ve toprak örnekleri, yaz ve kış örnekleme dönemleri boyunca Aliağa endüstri bölgesine yakın bir noktadan toplanmış; ayrıca Aliaga genelinde 48 farklı noktadan toprak örnekleri alınmıştır. Yarı uçucu toksik organik hava kirleticileri (SOC'lar: PAH'lar, PCB'ler ve OCP'ler) tüm örneklerde incelenmiştir. Dış havada ölçülen PAH seviyelerinin, evsel ısınmaya bağlı olarak kış mevsiminde arttığı görülmektedir. Yaz mevsiminde artan PCB ve OCP seviyeleri, önceden kirletilmiş olan yüzeylerden bu bileşiklerin sıcaklıkla orantılı olarak artan buharlaşma oranlarına ve kullanımda olan pestisitlerin bu mevsimde artan tarımsal uygulamalarına bağlı olabilir. Her iki mevsimde alınan dış hava örneklerinde düşük molekül ağırlıklı PAH'lar (phenanthrene, fluorene, fluoranthene) ve PCB'ler (tri-, tetra-, penta-CBs) baskındır. Yaz periyodu için dış havada ölçülen en yüksek seviyeler sırasıyla endosulfan-I, endosulfan-II ve chlorpyrifos'a, kış periyodunda ise chlorpyrifos, α-HCH ve endosulfan-I'e aittir. PCB'lerin tersine, partikül fazındaki PAH'lar ve OCP'ler yaz mevsiminde daha yüksek kuru çökelme akılarına sahiptirler. SOC'lar icin hesaplanan partikül çökelme hızları literatürdeki değerlerle tutarlıdır. Dış hava-toprak arakesitindeki net gaz akısı hesaplanmış; önceden kirletilmiş olan toprak yüzeyinin, düşük molekül ağırlıklı PAH'lar ve PCB'ler için atmosfere ikincil bir kaynak gibi davrandığı, daha ağır bileşikler içinse deponi vazifesi gördüğü gözlenmiştir. Chlordane grubundaki OCP'ler ve p,p'-DDT yaz mevsiminde; α-CHL, γ-CHL, t-nonachlor, endosulfan sulfate ve p,p'-DDT ise kış mevsiminde toprak yüzeyinden buharlaşma eğilimindedir. Çalışılan SOC'ların hava ile toprak arasındaki geçişleri tüm olası mekanizmalar için önemli ise de, toprakta absorpsiyonun daha baskın olduğu görülmüştür. Bunu, kuru ve yaş çökelme izlemektedir.

Anahtar Kelimeler: Polisiklik aromatik hidrokarbonlar (PAH'lar), poliklorlu bifeniller (PCB'ler), organoklorlu pestisitler (OCP'ler), dış hava konsantrasyonları, gaz-partikül dağılımı, kuru çökelme, çökelme hızı, hava/toprak arakesitinde taşınım.

CONTENTS

CHAPTER ONE
INTRODUCTION

1. Introduction

Persistent organic pollutants (POPs) are a class of compounds that are characterized by their physical/chemical properties including moderate vapor pressure, low water solubility, and high lipid solubility. Because of their semi-volatile nature, most POPs are capable of long-range transport through the atmosphere. POPs also resist to photolytic, biological, and chemical degradation in the environmental matrices at varying degrees (U.S. Environmental Protection Agency [U.S. EPA], 2002a). Although some natural sources of POPs are known to exist, most of them originate from anthropogenic sources. Some of these compounds are carcinogenic and mutagenic at the environmental levels, and they are likely to cause serious adverse human health or environmental effects (Park, Wade, & Sweet, 2002a; U.S. EPA, 2002a). It is the combination of persistence, bioaccumulation, long-range environmental transport, and toxicity that makes POPs or their breakdown products problematic.

In May 1995, the United Nations Environment Programme (UNEP) Governing Council decided to investigate POPs by dividing them into three general categories:

- Pesticides: aldrin, chlordane, DDT, dieldrin, endrin, heptachlor, mirex, toxaphene
- Industrial chemicals: PCBs (also a byproduct), hexachlorobenzene (HCB; also a pesticide and byproduct)
- By-products: polychlorinated dibenzo-p-dioxins/furans (PCDD/F)

Since then, this list has generally been extended to include substances including carcinogenic polycyclic aromatic hydrocarbons (PAHs), hexachlorocyclohexanes (HCHs and lindane), certain brominated flame-retardants (e.g. hexabromobiphenyl), as well as some organometallic compounds (e.g. chlordecone) (United Nations

Environment Programme [UNEP], 1999a). A treaty was signed by the United States, 90 other nations, and the European Community in Stockholm, Sweden, in May 2001, and under the treaty, known as the Stockholm Convention, countries make an agreement to reduce or eliminate the production, use, and/or release of the related POPs that are of greatest concern to the global community (U.S. EPA, 2002a).

Many POPs including polycyclic aromatic hydrocarbons (PAHs), polychlorinated biphenyls (PCBs), and organochlorine pesticides (OCPs) are classified as semi-volatile. Thus, they are also named as semi-volatile organic compounds (SOCs). SOCs coexist in the ambient air either as gases or attached to airborne particles. The relative amounts in gaseous and particle associated forms are controlled by the vapor pressure of the compound (roughly between 10^{-4}-10^{-11} atm at ambient temperatures), the meteorological conditions, as well as the type (i.e. the content of organic carbon, surface area), size distribution, and concentration of total suspended particles (TSP) in the air, and interactions between the compound and the aerosol (Cousins, Beck, & Jones, 1999; Park, Wade, & Sweet, 2001a; Vardar, Tasdemir, Odabası, & Noll, 2004).

Temperature has a strong influence on the volatilization rates of SOCs by affecting their vapor pressures (Backe, Cousins, & Larsson, 2004; Sofuoglu, Cetin, Bozacioglu, Sener, & Odabasi, 2004). Less volatile SOCs tend to partition into natural surfaces such as soil, vegetation, and water, where they may associate with organic matter. Warmer temperatures favor their volatilization and residence in the atmosphere as gases, while colder temperatures favor their deposition to the Earth's surface and their incorporation into airborne particles. Generally, the lower molecular weight SOCs are expected to exist mainly in gas-phase and tend to have the highest potential for long-range transport. However, the higher molecular weight ones are expected to be found mainly attached to particles and tend to remain concentrated around their sources (U.S. EPA, 2002a).

In the atmosphere, SOCs are subject to dispersion, transport over long distances, chemical conversion, and removal from the atmosphere by deposition. Even under the same meteorological conditions, gas- and particle-phase compounds are subject to different transport and removal mechanisms into the atmosphere (Bidleman, 1999). For airborne SOCs in gas-phase, environmental transformation in the atmosphere occurs principally from photo-chemical reaction with hydroxyl radicals. Photo-degradation by solar ultraviolet radiation and reaction with other species such as ozone and nitrogen are considered to be insignificant processes for their loss. If SOCs are as attached to particles, their lifetimes in the atmosphere are determined by particle removal mechanisms, in addition to reactions involving hydroxyl radicals or other free radical species in the particles and photo-degradation by solar ultraviolet radiation. However, the effectiveness of these processes for particle-phase has not been extensively studied as well as for gas-phase (U.S. EPA, 2002a).

Hipplein & McLachlan (2000) proposed atmospheric deposition (i.e. exchange of gaseous compounds between the air and the soil/vegetation/water surfaces, dry particulate deposition, and wet deposition) as the responsible mechanism for transferring of chemicals from air to the natural surfaces. Comparative loading estimates indicated that gas exchange dominates in many cases, followed by the respective contributions of dry and wet deposition (Asman et al., 2001; Gioia et al., 2005).

Once deposited, SOCs tend to accumulate in soil for a long period of time and they are subject to various partitioning, degradation, and transport processes. Considering their large reservoir in soils, gas exchange between the air and soil surfaces affects the fate and transport of SOCs into the environment (Meijer, Shoeib, Jones, & Harner, 2003b) and depends mainly on the difference in concentration between these compartments. If the concentration in the soil surface is higher than in the air, net volatilization occurs. In the opposite case, net deposition occurs (Asman et al., 2001). Other parameters affecting this mechanism are the soil physical-chemical properties (i.e. texture, structure, porosity, water and organic matter contents); the compound properties (i.e. vapor pressure, water solubility, phase

partitioning and diffusion coefficients); and meteorological conditions (i.e. temperature and wind speed) (Backe et al., 2004).

Gas transport across the soil-air interface occurs via diffusion. Magnitude and direction of the diffusive flux is determined by the concentration gradient in the soil-air matrices and the soil-air equilibrium partition coefficient (K_{SA}) (Hippelein & McLachlan, 1998). There are limited investigations on K_{SA} values, soil-air gas exchange fluxes, and equilibrium status of PAHs (Cousins & Jones, 1998; Demircioglu, 2008; Hippelein & McLachlan, 1998), PCBs (Backe et al., 2004; Cousins & Jones, 1998; Cousins, McLachlan, & Jones, 1998; Harner, Mackay, & Jones, 1995; Hippelein & McLachlan, 1998, 2000) and OCPs (Bidleman & Leone, 2004; Daly et al., 2007; Hippelein & Mclachlan, 1998, 2000; Kurt-Karakus, Bidleman, Staebler, & Jones, 2006; Meijer, Shoeib, Jantunen, & Harner, 2003a; Meijer et al., 2003b; Scholtz & Bidleman, 2006).

The main objectives of this study were to determine the ambient air and soil concentrations of SOCs (i.e. PAHs, PCBs, and OCPs) for the summer and winter sampling periods at an industrial site in Turkey and to describe the processes governing the movement of these compounds between the soil and air. In this respect, the following measurements and evaluations were aimed to:

- Measure atmospheric concentrations of PAHs, PCBs, and OCPs in both gas- and particle-phases, and to examine their seasonal variations,
- Investigate influence of the meteorological parameters on their atmospheric gas-phase concentrations,
- Calculate their particle-phase dry deposition fluxes and velocities,
- Measure soil concentrations of the studied compounds and to determine magnitude and direction of gas exchange fluxes and fugacity gradient between soil-air interface.

Particulate dry deposition and soil-air gas exchange fluxes were discussed together to show the relative importance of the processes affecting the PAH, PCB, and OCP levels in soil and air at the study site.

During the sampling periods, total suspended particulate matter (TSP) samples were also collected at the sampling site. Finally, additional soil samples were taken from the different points in Aliaga study area to see the contribution of the local sources to the SOC levels in ambient air and soil. These measurements allowed us to make additional assessments that can be summarized as:

- Determination of airborne total suspended particulate matter (TSP) levels and its organic matter (OM) content at the sampling site,
- Estimation of the particle/gas partitioning for PAHs, PCBs, and OCPs in ambient air,
- Determination of PAH, PCB, and OCP levels in soils at the study area, and mapping their spatial distribution.

All results were compared with previously reported values elsewhere.

This study consists of five chapters. An overview and objectives of the study were presented in Chapter 1. Chapter 2 reviews the concepts and previous studies related to this work. Experimental work and data analysis procedures are summarized in Chapter 3. Results and discussions are presented in Chapter 4. Chapter 5 includes the conclusions and suggestions drawn from this study.

CHAPTER TWO
LITERATURE REVIEW

This chapter presents background information on chemical structures, physical-chemical properties, health effects, production, uses, and sources of the studied substance groups of PAHs, PCBs and OCPs. Recent studies on their ambient air and soil concentrations, particle-phase dry deposition fluxes, and deposition velocities are also summarized.

2.1 Polycyclic Aromatic Hydrocarbons (PAHs)

Polycyclic aromatic hydrocarbons (PAHs, also known as polynuclear aromatic hydrocarbons) are a group of organic compounds that are generated primarily during the incomplete combustion of organic materials including wood and fossil fuels such as coal, oil, and gasoline (Vallack et al., 1998). There are hundreds of PAH compounds in the environment, but only 16 of them are included in the priority pollutants list of U.S. EPA based on a number of factors including toxicity, extent of information available, source specificity, frequency of occurrence at hazardous waste sites, and potential for human exposure (Agency for Toxic Substances and Disease Registry [ATSDR], 1995).

PAHs can be divided into two groups based on their physico-chemical, and biological characteristics: i) the low molecular weight PAHs with 2- to 3-rings, and ii) the high molecular weight PAHs with 4- to 7-rings (Nagpal, 1993). Because of their semi-volatile nature, PAH compounds may exist in the atmosphere both as gaseous and attached to airborne particles by nucleation and condensation. Atmospheric residence time and transport distance depend on the meteorological conditions and the size of the particles onto which PAHs are sorbed (ATSDR, 1995).

During their residence time in the atmosphere, PAHs undergo photo-chemical oxidation in the presence of sunlight. This photo-oxidation occurs much faster for

gaseous compounds than particulate bound ones. The most important atmospheric decomposition mechanism for PAHs is the reaction with hydroxyl radicals. PAHs in the air can also be oxidized by atmospheric pollutants such as ozone, nitrogen oxides, and sulfur dioxide, too, to be transformed into diones, nitro- and dinitro-derivatives, and sulfonic acids, respectively (Dabestani & Ivanov, 1999; Halsall, Sweetman, Barrie, & Jones, 2001; Possanzini, Di Palo, Gigliucci, Sciano, & Cecinato, 2004)

2.1.1 Chemical Structures, Properties, and Health Effects of PAHs

Chemical structures of the studied PAH compounds (U.S. EPA 16 plus carbazole) are illustrated in Fig. 2.1. PAHs are composed of two or more aromatic (benzene) rings which are fused together when a pair of carbon atoms is shared between them. The resulting structure is a molecule where the benzenoid rings are fused together in a linear fashion (e.g. anthracene) or in an angular arrangement (e.g. acenaphtylene) (Dabestani & Ivanov, 1999). In some PAHs, named as heterocyclic aromatic hydrocarbons, one carbon atom is substituted by an atom of another element, such as nitrogen, oxygen, sulphur, or chlorine (Toxic Organic Compounds in the Environment [TOCOEN], 2007).

The environmentally significant PAHs are the compounds which contain two (e.g. naphthalene with a chemical formula of $C_{10}H_8$) to seven benzene rings (e.g. coronene with a chemical formula of $C_{24}H_{12}$). Within this range, there is a large number of PAHs which differ in number of aromatic rings; position at which aromatic rings are fused to each other; and number, chemistry, and position of substituents on the basic ring system (Nagpal, 1993). Trivial names are used for some of the simple PAHs such as anthracene, phenanthrene, pyrene, fluoranthene, and perylene. More complicated compounds are named by their substitution on their basic structure, such as by benzo- dibenzo-, or naptho- groups (Odabasi, 1998).

Naphthalene Acenaphthylene Acenaphthene Fluorene

Phenanthrene Anthracene Carbazole Fluoranthene

Pyrene Benz[*a*]anthracene Chrysene

Benzo[*b*]fluoranthene Benzo[*k*]fluoranthene Benzo[*a*]pyrene

Dibenz[*a,h*]antracene Benzo[*ghi*]perylene Indeno[*1,2,3-cd*]pyrene
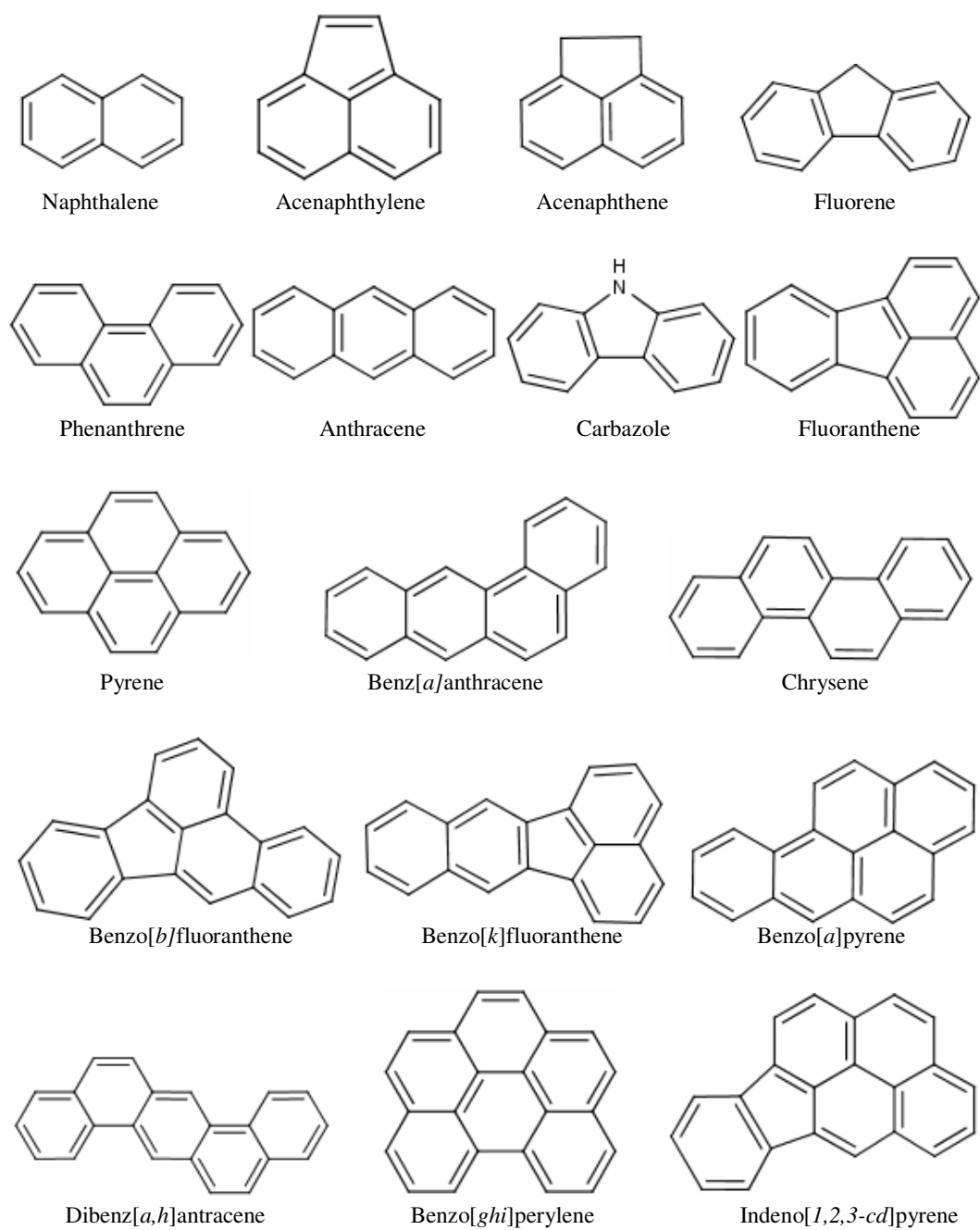
Figure 2.1 Chemical structures of the studied PAHs (National Library of Medicine [NLM], 2008a).

The distribution and partitioning of organic pollutants in various compartments of the environment (e.g. air, water, soil/sediment, and biota) is determined by their physical-chemical properties such as water solubility, vapor pressure, Henry's law constant, octanol-water partition coefficient (K_{OW}), and organic carbon partition coefficient (K_{OC}) (ATSDR, 1995). Table 2.1 shows the some important properties of the studied PAH compounds. The physical-chemical properties of PAHs vary with molecular weight. For instance, PAH resistance to oxidation, reduction, and vaporization increases with increasing molecular weight, whereas the aqueous solubility of these compounds decreases (Nagpal, 1993). Pure PAHs generally exist as colorless, white, or pale yellow-green solids at room temperature and most of them have high melting and boiling points (ATSDR, 1995).

Since PAHs are non-polar and hydrophobic compounds, they are poorly soluble in aqueous environments, but are soluble in organic solvents or organic acids. This means that they are generally found adsorbed on particulates and on humic matter in aqueous environments, or solubilized in any oily matter which may co-exist in water, sediments and soil as contaminants (Dabestani & Ivanov, 1999). Temperature and dissolved/colloidal organic fractions of water enhance the solubility of the PAH compound in water (Nagpal, 1993), and solubility decreases as the molecular weight and number of rings increases. Thus, the high molecular weight PAHs (≥4 rings) are almost exclusively bound to particulate matter, while the lower molecular weight ones (≤3 rings) can also be found dissolved in water (ATSDR, 1995).

PAHs tend to have low vapor pressures. As molecular weight and the number of rings increase, their vapor pressure decreases. At a given temperature, substances with higher vapor pressures vaporize more readily than substances with a lower vapor pressure. As a result, the high molecular weight PAHs (≥ 4 rings) are found predominantly in particle-phase, while the lower molecular weight ones (≤3 rings) are present predominantly in gas-phase in the air (Dabestani & Ivanov, 1999).

Table 2.1 Selected physical-chemical properties of individual PAH compounds.

PAHs[**]	Cas-No[a]	Molecular Formula[a]	MW^a (g mol^{-1})	T_M^a (°C)	T_B^a (°C)	S_W^a (25°C) (mg L^{-1})	VP^a (25°C) (mm Hg)	H^a (25°C) (atm m^3 mol^{-1})	log K_{OA}^c (25°C)	log K_{OW}^a
NAP	91-20-3	$C_{10}H_8$	128	80	218	31	8.50E-02	4.40E-04	-	3.36
ACL	208-96-8	$C_{12}H_8$	152	93	280	16.1	6.68E-03	1.14E-04	6.34	3.94
ACT	83-32-9	$C_{12}H_{10}$	154	93	279	3.9	2.15E-03	1.84E-04	6.52	3.92
FLN	86-73-7	$C_{13}H_{10}$	166	115	295	1.69	6.00E-04	9.62E-05	6.9	4.18
PHE	85-01-8	$C_{14}H_{10}$	178	99	340	1.15	1.21E-04	3.35E-05[b]	7.68[b]	4.46
ANT	120-12-7	$C_{14}H_{10}$	178	215	340	0.0434[*]	2.67E-06[d]	5.56E-05	7.71	4.45
CRB	86-74-8	$C_{12}H_9N$	167	246	355	1.8	7.50E-07[e]	1.16E-07[b]	8.03[b]	3.72
FL	206-44-0	$C_{16}H_{10}$	202	108	384	0.26	9.22E-06	8.86E-06	8.76	5.16
PY	129-00-0	$C_{16}H_{10}$	202	151	404	0.135	4.50E-06	1.19E-05	8.81	4.88
BaA	56-55-3	$C_{18}H_{12}$	228	84	438	0.0094	2.10E-07	1.20E-05	10.28	5.76
CHR	218-01-9	$C_{18}H_{12}$	228	258	448	0.002	6.23E-09	5.23E-06	10.30	5.81
BbF	205-99-2	$C_{20}H_{12}$	252	168	-	0.0015	5.00E-07	6.57E-07	11.34	5.78
BkF	207-08-9	$C_{20}H_{12}$	252	217	480	0.0008	9.70E-10[d]	5.84E-07	11.37	6.11
BaP	50-32-8	$C_{20}H_{12}$	252	177	495[f]	0.00162	5.49E-09[d]	4.57E-07	11.56	6.13
IcdP	193-39-5	$C_{22}H_{12}$	276	164	536	0.00019	1.25E-10	3.48E-07	12.43	6.7
DahA	53-70-3	$C_{22}H_{14}$	278	270	524	0.00249	1.00E-10	1.23E-07	12.59	6.75
BghiP	191-24-2	$C_{22}H_{12}$	276	278	>500	0.00026	1.00E-10	3.31E-07	12.55	6.63

[**] Naphthalene (NAP), acenaphthylene (ACL), acenaphthene (ACT), flourene (FLN), phenanthrene (PHE), anthracene (ANT), carbozole (CRB), fuoranthene (FL), pyrene (PY), benz[*a*]anthracene (BaA), chrysene (CHR), benz[*b*]fluoranthene (BbF), benz[*k*]fluoranthene (BkF), benz[*a*]pyrene (BaP), indeno[1,2,3-*cd*]pyrene (IcdP), dibenzo[*a,h*]anthracene (DahA), benzo[*g,h,i*]perylene (BghiP).

MW: Molecular weight, T_M: Melting point, T_B: Boiling point, S_W: Solubility in water, VP: Vapor pressure, H: Henry's law constant, log K_{OW}: Octanol-water coefficient, log K_{OA}: Octanol-air coefficient, [*] at 24°C.

[a] NLM, 2008a, [b] Odabasi, Cetin, & Sofuoglu, 2006a, [c] Odabasi, Cetin, & Sofuoglu, 2006b, [d] NLM, 2008b, [e] Virtual Computational Chemistry Laboratory [VCCL], 2007, [f] Estimation Program Interface [EPI], 2007.

The ratio of a chemical's concentration in air and water at equilibrium can be expressed by Henry's law constant. This partition coefficient is used as a measure of a compound's volatilization. Henry's law constants for low molecular weight PAHs are in the range of 10^{-3}-10^{-5} atm m^3 mol^{-1} and for the high molecular weight PAHs they are in the range of 10^{-5}-10^{-8} atm m^3 mol^{-1}. Thus, significant volatilization can take place for compounds with Henry's law constant values ranging from 10^{-3}-10^{-5} while PAHs with values $<10^{-5}$ do not volatilize much (ATSDR, 1995; Dabestani & Ivanov, 1999).

The K_{OW} is used to estimate the potential for an organic chemical to move from water into lipid, and has been correlated with bio-concentration in aquatic organisms. For PAH compounds, the values of log K_{OW} increase with increasing number of rings. K_{OW} values for PAHs are relatively high indicating a relatively high potential for adsorption to suspended particulates in air and water, and for bio-concentration in organisms (ATSDR, 1995).

The K_{OC} indicates the chemical's potential to bind to organic carbon in soil and sediment. The log K_{OC} values for PAHs increase with increasing number of rings. The low molecular weight PAHs have K_{OC} values in the range of 10^3-10^4 indicating a moderate potential to be adsorbed to organic carbon in the soil and sediments. High molecular weight PAHs have K_{OC} values in the range of 10^5-10^6 indicating stronger tendencies to adsorb to organic carbon (ATSDR, 1995). Persistence of the PAHs also varies with their molecular weight. The low molecular weight PAHs are most easily degraded. The reported half-lives of naphthalene, anthracene, and benzo[*e*]pyrene in sediment are 9, 43, and 83 hours, respectively, while for higher molecular weight PAHs, their half-lives are up to several years in soils/sediments (UNEP, 2002).

In human beings, systemic, immunological, neurological, reproductive, developmental, genotoxic, and carcinogenic adverse health effects have been linked to several PAHs (ATSDR, 1995). The International Agency for Research on Cancer (IARC) has reported that benz[*a*]anthracene and benzo[*a*]pyrene are probably

carcinogenic to human (Group B2); benzo[*b*]fluoranthene, benzo[*k*]fluoranthene, and indeno[1,2,3-*c,d*]pyrene are possibly carcinogenic to human (Group 2A). In the U.S. EPA list, benz[*a*]anthracene, benzo[*a*]pyrene, benzo[*b*]fluoranthene, benzo[*k*]fluoranthene, chrysene, dibenz[*a,h*]anthracene, and indeno[1,2,3-*c,d*]pyrene are classified as Group B2, probable human carcinogens (ATSDR, 1995).

2.1.2 Production and Uses of PAHs

Among a large number of compounds, only a few PAHs (e.g. acenaphthene, anthracene, fluorene, fluoranthene, naphthalene, and phenanthrene) are produced for commercial use. They are mostly used as intermediaries in pharmaceutical, photographic, and chemical industries. Limited uses in the production of fungicides, insecticides, moth repellent, and surfactants have been also reported (ATSDR, 1995; Nagpal, 1993).

Acenaphthene is used as a chemical intermediary in pharmaceutical and photographic industries, and to a limited extent, in the production of soaps, pigments and dyes, insecticides, fungicides, plastics, and processing of certain foods (ATSDR, 1995; Nagpal, 1993; Spectrum, 2003a)

Anthracene is used as a raw material for the manufacture of fast dyes, pigments, and coating materials; as a chemical intermediary for dyes; and as a diluent for wood preservatives. It is used in the manufacture of synthetic fibers, plastics, mono-crystals, and scintillation counter crystals. Its uses in insecticides, smoke screens and organic semiconductor researches have been also reported (ATSDR, 1995; Nagpal, 1993; Spectrum, 2003b).

Fluorene is used as a chemical intermediate in many chemical processes, in the formation of poly-radicals for resins, and in the manufacture of resinous products and dyestuffs. Derivatives of fluorene show activity as herbicides and growth regulators (ATSDR, 1995; Spectrum, 2003d).

Fluoranthene is a constituent of coal tar and petroleum derived asphalt. This compound is used as a lining material to protect the interior of steel and ductile-iron drinking water pipes and storage tanks (ATSDR, 1995; Spectrum 2003c).

Naphthalene is the most abundant distillate of coal tar. Its most common use is as a household fumigant against moths. In the past, it was used in the manufacture of carbaryl insecticide and vermicide. Naphthalene is also an important hydrocarbon raw material used in the manufacture of phthalic anhydride (intermediate for polyvinyl chloride, PCV, plasticizers), celluloid and hydronapthalenes (used in lubricants), and motor fuels. Naphthalene is also used in the production of beta-naphthol, synthetic tanning agents, leather, resins, dyes, surfactants and dispersants. Some uses as an antiseptic and as a soil fumigant have been reported as well (ATSDR, 1995; Nagpal, 1993; U.S. EPA, 2002b; Spectrum, 2003e).

Phenanthrene is used in the manufacture of dyestuffs, explosives, and phenanthrenequinone which is an intermediate for pesticides. It is also an important starting material for phenanthrene based drugs. This leads directly to use in biochemical research for the pharmaceutical industry. A mixture of phenanthrene and anthracene tar is used to coat water storage tanks to keep them from rusting (ATSDR, 1995; Spectrum, 2003f).

There are no known commercial uses for acenaphthylene, benz[a]anthracene, benzo[b]fluoranthene, benzo[e]pyrene, benzo[j]fluoranthene, benzo[k]fluoranthene, benzo[g,h,i]erylene, benzo[a]pyrene, chrysene, dibenz[a,h]anthracene, indeno(1,2,3-c,d]pyrene, and pyrene except as research chemicals (ATSDR, 1995)

2.1.3 Sources of PAHs

The sources of PAHs can be divided into two categories: natural and anthropogenic sources. Emissions from anthropogenic activities predominate, but some PAHs in the environment originate from natural sources.

2.1.3.1 Natural Sources

In nature, PAHs may be formed by three ways: (i) high temperature pyrolysis of organic materials, (ii) low to moderate temperature diagenesis of sedimentary organic material to form fossil fuel, and (iii) direct biosynthesis by microbes and plants (Nagpal, 1993).

Emissions from agricultural burning, forest and prairie fires contribute the largest volumes of PAHs from a natural source to the environment. Volcanic activity and biosynthesis by plants, algae/phytoplankton, and microorganisms are other natural sources of PAHs. But compared to fires, these sources emit smaller amounts to the environment (Nagpal, 1993; Odabası, 1998). PAHs occur naturally in bituminous fossil fuels, such as coal and crude oil deposits, as a result of diagenesis (i.e. the low temperature, 100-150 °C, decomposition of organic material over a significant span of time) (Nagpal, 1993). Slow transformation of organic materials in lake sediments by diagenesis is another minor natural source of PAHs to the environment (Dabestani & Ivanov, 1999). They also form as significant components of petroleum products such as some paints, creosote (used in wood preservation), and asphalt (used for road paving) (U.S. EPA, 2002a).

2.1.3.2 Anthropogenic Sources

Anthropogenic emission sources include combustion and industrial production. Incomplete combustion of organic matter at high temperature is one of the major anthropogenic sources of environmental PAHs. Emissions into the atmosphere during the production of some PAHs for commercial uses are not expected to be significant (ATSDR, 1995).

Atmospheric PAH emissions from anthropogenic sources fall into two groups: (i) stationary sources and (ii) non-stationary sources. Stationary sources include coal and gas-fired boilers; coal gasification and liquefaction plants; carbon black, coal tar

pitch and asphalt production; aluminum production; coke-ovens; the iron-steel industries; catalytic cracking towers; petroleum refineries and related activities; electrical generating plants; industrial and municipal incinerators (waste burning); residential heating; and any other industry that entails the use of wood, petroleum or coal to generate heat and power (Dabestani & Ivanov, 1999; Nagpal, 1993).

Non-stationary sources of PAHs refer to automobiles or other vehicles which use petroleum derived fuels. Temperatures within an internal combustion engine are often sufficient enough to convert a fraction of the fuel or oil into PAHs via incomplete combustion. These compounds are then emitted to the atmosphere through exhaust fumes and then they sorb onto airborne particulates (Nagpal, 1993).

2.2 Polychlorinated Biphenyls (PCBs)

Polychlorinated biphenyls (PCBs) have no natural sources and have been commercially prepared by chlorination of biphenyl (Park, 2000). Due to their thermal stability, excellent dielectric properties, and resistance to oxidation, acids, and bases, they were widely used in electrical equipment (mostly in capacitors and transformers) and other industrial applications where chemical stability has been required for safety, operation and durability until recently (UNEP, 1999b).

Because of their toxicity and resistance to degradation into the environment, the production and use of PCBs have been banned in many countries for decades. However, due to their persistence, PCB levels in the environmental matrices are declining slowly, and this makes them ubiquitous. Breivik, Sweetman, Pacyna, & Jones (2007) have estimated that PCB emissions during 2005 were approximately 10% of what was released in 1970.

In the atmosphere, PCBs may exist in both gas- and particle-phases and are capable to long-range transport. Low molecular weight PCBs are more in the gas-phase, and thus are easily transported further away from the sources compared to the

particle-phase ones. The heavier PCBs tend to be particle-phase and more readily degraded in the atmosphere (ATSDR, 2000a).

Commercial PCBs consist of a mixture of PCB congeners. However, after release into the environment, the composition of PCB mixtures changes over time through processes such as volatilization, partitioning, chemical and biological transformation, and preferential bioaccumulation (U.S. EPA, 1996). Generally, biodegradability decreases with increasing degree of chlorination. Congeners with 3 or fewer chlorine atoms are significantly biodegradable and are also more likely to evaporate to air. However, PCBs having more than 5 chlorine atoms tend to sorb to suspended particulates, sediments and soil, and resist biodegradation (Nagpal, 1992). In the air, photo-chemical reaction with hydroxyl radicals is the dominant transformation process for gaseous PCBs, but photolysis for particle-phase ones is not important (ATSDR, 2000a)

2.2.1 Chemical Structures, Properties, and Health Effects of PCBs

PCBs is a group of aromatic, synthetic compounds formed by the addition of chlorine atoms (Cl_2) to biphenyl molecule ($C_{12}H_{10}$) which is a dual-ring structure comprising two 6-carbon benzene rings (Nagpal, 1992). The general formula for PCBs is $C_{12}H_{10-n}Cl_n$, where n ranges from 1 to 10 (UNEP, 1999b).

Fig. 2.2 shows the basic structure of a biphenyl molecule where the numbers 2-6 and 2'-6' represent possible substitution locations for chlorine. Positions 2, 2', 6, and 6' are called *ortho* positions, positions 3, 3', 5, and 5' are called *meta* positions, and positions 4 and 4' are called *para* positions. The benzene rings can rotate around the bond connecting them. Their two extreme configurations are planar (i.e. two benzene rings in the same plane) and non-planar (the benzene rings are at a 90° angle to each other). The benzene rings of non-*ortho* substituted PCBs, as well as mono-*ortho* substituted PCBs, may assume a planar configuration, referred to as planar or

coplanar congeners (ATSDR, 2000a). There are 20 non-*ortho* substituted PCB congeners that are often called "dioxin-like compounds" in terms of their toxicity (World Health Organization [WHO], 2000).
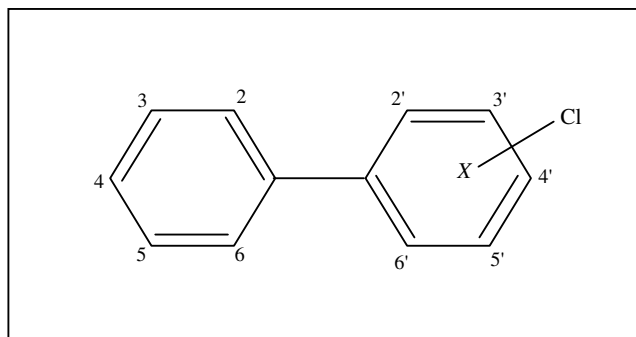
Figure 2.2 Basic molecular structure of a biphenyl molecule (UNEP, 1999b).

The nature of an aromatic (benzene) ring allows a single attachment to each carbon. This means that there are 10 possible positions for chlorine substitution by replacing the hydrogens in the original biphenyl. There are, thus, 10 different PCB homologues depending on the number of chlorines (Nagpal, 1992). Species with a single chlorine substituent are called mono-chlorobiphenyl (mono-CBs). Species with two through ten chlorines, in order, are called di-, tri-, tetra-, penta-, hexa-, hepta-, octa-, nona-, and deca-CBs (ATSDR, 2000a).

Congener is a single, unique, well-defined chemical compound in the PCB category. The name of the congener specifies the total number of chlorine substituents and the position of each chlorine atoms (ATSDR, 2000a). For example, 4,4'-dichlorobiphenyl is a congener comprising the biphenyl structure with two chlorine substituents, one on each of the two carbons at the *para* positions of the two rings. Theoretically, 209 different congeners are possible, but only about 130 of these have been identified in commercial products (UNEP, 1999b).

Table 2.2 Selected physical-chemical properties of PCB congeners (1/2).

PCBs	Cas-No[a]	Molecular Formula[a]	Molecular Structure[a]	MW[a] (g mol^{-1})	T_M[a] (°C)	T_B[a] (°C)	S_W[b] (25°C) (mg L^{-1})	VP[b] (25°C) (mm Hg)	H[c] (at 25°C) (atm m^3 mol^{-1})	log K_{OA}[d] (at 20°C)	log K_{OW}[g]
PCB-18	37680-65-2	$C_{12}H_7Cl_3$	2,2',5	258	101	341	0.4	1.05E-03	2.52E-04	7.79	5.19
PCB-17	37680-66-3	$C_{12}H_7Cl_3$	2,2',4	258	101	341	0.0833	4.00E-05	6.02E-04	7.74	5.33
PCB-31	16606-02-3	$C_{12}H_7Cl_3$	2,4',5	258	101	341	0.143	4.00E-04	2.68E-04	8.4	5.66
PCB-28	7012-37-5	$C_{12}H_7Cl_3$	2,4,4'	258	101	341	0.27	1.95E-04	3.63E-04	8.4	5.63
PCB-33	38444-86-9	$C_{12}H_7Cl_3$	2',3,4	258	101	341	0.133[*]	1.03E-04	5.97E-04	8.52	5.46[h]
PCB-52	35693-99-3	$C_{12}H_6Cl_4$	2,2',5,5'	292	122	360	0.0153	8.45E-06	3.11E-04	8.49	5.74
PCB-49	41464-40-8	$C_{12}H_6Cl_4$	2,2',4,5'	292	122	360	0.0781[*]	8.48E-06	4.17E-04	8.63	5.91
PCB-44	41464-39-5	$C_{12}H_6Cl_4$	2,2',3,5'	292	122	360	0.10[*]	8.45E-06	2.68E-04	8.71	5.62
PCB-74	32690-93-0	$C_{12}H_6Cl_4$	2,4,4',5	292	122	360	0.00496	8.45E-06	4.17E-04	9.14	6.2
PCB-70	32598-11-1	$C_{12}H_6Cl_4$	2,3',4',5	292	122	360	0.041	4.08E-05	2.77E-04	9.22	6.2
PCB-95	38379-99-6	$C_{12}H_5Cl_5$	2,2',3,5',6	326	135	378	0.0211[*]	2.22E-06	6.29E-04	9.06	6.15
PCB-101	37680-73-2	$C_{12}H_5Cl_5$	2,2',4,5,5'	326	135	378	0.0154	2.52E-05	4.29E-04	9.28	6.26
PCB-99	38380-01-7	$C_{12}H_5Cl_5$	2,2',4,4',5	326	135	378	0.00366	2.20E-05	4.27E-04	9.38[f]	6.4
PCB-87	38380-02-8	$C_{12}H_5Cl_5$	2,2',3,4,5'	326	135	378	0.0294[*]	1.70E-05	3.63E-04	9.25[f]	6.12
PCB-110	38380-03-9	$C_{12}H_5Cl_5$	2,3,3',4',6	326	135	378	0.00731	2.22E-06	3.99E-04	9.58	6.22
PCB-82	52663-62-4	$C_{12}H_5Cl_5$	2,2',3,3',4	326	135	378	0.0291[*]	2.22E-06	5.97E-04	9.16[f]	6.11
PCB-151	52663-63-5	$C_{12}H_4Cl_6$	2,2',3,5,5',6	361	146	397	0.0136[*]	2.29E-06	1.35E-03	9.58	6.57
PCB-149	38380-04-0	$C_{12}H_4Cl_6$	2,2',3,4',5',6	361	146	397	0.00424	8.43E-06	3.96E-04	9.74	6.46
PCB-118	31508-00-6	$C_{12}H_5Cl_5$	2,3,4,4',5	326	135	378	0.0134[*]	8.97E-06	3.62E-04	10.04	6.72
PCB-153	35065-27-1	$C_{12}H_4Cl_6$	2,2',4,4',5,5'	361	146	397	0.00095[**]	3.43E-06	5.40E-04	9.99	6.76
PCB-132	38380-05-1	$C_{12}H_4Cl_6$	2,2',3,3',4,6'	361	146	397	0.00808	5.81E-07	2.83E-04	10.07	6.42
PCB-105	32598-14-4	$C_{12}H_5Cl_5$	2,3,3',4,4'	326	135	378	0.0034	6.53E-06	3.39E-04	10.20	6.59
PCB-138	35065-28-2	$C_{12}H_4Cl_6$	2,2',3,4,4',5'	361	146	397	0.0015[*]	3.80E-06	4.55E-04	10.20	6.68
PCB-158	74472-42-7	$C_{12}H_4Cl_6$	2,3,3',4,4',6	361	146, 107[b]	397	0.00807[*]	1.55E-06[a]	8.11E-04	10.14	6.74
PCB-187	52663-68-0	$C_{12}H_3Cl_7$	2,2',3,4',5,5',6	395	164	416	0.00451[*]	1.30E-07	6.64E-04	10.22	7.04

Table 2.2 Selected physical-chemical properties of PCB congeners (2/2).

PCBs	Cas-No[a]	Molecular Formula[a]	Molecular Structure[a]	MW[a] (g mol^{-1})	T_M[a] (°C)	T_B[a] (°C)	S_W[b] (25°C) (mg L^{-1})	VP[b] (25°C) (mm Hg)	H[c] (at 25°C) (atm m^3 mol^{-1})	log K_{OA}[d] (at 20°C)	log K_{OW}[g]
PCB-183	52663-69-1	$C_{12}H_3Cl_7$	2,2',3,4,4',5',6	395	164, 83[b]	416	0.0049[*]	9.66E-07[a]	3.46E-04	10.26	7.04
PCB-128	38380-07-3	$C_{12}H_4Cl_6$	2,2',3,3',4,4'	361	146	397	0.00035	2.56E-06	3.31E-04	9.93[f]	7.24[e]
PCB-177	52663-70-4	$C_{12}H_3Cl_7$	2,2',3,3',4',5,6	395	164	416	0.0015	1.30E-07[a]	3.36E-04	10.58	6.92[h]
PCB-171	52663-71-5	$C_{12}H_3Cl_7$	2,2',3,3',4,4',6	395	164	416	0.00217	1.40E-06	2.38E-04[a]	10.51	7.06
PCB-156	38380-08-4	$C_{12}H_4Cl_6$	2,3,3',4,4',5	361	146	397	0.00533[*]	1.61E-06	3.36E-04	10.87	7.12
PCB-180	35065-29-3	$C_{12}H_3Cl_7$	2,2',3,4,4',5,5'	395	164	416	0.00385[*]	9.77E-07	3.79E-04	10.72	7.18
PCB-191	74472-50-7	$C_{12}H_3Cl_7$	2,3,3',4,4',5',6	395	164	416	0.000314	1.30E-07[a]	2.38E-04[a]	10.91	7.24
PCB-169	32774-16-6	$C_{12}H_4Cl_6$	3,3',4,4',5,5'	361	146	397	0.00051	5.81E-07	4.43E-04	11.32	7.49
PCB-170	35065-30-6	$C_{12}H_3Cl_7$	2,2',3,3',4,4',5	395	164	416	0.00347[*]	6.28E-07	1.98E-04	11.07	7.07
PCB-199	52663-75-9	$C_{12}H_2Cl_8$	2,2',3,3',4,5,6,6'	430	181	434	0.00022	2.87E-08	9.91E-04	11.05	7.31
PCB-208	52663-77-1	$C_{12}HCl_9$	2,2',3,3',4,5,5',6,6'	464	191	453	0.000018	7.60E-09	3.56E-05[a]	11.26	7.71
PCB-195	52663-78-2	$C_{12}H_2Cl_8$	2,2',3,3',4,4',5,6	430	181	434	0.00022	2.87E-08	1.54E-04	11.44	7.52
PCB-194	35694-08-7	$C_{12}H_2Cl_8$	2,2',3,3',4,4',5,5'	430	181	434	0.000272	2.87E-08	8.76E-05	11.59	7.54
PCB-205	74472-53-0	$C_{12}H_2Cl_8$	2,3,3',4,4',5,5',6	430	181	434	0.0000858	2.87E-08[a]	3.23E-04[a]	11.62	7.68
PCB-206	40186-72-9	$C_{12}HCl_9$	2,2',3,3',4,4',5,5',6	464	191	453	0.000025	7.60E-09	2.45E-04[a]	11.79	7.86
PCB-209	2051-24-3	$C_{12}Cl_{10}$	2,2',3,3',4,4',5,5',6,6'	499	199, 306[b]	472	0.00000743	1.06E-07	1.06E-06[a]	11.96	8.09

MW: Molecular weight, T_M: Melting point, T_B: Boiling point, S_W: Solubility in water, VP: Vapor pressure, H: Henry's law constant, log K_{OW}: Octanol-water coefficient, log K_{OA}: Octanol-air coefficient, [*] at 20 °C, [**] at 24 °C.
[a] EPI, 2007, [b] NLM, 2008a, [c] Bamford, Poster, & Baker, 2000; Bamford, Poster, Huie, & Baker, 2002, [d] Zhang et al., 1999, [e] Jabusch & Swackhamer, 2005, [f] Chen et al., 2002, [g] Zhou, Zhai, Wang, & Wang, 2005, [h] Padmanabhan, Partasarathi, Subramanian, & Chattaraj, 2006 .

Table 2.2 shows some physical-chemical properties of the studied PCB congeners that vary widely depending on the degree of chlorination and the position of chlorine atom on the biphenyl molecule. Although most PCB congeners are solids at room temperature, the commercial mixtures are mobile oils, viscous fluids, or sticky resins (Nagpal, 1992). Pure individual PCB congeners are colorless to light yellow and have no known smell or taste (ATSDR, 2000a). They have extremely high boiling points and are practically nonflammable. The important characteristics of PCBs that have led to their widespread use are (i) thermal stability, (ii) high degree of chemical stability, (iii) resistance to oxidation, acids, bases, and other chemical agents, and (iv) excellent dielectric properties (i.e. low electrical conductivity) (UNEP, 1999b).

PCBs exhibit low vapor pressure (Nagpal, 1992) and their vapor pressures and Henry's law constants tend to decrease with increased chlorination. Thus, the more chlorinated congeners are relatively non-volatile. PCBs with vapor pressures $>10^{-4}$ mm Hg (mono- and di-CBs) appear to exist in the atmosphere almost entirely in the gas-phase, while PCBs with vapor pressures $<10^{-8}$ mm Hg appear to exist almost entirely in the particle-phase, and PCBs with vapor pressures between 10^{-4} and 10^{-8} mm Hg (tri- to hepta-CBs) exist in both phases (ATSDR, 2000a).

PCBs are non-polar compounds. Their non-polar nature makes them only slightly soluble in water, but they dissolve easily in fats, oils, and most organic solvents (UNEP, 1999b). Generally, water solubility of PCBs decreases as the degree of chlorine substitution increases. Within a homologue group, the solubility depends on the positions of the chlorine atoms on the biphenyl ring (Nagpal, 1992).

PCBs are often associated with the solid fraction (e.g. particulate matter, sediment, soil) of the aquatic and terrestrial environments. In general, sorption tendency of PCBs increases with increasing degree of chlorination, the surface area and the organic carbon content of the sorbents (Nagpal, 1992). The higher chlorinated PCBs with lower water solubility and higher K_{OW} values have a greater tendency to bind to solids as a result of strong hydrophobic interactions. In contrast,

the low molecular weight PCBs with higher water solubility and lower K_{OW} values sorb to a lesser extent on solids and remain largely in the aquatic environments. Therefore, in comparison with the lower chlorinated PCBs, volatilization of highly chlorinated ones in the aquatic and terrestrial environments is reduced significantly by binding these compounds to solids (ATSDR, 2000a).

Most PCB congeners are extremely persistent in the environment. They are estimated to have half-lives ranging from three weeks to two years in air and more than six years in aerobic soils and sediments, with the exception of mono- and di-chlorobiphenyls (UNEP, 2002). Due to their stability and lipophilicity, PCBs bio-accumulate in food chains and are stored in fatty tissues of exposed animals and humans (ATSDR, 2000a).

In people, some acute (e.g. skin conditions, spasms, hearing and vision problems) and chronic (e.g. irritation of nose and lungs, gastrointestinal discomfort, changes in blood and liver, depression, fatigue, and possibly cancer) adverse health effects have been linked to PCBs. The U.S. EPA and the IARC have determined that certain PCB mixtures including Araclor-1016, -1242, -1254 and -1260 are probably carcinogenic (Group B2) to humans (U.S. EPA, 2002b).

2.2.2 Production and Uses of PCBs

PCBs are synthetic chemical compounds and their production involves the chlorination of biphenyl in the presence of a catalyst. Depending on the reaction conditions, the degree of chlorination varies between 21 and 68% chlorine on a weight-by-weight basis (Breivik, Sweetman, Pacyna, & Jones, 2002a). Commercially produced PCBs are a complex mixture of individual PCB congeners, and they were marketed under several trade names including Aroclor, Askarel, Pyroclor, Santotherm, Kennechlor, Hyvol, Chlorextol, and Pyranol (Nagpal, 1992). The most common trade name is Aroclor.

There are many types of Aroclors and each of them is characterized by a four digit number that indicates the degree of chlorination. The first two digits generally refer to the number of carbon atoms in the phenyl rings. For PCBs, this is 12. The last two digits indicate the percentage of chlorine by mass in the mixture. For example, the name Aroclor 1254 means that the mixture contains approximately 54% chlorine by weight. Therefore, higher Aroclor numbers reflect higher chlorine content (ATSDR, 2000a; UNEP, 1999b).

The industrial and commercial uses of PCBs (ATSDR, 2000a; Breivik, Sweetman, Pacnya, & Jones, 2002b; U.S. EPA & Oregon Department of Environmental Quality [DEQ] 2005; UNEP, 1999b; Vallack et al., 1998) can be classified based on their presence in closed, partially closed, and open systems as follows:

- Closed system applications (as coolants and dielectric fluids in transformers, capacitors, electric motors, and electrical household appliances such as television sets, refrigerators, air conditioners, microwave ovens; in fluorescent light ballast, and electromagnets),

- Partially closed system applications (as heat transfer fluids in mechanical operations at the inorganic/organic chemicals, plastics and synthetics, and petroleum refining industries; as hydraulic fluids in mining equipment, aluminum, copper, steel, and iron forming industries; in gas turbines and vacuum pumps; in electrical equipment such as voltage regulators, switches, circuit breakers; as stabilizing additives in flexible PVC coatings of electrical wiring and electronic components, in cable insulation materials), and

- Open system applications (as ink solvents in carbonless copy paper; as plasticizers in polyvinyl chloride (PVC) plastics, rubber, synthetic resins, and sealants; as additives in cement and plaster; in casting waxes; in paints, textiles, surface coatings, de-dusting agents, asphalt, natural gas pipelines, flame retardants; adhesives; in insulating materials; pesticide extenders; in lubricating and cutting oils; in dyes and printing inks).

Products such as oil, carbonless copy paper and plastics made with recycled PCB materials, and automobiles with PCB containing oil, fluids and cables have been also reported (UNEP, 1999b; U.S. EPA & DEQ, 2005).

The production and use of PCBs have been banned for decades in many countries. In Turkey, the uses of PCBs were banned in 1995, except for the closed system uses such as capacitors and transformers that are already in-use (Acara et al., 2006).

2.2.3 Sources of PCBs

Generally, closed and partially closed systems contain PCB oils and fluids. PCBs in closed systems can not readily escape into the environment. However, they may be released during equipment servicing, repairing, or as a result of damaged equipment. Also, the reclamation process for used out instruments and wasted material is a possible source. PCBs in partially closed systems are not directly exposed to the environment, but may be released periodically during typical use or discharge. The PCBs in open systems take on the form of the product used in as a component. Open systems are applications in which PCBs are in direct contact with their surroundings and thereby, they may be easily transferred to the environment (UNEP, 1999b).

Because their hazardous nature has only recently been understood, PCBs have been routinely disposed of over the years without any precautions being taken. As a result, large volumes of PCBs have been released into the environment from illegal or improper dumping of PCB wastes into landfills; open burning; incineration of industrial and municipal wastes (e.g. refuse, sewage sludge, products containing PCBs); vaporization from contaminated surfaces and products containing PCBs; accidental spills and leakage from products to soils; direct entry or leakage into sewers and streams; leakage from older electrical equipment in use; the repair and maintenance of PCB containing equipment (Breivik et al., 2002b; UNEP, 1999b; U.S. EPA & DEQ, 2005; Vallack et al., 1998).

Recycling operations of PCB containing materials (e.g. oil, carbonless copy paper, PVC plastic, and scrap metal) are the other PCB source to the environment. In scrap metal recycling operation, PCBs are emitted from transformer shell salvaging; heat transfer and hydraulic equipment; and shredding and smelting of waste materials such as cars, electrical household appliances (e.g. refrigerators, air conditioners, television sets, and microwave ovens) and other appliances used for upholstery, padding, and insulation. In iron-steel industries, PCBs are also released from non-ferrous metal salvaging as parts from PCB containing electrical equipment, and oil/grease insulated electrical cable (UNEP, 1999b; U.S. EPA & DEQ, 2005).

PCBs emissions may be generated from various thermal processes in the production of organic pigments, pesticides, chemicals (such as PVC manufacturing and petroleum refining industries), cement, copper, iron-steel, and aluminum refining industries. In these processes, they may be synthesized like dioxins. The forming of PCBs as a by-product is possible when chlorine, hydrocarbon and elevated temperatures together with catalysts (UNEP, 1999b).

PCBs are combustible liquids, and the products of combustion may be more hazardous than the original material. Combustion by-products include hydrogen chloride, polychlorinated dibenzodioxins/dibenzofurans (PCDD/DFs). The pyrolysis of commercial PCB mixtures produces several PCDFs. PCDFs are also produced as a by-product during the commercial production and handling of PCBs, and as impurities in various commercial PCB mixtures (ATSDR, 2000a).

2.3 Organochlorine Pesticides (OCPs)

Organochlorine pesticides (OCPs) are mostly used as insecticides in agriculture. Some OCPs have been banned for decades in many countries because of concerns about environmental and human health impacts (Acara et al., 2006). However, banned OCPs are still found in the environment, probably due to their persistence, illegal uses or emissions from certain industrial sources. OCPs restricted/banned or

remained in-use are mainly released to the atmosphere by agricultural usage, volatilization from contaminated soil, and particulate matter re-entrainment from the surface cover by the wind at contaminated areas (Bidleman, 1999).

Once released, OCPs can be partitioned to all environmental matrices such as air, water, soil, and sediment. Due to their semi-volatile nature, they can exist in the atmosphere as a gas and/or attached to airborne particles, and can be transported over long distances. Although their atmospheric lifetime is long, they can be degraded by reacting with photo-chemically produced hydroxyl radicals or can be removed from the air by wet and dry deposition (ATSDR, 2005).

OCPs are generally stable in the environmental matrices and undergo limited decomposition and/or degradation. In soil, sediment, and water, they are broken down to less toxic substances by algae, fungi, and bacteria, but this process can take a long time. Biodegradation is believed to be the dominant decomposition process for OCPs in soil and water, although hydrolysis and photolysis may also occur to a lesser extent. The rates of degradation processes depend on the ambient environmental conditions. Since most OCPs are bio-accumulative, they build up in the food chain as well as in fatty tissues of animals and humans (ATSDR, 2005; Regional Water Quality Control Plant [RWQCP], 1997).

2.3.1 Chemical Structures, Properties, and Health Effects of OCPs
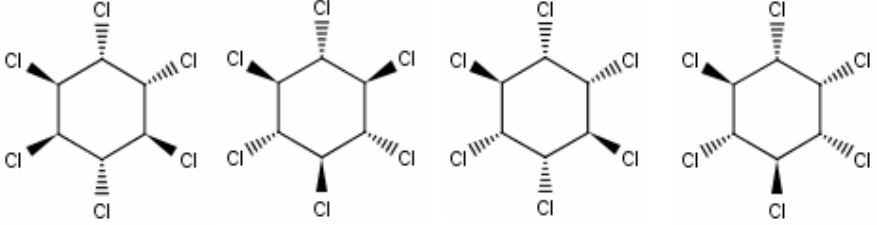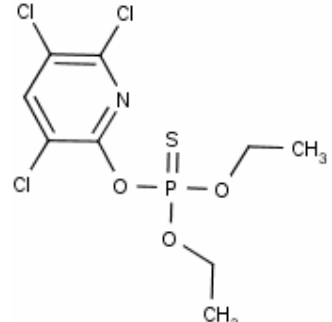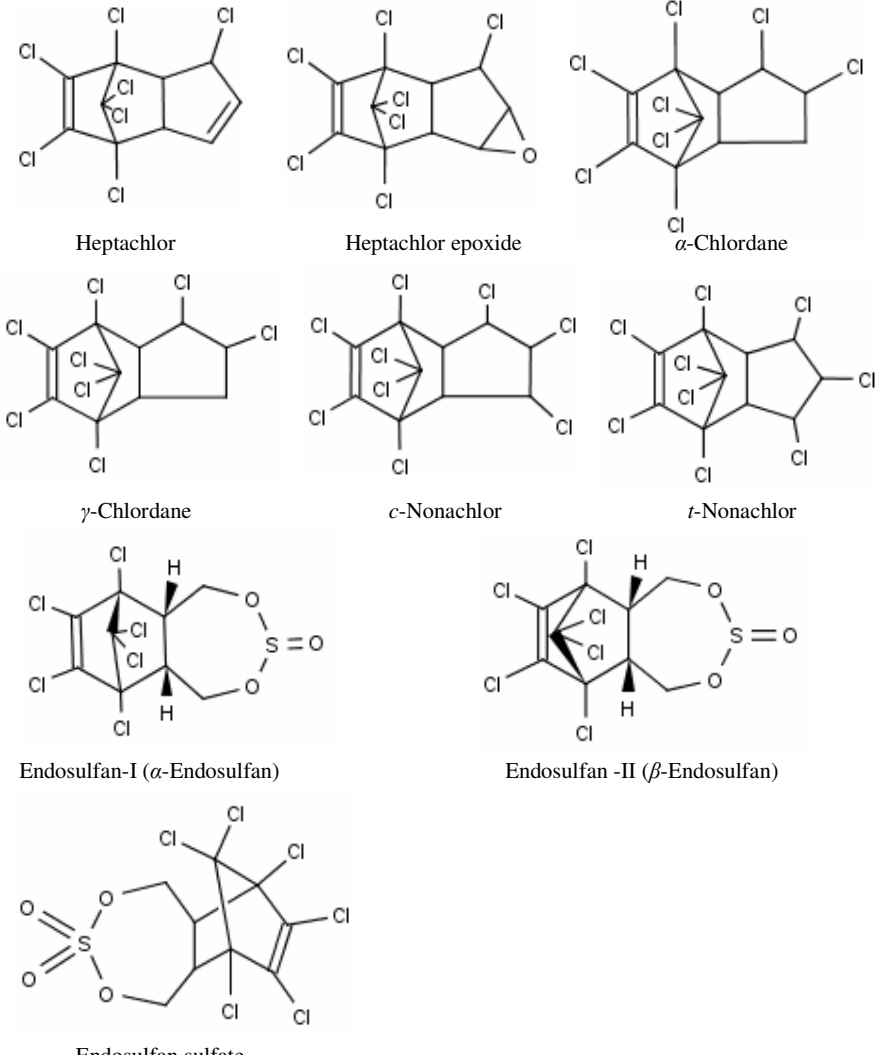
Organochlorine pesticides vary in their chemical structures and mechanisms of toxicity. Subcategories of this group include dichlorodiphenylethanes (e.g. DDT, methoxychlor, dicofol, chlorobenzilate); cyclodienes (e.g. aldrin, dieldrin, endrin, chlordane, heptachlor, endosulfan, mirex); chlorinated benzenes (e.g. hexachlorobenzene [HCB]); and cyclohexanes (e.g. hexachlorocyclohexane [HCH], lindane) (U.S. EPA, 2002a, 2002b; WHO, 1979). In this study, chlorpyrifos is the only studied compound that belongs to the group of organophosphate insecticide.

Chemical structures of some pesticides and their degradation products are illustrated in Fig. 2.3, and selected physical-chemical properties of studied pesticides are given in Table 2.3. In this section, studied pesticides were evaluated according to their related groups and metabolites. The structures and many physical-chemical properties of related pesticides are very similar. For example, cyclodiene pesticides are a large group of highly chlorinated cyclic hydrocarbons with characteristic endomethylene bridged structures. They are highly persistent compounds, exhibiting especially high resistance to degradation in soil (U.S. EPA, 2002a). DDT related pesticides have a different type of structure, but they also share some properties with other OCPs such as chlordane, dieldrin, and heptachlor (RWQCP, 1997).

2.3.1.1 Hexachlorocylclohexane (HCH)

Hexachlorocylclohexane (HCH) is an organochlorine insecticide consisting of eight isomers. But, only alpha- (α), beta- (β), gamma- (γ), and delta- (δ) isomers are of commercial significance. Different isomers are named according to the position of the hydrogen atoms in the structure. Pure γ-HCH, commonly called lindane, is the only isomer with insecticidal activity. Technical HCH mixture is comprised of approximately 60-70% α-HCH, 5-12% β-HCH, 10-15% γ-HCH, 6-10% δ-HCH, and other isomers. HCHs are brownish- to white-colored crystalline solids or fine plates with a phosgene-like odor (ATSDR, 2005).

γ-HCH can be released into the atmosphere both as lindane and as a component of technical HCH. Agricultural application of lindane constitutes the largest source of γ-HCH to the environment. α-HCH has the highest proportion in technical HCH mixtures, and it can be released into the atmosphere only as a component of technical HCH. The main degradation of HCH isomers in the air occurs through the photochemical reaction with hydroxyl radicals (ATSDR, 2005).

HCHs				
	α-HCH	β-HCH	γ-HCH (Lindane)	δ-HCH
Chlorpyrifos				
Cyclodienes (Heptachlor, Chlordane and metabolites)	Heptachlor	Heptachlor epoxide	α-Chlordane	
	γ-Chlordane	c-Nonachlor	t-Nonachlor	
(Endosulfan and metabolites)	Endosulfan-I (α-Endosulfan)		Endosulfan -II (β-Endosulfan)	
	Endosulfan sulfate			

(Aldrin Dieldrin)	Aldrin Dieldrin
(Endrin and metabolites)	Endrin Endrin aldehyde Endrin ketone
DDT related pesticides (DDT and metabolites, methoxychlor)	p,p'-DDT p,p'-DDD p,p'-DDE Methoxychlor
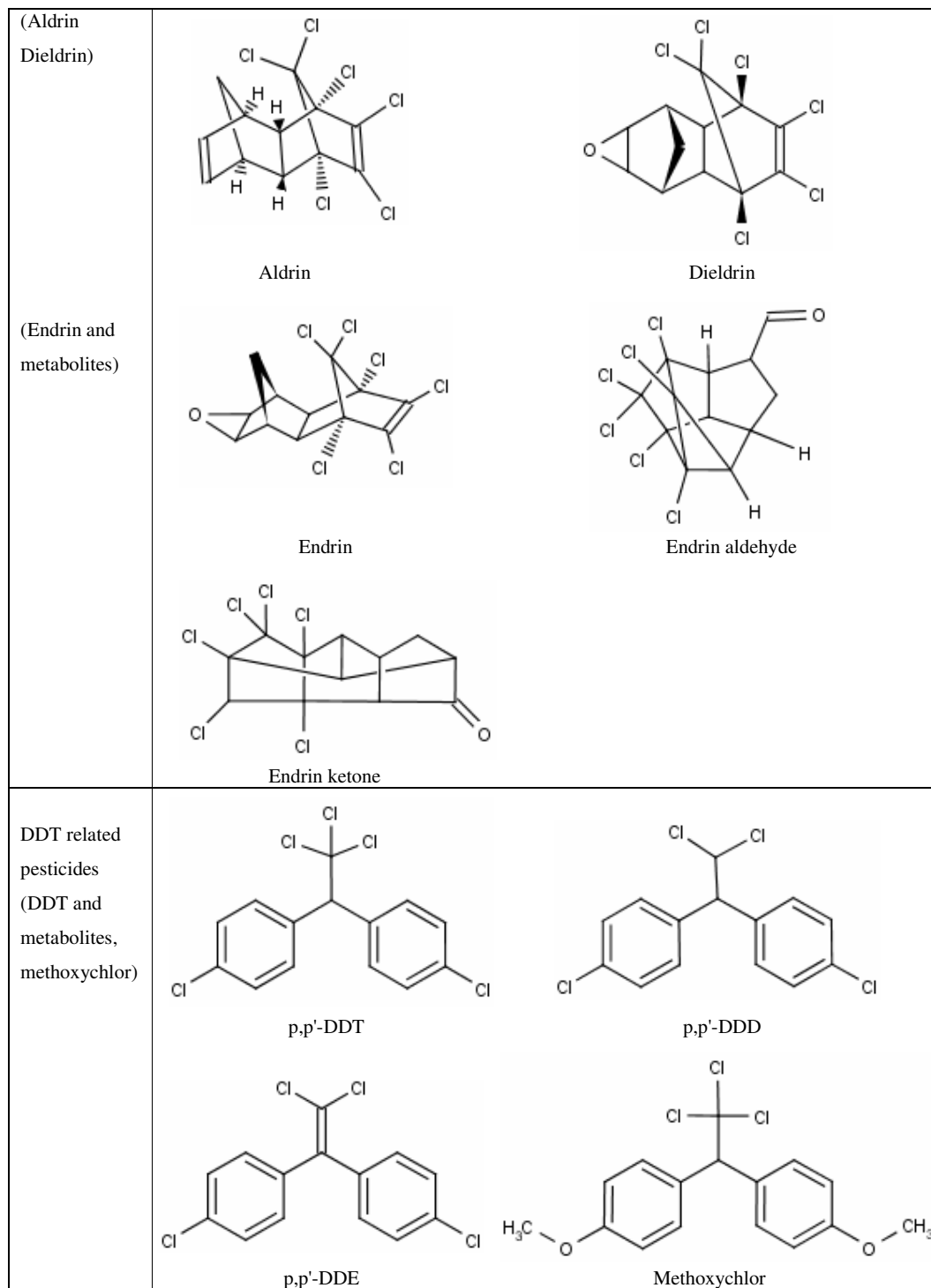
Figure 2.3 Chemical structures of the some related pesticides and their metabolites (NLM, 2008a).

Table 2.3 Selected physical-chemical properties of the studied pesticides.

OCPs[**]	CAS-No[a]	Molecular Formula[a]	MW[a] (g mol⁻¹)	T_M[b] (°C)	T_B[b] (°C)	S_W[a] (25°C) (mg L⁻¹)	VP[a] (25°C) (mm Hg)	H[c] (25°C) (atm m³ mol⁻¹)	log K_{OA}[e] (25°C)	log K_{OW}[a]
α-HCH	319-84-6	$C_6H_6Cl_6$	291	57, 160[a]	304, 288[a]	2.0	4.50E-05	2.96E-06	7.61	3.80
β-HCH	319-85-7	$C_6H_6Cl_6$	291	57, 315[a]	304	0.24	3.60E-07[*]	3.55E-07[d]	8.88	3.78
γ-HCH	58-89-9	$C_6H_6Cl_6$	291	57, 113[a]	304, 323[a]	7.3	4.20E-05[*]	2.66E-06	7.85	3.72
δ-HCH	319-86-8	$C_6H_6Cl_6$	291	57, 142[a]	304	10.0[*]	3.52E-05	4.29E-07[a]	8.84	4.14
CHLPYR	2921-88-2	$C_9H_{11}Cl_3NO_3PS$	351	83, 42[a]	377	1.12[**]	2.03E-05	3.55E-05	8.41[f]	4.96
HEP EPOX	1024-57-3	$C_{10}H_5Cl_7O$	389	133, 160[a]	341	0.20	1.95E-05[***]	2.27E-05	8.50[f]	4.98
α-CHL	5103-71-9	$C_{10}H_6Cl_8$	410	133	351	0.056	3.60E-05	5.43E-05	8.92	6.10
γ-CHL	5103-74-2	$C_{10}H_6Cl_8$	410	133	351	0.056	5.03E-05	1.57E-04	8.87	6.22
c-NONA	5103-73-1	$C_{10}H_5Cl_9$	444	148	372	0.0104	9.00E-07	5.92E-06	9.66	6.08
t-NONA	39765-80-5	$C_{10}H_5Cl_9$	444	148	372	0.0104	1.00E-06	1.06E-04	9.29	6.35
ESLF-I	959-98-8	$C_9H_6Cl_6O_3S$	407	166	401	0.51[*]	3.00E-06	8.09E-06	8.64	3.83
ESLF-II	33213-65-9	$C_9H_6Cl_6O_3S$	407	166	401	0.45[*]	6.00E-07	6.51E-07	9.28[f]	3.83
ESULFATE	1031-07-8	$C_9H_6Cl_6O_4S$	423	170, 181-182[a]	409	0.48[*]	2.80E-07	3.25E-07[a]	9.68[f]	3.66
p,p'-DDT	50-29-3	$C_{14}H_9Cl_5$	354	123, 109[a]	368	0.0055	1.6E-07[*]	9.57E-06	9.82	6.91
p,p'-DDD	72-54-8	$C_{14}H_{10}Cl_4$	320	114, 110[a]	367, 350[a]	0.09	1.35E-06	9.47E-06	10.10	6.02
DIELD	60-57-1	$C_{12}H_8Cl_6O$	381	135, 176[a]	340, 330[a]	0.195	5.89E-06	9.77E-06	8.90	5.40
END	72-20-8	$C_{12}H_8Cl_6O$	381	135, 226-230[a]	340	0.25	3.00E-06[*]	5.62E-06	8.13	5.20
END AL	7421-93-4	$C_{12}H_8Cl_6O$	381	138	340	0.024	2.00E-07	4.18E-06[a]	9.47[f]	4.80
END KET	53494-70-5	$C_{12}H_8Cl_6O$	381	146	357	0.222	5.51E-06	2.02E-08[a]	10.11[f]	4.99
MEOCL	72-43-5	$C_{16}H_{15}Cl_3O_2$	346	129, 87[a]	378, 346[a]	0.10	2.58E-06	2.03E-07[a]	10.57[f]	5.08

[**] α,β,γ,δ-Hexachlorocyclohexane isomers (α,β,γ,δ-HCH), chlorpyrifos (CHLPYR), heptachlor epoxide (HEP EPOX), α-chlordane (α-CHL), γ-chlordane (γ-CHL), cis-nonachlor (c-NONA), trans-nonachlor (t-NONA), endosulfan-I (ESLF-I), endosulfan-II (ESLF-II), endosulfan sulfate (ESLF SUL), dichlorodiphenyl trichloroethane (p,p'-DDT), tetrachlorodiphenylethane (p,p'-DDD), dieldrin (DIELD), endrin (END), endrin aldehyde (END AL), endrin ketone (END KET), methoxychlor (MEOCL).

MW: Molecular weight, T_M: Melting point, T_B: Boiling point, S_W: Solubility in water, VP: Vapor pressure, H: Henry's law constant, log K_{OA}: Octanol-air coefficient, log K_{OW}: Octanol-water coefficient, [*] at 20 °C, [**] at 24 °C, [***] at 30 °C.

[a] NLM, 2008a, [b] EPI, 2007, [c] Cetin, Ozer, Sofuoglu, & Odabasi, 2006, [d] Sahsuvar, Helm, Jantunen, & Bidleman, 2003, [e] Shoeib & Harner, 2002, [f] Odabasi , 2007a.

Among HCH isomers, α- and γ-HCH are more ubiquitous in the environment. Although both isomers have relatively high vapor pressures, γ-HCH has a higher value than that of α-HCH (Gioia et al., 2005). Thus, atmospheric lindane concentrations tend to be more strongly correlated with temperature and more influenced by volatilization from terrestrial surfaces. However, global atmospheric background concentrations are higher for α-HCH than γ-HCH possibly because α-HCH is more persistent (Wania, Haugen, Lei, & Mackay, 1998).

The occurrence of HCH isomers in water supplies is more important potential problem than many other OCPs (e.g. DDT, endrin, aldrin, heptachlor) due to their high water solubility. γ-HCH has a low residence time in the aquatic environment and the principal dissipation routes are sedimentation, biodegradation, and volatilization. Thus, γ-HCH is generally found to contribute less to aquatic pollution than the other HCH isomers (U.S. EPA, 1980a).

HCHs are much less bio-accumulative than other OCPs because of their relatively low liphophilic properties. Lindane and other HCH isomers are relatively persistent in soils and water, with half-lives generally greater than 1 and 2 years, respectively (UNEP, 2002). HCHs in soil or sediment are degraded primarily by biodegradation. The biological transformation of HCHs results in the formation of various cyclophenols including 2,3,5-, 2,4,5- and 2,4,6-trichlorophenol; 3,4-dichlorophenol; 2,3,4,5- and 2,3,4,6-tetrachlorophenol (U.S. EPA, 1980a). γ-HCH is also transformed to tetrachlorohexene; tri-, tetra-, and penta-chlorinated benzenes; penta- and tetra-cyclohexanes; and other isomers of HCH (ATSDR, 2005).

Several hepatic, immunological, hematological, neurological, reproductive, and carcinogenic effects have been reported in humans exposed to HCHs. Among HCH isomers, γ-HCH (lindane) has the highest acute toxicity (U.S. EPA, 1980a). The World Health Organization (WHO) has determined that HCH and lindane are classified as Class II, moderately hazardous chemicals (WHO, 2005). The IARC has classified all HCH isomers as possibly carcinogenic to humans. The U.S. EPA has

determined technical HCH and *α*-HCH as Group B2, probable human carcinogens, and *β*-HCH as Group C, possible human carcinogen. The U.S. EPA has also classified lindane as having "suggestive evidence of carcinogenicity, but not sufficient to assess its human carcinogenic potential" (ATSDR, 2005).

2.3.1.2 Chlorpyrifos

Chlorpyrifos, also known as chlorpyrifos ethyl, is an organophosphate pesticide. However it is rather unusual in this group, since it has a high degree of chlorination. This chlorination gives certain properties that are not typically noted for this general class of compounds. The important properties are its low water solubility, more lipid solubility, and adsorption tendency to particulate matter, soil or sediment. These properties make it more persistent than most other pesticides in this general group (U.S. EPA, 2002b).

Chlorpyrifos is a white crystalline solid that has a strong odor (U.S. EPA, 2002b). Chemical hydrolysis, photo-degradation, and biodegradation are all important processes for the transformation and degradation of chlorpyrifos (Miller, 1996). Because of its low water solubility and its affinity for organics, it has little mobility in most soils. When chlorpyrifos enters an aquatic system, it appears to be sorbed readily to suspended organics and sediment, although some is removed by volatilization and degradation. Its penetration into sediment appears to be shallow, with most occurring in the upper layers. Although chlorpyrifos is hydrophobic, it bio-concentrates or accumulate in living tissues to only a limited extent because of its rapid metabolism (ATSDR, 1997; U.S. EPA, 1986). 3,5,6-trichloro-2-pyridinol (TCP) is a major metabolite of this compound (ATSDR, 1997).

In people, short-term oral exposure to low levels of chlorpyrifos can cause dizziness, fatigue, runny nose or eyes, salivation, nausea, intestinal discomfort, sweating, and changes in heart rate. Much higher levels of chlorpyrifos may cause paralysis, seizures, loss of consciousness, and death. Other effects of exposure to

chlorpyrifos include changes in behavior or sleeping pattern, mood changes, and effects on the nerves and/or muscles in the limbs, which may appear as odd sensations such as numbness, tingling, or muscle weakness. Chlorpyrifos is classified as Class II, moderately hazardous chemical by WHO (2005). The U.S. EPA has not classified chlorpyrifos for carcinogenicity (Class D) (ATSDR, 1997).

2.3.1.3 Heptachlor

Heptachlor is a cyclodiene insecticide that has a chemical structure and mechanism of toxicity similar to that of chlordane. It is also both a breakdown product and a minor component of chlordane (U.S. EPA, 2002b). Pure heptachlor is a white powder that does not burn easily and does not explode. Technical product is a tan powder and usually consists of 72% heptachlor and 28% impurities such as *trans*-chlordane, *cis*-chlordane, and nonachlor (ATSDR, 2007).

Heptachlor epoxide is an oxidation breakdown product of heptachlor and chlordane. It degrades more slowly, and thus, it is more persistent in the environment than heptachlor. Heptachlor epoxide is also considered more toxic than its parent compound. Although both of them do not dissolve easily in water, heptachlor epoxide dissolves more easily in water than heptachlor does (ATSDR, 2007)

Both heptachlor and heptachlor epoxide have relatively high log K_{OC} values that suggest a high sorption tendency. This means that these compounds are not mobile in soil and have a low potential to leach. However, they have some volatilization potential from the contaminated surfaces to the air (Miller, 1996). The half-life of heptachlor in soil is 0.75-2 years in temperate regions (UNEP, 2002). Based on their high partition coefficient, both are bio-concentrated in aquatic and terrestrial organisms. Because of its lipophilicity and its more persistent nature, bio-magnification of heptachlor epoxide in food chain is significant (ATSDR, 2007).

In humans, heptachlor results in a variety of adverse health effects including liver effects, neurological effects, reproductive system dysfunction, and developmental effects. The U.S. EPA and the IARC have classified heptachlor as a possible human carcinogen. The U.S. EPA also considers heptachlor epoxide as a possible human carcinogen (ATSDR, 2007).

2.3.1.4 Chlordane

Chlordane belongs to the cyclodiene group of insecticides, and it is structurally quite similar to heptachlor and heptachlor epoxide. Technical chlordane is a mixture of various related chemicals with a typical composition of ~15% *cis-* (or *α-)* chlordane, 15% of *trans-* (or *γ-)* chlordane, 9.7% of *tran*s-nonachlor, 3.9% *octa-*chlordane, 3.8% heptachlor, 2.7% *cis*-nonachlor and other compounds. The composition of technical chlordane varies according to conditions during its manufacture (U.S. EPA, 1997).

Chlordane is a thick liquid whose color ranges from colorless to amber, depending on its purity. It may have no smell or a mild, irritating smell. The physical-chemical properties of technical chlordane are difficult to specify, since the technical product is a mixture of over 140 compounds. Properties of a mixture also differ from the properties of the components. Compositional changes with time may result from different rates of degradation and transport among the constituents of the mixture (ATSDR, 1994).

Generally, chlordane and related compounds are insoluble in water, but soluble in fat and bio-concentrate in fatty tissues. Especially *cis-* and *trans*-chlordane have high Henry's law coefficients which make them more volatile than other pesticides (Table 2.3). Combined with their persistence in the environment, they are likely to undergo long-range transport (U.S. EPA, 2002b).

In the environment, chlordane is metabolized to *oxy*-chlordane and heptachlor. Heptachlor is also metabolized to heptachlor epoxide as described above. Chlordane is an unlikely source of exposure if heptachlor epoxide is found in the absence of either *oxy*-chlordane or *trans*-nonachlor. The most persistent compounds in biological tissue are *oxy*-chlordane and heptachlor epoxide which are of primary toxicological significance (U.S. EPA, 1997).

Like most of the other cyclodiene pesticides, chlordane is highly immobile within the soil, since it is both insoluble in water and rapidly binds to soil particles. It has a half-life of about 4 years in soils depending on the environmental conditions (UNEP, 2002). Evaporation is the major route of removal from soils. Also, it has a low potential for groundwater contamination (Miller, 1996; ATSDR, 1994).

Major health effects in humans that may be linked to chlordane exposure are on the nervous system, the digestive system, and the liver. Large amounts of chlordane taken by mouth can cause convulsions and death. Swallowing small amounts or breathing air containing high concentrations of chlordane vapors can cause a variety of nervous system effects, including headaches, irritation, confusion, weakness, and vision problems, as well as upset stomach, vomiting, stomach cramps, diarrhea, and jaundice (ATSDR, 1994). The WHO classified chlordane as Class II, moderately hazardous (WHO, 2005). The IARC has determined that chlordane is not classifiable as to its carcinogenicity to humans. However, the U.S. EPA lists chlordane in Group B2, probable human carcinogen (ATSDR, 1994).

2.3.1.5 Endosulfan

Endosulfan belongs to the group of chlorinated cyclodiene insecticides (U.S. EPA, 1980b). Technical endosulfan contains a mixture of its two different forms: ~70% of endosulfan-I (*α*-isomer) and 30% of endosulfan-II (*β*-isomer). Endosulfan is a light to dark brown crystalline solid that does not burn. It has a distinct odor similar to turpentine (ATSDR, 2000b).

Endosulfan sulfate is the main degradation product of endosulfan as a result of oxidation, biotransformation or photolysis mechanisms (Hafner & Hites, 2003). Both isomers of endosulfan are also metabolically converted by microorganisms, plants, and animals to endosulfandiol, endosulfan ether, endosulfan hydroxyether, and endosulfan lactone in the environment (U.S. EPA, 1980b). ATSDR (2000b) has reported that the β-isomer (endosulfan-II) is also slowly converted to the more stable α-isomer (endosulfan-I) at high temperatures.

In soil, endosulfan is most likely subjected to photolysis (on soil surfaces), hydrolysis (under alkaline conditions), or biodegradation. Because of its very low solubility, it does not easily dissolve in water. Based on the relationship between the partition coefficients of K_{OW} and K_{OC}, endosulfan has a moderate capacity to adsorb to soils and it is not likely to leach to groundwater. Thus, it is also moderately persistent in the soil environment with a reported average field half-life of 50 days. The α- and β-isomers have different degradation times in soil with half-lives of 35 and 150 days (in neutral conditions), respectively (UNEP, 2002). Due to their low K_{OW} values, endosulfan and metabolites do not bio-accumulate to high concentrations in terrestrial or aquatic ecosystems (ATSDR, 2000b).

There is very little difference in toxicity between endosulfan and its metabolite, endosulfan sulfate. However, the α-isomer has been shown to be about three times as toxic as the β-isomer of endosulfan (ATSDR, 2000b). Exposure to very large amounts of endosulfan for short periods can cause adverse effects on nervous system such as hyper-excitability, tremors, convulsions, and dizziness. Chronic signs include intermittent muscle twitching, psychological disorders, loss of consciousness, and convulsions. In animal studies, long-term exposure to low levels of endosulfan has been shown to affect the kidney, testes, and liver. Effects on the immune system, and decreased weight gain were also noted (U.S. EPA, 2002b). The WHO classified endosulfan as Class II, moderately hazardous substance (WHO, 2005). The IARC and U.S. EPA have not classified endosulfan regarding its ability to cause cancer (ATSDR, 2000b).

2.3.1.6 Aldrin and Dieldrin

Aldrin and dieldrin are structurally similar compounds that belong to cyclodiene series of insecticides. Since aldrin is readily converted to dieldrin in the environment, these two compounds are discussed together in this section. Technical aldrin contains at least 85.5% aldrin, and technical dieldrin contains at least 85% dieldrin. Pure aldrin and dieldrin are white powders, while technical-grade aldrin and dieldrin are tan powders. Both insecticides have mild chemical odors (ATSDR, 2002b).

Aldrin is readily converted by natural processes into the more stable and persistent compound of dieldrin. Thus, as a pesticide residue, aldrin is rarely detected in its original chemical form into the environment (U.S. EPA, 2002b; RWQCP, 1997). Since dieldrin is more resistant to biotransformation and abiotic degradation, it is found ubiquitously in all environmental media where aldrin and dieldrin were originally released (ATSDR, 2002b).

Aldrin and dieldrin are non-polar compounds. Therefore, they have a strong affinity for organic matter and sorbs tightly to soil particulates. Movement of dieldrin through the soil column is extremely slow, indicating little potential for groundwater contamination. Based on their physical properties, volatilization from soil or water surfaces is expected, however, this may be decreased by adsorption to suspended solids and sediment in the water column. Most aldrin and dieldrin found in surface water are the result of runoff from contaminated soil (ATSDR, 2002b).

Aldrin undergoes photolysis to dieldrin which in turn may be degraded by ultraviolet radiation or microbial action into the more persistent compound, photo dieldrin (ATSDR, 2002b). Aldrin is classified as moderately persistent with half-life in soil and surface waters ranging from 20 days to 1.6 years. Dieldrin is much more resistant to biodegradation than aldrin. It is highly persistent in soils, with a half-life of 3-4 years in temperate climates (UNEP, 2002). Both aldrin and dieldrin are bio-concentrated by plants, animals, and aquatic organisms, and biomagnified in aquatic

and terrestrial food chains. Food chain bioaccumulation appears to be a more important fate process for dieldrin than for aldrin, since aldrin is rapidly converted to more stable form, dieldrin. Atmospheric aldrin and dieldrin compounds in gas-phase are expected to react with hydroxyl radical. Gas-phase aldrin may also be degraded in the air by reaction with ozone (ATSDR, 2002b). The persistence in air has been estimated in 4-40 hrs (UNEP, 2002)

Aldrin and dieldrin affect human health in similar ways. Exposure to large amount of both pesticides for short periods can cause convulsions or other nervous system effects, and kidney damage. Some people who intentionally ate or drank large amounts of aldrin or dieldrin died. In people exposed to smaller amounts of aldrin or dieldrin, adverse health effects occur, because levels of the chemicals build up in the body over time. Exposure to moderate levels of aldrin or dieldrin for a long time causes headaches, dizziness, irritability, vomiting, or uncontrollable muscle movements. They also can destroy the blood cells in human body. The IARC has determined that aldrin and dieldrin are not classifiable as to their carcinogenicity to humans. However, aldrin and dieldrin are both classified by the U.S. EPA as Group 2, probable human carcinogens (ATSDR, 2002b).

2.3.1.7 Endrin

Endrin is a stereoisomer of dieldrin, and a member of cyclodiene group of pesticides (U.S. EPA, 2002b). Endrin is also a contaminant in dieldrin. Endrin aldehyde and endrin ketone occurred as impurities of eldrin or as degradation products. While technical-grade endrin is typically 95-98% pure, some chemicals are found as impurities including aldrin, dieldrin, isodrin, heptachloronorbornadiene, and heptachloronorborene in addition to endrin aldehyde and endrin ketone (ATSDR, 1996). Pure endrin is a white crystalline solid that is almost odorless, while the technical compound is a light tan powder (U.S. EPA, 1980c).

Endrin is a highly persistent chemical in the environment, particularly in soils. Because of its low solubility in water, leaching may be possible in some soils under certain conditions. Half-lives of up to 12 years have been reported in some cases (UNEP, 2002). Biodegradation and hydrolysis does not appear to be a significant fate process for endrin in soils. In combination with losses from volatilization, photo-degradation, and heat transformation (primarily to endrin ketone with minor amounts of endrin aldehyde) account for the rapid decrease in endrin residues on soil surfaces exposed to sunlight (ATSDR, 1996).

Endrin is the most acutely toxic compound among the cyclodiene group of insecticides (U.S. EPA, 2002b). In humans, the primary toxic effect of acute exposure to endrin is on the nervous system. Symptoms are headache, dizziness, nervousness, confusion, nausea, vomiting, convulsions, hyper-excitability, and seizures (ATSDR, 1996). Chronic signs of toxicity include intermittent muscle twitching, psychological disorders, loss of consciousness, and convulsions (U.S. EPA, 2002b). The U.S. EPA and the IARC have determined that endrin is not classifiable for its human carcinogenety (ATSDR, 1996).

2.3.1.8 Dichlorodiphenyltrichloroethane (DDT)

Technical-grade DDT consists of different isomers with similar properties. Its formulation mainly contains 65-80% of *p,p'*-DDT and other chemical forms of DDT including *o,o*'-DDT, and *o,p*'-DDT. Isomers of *p,p'*-DDD and *p,p'*-DDE occurs as impurities in technical DDT as well as its degradation product. Although both of the degradation products are toxic, DDE is the more persistent and more toxic metabolite of DDT (ATSDR 2002a).

Technical DDT is a white amorphous powder that is odorless or may have a slight aromatic odor. It melts over the range of 80-94 °C. Pure *p,p´*-DDT is a colorless crystalline solid or powder-like substance with weak aromatic odors. It is very

soluble in fats and most organic solvents, but insoluble in water. $p,p´$-DDT is a flammable substance with a range of flash point 72-75 °C (UNEP, 2006).

Because of their semi-volatile nature, p,p'-DDT, p,p'-DDE, and p,p'-DDD are found in the atmosphere both as gaseous or attached to airborne particulates, and undergo long-range transport. Both p,p'-DDE and p,p'-DDD have higher vapor pressures than p,p'-DDT, and thus, a smaller fraction of p,p'-DDE and p,p'-DDD are adsorbed to particulate matter than p,p'-DDT (ATSDR, 2002a). Gas-phase p,p'-DDT and its metabolites are subject to direct photo-degradation and reaction with photo-chemically produced hydroxyl radicals (UNEP, 2006).

When deposited on soil, routes of loss and degradation include runoff, volatilization, photolysis, and biodegradation. p,p'-DDT biodegrades primarily to p,p'-DDE under un-flooded conditions (e.g. aerobic) and to p,p'-DDD under flooded (e.g. anaerobic) conditions (ATSDR, 2002a). However, these processes generally occur only very slowly. DDT is highly persistent in soils with a half-life of up to 15 years and of 7 days in air depending on conditions (UNEP, 2002). As a result of their strong binding to soil (as reflected by their high K_{OC} values), p,p'-DDT, p,p'-DDE, and p,p'-DDT mostly remain on the surface layers of soil. They do not dissolve in water, and are essentially immobile in soil. Thus, there is little leaching into the lower soil layers and groundwater. As reflected by their high log K_{OW} values (Table 2.3), p,p'-DDT and its degradation products adsorb strongly to particulate matter in the water column and primarily partition into the sediment. But, some of them may volatilize into the air. The persistence of DDT and its metabolites in combination with their high lipophilicity have contributed to the bioaccumulation and bio-magnification of these compounds in the environment (ATSDR, 2002a).

In humans, acute overdoses of DDT affect most likely the nervous system. People who swallowed large amounts of DDT may become excitable and may have tremors and seizures. Other symptoms are sweating, headache, nausea, vomiting, and dizziness. The same types of effects are expected by breathing DDT particles in the

air or by contact of the skin with high amounts of DDT. People exposed for a long time to small amounts of DDT have some minor changes in the levels of liver enzymes in the blood. Studies in animals have shown that DDT, DDE, and DDD can cause cancer, primarily in the liver (ATSDR, 2002a). The WHO classified DDT as Class II, moderately hazardous substance (WHO, 2005). The IARC classifies DDT (p,p'-DDT) as a possible human carcinogen. The U.S. EPA has determined that DDT, DDE, and DDD are probable human carcinogens (ATSDR, 2002a).

2.3.1.9 Methoxychlor

Methoxychlor, also known as methoxy-DDT, belongs to an insecticide group of dichlorodiphenylethanesis. It is essentially a less-toxic form of the DDT in which a methoxy group replaces the more persistent and biologically active chlorine molecule on one of the phenyl groups of the basic DDT molecule (U.S. EPA, 2002b). Pure methoxychlor is a pale-yellow powder with a slightly fruity or musty odor. Technical-grade methoxychlor typically contains 88-90% of the pure chemical and 10-12% of impurities including methoxychlor isomers and other reaction products (ATSDR, 2002c).

In air, methoxychlor exists in both the particle- and, to a small degree, gas-phases. Methoxychlor is rapidly degraded by photo-chemically produced hydroxyl radicals in air, but most is probably removed from the atmosphere by wet and dry deposition processes. The residence time for methoxychlor in the atmosphere is less than 1 month (ATSDR, 2002c).

Methoxychlor is moderately soluble in water and soluble in a variety of organic solvents. Because of its relatively high K_{OC} value, it binds tightly to soils, but most does not persist due to degradation by microorganisms in the soil. Methoxychlor is generally not detected in surface water or groundwater probably due to its degradation and affinity for sediments and organic matter. Although methoxychlor is not as persistent as DDT, it can persist in soils for more than a year after its

application. Methoxychlor in water and sediment is degraded to dechlorinated, dehydrochlorinated, and demethylated products by chemical, photochemical, and biological processes. Half-lives of metoxychlor are less than 30 days in anaerobic soils and greater than 100 days in aerobic soils depending on the environmental conditions. Methoxychlor can accumulate in living tissues. However, most fish and animals change methoxychlor into other substances that are rapidly released from their bodies. Thus, it does not usually build up in the food chain (ATSDR, 2002c).

Exposure to high levels of methoxychlor can cause effects on the nervous system Symptoms include tremors, convulsions, and seizures. Some of the breakdown products of methoxychlor cause effects similar to those produced by estrogen. WHO has determined that metoxychlor is a substance, unlikely to present acute hazard in normal use (WHO, 2005). According to the IARC and the U.S. EPA, methoxychlor is not classifiable for its carcinogenicity to humans (ATSDR, 2002c).

2.3.2 Production and Uses

2.3.2.1 Hexachlorocylclohexane (HCH)

The manufacturing of technical-grade HCH involves the photo-chlorination of benzene which yields an isomeric mixture consisting of α-HCH, β-HCH, γ-HCH, δ-HCH, and impurities (IARC 1979). In the manufacture of technical-grade γ-HCH (lindane), it is concentrated to 99.9% γ-HCH by treatment with methanol or acetic acid followed by fractional crystallization (ARSDR, 2005).

Technical HCH was produced as an insecticide and used in agriculture as exterminating agent of soil pest, beetle, human and animal parasites, and in forestry and wood protection. Technical HCH mixture was also previously used as an additive in plasticizer production (e.g. in PVC sheathing of electric cables) (Manz, Wenzel, Dietze, & Schuurmann, 2001). In Turkey, the use of technical HCH was restricted in 1978 and then it was banned in 1985 (Acara et al., 2006).

Lindane is an insecticide used on a wide variety of fruit and vegetable crops, forestry, tobacco, greenhouse vegetables and ornamentals. The use of lindane as a seed treatment for control of wireworms and other soil pests is also reported. It is used in lotions, creams, and shampoos for the pharmaceutical treatment of scabies and head lice in humans. Additionally, γ-HCH is used in veterinary products to control external parasites like fleas, mites, lice, and other pests (ATSDR, 2005; RWQCP, 1997; U.S. EPA, 2002b). In Turkey, the use of lindane was banned in 1979 (Acara et al., 2006), but it is currently used in Europe (Lee, Burnett, Harner, & Jones, 2000; Sofuoglu et al., 2004).

2.3.2.2 Chlorpyrifos

Chlorpyrifos is an organophosphate pesticide that has been widely used to control a variety of insects. It is effective in controlling cutworms, corn rootworms, cockroaches, grubs, fleas, flies, termites, fire ants, ticks, and lice. Chlorpyrifos is also an active ingredient in some pet flea and tick collars. It has additional uses as an insecticide on grain, cotton, field, fruit, nut, and vegetable crops, as well as on lawns and ornamental plants (ATSDR, 1997; Miller, 1996; U.S. EPA, 2002b). Chlorpyrifos is a currently used pesticide in Turkey (Sofuoglu et al., 2004).

2.3.2.3 Heptachlor

Heptachlor was used extensively as a soil and seed treatment to protect cotton, and some food crops like corn, grains, and sorghum from pests. It was used to control ants, cutworms, maggots, termites, weevils, and wireworms in both cultivated and uncultivated soils. Heptachlor was also used non-agriculturally to control termites and household insects for homes, buildings, lawns, and gardens. The other uses were to kill fire ants, to control disease vectors like mosquitoes, and to combat malaria (ATSDR, 2007; U.S. EPA, 2002b; RWQCP, 1997). In Turkey, the use of heptachlor was banned in 1979 (Acara et al., 2006).

2.3.2.4 Chlordane

Chlordane is an insecticide, produced by chlorinating cyclopentadiene to form hexachlorocyclopentadiene and condensing the latter with cyclopentadiene to form chlordene. The chlordene is further chlorinated at high temperature and pressure to chlordane (ATSDR, 1994).

Chlordane was used on agricultural crops including vegetables, small grains, potatoes, sugarcane, sugar beets, fruits, nuts, citrus, and cotton. It was also used extensively to control termites and on home lawns and garden pests (RWQCP, 1997). In Turkey, the use of chlordane was banned in 1979 (Acara et al., 2006).

2.3.2.5 Endosulfan

Technical-grade endosulfan contains at least 94% endosulfan. The formulation consists of mainly endosulfan-I and -II with a ratio of approximately 7:3, as well as a few impurities or degradation products including endosulfan sulfate, endosulfan ether, and endosulfan alcohol (ATSDR, 2000b).

Endosulfan is an insecticide that is used on a wide variety of food crops (e.g. tea, fruits, vegetables, and grains) and nonfood crops (e.g. cotton, tobacco, ornamental plants, and trees). It is also used as wood preservative (ATSDR, 2000b; RWQCP, 1997; U.S. EPA, 2002b). Endosulfan is a currently used pesticide in Turkey (Sofuoglu et al., 2004).

2.3.2.6 Aldrin and Dieldrin

Aldrin is an insecticide that was used on crops such as corn and cotton. As a termiticide, aldrin was also applied to soil to control root worms, beetles, and termites. Two minor uses of this compound for mothproofing in manufacturing

processes, and dipping roots and tops of nonfood plants have been also reported (RWQCP, 1997).

Dieldrin was manufactured by the epoxidation of aldrin (ATSDR, 2002b). It was used to control insects on crops such as corn, cotton, and citrus. Dieldrin was also used for termite control, soil and seed treatment, wood preservative, controlling disease carrying vectors (e.g. mosquitoes), sheep dip (used prior to shearing), and mothproofing in manufacturing of wool products (RWQCP, 1997).

Other past uses of aldrin and dieldrin included timber preservation, and termite-proofing of plastic and rubber coverings of electrical and telecommunication cables, and of plywood and building boards (ATSDR, 2002b). In Turkey, the uses of dieldrin and aldrin were banned in 1971 and 1979, respectively (Acara et al., 2006).

2.3.2.7 Endrin

Endrin is produced by the reaction of vinyl chloride and hexachlorocyclopentadiene to yield the intermediate product. This product is dehydrochlorinated and condensed with cyclopentadiene to produce isodrin. Isodrin is then epoxidized with peracetic or perbenzoic acid to yield endrin (ATSDR, 1996).

Endrin was used as an insecticide, rodenticide, and avicide. It was used to control cutworms, voles, grasshoppers, borers, and other pest on various crops in food (e.g. grains, sugarcane, citrus, potatoes, wheat, apples) and nonfood (e.g. cotton, tobacco, flowers, bark treatment for ash and hackberry tree) commodities (RWQCP, 1997). Endrin was also used to control nuisance birds, rodents, and pests including termites, mice, and army worms (U.S. EPA, 1980c). In Turkey, the use of endrin was banned in 1979 (Acara et al., 2006)

2.3.2.8 Dichlorodiphenyltrichloroethane (DDT)

Technical DDT is produced by condensing chloral hydrate with chlorobenzene in concentrated sulfuric acid. The active ingredient is *p,p'*-DDT. It contains also trace amounts of *o,o'*-DDT, *o,p'*-DDT, and *p,p'*-DDD. DDD was once manufactured and used as an insecticide, but its use was a much lesser extent than DDT (ATSDR, 2002a).

DDT was introduced in 1946 and has found broad application all over the world (RWQCP, 1997). It was used to control insects on crops, including cotton and tobacco. It was also used to control tsetse flies and against mosquitoes carrying diseases such as malaria, yellow fever, and typhus. DDT was used on animals and humans to control ticks and lice, too (UNEP, 2006). It was reported that DDT/lindane preparations were used to protect the copper cables from termites. The sheeting of cable had been coated with the insecticides lindane for immediate toxic effect and p,p'-DDT for long term effect (Manz et al., 2001; Wenzel et al., 2006). DDT is used as a chemical intermediate in the production of the pesticide dicofol (UNEP, 2006).

In Turkey, the usage of DDT was restricted in 1978, and then, it was banned in 1985 (Acara et al., 2006). However, in some countries, it is still used today under restrictions for vector control to prevent malaria transmission, and for controlling epidemics (UNEP, 2006).

2.3.2.9 Methoxychlor

Methoxychlor is produced commercially by the condensation of anisole with chloral in the presence of an acidic condensing agent. Because of its low toxicity in animals and humans, methoxychlor has been viewed as an attractive replacement for DDT (ATSDR, 2002c).

Methoxychlor is an insecticide effective against a wide range of pests including houseflies, mosquitoes, cockroaches, chiggers, and various arthropods. It is used on agricultural crops, vegetables, fruits, ornamental plants, stored grain, livestock, and domestic pets, and in forestry. This insecticide can be applied to large areas such as beaches, estuaries, lakes, and marshes for controlling fly and mosquito larvae. Other uses include the spray treatment of barns, grain bins, mushroom houses, and other agricultural premises and the spraying or fogging of garbage containers, sewer manholes, and sewage disposal areas. Methoxychlor is also registered for veterinary use to kill parasites on dairy and beef cattle (ATSDR, 2002c; Miller, 1996).

2.3.3 Sources of OCPs

OCPs do not occur naturally in the environment. There is some debate regarding the primary global emission source of many OCP compounds, since some countries continue to use large quantities. Ongoing uses are referred to as new or current sources, because they represent fresh emissions into the environment. Another potential source is old pesticide used previously and continues to from previously contaminated surfaces. Agricultural soils are suspected to be an important emission source of old pesticides because of the historically large quantities that were applied (Harner, Wideman, Jantunen, Bidleman, & Parkhurst, 1999).

OCPs restricted, banned or used can enter the environment through agricultural uses; illegal uses; volatilization from contaminated soil; dry/wet deposition and runoff; particulate matter re-entrainment by the wind at contaminated areas; emissions from certain industrial sources; emissions from waste incinerators; disposal of contaminated wastes into landfills; and releases from manufacturing plants that produce these chemicals (ATSDR, 2005; Bidleman, 1999; Hafner & Hites, 2003; RWQCP, 1997).

Due to the previous uses of HCHs, lindane, and DDT as an additive in plasticizer production (e.g. in PVC sheathing of electric cables), these pesticides can also be

emitted by chemical production and formulating plants, hazardous waste dumps, cable manufacturing, cable scrapping, and incineration in smelting plants (Manz et al., 2001; Wenzel et al., 2006).

2.4 Reported Levels of SOCs in Air, Dry deposition and Soil Samples

Dry deposition fluxes, ambient air and soil concentrations of the studied groups of compounds (i.e. PAHs, PCBs, and OCPs) have been previously measured at the rural, coastal, suburban, urban, and industrial sites throughout the world. Although there are numerous studies, they differ from each other in terms of effects of their local sources, sampling method, sampling duration, sample preparation, and analysis (Odabası, 1998). There is considerable interest in whether studied compounds exhibit seasonality in air concentrations, because this provides clues as to the link with sources (e.g. some combustion sources are greater in winter) and certain atmospheric loss processes (e.g. photolysis) which may also vary seasonally. The total number and the types of compounds studied also vary from one article to another. This makes it difficult to compare results from different studies in the world.

2.4.1 Levels Measured in the Air

A summary of atmospheric total (gas+particle) concentrations of PAHs, PCBs, and OCPs previously reported for the different sites through the world are presented in Table 2.4, 2.5, and 2.6, respectively. To measure the atmospheric concentrations of SOCs, high volume (Hi-Vol) air sampler has been used during this study and other recent studies given in these tables. In this technique, ambient air is drawn through a filter to retain the particle-phase and then through a sorbing medium such as polyurethane foam (PUF), XAD resin or Tenax to trap the gas-phase (Temime-Roussel, Monad, Massiani, & Wortham, 2004; Tsapakis & Stephanou, 2003).

2.4.1.1 Atmospheric PAH Levels

The results in Table 2.4 showed that atmospheric PAH levels measured at the industrial and urban sites were relatively higher than those measured at the suburban, rural, and coastal sites in the world. Since PAHs are byproducts of incomplete combustion, their current sources including vehicle emissions, residential heating, and industrial activities significantly contribute to the ambient PAH levels mainly at the industrial and urban sites. According to the previously reported studies (Bae, Yi, & Kim, 2002; Gevao, Hamilton-Taylor, & Jones, 1998; Kiss et al., 2001; Park, Kim, & Kang, 2002b; Park et al., 2001a; Odabasi et al., 2006a; Schnelle-Kreis, Sklorz, Peters, Cyrys, & Zimmermann, 2005; Vardar, Esen, & Tasdemir, 2007), higher atmospheric PAH concentrations were generally observed during winter. This increase in atmospheric concentrations of PAHs during winter was attributed to the increasing emissions from residential heating.

There have been several studies on the atmospheric PAH levels measured in Turkey (Table 2.4). At a study conducted by Demircioglu (2008), atmospheric Σ_{14}-PAH (fluorene through benzo[*g,h,i*]perylene) concentrations were measured at the different sites in Izmir, and the highest level were found for urban Yesildere (a residential/commercial site with heavy traffic), and was followed by urban Guzelyali (a residential/coastal site with heavy traffic) and suburban Izmir. In urban Yesildere, Odabasi et al. (2006a) found average total Σ_{13}-PAH (fluorene through benzo[*g,h,i*]perylene) concentrations of 143 ± 163 ng m^{-3} that agreed well with the other measurement in Izmir (Demircioglu, 2008). In an urban/industrial site of Bursa, Tasdemir & Esen (2007a) measured relatively higher total Σ_{16}-PAH (naphthalene through benzo[*g,h,i*]perylene) levels in the air with an average of 456 ng m^{-3}. This was ascribed to the heavy traffic and industrial activities in this site. Vardar et al. (2007) also performed a study on atmospheric PAH levels for a suburban site of Bursa and they reported average total Σ_{15}-PAH (acenaphthene through benzo[*g,h,i*]perylene) concentrations that were higher in winter (231 ng m^{-3}) than in summer (20 ng m^{-3}). PAH concentrations measured at suburban Bursa were relatively lower than those measured at urban Bursa (Tasdemir & Esen, 2007a).

Table 2.4 Average total concentrations (gas+particle, ng m^{-3}) of PAHs* in the air.

Location	Site	Sampling Period	ACT*	FLN*	PHE*	ANT*	CRB*	FL*	PY*	BaA*	CHR*	BbF*	BkF*	BaP*	IcdP*	DahA*	BghiP*	ΣPAHs
Izmir, Turkey[a]	Suburban	A	-	4.7	13.6	0.60	0.60	5.2	3.8	0.60	1.9	0.95	0.82	0.72	0.91	0.42	0.93	35.8
	Urban (Yesildere)	S-W	-	12.6	41.8	5.7	1.1	30.1	23.3	3.6	7.8	3.4	3.6	3.1	3.4	1.3	3.4	144
	Urban (Guzelyali)	S-W	-	11.5	38.6	2.2	0.60	14.3	11.2	1.4	3.9	2.2	1.7	1.3	1.3	0.44	1.4	92.1
Bursa, Turkey[b]	Urban	S-W	2.5	22.6	76.2	7.0	-	47.8	31.1	4.7	10.6	5.8	4.7	3.3	3.9	1.3	5.6	227
Heraklion, Greece[c]	Urban	A	-	5.2	20	3.3	-	4.9	6.6	1.1	-	1.5	1.8	1.2	2.5	0.12	3.4	51.6
Taichung, Taiwan[d]	Industrial	S-W	202	139	94.2	164	-	84.4	81.6	14.2	50.7	12.8	14.5	9.0	3.9	4.3	6.7	881
	Urban	S-W	143	95.7	63.2	109	-	58.9	54.5	20.3	34.3	9.1	12.6	6.4	4.2	2.9	5.5	620
Rome[e]	Urban	A	59.2	18.9	78.2	6.1	-	21.5	16.8	1.8	4.4	-	-	2.7	1.6	-	2.9	214
Fuji, Japan[f]	Industrial	S	6.4	9.8	26.3	0.4	-	4.6	3	0.1	0.4	0.5	0.2	0.2	0.2	-	0.3	52.4
		W	2.9	5.8	12.6	0.9	-	3.2	2.9	1	1.6	1.5	0.7	1.1	1.1	0.1	1.3	36.7
Shimizu, Japan[f]	Industrial	S	3.5	5.6	17.3	0.3	-	1.9	1.5		0.1	0.1	0.1	0.1	0.1	-	0.1	30.7
		W	2.5	4.7	10.1	0.3	-	1.6	1.2	0.4	0.9	1.1	0.4	0.5	0.6	0.1	0.6	25.1
Athens, Greece[g]	Urban	S	-	1.4	6.5	1.0	-	3.0	2.1	0.27	-	-	-	0.17	0.45	0.08	0.44	15.4
	Coastal		-	1.3	7.5	0.95	-	1.3	1.4	0.20	-	-	-	0.02	0.05	0.01	0.05	12.8
	Background		-	0.16	1.2	0.27	-	0.66	0.46	0.03	-	-	-	0.10	0.18	0.10	0.20	3.4
Baltimore, USA[h]	Urban/Industrial	S	-	4.1	12.6	0.33	-	3.6	2.3	0.09	0.09	-	-	0.12	0.29	0.01	0.32	23.8
Galveston Bay, USA[i]	Coastal	A	0.53	1.64	12.4	0.56	-	5.97	3.29	0.05	0.29	0.11	0.03	0.05	0.05	0.01	0.06	25.0
Chicago, USA[j]	Urban	S-F	76.9	74.8	200	14.1	6.1	44.1	24.6	2.1	3.6	2.3	1.9	1.6	1.2	-	1.1	454

S: Summer, W: Winter, F: Fall, A: Annual.

[a] Demircioglu, 2008, [b] Tasdemir & Esen, 2007a, [c] Tsapakis & Stephanou, 2005, [d] Fang et al., 2004, [e] Possanzini et al., 2004, [f] Ohura, Amagai, Fusaya, & Matsushita, 2004,
[g] Mandalakis, Tsapakis, Tsoga, & Stephanou, 2002, [h] Dachs et al., 2002, [i] Park et al., 2001a, [j] Odabasi, Vardar, Sofuoglu, Tasdemir, & Holsen 1999b.

Recent studies (Dachs et al., 2002; Demircioglu, 2008; Gevao et al., 1998; Mandalakis et al., 2002; Odabasi, Sofuoglu, Vardar, Tasdemir, & Holsen, 1999a; Ohura et al., 2004; Tasdemir & Esen, 2007a; Terzi & Samara, 2004; Vardar et al., 2007) noted that gas-phase percentage of total PAH mass in the air was higher in summer than in winter. Vardar et al. (2007) found gas-phase concentrations accounting for 66% and 89% of total PAH mass in air for winter and summer seasons, respectively. Sofuoglu, Odabasi, Tasdemir, Khalili, & Holsen (2001) performed a study on the temperature dependent gas-phase PAH and OCP levels in Chicago air, and they concluded that for three- to four- ring PAHs (acenaphtene through chrysene), temperature accounted for 23-49% of the variability in their atmospheric concentrations.

As shown in Table 2.4, total PAH mass in the air were dominated by low molecular weight ones and this was attributed to their high vapor pressures controlling gas-particle partitioning. Generally, phenanthrene was the most abundant compound among PAHs in the air. Odabasi et al. (1999b) reported that the gas-phase percentage for the individual PAHs generally decreased with increased molecular weight, and ranged between 1.1-99.4%. Similar results were also reported by the recent studies (Dachs et al., 2002; Gevao et al., 1998; Ohura et al., 2004; Tasdemir & Esen, 2007a; Terzi & Samara, 2004).

2.4.1.2 Atmospheric PCB Levels

The results given in Table 2.5 showed that atmospheric PCB levels measured at the industrial and urban sites were higher than those measured at the rural and coastal sites through the world. Generally higher PCB concentrations were measured during summer months in recent studies (Cetin, Yatkin, Bayram, & Odabasi, 2007; Yeo, Choi, Chun, & Sunwoo, 2003; Cousins & Jones, 1998; Currado & Harrad, 2000; Hillery, Basu, Sweet, & Hites, 1997; Montone, Taniguchi, & Weber, 2003; Lee & Jones, 1999; Odabasi, Cetin, Demircioglu, & Sofuoglu, 2008; Simcik, Franz, Zhang, & Eisenreich, 1998; Stern et al., 1997). Since PCB production and uses have

been banned for decades in many countries, the current atmospheric levels are mainly released by the volatilization from previously polluted surfaces (e.g. soil, water, vegetation) or equipments containing PCBs.

The results reported by Gioia et al. (2005) and Odabasi et al. (2008) showed that gas-phase percentage of individual OCPs was generally higher in summer than in winter. Mandalakis & Stephanou (2006) performed a study on the atmospheric PCB concentrations being influenced by temperature, and they found that air temperature accounted for 5% (for octa-CBs) and 64% (for tetra-CBs) of the variability in gas-phase concentrations of di- through octa-CBs.

There have been several studies on the atmospheric PCB levels measured at the different sites in Turkey (Table 2.5). PCB concentrations measured by Odabasi et al. (2008) at a coastal/urban site of Izmir was found relatively higher than the ones reported for the other urban sites in Turkey. In Bursa, atmospheric PCB levels were measured at an urban site (Cindoruk & Tasdemir, 2007a) and an urban/industrial site (Cindoruk, Esen, & Tasdemir, 2007). The results are consistent with PCB levels reported for urban areas in Table 2.5. In urban and industrial sites of Aliaga in Izmir, Cetin et al. (2007) performed a study on atmospheric PCB levels. The results found for urban Aliaga were similar to the ones observed for urban air. However, higher PCB concentrations at sites of close proximity with the scrap iron smelters and steel plants in Aliaga were found, and this was attributed to the emissions from stacks and fugitive sources at the steel plants as well as volatilization and re-suspension from the previously contaminated soils. In the same study conducted by Cetin et al. (2007), sources of particle-phase PCBs were apportioned using factor analysis (FA) and chemical mass balance (CMB) models. FA suggested that the steel industry, fuel oil combustion or the nearby vinyl chloride process in the petrochemical plant, and soil were significant PCB sources. CMB results showed that at the industrial site, the contribution of steel industry and soil to particle-phase PCBs were 71 and 22%, respectively, while at the urban site, the contributions were 33 and 49%, respectively (Cetin et al., 2007).

Table 2.5 Average total ΣPCB concentrations (gas+particle, pg m^{-3}) reported for the different sites throughout the world.

Location	Site	ΣPCB Concentrations[*]	Sampling Period	No of PCBs	Reference
Izmir, Turkey	Coastal/Urban	1642±817[**]	February-March, 2005	29	Odabasi, Cetin, Demircioglu, & Sofuoglu, 2008
		2078±1026[**]	July, 2005		
Aliaga, Izmir, Turkey	Industrial	3136±824	June, 2005	36	Cetin, Yatkin, Bayram, & Odabasi, 2007
		1371±642	March-April, 2005		
	Urban	314±129	June, 2005		
		847±610	March-April, 2005		
Bursa, Turkey	Urban	492±189	August, 2004-May, 2005	37	Cindoruk & Tasdemir, 2007a
Bursa, Turkey	Urban/Industrial	287±175	July, 2004-May, 2005	28	Cindoruk, Esen, & Tasdemir, 2007
Melpitz, Germany	Rural	110±80	April, 2001	54	Mandalakis & Stephanou, 2006
Chicago, IL, USA	Urban	1900±1700	June-October, 1995	50	Tasdemir, Vardar, Odabasi, & Holsen, 2004a
Birmingham, UK	Urban	252	April, 1999-July, 2000	41	Harrad & Mao, 2004
Ansung, Korea	Rural	19.9 (6.13-71.9)	July, 1999-January, 2000	22	Yeo, Choi, Chun, & Sunwoo, 2003
King George Island, Antarctica	Pristine	37.4±27.0	December, 1995-February, 1996	10	Montone, Taniguchi, & Weber, 2003
Athens, Greece	Urban	349	July, 2000	38	Mandalakis, Tsapakis, Tsoga, & Stephanou, 2002
	Coastal	184			
	Background	80.5			
Baltimore, USA	Urban	1180±420[**]	July, 1997	83	Brunciak et al., 2001a
Chesapeake Bay, USA	Coastal	550±220[**]			
Liberty Science Center, NJ, USA	Urban/Industrial	1000±820	July, 1998; October, 1998-May,1999	83	Brunciak, Dachs, Gigliotti, Nelson, & Eisenreich, 2001b
New Brunciak, NJ, USA	Suburban	546±400	October, 1997-May, 1999		
Sandy Hook, NJ, USA	Coastal	450±300	February, 1998-Februray, 199		
Scania, Sweden	Rural/urban areas (11 different sites)	7-983	July, 1992-July, 1993	51	Backe, Larsson, & Okla, 2000
Birmingham, UK	Urban	290 (76-1000)	August, 1997-August, 1998	57	Currado & Harrad, 2000
Lanchester, UK	Semirural	164	March-October, December, 1994	30	Lee & Jones, 1999

[*] As average±SD, average, and/or range, [**] Gas-phase.

According to the results of several other studies (Brunciak et al., 2001a, 2001b; Cetin et al., 2007; Cindoruk & Tasdemir, 2007a; Cindoruk et al., 2007; Mandalakis & Stephanou, 2006; Montone et al., 2003; Odabasi et al., 2008; Tasdemir et al., 2004a; Yeo et al., 2003), total PCB mass in air were dominated by lower chlorinated congeners. Low molecular weight congeners had higher percentages of gas-phase, while higher molecular weight ones had greater percentages of particle-phase. The contribution of gas-phase to the total PCB mass in air was reported between the range of 85 and up to 98% (Cetin et al., 2007; Cindoruk & Tasdemir, 2007a; Cindoruk et al., 2007; Mandalakis & Stephanou, 2006; Odabasi et al., 2008; Tasdemir et al., 2004a). A tendency for atmospheric PCB concentrations to decrease with increasing number of chlorine atoms was observed by Cetin et al. (2007), Cindoruk & Tasdemir (2007a), Cindoruk et al. (2007), Odabasi et al. (2008), and Yeo et al. (2003). They concluded that the concentration patterns in the air showed the highest level for tri-CBs, and followed by tetra-CBs, penta-CBs, hepta-CBs, hexa-CBs, and deca-CBs.

2.4.1.3 Atmospheric OCP Levels

Since many of the pesticides have been banned or restricted, the current atmospheric levels of OCPs are mainly influenced by the temperature dependent volatilization from soil. Increased summertime OCP concentrations in the air was reported by Cortes, Hoff, Brice, & Hites (1999), Gioia et al. (2005), Halsall et al. (1998), Harrad & Mao (2004), Lee et al. (2000), Odabasi et al. (2008), and Sun, Blanchard, Brice, & Hites (2006). This was attributed to the enhanced local/regional applications of in-use pesticides and enhanced volatilization rates of the compounds during the warmer months. Sofuoglu et al. (2004) reported that the temperature accounted for 0 (heptachlor epoxihe, endrin aldehyde, *p,p'*-DDT) to 21% (endosulfan sulfate) of the variability in atmospheric concentrations of gas-phase OCPs measured at a suburban site of Izmir.

Table 2.6 Average atmospheric concentrations (pg m^{-3}) of individual OCPs reported recently.

OCPs	Izmir, Turkey[a] Febr.-March, 2005 GP	PP	July, 2005 GP	PP	Germany[b] July-Sept., 1995 T	T	Chiapas, Mexico[c] Aug., 2000-June, 2001 T	New Jersey, USA[d] Jan., 2000-May, 2001 GP	GP	GP	Izmir, Turkey[e] May, 2003 T	Chicago, USA[f] June-Oct., 1995 GP	Galveston Bay, USA[g] Febr., 1995-Aug., 1996 GP	PP	Alabama, Canada[h] Jan.-Oct., 1996 May, 1997 T
α-HCH	43	1.4	62	0.8	111	19.9	27	96	84	55	111	110	79.4	-	92
β-HCH	-	-	-	-	130	28.3	-	-	-	-	320	-	4.1	0.3	-
γ-HCH	88	3	28	2	3900	121	76	158	65	48	117	150	135	0.6	50
δ-HCH	-	-	-	-	28.7	18.8	-	-	-	-	38	-	47.1	0.1	-
CHLPYR	1154	10	864	379	-	-	-	-	-	-	391	-	-	-	-
HEP EPOX	91	5	9	1	-	-	18	45	19	14	34	-	13.1	-	16
α-CHL	6	0.3	2	0.2	-	-	42	518[*]	474[*]	127[*]	-	120	29.6	0.2	25
γ-CHL	9	0.2	0.8	0.2	-	-	56	-	-	-	158	130	38.2	0.4	47
c-NONA	0.2	0.1	0.4	0.1	-	-	2	-	-	-	-	-	4.2	0.2	3.1
t-NONA	1.4	0.3	0.2	0.1	-	-	35	-	-	-	50	80	25.6	0.4	23
ESLF I	80	4	4474	13	-	-	367	102	168	59	171[***]	-	-	-	-
ESLF II	11	2	879	77	-	-	-	1.8	10	10	20	-	-	-	-
ESLF SUL	3	1.1	28	22	-	-	-	-	-	-	369	-	-	-	-
p,p′-DDT	8	2	5	2	21.5	0.8	395	133[**]	237[**]	31[**]	29	70	7.6	1.4	-
p,p′-DDD	-	-	-	-	3.5	0.3	28	-	-	-	5	100	2.1	0.8	-
DIELD	-	-	-	-	-	-	15	75	36	38	35	-	19	0.5	38
END	-	-	-	-	-	-	-	-	-	-	16	-	1.4	4.6	-
END AL	-	-	-	-	-	-	-	-	-	-	48	-	-	-	-
END KET	-	-	-	-	-	-	-	-	-	-	41	-	-	-	-
MEOCL	-	-	-	-	-	-	-	-	-	-	220	-	-	-	-

GP: Gag-phase, PP: Particle-phase, T: Total (gas+particle), [*] ΣChlordanes, [**] ΣDDTs (including 6 isomers of DDT), [***] α-CHL+ESLF-I.

[a] Odabasi et al., 2008 (Coastal/urban site), [b] Wenzel et al., 2006 (Industrial with metalworking/smelting plants and remote sites, respectively), [c] Alegria, Bidleman, & Figueroa, 2006 (Residential/agricultural site), [d] Gioia et al., 2005 (Urban/industrial, suburban, and rural/forested sites, respectively), [e] Sofuoglu et al., 2004 (Suburban site), [f] Sofuoglu et al., 2001 (Urban site), [g] Park, Wade, & Sweet, 2001b (Coastal site), [h] Jantunen, Bidleman, Harner, & Parkhurst, 2000 (Farmland).

Unlike PAHs and PCBs, OCP sources are expected to be associated with rural agricultural regions rather than urban or industrial areas. Table 2.6 shows the average atmospheric OCP concentrations measured at the different sites through the world. Considerably high DDT level was observed at a residential/agricultural site in Mexico, because DDT was widely used until recently in Mexico and was phased out in 2002 (Alegria et al., 2006). High endosulfan and lindane (γ-HCH) levels found in Mexico air were attributed to their current uses. Wenzel et al. (2006) found high lindane and p,p'-DDT concentrations at an industrial site in Germany that was ascribed to their direct sources from cable scrapping operations at the metalworking/smelting plants located at this site. Gioia et al. (2005) also measured high ΣDDT levels at urban/industrial and suburban sites in USA, and the results were correlated with their past uses at the suburban site, and the presence of a DDT manufacturing plant that was used in the past, close to the urban/industrial site.

In Turkey, some studies have been performed on the OCP levels in Izmir air (Table 2.6). A study on atmospheric OCP concentrations at a coastal/urban site of Izmir was investigated by Odabasi et al. (2008). In this study, chlorpyrifos and endosulfan (currently used pesticides in Turkey) had relatively higher concentrations among the studied OCPs, and was followed by α-HCH, γ-HCH, and endosulfan sulfate (a degradation product of endolsulfan). At another study conducted by Sofuoglu et al. (2004) in a suburban site of Izmir, relatively high ambient air concentrations were obtained for pesticides excepting chlorpyrifos and heptachlor epoxide. Similarly, chlorpyrifos had the highest atmospheric concentrations among the studied OCPs, followed by endosulfan sulfate, and β-HCH.

It was reported by Murayama et al. (2003) and Lee et al. (2000) that α- to γ-HCH ratio was close to 1 in areas where γ-HCH was used, and between 3-7 in areas where α-HCH was used or in remote areas. Average α- to γ-HCH ratio was found as 0.38 in Mexico air, indicating the continued use of lindane (Alegria et al., 2006). In the studies performed in Izmir air, average α- to γ-HCH ratio was 1.1±0.3 (Odabasi et al, 2008) and 1.2±0.5 (Sofuoglu et al., 2004). The use of technical HCH and lindane has

been banned for decades in Turkey (Acara et al., 2006), but lindane is currently used in Europe (Lee et al., 2000; Wania et al., 1998). Thus, the relatively low α- to γ-HCH ratios in Izmir air were likely to be associated with the effect of regional sources.

2.4.2 Levels Measured in Particle Dry Deposition Fluxes and Velocities

Atmospheric deposition is a major source for SOCs in soils. Direct and indirect methods are used to measure dry deposition flux. In the direct method, an artificial surface (e.g. Teflon plates, various types of filters, Petri dishes, buckets, oil-coated glass plates, greased strips and water surface) is employed to estimate experimental dry deposition flux, while in the indirect method, measured ambient concentrations are multiplied by an assumed or modeled deposition velocity to determine the dry deposition flux (Odabasi et al., 1999a). Deposition velocity is affected by the meteorological parameters, physical properties of the particle (i.e. size, shape and density), and the type and roughness characteristics of the receptor surface (Golomb et al., 2001). Thus, the selection of an appropriate deposition velocity is crucial since it may introduce large uncertainties in the calculation of dry deposition fluxes.

Recently reported average particulate fluxes of PAHs and PCBs are presented in Table 2.7 and 2.8, respectively. The results showed that lower dry deposition fluxes were generally measured at the rural and coastal sites. This was attributed to both the removal of large particles from the air close to their source and the low atmospheric concentrations of PAH and PCB compounds at the rural sites in comparison with the urban and industrial sites (Franz, Eisenreich, & Holsen, 1998).

There have been some studies on the particle-phase dry deposition fluxes of PAHs measured in Turkey (Table 2.7). Demircioglu (2008) conducted a study on the particulate PAH fluxes in urban and suburban sites of Izmir, and the results were higher than the ones reported for urban Bursa (Tasdemir & Esen, 2007b) and for rural Lake Michigan (Franz et al., 1998). In urban Bursa, PAH fluxes measured by Tasdemir & Esen (2007b) were lower than the ones reported for the other urban sites

in Table 2.7. Tasdemir & Esen (2007b) reported phenanthrene, florene, and pyrene as the dominant compounds in the particulate PAH fluxes. The dominance of low molecular weight compounds in ΣPAH fluxes was also reported by the recent studies (Demircioglu, 2008; Franz et al., 1998; Odabasi et al., 1999a), and this was ascribed to their association with large airborne particles.

Table 2.7 Average particle-phase dry deposition fluxes (F_d, ng m^{-2} day^{-1}) of individual PAHs reported previously.

PAHs	Izmir, Turkey[a]		Bursa, Turkey[b]	Taichung, Taiwan[c]			Chicago, IL, USA[d]	Chicago, IL, USA[e]	Lake Michigan, USA[e]
	Suburban	Urban	Urban	Industrial	Urban	Rural	Urban	Urban	Rural
ACT	-	-	-	860	900	560	3300	120	12
FLN	1338	622	140	3470	2480	2300	4200	110	5
PHE	3144	1492	710	1160	640	780	47100	1560	60
ANT	172	63	50	2370	1450	1660	1600	190	8
CRB	170	90	-	-	-	-	1900	-	-
FL	615	732	540	1620	1840	1090	25500	2710	106
PY	815	428	360	690	210	460	22900	2240	77
BaA	132	78	110	140	330	80	7000	1090	25
CHR	237	350	290	950	800	600	9100	1880	94
BbF	441	162	110	1720	1120	1140	9600	2910[*]	114[*]
BkF	170	94	100	1340	1090	880	8600	-	-
BaP	154	66	80	350	550	230	7700	1100	49
IcdP	313	90	80	2040	1850	1340	6300	770	31
DahA	393	34	20	3190	1180	2100	-	330	17
BghiP	242	113	130	2820	1900	1850	5400	990	48
ΣPAHs	8160	4286	2720	22720	16340	15070	160200	16000	646

[*] Benzo[*b*]fluoranthene+ Benzo[*k*]fluoranthene.

[a] Demircioglu, 2008 (May, 2003-May, 2004 and March, July, 2004, respectively; with dry deposition plates).

[b] Tasdemir & Esen, 2007b (August, 2004-May, 2005; with a modified water surface sampler).

[c] Fang, Chang, Lu, & Bai, 2004 (August-December, 2002; using a model).

[d] Odabasi et al., 1999a (June-October, 1995; with dry deposition plates).

[e] Franz et al., 1998 (November, 1993-October, 1995; with dry deposition plates).

At a study conducted by Franz et al. (1998), the particle-phase dry deposition fluxes of PAHs and PCBs were measured at urban Chicago and rural Lake Michigan. Similar conclusions were observed for PCBs as for PAHs. The increased fluxes of PAHs and PCBs during winter were measured in urban Chicago. The result was attributed to the higher wind speeds that suspended more soil particles and road dust in winter than in summer. Dry deposition fluxes of PAHs and PCBs for urban

Chicago were higher than for rural Lake Michigan. The rapid decrease in the deposition flux with distance from urban site supported the hypothesis that large particles are efficiently removed from the urban plume in the coastal zone. Small particles are also being deposited, but coarse particles with large settling velocities (>0.5 cm s^{-1}) contribute most of the deposition flux. It was suggested by Franz et al. (1998) that the patterns of PAH and PCB compounds measured in particulate fluxes were similar to the patterns measured in atmospheric particulate concentrations. This verified that dry deposition to surrogate surface reflects atmospheric particulate matter.

Table 2.8 Average particle-phase dry deposition fluxes (F_d, ng m^{-2} day^{-1}) of ΣPCBs reported previously (avg±SD or avg).

Location	Site	F_d for ΣPCB	Sampling Period	No of PCBs	Method
Bursa, Turkey[a]	Suburban	46.3±40.6	July, 2004-May, 2005	29	WSS
Chicago, IL, USA[b]	Urban	240±160	June-Oct., 1995	50	WSS
Chicago, IL, USA[c]	Urban	190±80	June-Oct., 1995	50	DDP
C. Christi Bay, TX, USA[d]	Mixed	2.7	Aug., 1998-Sept., 1999	22	Calculation[*]
Galveston Bay, TX, USA[e]	Coastal	13.3	Febr., 1995-Aug., 1996	22	Calculation[*]
Chicago, IL, USA[f]	Urban	210	Nov., 1993-Oct., 1995	44	DDP
Lake Michigan, USA[f]	Rural	79			

WSS: Water surface sampler, DDP: Greased dry deposition plate.

[*] V_d is assumed as 0.34 cm s^{-1}.

[a] Cindoruk & Tasdemir, 2007b.

[b] Tasdemir & Holsen, 2005.

[c] Tasdemir et al., 2004b.

[d] Park et al., 2002a.

[e] Park et al., 2001b.

[f] Franz et al., 1998.

Although dry deposition fluxes of particle-phase PAH and PCB compounds have been measured experimentally at different sites through the world, no previous measurement for OCPs obtained with experimental techniques is available. In some studies, deposition fluxes of OCP were estimated using indirect method. Odabasi et al. (2008) estimated particle dry deposition fluxes of OCPs in a coastal/residential site of Izmir, using measured atmospheric particle-phase concentrations and assumed deposition velocities of PAHs. Among the studied OCPs, chlorpyrifos had the highest deposition flux (388 ng m^{-2} day^{-1}), and was followed by endosulfan-II,

endosulfan-I, heptachlor epoxide, endosulfan sulfate, γ-HCH, and p,p'-DDT (79, 29, 21, 16, 15, and 10 ng m^{-2} day^{-1}, respectively). In coastal Galveston Bay, Park et al. (2001b) calculated the dry deposition fluxes of related OCPs by taking the dry deposition velocity as 0.34 cm s^{-1} based on the literature survey. Deposition fluxes for Σcyclodienes, ΣDDTs, Σchlordanes, and ΣHCHs were found to be 1.5, 1.2, 0.6, and 0.3 ng m^{-2} day^{-1}, respectively. Gioia et al. (2005) also assumed a deposition velocity of 0.5 cm s^{-1} to calculate dry deposition fluxes of OCPs at the different sites in New Jersey. The calculated fluxes for Σchlordanes, ΣDDTs, endosulfan-I, -II, and endosulfan sulfate were 2.8, 1.5, 0.9, 1.8, and 0.7 ng m^{-2} day^{-1} for urban/industrial site; 1.8, 1.2, 0.2, 0.9, and 0.4 ng m^{-2} day^{-1} for suburban site; and 0.5, 0.3, 0.4, 0.9, and 0.6 ng m^{-2} day^{-1} for rural/forested site, respectively.

Table 2.9 Reported overall average particle dry deposition velocities (V_d, avg±SD or avg) for SOCs.

Location	Parameter	V_d (cm s^{-1})	Sampling Period	Reference
Izmir, Turkey	PAHs	1.5±2.4	May, 2003-May, 2004	Demircioglu, 2008
		1.0±2.3	March, July, 2004	
Bursa, Turkey	PAHs	0.45±0.35[*]	July, 2004-May, 2005	Esen, Cindoruk, Tasdemir, 2008
Bursa, Turkey	PAHs	0.39±0.33	Aug., 2004-May, 2005	Tasdemir & Esen, 2007b
Chicago, IL, USA	PAHs	4.5±3.1	Winter, 1996-1997	Vardar, Odabasi, Holsen, 2002
Chicago, IL, USA	PAHs	6.7±2.8	June-Oct., 1995	Odabasi et al., 1999a
Chicago, IL, USA	PAHs	0.64	July, 1994	Franz et al., 1998
		2.2	January, 1995	
Bursa, Turkey	PCBs	0.74±0.23[*]	July, 2004-May, 2005	Esen et al., 2008
Bursa, Turkey	PCBs	1.26±1.86	July, 2004-May, 2005	Cindoruk & Tasdemir, 2007b
Chicago, IL, USA	PCBs	4.2±2.7	June-Oct., 1995	Tasdemir & Holsen, 2005
Chicago, IL, USA	PCBs	5.2±2.9	June-Oct., 1995	Tasdemir et al., 2004b
Chicago, IL, USA	PCBs	4.4	July, 1994	Franz et al., 1998
	PCBs	7.2	January, 1995	

[*] Calculated from bulk deposition fluxes and particle-phase concentrations.

Table 2.9 shows the reported overall average dry deposition velocities for particulate SOCs. They varied widely and ranged between 0.39-6.7 cm s^{-1} for ΣPAHs and between 0.74-7.2 cm s^{-1} for ΣPCBs. These differences may be due to different measurement techniques, artifacts related to the collection surfaces, and affinity of SOCs to atmospheric particles and ground dust (Cindoruk & Tasdemir, 2007b).

The variation in the dry deposition velocities is a function of particle size distributions and meteorological conditions including wind speed, air temperature, and atmospheric stability. The seasonal difference in particle-phase PAH and PCB deposition velocities were observed by Franz et al. (1998), and the higher wintertime deposition velocities were related to the increased wind speed during this season. Demircioglu (2008) found the difference in deposition velocities of PAHs measured at suburban and urban sites of Izmir, and this was attributed to different size distributions of urban and suburban particles.

2.4.3 Levels Measured in Soils

Once deposited, SOCs tend to accumulate in soils for a long period of time depending on their physical-chemical properties and microbiological degradability. As the soil is a main reservoir for SOCs in the terrestrial environment (Cousins & Jones, 1998; Hippelein & McLachlan, 1998; Motelay-Massei et al., 2004), it is important to monitor any long-term changes in its burden, and to determine whether the soil is a sink for SOCs or a potential source through volatilization or wind driven transport of polluted soil/dust particles back to the atmosphere (Cousins, Kreibich, Hudson, Lead, & Jones, 1997).

Because anthropogenic activities are main sources of PAHs and PCBs, generally the industrial site had the highest level in soils and was followed by the urban, suburban, rural, and remote sites. However, the parameters affecting the OCP level in soils are more specific. Besides the deposition from the air, the type of land-use and the type of pesticide used for agricultural purposes mainly influence the OCP concentrations and patterns in soils. However, it must be kept in mind that the distinctions between the various land-use types may not be sharp. For example, agricultural or forest soils may be located in an urban area.

2.4.3.1 PAH Levels in Soils

The reported PAH concentrations in soils are presented in Table 2.10. Motelay-Massei et al. (2004) performed a study on PAH levels in soils at seven different sites in France, and they found the highest PAH concentrations for the industrial sites followed by suburban, urban and remote sites. Similarly, soil PAH concentrations were measured by Nadal, Schuhmacher, & Domingo (2004), and the highest level was found for the industrial 1 site (chemical industry) followed by residential, industrial 2 (petrochemical complex) and unpolluted sites in Spain. Zhang, Luo, Wong, Zhao, & Zhang (2006) also found relatively higher PAH concentrations in soils for the urban site than those for the rural site in China.

Table 2.10 Average soil concentrations ($\mu g\ kg^{-1}$, dry wt) of individual PAHs reported previously.

PAHs	Hong Kong, China[a]		The Siene River basin, France[b]							Tarragana, Spain[c]			
	Dec., 2000		Nov., 2000							Jan., 2002			
	Urban	Rural	Industrial 1, 2		Urban	Suburbs 1, 2		Remote 1, 2		Industrial 1, 2		Residential	Unpolluted
ACT	0.53	nd	20.1	35.9	nd	28.5	12.5	2.5	nd	1.3	<2.0	4.8	<2.0
FLN	4.6	2.4	nd	9.9	4.8	43.5	23.4	4.7	nd	23	2.1	13	1.1
PHE	16.7	2.1	239	254	132	216	173	38.0	21.9	131	16	114	7.9
ANT	3.6	1.1	31	9.8	16.8	9.4	26.5	3.9	1	51	3.1	17	<2.0
CRB	-	-	-	-	-	-	-	-	-	-	-	-	-
FL	28.0	8.8	1496	834	292	437	510	144	282	180	21	97	5.6
PY	27.1	3.3	1178	581	219	527	334	160	151	159	20	96	2.5
BaA	9.0	1.5	222	244	127	70.4	217	30.9	43.5	137	12	68	1.9
CHR	16.2	0.35	253	319	196	68.1	343	31.7	61.6	120	14	68	3.7
BbF	26.7[*]	1.5[*]	261	313	161	76.5	321	24.7	76.6	9	2.9	2.4	2.3
BkF	-	-	115	139	72.7	25.3	143	8.9	1.3	9	13	47	1.2
BaP	9.9	3.4	246	249	126	38.5	284	14.4	0.4	100	18	56	22
IcdP	8.3	0.04	1409	145	116	36.9	223	9.8	296	16	9	60	5.3
DahA	-	-	14	21.2	16.4	1.86	28.7	0.4	5.2	6	1.8	21	<2.0
BghiP	9.8	2.2	158	239	166	92.3	351	21.1	2.5	41	17	40	50
ΣPAHs	160	26.6	5642	3394	1646	1671	2990	495	943	983	152	704	110

nd: Not detected, [*] For B(b+k)F.
[a] Zhang et al., 2006.
[b] Motelay-Massei et al., 2004.
[c] Nadal et al., 2004.

In Turkey, soil PAH concentrations in a suburban site of Izmir were measured by Demircioglu (2008). The average concentrations of individual PAHs ranged between

0.4±0.3 (benzo[*a*]pyrene) and 20±9 (phenanthrene) µg kg^{-1} dry weight (dry wt), and the average Σ_{14}-PAH concentration was found to be 56±14 µg kg^{-1} (dry wt). This result was lower than the ones reported for the other sites in Table 2.10, except for the rural site in Hong Kong (Zhang et al., 2006).

Demircioglu (2008) reported that the PAH profile in soils was dominated by lower molecular weight compounds at suburban Izmir. The most abundant individual PAHs were phenanthrene, fluoranthene, pyrene, and chrysene accounting for 34, 14, 11, and 11% of the Σ_{14}-PAHs in soils, respectively. A variation in the soil PAH profile at the different sites was observed by Motelay-Massei et al. (2004), Nadal et al. (2004), and Zhang et al. (2006), and this was explained the nature of the sites and their proximity to the sources.

2.4.3.2 PCB Levels in Soils

Table 2.11 shows the PCB levels in soils reported recently elsewhere. In Turkey, soil Σ_{36}-PCB concentrations at six different sites of Aliaga were reported by Cetin et al. (2007) and the highest concentrations were observed for the industrial sites. Based on the results of factor analysis and chemical mass balance modeling, Cetin et al. (2007) concluded that the steel industries and local soil may be potential PCB sources for urban and industrial sites in Aliaga, Izmir.

The reported range for average soil Σ_7-PCB concentrations at 47 different sites in Central and Southern Europe was between 2.3 (background sites) and 839 (heavily polluted sites) µg kg^{-1} (dry wt) (Ruzickova, Klanova, Cupr, Lammel, & Holoubek, 2008). A large variation in average soil Σ_{69}-PCB concentrations ranging between 2.6-332 µg kg^{-1} (dry wt) was also found by Backe et al. (2004) for the 11 different sites in Sweden. Harner et al. (1995) reported soil ΣPCB concentrations for four congeners (28, 52, 138, and 153) between 10-670 µg kg^{-1} (dry wt) at 10 different sites in England. According to Motelay-Massei et al. (2004), PCB concentrations at the industrial sites were 100 times higher than at the remote sites. The variation in

soil PCB levels between the sites were explained by differences in soil properties and other environmental conditions such as proximity to sources of pollutants, land use, and the wind direction (Backe et al., 2004).

Table 2.11 Average soil concentrations (µg kg^{-1}, dry wt) of ΣPCBs reported previously.

Location	Site	ΣPCB Conc.	Sampling Period	No of PCBs	Reference
Aliaga, Izmir, Turkey	Industrial 1	66.0	March-April, June, 2005	36	Cetin et al., 2007
	Industrial 2	48.5			
	Industrial 3	44.0			
	Residential/Industrial	4.9			
	Suburban 1	15.9			
	Suburban 2	14.9			
Central and Southern Europe	Background	1.8	July-Dec., 2005	7	Ruzickova et al., 2008
	Residential/Urban	6.8			
	Industrial	27.2			
	Heavily Polluted	839			
Hong Kong	Urban	9.9	Dec., 2000	7	Zhang, Luo, Wong, Zhao, & Zhang, 2007
	Rural	0.07			
Seine River Basin, France	Industrial 1	342	Nov., 2000	22	Motelay-Massei et al., 2004
	Industrial 2	85.4			
	Urban	5.53			
	Suburban 1	40.1			
	Suburban 2	0.13			
	Remote 1	18.2			
	Remote 2	*nd*			
Sweden	Coastal 1	332	Sept., 1993	69	Backe et al., 2004
	Coastal 2	46.0			
	Rural 1	8.03			
	Rural 2	11.0			
	Rural 3	4.5			
	Rural 4	12.0			
	Rural 5	3.8			
	Grassy plain	3.7			
	Urban 1	4.3			
	Urban 2	7.1			
	Urban 3	2.6			
Bayreuth, Germany	Industrial	21.9	Not Given	12	Krauss & Wilcke, 2003
	Urban	13.0			
	Rural	1.7			

Backe et al. (2004) reported a large variation in the PCB patterns in soils taken from different sites. It was observed that areas with the highest soil concentrations had the higher degree of heavier congeners, explained by faster volatilization rates of

lighter congeners and a larger fraction of heavier congeners left in the soil. Motelay-Massei et al. (2004) also reported that the soil ΣPCB concentrations dominated by the high molecular weight PCBs at the urban sites, by many light congeners as well as heavy ones for the industrial sites, and by a greater contribution of lightest molecular weight PCBs for the remote sites. Background and remote areas are probably subjected to long range transport of lighter molecular weight compounds rather than short range transport from local sources.

2.4.3.3 OCP Levels in Soils

Average soil concentrations of individual OCPs previously reported for the different sites through the world are presented in Table 4.12. Generally, the highest pesticide level in agricultural soils was observed for DDT related compounds which were once heavily used at these sites (Bidleman & Leone, 2004; Harner et al., 1999). Meijer et al. (2003a) conducted a study at two agricultural sites in Canada, and they also found the highest concentrations for dieldrin and the individual DDTs (except *o,p'*-DDE). The concentration range for these compounds was between 10-10,000 μg kg^{-1} (dry wt). But for the other studied pesticides (HCB, *α*- and *γ*-HCHs, aldrin, endrin, heptachlorepoxide, *t*-nonachlor, *α*- and *γ*-chlordane), this range was between 0.1-10 μg kg^{-1} (dry wt). At agricultural/industrial sites in Brazil, the in-use pesticides (endosulfan, dieldrin, and endrin) were reported as the most abundant compounds in soils (Rissato et al., 2006).

It was reported by Harner et al. (1999) that insight to the aging process of pesticides in soils can be gained by comparing isomer patterns in soils to the original compositions in technical mixtures. According to the Harner et al. (1999), the ratio of TC:CC:TN (*t*-chlordane:*c*-chlordane:*t*-nonachlor) in technical chlordane mixture is 1.00:0.77:0.62 with a relative removal rates in the order TC>CC>TN. The average ratios of TC:CC:TN was found to be 1.00:1.10:1.76 that were different from their original ratios. A large variation in the TC:CC ratios (1.00:3.57-1.00:0.17) between the sites was also reported and this was attributed to differences in degradation

preference among soils or to former application of technical heptachlor containing chlordane isomers.

Table 2.12 Average soil concentrations (μg kg^{-1}, dry wt) of OCP compounds reported previously.

OCPs	Sao Paulo, Brezil[a]			Hong Kong[b]	Alabama, Luisiana, Texas, USA[c]	Alabama, USA[d]
	March-June, 2005			Dec., 2000	1999-2000	1996
	Industrial/Agricultural 1, 2		Unpolluted	Farmland	Agricultural	Agricultural
α-HCH	0.06	0.26	<0.03	0.14±0.08	0.17±0.14 (<0.05)[*]	0.10±0.12 (0.05)[*]
β-HCH	<0.05	0.15	<0.05	6.37±0.24	-	-
γ-HCH	<0.05	0.15	*nd*	0.02±0.02	0.13±0.07 (<0.05)	0.13±0.11 (0.06)
δ-HCH	*nd*	0.07	*nd*	-	-	-
CHLPYR	-	-	-	-	-	-
HEP EPOX	*nd*	0.05	*nd*	-	-	0.19±0.14 (0.10)
α-CHL	-	-		-	0.29±0.40 (0.06)	0.54±0.59 (0.18)
γ-CHL	-	-		-	0.30±0.35 (0.06)	0.49±0.49 (0.17)
c-NONA	-	-		-	0.38±0.41 (0.06)	-
t-NONA	-	-		-	0.25±0.37 (0.09)	0.86±0.82 (0.25)
ESLF I	0.71	<0.05	<0.05	*nd*	-	-
ESLF II	1.77	0.12	<0.05	-	-	-
ESLF SUL	1.77	0.15	<0.05	-	-	-
p,p'-DDT	0.50	0.64	0.07	0.02±0.04	60±92 (11)	24.6±30.5 (6.61)
p,p'-DDD	0.48	0.10	0.07	0.05±0.12	2±2 (0.31)	2.40±2.41 (1.15)
DIELD	<0.05	0.21	*nd*	-	2.3±4.1 (0.33)	4.87±6.67 (1.46)
END	0.08	0.11	*nd*	*nd*	-	-
END AL	-	-	-	-	-	-
END KET	-	-	-	-	-	-
MEOCL	*nd*	<0.10	*nd*	-	-	-

[*] Geometric mean, *nd*: Not detected.
[a] Rissato et al., 2006.
[b] Zhang et al., 2006.
[c] Bidleman & Leone, 2004.
[d] Harner et al., 1999.

Zhang et al. (2006) found high β-HCH level in Hong Kong soils and this was ascribed its persistence in soil, due to higher K_{OW} and lower vapor pressure values of β-HCH in comparison with other HCH isomers. They found an average α-HCH to γ-HCH ratio of 6 which was close to the original ratio of technical HCH. Since technical HCH was banned in Hong Kong, estimated high α-HCH to γ-HCH ratio was explained by higher volatilization rate of γ-HCH than α-HCH.

It was suggested by Harner et al. (1999) that for a soil-air system in equilibrium, the concentration of a hydrophobic chemical in the soil is expected to be proportional to the organic content of the soil because organic matter is the major reservoir for these compounds. Pesticide concentrations in soils were correlated with percent organic carbon by Harner et al. (1999) and a poor relationship for all compounds were observed. They concluded that this indicates disequilibrium in the soil-air system, since the soils are oversaturated with respect to the atmosphere for most of the compounds, resulting net gas volatilization from the soil.

CHAPTER THREE
MATERIALS AND METHODS

Sampling site and program, sampling techniques and the experimental methods used for the measurement of PAHs, PCBs and OCPs in this study are discussed in Chapter 3. Data analysis methods are also presented in this chapter.

3.1 Sampling Site and Program

Sampling was performed at a site located at the Horozgedigi village in the Aliaga industrial region, ~5 km south of the Aliaga town center and ~50 km north of the metropolitan city of Izmir, Turkey. The site is located in the vicinity of significant pollutant sources including a large petroleum refinery, a petrochemicals complex, iron smelters with scrap iron storage and classification sites, steel rolling mills, a natural gas-fired power plant (1500 MW), a chemical fertilizer plant, a very dense transportation activity of scrap iron trucks, heavy road and rail traffic, ship dismantling areas, busy ports with scrap iron and petroleum coke storage, and nearby agricultural and residential areas (Fig. 3.1). Aliaga's land surface area is 274 km^2, and according to the statistical data given for 2006, ~44% of total area has been used for crop production (e.g. olive trees, vegetables, vineyard, cotton, corn, barley and wheat) (Ministry of Agriculture and Rural Affairs [MARA], 2007).

Concurrent ambient air, total suspended particulate matter (TSP), and dry deposition samples were collected during two sampling campaigns conducted between August 2-17, 2004 and March 20-April 5, 2005. For all ambient air, TSP, and dry deposition samples, average sampling duration was ~24 h. Both sampling periods coincided with dry weather days. Meteorological data was provided from a meteorological station located at the sampling site. Average air temperatures were 24°C and 9°C for the summer and winter sampling periods, respectively. Wind speed ranged between 1.5-5.5 and 1.7-9.4 m s^{-1} during the summer and winter sampling periods, respectively. Generally northerly winds (WNW, NW) have prevailed

(except for four days wind was from SE) during the sampling programs (Fig. 3.1). Detailed sampling information, TSP and its organic matter (OM) data is given in Table 3.1. Meteorological parameters (i.e. temperature, wind speed and direction) measured during the sampling programs of the present study were not significantly different than the seasonal averages (Table 3.1). This suggests that the measured ambient PAH, PCB, and OCP concentrations during the sampling periods are representative for the summer and winter seasons.
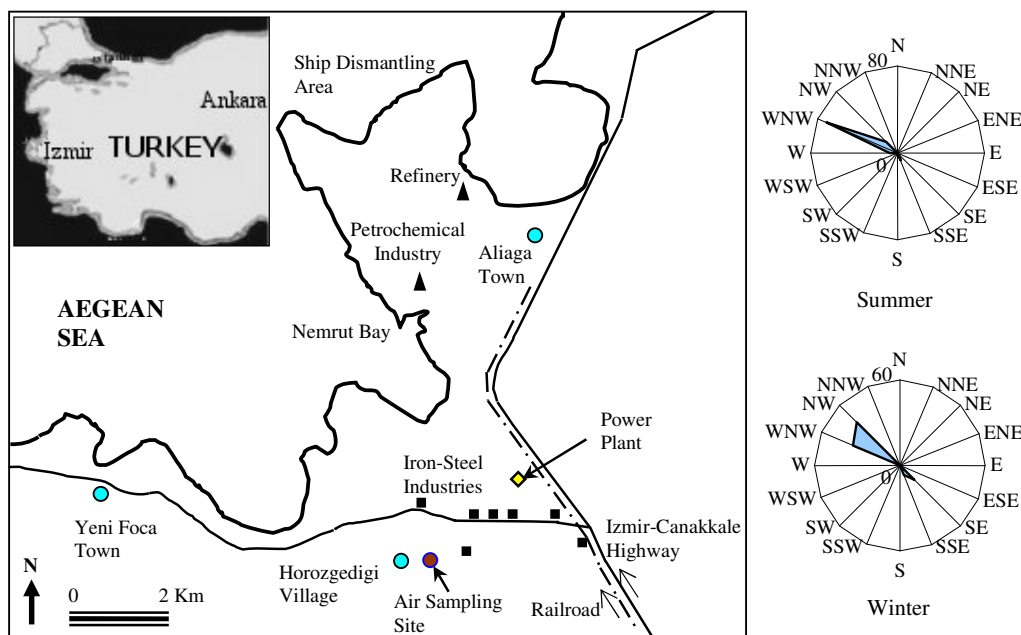
Figure 3.1 General layout of the study site. Wind roses show the frequency (%) of prevailing wind directions during the sampling programs.

Seven soil samples (*n*=4 for summer and 3 for winter) were taken around the air sampling site during the sampling campaigns. Additional soil samples were also collected at 48 different points in the study area in March 2006 to determine the spatial distribution of PAH, PCB, and OCP contaminations in soils that can be related to the local sources. Locations of the sampling points are illustrated in Fig. 3.2 and the sampling information, and water and organic matter (OM) contents of all soil samples (*n*=55) are summarized in Table 3.2.

Table 3.1 Summary of sampling information, TSP and its OM data obtained from the air sampling site in Aliaga during two sampling periods.

Date	Duration (min)	T (°C)	U (m s^{-1})	WD	RH (%)	C_{TSP} (µg m^{-3})	C_{OM} (µg m^{-3})	OM (%)
08/02-03/2004	1460	24.1	3.9	NW	62	71.1	30.5	43
08/03-04/2004	1426	23.9	2.4	WNW	66	63.3	34.0	54
08/04-05/2004	1412	24.4	1.8	WNW	61	-	-	-
08/05-06/2004	1490	24.1	1.9	WNW	70	65.0	30.1	46
08/06-07/2004	1423	25.1	1.5	W	64	92.5	43.5	47
08/07-08/2004	1301	24.1	2.5	WNW	76	69.2	32.6	47
08/08-09/2004	1394	24.3	3.3	WNW	71	67.9	33.1	49
08/09-10/2004	1316	24.7	2.5	WNW	67	54.5	22.2	41
08/10-11/2004	1607	23.3	2.9	WNW	72	74.6	27.6	37
08/11-12/2004	1302	23.4	4.1	NW	66	112	25.5	23
08/12-13/2004	1441	24.3	3.1	WNW	60	113	40.0	35
08/13-14/2004	1476	24.8	1.7	WNW	56	92.5	35.3	38
08/14-15/2004	1528	26.4	1.6	SSE	57	71.0	28.4	40
08/15-16/2004	1419	24.4	5.5	WNW	68	287	49.1	17
Sampling period Avg±SD	1428	24.4±0.8	2.8±1.1	WNW	66±6	94.9±58.2	33.2±7.2	40±10
Seasonal Avg±SD [a]		23.8±1.6	3.4±1.4	WNW	62±9			
03/20-21/2005	1333	6.4	4.0	WNW	64	178	37.8	21
03/21-22/2005	1360	7.9	2.7	NW	46	82.5	30.4	37
03/22-23/2005	1433	8.0	3.1	NW	30	88.3	28.8	33
03/23-24/2005	1455	8.5	2.5	NW	37	135	50.3	37
03/24-25/2005	1384	9.9	2.3	NW	36	114	40.5	36
03/25-26/2005	1502	11.0	1.7	SSE	54	-	-	-
03/27-28/2005	1383	16.1	6.7	SE	60	-	-	-
03/28-29/2005	1340	16.2	6.1	SE	62	89.9	19.3	21
03/29-30/2005	1418	13.4	2.1	WNW	74	40.6	10.1	25
03/30-31/2005	1452	12.1	2.7	NW	77	149	44.3	30
04/01-02/2005	1243	5.0	9.4	NW	58	470	112	24
04/02-03/2005	1466	4.8	8.2	WNW	56	267	70.1	26
04/03-04/2005	1361	4.8	5.6	WNW	50	399	99.8	25
04/04-05/2005	1454	6.6	4.7	WNW	45	373	71.9	19
Sampling period Avg±SD	1399	9.3±3.9	4.4±2.5	NW	54±14	199±137	51.3±30.1	28±6
Seasonal Avg±SD [b]		7.8±3.7	3.7±2.1	NW	44±31			

T: Air temperature, U: Wind speed, WD: Prevailing wind direction, RH: Relative humidity, C_{TSP}: Concentration of total suspended particulate matter, C_{OM}: Concentration of organic matter content of TSP.

[a] Refers to the average of a period from 06.01.2004 to 08.31.2004.

[b] Refers to the average of a period from 12.01.2004 to 04.05.2005.

Table 3.2 Summary of sampling information, water and OM contents of soil samples.

Sampling Date	SN	Site	WC (%)	OM (%)	OM (%) (Dry S.)	Sampling Date	SN	Site	WC (%)	OM (%)	OM (%) (Dry S.)
08/05/2004	1	29[a]	5.1	9.6	10.1	03/28/2006	21	23	10.9	3.9	4.4
08/08/2004	2		4.7	9.6	10	03/28/2006	22	24	8.5	5.1	5.5
08/10/2004	3		5.5	9.5	10	03/28/2006	23	25	8.3	9.1	9.9
08/17/2004	4		4.9	8.4	8.8	03/21/2006	24	26	19.4	7.0	8.7
03/24/2005	5		13.3	6.6	7.6	03/28/2006	25	29[a]	8.5	6.5	7.1
03/29/2005	6		7.7	7.2	7.9	03/21/2006	26	30	17.7	6.0	7.2
04/05/2005	7		9.4	6.7	7.4	03/28/2006	27	32	10.9	4.9	5.5
Avg±SD			7.2±3.2	8.2±1.4	8.8±1.2	03/28/2006	28	33	11.7	6.7	7.5
03/28/2006	1	1	4.2	3.6	3.7	03/28/2006	29	34	8.0	4.2	4.6
03/28/2006	2	2	14.8	5.6	6.6	03/21/2006	30	35	19.8	5.9	7.4
03/21/2006	3	3	12.7	3.7	4.2	03/21/2006	31	36	18.1	8.6	10.5
03/28/2006	4	4	10.8	3.9	4.4	03/21/2006	32	37	11.6	2.7	3.0
03/21/2006	5	5	6.9	2.3	2.5	03/28/2006	33	39	11.8	5.2	5.8
03/28/2006	6	6	11.3	7.3	8.3	03/21/2006	34	42	13.1	7.1	8.2
03/28/2006	7	7	18.8	5.9	7.3	03/28/2006	35	43	4.1	2.7	2.8
03/21/2006	8	9	10.7	3.1	3.5	03/28/2006	36	44	7.2	4.3	4.7
03/21/2006	9	10	17.8	4.5	5.5	03/21/2006	37	45	13.6	3.6	4.2
03/28/2006	10	11	4.8	5.3	5.6	03/21/2006	38	46	14.9	5.7	6.7
03/28/2006	11	12	13.1	7.6	8.8	03/21/2006	39	47	13.1	5.8	6.7
03/28/2006	12	13	9.9	6.8	7.6	03/21/2006	40	48	9.6	4.0	4.5
03/21/2006	13	14	13.0	4.2	4.9	03/28/2006	41	49	7.0	3.4	3.7
03/21/2006	14	15	10.0	3.0	3.4	03/21/2006	42	50	16.1	7.2	8.6
03/28/2006	15	16	6.2	3.6	3.9	03/28/2006	43	53	7.8	4.0	4.3
03/28/2006	16	17	12.9	9.0	10.3	03/28/2006	44	54	4.9	3.7	3.9
03/28/2006	17	18	13.2	5.8	6.7	03/28/2006	45	55	5.6	5.1	5.4
03/28/2006	18	19	4.9	4.2	4.4	03/28/2006	46	58	6.5	6.7	7.2
03/21/2006	19	20	11.7	6.4	7.3	03/21/2006	47	59	18.4	4.6	5.6
03/21/2006	20	22	11.8	4.9	5.5	03/28/2006	48	60	10.3	5.8	6.5

SN: Sample number, WC: Water content, OM: Organic matter.

[a] Air sampling site.

Spatial distributions of PAH, PCB and OCP levels in soils (n=48) were mapped using MapInfo Professional with Vertical Mapper which is a GIS (geographic information system) mapping software. The maps were created in MapInfo, and then the point concentrations of the contaminants were displayed by creating thematic maps of the contaminant concentration attribute. The contour maps were interpolated from the point concentrations using Vertical Mapper. Interpolation method used in this study was the triangulation with smoothing where the data points are connected by a series of triangles.
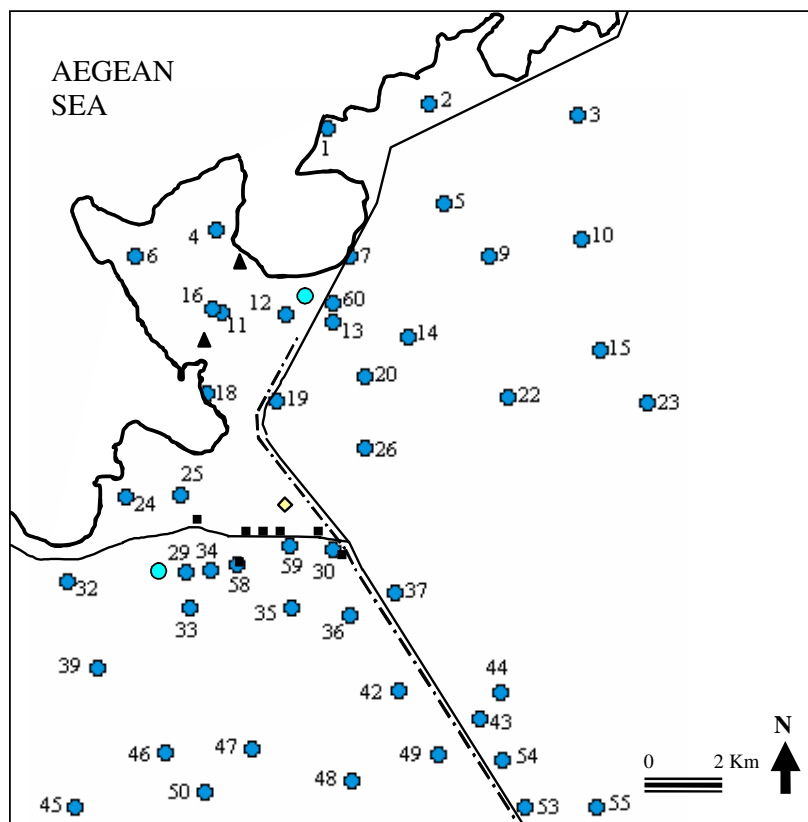
Figure 3.2 Locations of the sampling points for the soil samples (*n*=48) in the Aliaga study area. Sample 29 was taken from the air sampling site. (● : soil sampling points, ○ : residential areas).

3.2 Sampling Methods

3.2.1 Ambient Air Samples

Ambient air samples in particle- and gas-phases were collected using a modified high-volume sampler (PS-1), Model GPS-11 (Thermo-Andersen Inc.). Particles were collected on 10.5 cm diameter quartz filters while the gas-phase compounds were collected using a modified cartridge containing XAD-2 resin placed between polyurethane foam (PUF) plugs. Average sampling volumes for ambient air samples were 257 ± 22 and 309 ± 21 m^3 for the summer and winter periods, respectively.

A second high volume sampler was deployed at the same sampling site to determine total suspended particulate matter (TSP) and its organic matter (OM) content in the ambient air. Particles were collected on 11 cm glass fiber filters (GFFs). The average sampling volumes for TSP samples were 63.7±19 and 33.1±11.6 m^3 for the summer and winter periods, respectively. Both high volume air samplers were calibrated before sampling campaigns.

3.2.2 Dry Deposition Samples

The particle dry deposition flux was measured using a smooth deposition plate (22x7.5 cm) with a sharp (<10°) leading edge mounted on a wind vane. Glass fiber filter (GFF) sheets mounted with cellulose acetate strips on the plates were used to collect the deposited particles. The dimensions of the GFF sheet's deposition surface were 5.5x12.5 cm. Five plates and sheets with a total collection area of 344 cm^2 were used for sampling.

3.2.3 Soil Samples

To represent each sampling site, multiple soil samples (n=3-4) were collected from different points around the sampling site. For each site, soil samples were collected over a ~100 m^2 area. Approximately 0.5-1 kg of soil samples were taken manually from the top 5 cm of the soil after removal of the large stones and pieces of vegetation. After packing in aluminum foil, soil samples were placed in airtight plastic bags.

3.3 Preparation for Sampling

3.3.1 Glassware

All glassware used for the sampling and analysis procedures was washed with hot water and detergent, and then rinsed a number of times with water, distilled water,

and a series of polar and non-polar solvents (acetone, hexane), respectively. Subsequently, they were dried in an oven at 105°C for several hours. The openings of the glassware were wrapped with aluminum foil to remove any contamination.

3.3.2 Quartz and Glass Fiber Filters

After wrapping loosely with aluminum foils, quartz filters (used for ambient air sampling) and glass fiber filters (GFFs, used for dry deposition sampling) were baked in a muffle furnace at 450°C overnight to remove any organic residues. Then, they were allowed to cool to room temperature in a desiccator, sealed in airtight plastic bags, and stored frozen prior to sample collection.

Similarly, GFFs used for TSP sampling were wrapped loosely with aluminum foil and baked in a muffle furnace at 450°C for 2 h to remove any organic residues. Then, they were allowed to cool to room temperature in a desiccator and weighed using a micro balance capable of weighing 0.1 mg.

3.3.3 PUF Cartridges

PUF cartridges were cleaned by Soxhlet extraction using a dichloromethane (DCM): petroleum ether (PE) mixture (20:80, volumetric) for 24 h. After extraction, they were wrapped loosely with aluminum foil, dried in an oven at 70°C overnight, and stored frozen in glass jars capped with Teflon-lined lids.

3.3.4 Dry Deposition Plates and Cellulose Acetate Strips

Plates and cellulose acetate strips used for dry deposition sampling were cleaned with detergent and hot water, and then rinsed several times with water, distilled water, acetone, and hexane, respectively. Subsequently, they were wrapped with aluminum foil. Before sampling, prepared glass fiber filter sheets (7.5x12.5 cm) were mounted on dry deposition plates and both sides were covered with cellulose acetate

strips (1x12.5 cm) to prevent exposure to the deposited material during field sampling.

3.3.5 Sample Handling

All cleaned and prepared sampling materials including GFFs, quarz filters, PUF cartridges, and dry deposition plates were transported to the field in their containers to avoid exposure to ambient air. After sampling, PUF cartridges, PS-1 and dry deposition filters were wrapped with aluminium foil, placed back into their containers, returned to the laboratory together with the field blanks, and stored in a freezer at -20°C.

After sampling, GFFs used in TSP sampling were placed back into their storage boxes and returned with the field blanks to the laboratory. They were placed in a desiccator overnight, and reweighed.

Soil samples were packed in aluminum foil, put into airtight plastic bags, and carried to the laboratory. At once, they were sieved through a 0.5 mm mesh sieve to remove remaining large particles and organic debris. A number of soil samples (usually n=3-4) collected at each sampling point were combined by taking equal amounts for each, and then the mixture was homogenized to obtain one representative sample for each site. From this soil mixture, approximately 30 g of soil samples were used to determine their water and organic matter contents. The remaining part was packed again in aluminum foil, put into airtight plastic bags, and stored in a freezer at -4°C until the analysis. For the PAH, PCB, and OCP analysis procedure, 15 g of soil samples were used.

3.4 Preparation for Analysis

3.4.1 Sample Extraction and Concentration

All ambient air and dry deposition samples were Soxhlet extracted with a volumetric mixture of DCM: PE (20:80, volumetric) for 24 h. Prior to extraction, all samples were spiked with 0.5 ml surrogate standard mixtures of PAHs and PCBs to monitor the analytical recovery efficiency. The extracts were concentrated and transferred into hexane using a rotary evaporator. The temperature of water bath was maintained at 30°C. After volume reduction to ~5 ml, the extract was transferred into hexane by adding 15 ml of hexane. Then, the mixture was evaporated again down to ~5 ml, and 10 ml of hexane were added to the flask. After volume reduction to ~5 ml, the sample was transferred into a 40 ml amber vial sealed with Teflon cap. The flask used for evaporation was rinsed with 5 ml of hexane and this was added into the same vial. The concentrated sample in the 10 ml of hexane was reduced to ~2 ml by gentle flow of pure N_2 (~150-200 ml min^{-1}).

For the PAH, PCB, and OCP analysis in soils, 15 g of sub-samples were placed in glass jars capped with Teflon-lined lids. Samples were spiked with 0.5 ml of PAH and PCB surrogate standards, and soaked in 50 ml of a 1:1 (volumetric) acetone: hexane mixture overnight. Then, they were ultrasonically extracted for 30 min. For the concentration and clean up steps, the same procedures used for the air and dry deposition samples were applied.

3.4.2 Clean Up and Fractionation

To remove interferences before GC/MS analysis, the samples were cleaned up and fractionated on an alumina-silicic acid column. Before use, Na_2SO_4 and alumina were placed in ceramic plates covered loosely with aluminum foil, and then they were baked in a muffle furnace at 450°C for 4 h. Silicic acid was placed in a flask

covered loosely with aluminium foil, dried in an oven at 105°C overnight to remove moisture. Then, they were allowed to cool to room temperature in a desiccator.

In an amber vial, three grams of silicic acid was deactivated by adding 100 µL of DI water (3% water), and then the mixture was shaken until homogenized. Similarly, two grams of alumina was deactivated by adding of 120 µL of DI water (6% water) and the mixture was homogenized by shaking. These mixtures were left at room temperature at least 1 h before use, and used within 12 hours.

Alumina-silicic acid column was prepared by adding a piece of glass wool, 3 g of silicic acid (3% water), 2 g of alumina (6% water), and ~1 cm column height of anhydrous Na_2SO_4 in series. The column was pre-washed with 20 ml of DCM followed by 20 ml of PE. Then, the sample in 2 ml of hexane was added to the top of the column with a 2 ml rinse of PE, and eluent was collected in a vial at a rate of two drops per second. After letting the sample pass through the column, 20 ml of PE was added and eluent collected in the same vial (fraction 1). Fraction 1 contained PCBs. Then the vial used for eluent collection was changed, 20 ml of DCM was added into the column, and eluent was collected at the same rate (fraction 2). Fraction 2 contained PAHs and OCPs. For both fractions, the sample volume was reduced, and the solvent was exchanged into hexane using a high purity stream of nitrogen (~150-200 ml min^{-1}). The sample was blown-down to ~5 ml, and 10 ml of hexane was added to the vial. After volume reduction to ~5 ml, again 10 ml of hexane was added into the sample volume. Then, the final sample volume was adjusted to exactly 1 ml by N_2 blow-down. All samples were stored in a freezer until analysis.

3.5 Determination of TSP and its OM Content

Before TSP sampling, prepared GFFs were weighed using a micro balance capable of weighing 0.1 mg. After sampling, GFFs (samples and blank filters) were kept in a desiccator overnight, and reweighed. TSP amount in ambient air was

calculated by subtracting the initial weight from the final weight. Then, GFFs were baked in a muffle furnace at 450°C for 1 h. They were allowed to cool to room temperature in a desiccator overnight, and again weighed to determine OM content of total suspended particulates. OM content was calculated by subtracting the final weight (after baking) from the initial weight (before baking). To minimize the interference from weight loss of filters during baking at high temperatures, concurrent blank filters were used for each sample. OM contents of particles were corrected using the weight loss in blank filters.

3.6 Determination of Water and OM Contents of Soil Samples

Soil moisture content was determined by weighing sub-samples of soils before and after drying at 103°C in an oven for 24 h, and the organic matter content was determined by loss on ignition in a muffle furnace at 600°C for 4 h using Standard Methods of 2540-B and 2540-E, respectively (Eaton, Clesceri, Rice, & Greenberg, 2005). Method 2540-E has been commonly used because it offers an approximation of the amount of organic matter present in the solid fraction (Backe et al., 2004; Nadal et al., 2004).

3.7 Analysis of Samples

All the sample and blank extracts (i.e. n=32 for PS-1 PUF, 32 for PS-1 filter, 32 for dry deposition filter, 59 for soil) were analyzed for PAH, PCB, and OCP compounds with a gas chromatograph (GC) (Agilent 6890N) equipped with a mass selective detector (Agilent 5973 inert MSD). They were analyzed with the same capillary column (HP-5ms, 30 m, 0.25 mm, 0.25 μm).

For PAH analysis, the initial oven temperature was held at 50°C for 1 min, was raised to 200°C at 25°C min^{-1} and from 200 to 300°C at 8°C min^{-1}, and was held for 5.5 min. The injector, ion source, and quadrupole temperatures were 295, 300, and

180°C, respectively. High purity helium was used as the carrier gas at constant flow mode (1.5 ml min^{-1}, 45 cm s^{-1} linear velocity).

PCBs were analyzed at electron impact ionization mode. The initial oven temperature was held at 70°C for 2 min and was raised to 150ºC at 25ºC min^{-1}, to 200ºC at 3ºC min^{-1}, to 280ºC at 8ºC min^{-1}, and was held for 10 min. The injector, ion source, and quadrupole temperatures were 250, 230, and 150°C, respectively.

Before the OCP analysis, all extracts were spiked with the internal standard (BDE-77, 3,3′,4,4′-tetrabromodiphenyl ether). All OCPs except *p,p'*-DDE were analyzed at electron capture negative chemical ionization (ECNI) mode. The carrier gas (helium) was used at constant flow mode (1.0 ml min^{-1}) with a linear velocity of 36 cm s^{-1}. The initial oven temperature was held at 50°C for 1 min, was raised to 100ºC at 25ºC min^{-1}, to 260ºC at 5ºC min^{-1}, to 300ºC at 10ºC min^{-1}, and was held for 2 min. The injector, ion source, and quadrupole temperatures were 250, 150, and 150°C, respectively. High-purity methane was the reagent gas. At the same GC/MS conditions, analysis of *p,p'*-DDE for the soil samples collected around the study area (*n*=48 sample plus 4 blanks) were carried out at electron impact ionization mode. The injector, ion source, and quadrupole temperatures for *p,p'*-DDE analysis were 250, 230, and 150°C, respectively.

The MSD was run in selected ion-monitoring mode. Compounds were identified on the basis of their retention times, target and qualifier ions. Qualification was based on the internal standard calibration procedure.

3.8 Quality Control and Assurance

3.8.1 Procedural Recoveries

Prior to extraction, all sample and blank matrices were spiked with internal standard mixtures of PAHs (naphthalene-d_8, acenaphthene-d_{10}, phenanthrene-d_{10}, chrysene-d_{12} and perlylene-d_{12}) and PCBs (PCB-14, 65, and 166) to monitor the analytical recovery efficiency. Each sample was checked for the recovery efficiencies if they were in the range of 50-120%. The recoveries of the internal standards were used to correct the amounts of the specific PAHs and PCBs found in the samples, correspondingly.

Table 3.3 shows the average recovery efficiencies (%) of PAH and PCB internal standards in all blank and sample matrices. Naphthalene and acenaphthylene were identified but not quantified for all samples because of uncertainties with recoveries (<50%) resulting in reduced precision.

Table 3.3 Average recovery efficiencies (%) of PAH and PCB internal standards (avg±SD) in all blank and sample matrices.

Internal Standards	PS-1 PUFs	PS-1 Filters	DD Filters	Soil
Acenaphthene-d_{10}	62±8	72±11	63±12	50±13
Phenanthrene-d_{10}	85±12	92±20	88±14	68±12
Chrysene-d_{12}	81±3	90±14	88±5	72±10
Perlylene-d_{12}	77±10	94±17	87±7	75±14
PCB-14	96±14	80±13	84±15	88±10
PCB-65	103±16	86±17	98±11	90±14
PCB-166	94±30	90±34	86±31	104±10

Procedural recoveries of PAH, PCB, and OCP compounds were tested also by spiking experiments (n=15, 12, and 6, respectively). Average recovery efficiencies for PAHs ranged between 80±19% (dibenz[*a,h*]anthracene) and 120±6% (pyrene) (Demircioglu, 2008). The range for PCB congeners was between 69±15% (PCB-18) and 115±5% (PCB-49), and they were generally >85% (Cetin et al., 2007).

Procedural recoveries of OCPs were generally >70% with an overall average of 85±21% (Odabasi, 2007a). Since the recoveries were generally high, OCP amounts in the samples were not corrected.

3.8.2 Blanks

Blank PUF cartridges, PS-1 and dry deposition filters were routinely placed in the field. To determine the contribution of PAHs, PCBs, and OCPs from the sample preparation, solvent blanks were processed for the soil samples. All blanks were extracted and analyzed in the same manner as the samples to determine if there was any contamination during sample handling and preparation.

Table 3.4 Average PAH amounts (ng, avg±SD) in blank matrices (n=4 for each).

PAHs	PS-1 PUF	PS-1 Filter	DD Filter	Soil
ACT	12±3.2	7.6±3.3	5.7±1.3	8.4±0.9
FLN	19±9.2	16±7.1	14±1.9	16±1.3
PHE	88±28	65±16	53±2.9	44±2.5
ANT	1.5±0.4	1.0±0.4	0.9±0.07	1.0±0.1
CRB	0.5±0.8	*nd*	*nd*	0.5±0.04
FL	12±5.0	12±6.8	6.9±1.3	5.5±0.5
PY	13±5.7	9.4±4.9	6.5±0.7	4.2±0.4
BaA	*nd*	0.2±0.4	*nd*	0.2±0.01
CHR	5.4±2.9	3.5±0.8	2.6±0.9	1.1±0.07
BbF	*nd*	1.0±0.9	*nd*	*nd*
BkF	*nd*	0.7±0.6	*nd*	*nd*
BaP	*nd*	0.4±0.7	*nd*	*nd*

nd: Not detected.

Average PAH amounts mostly detected in the blank matrices are presented in Table 3.4. Indeno[1,2,3-*cd*]pyrene, dibenz[*a,h*]anthracene, and benzo[*g,h,i*]perylene were not detected in any blanks (n=16). Phenanthrene had the largest amounts found in blanks with an average of 88.1±28.3 ng for PUFs, 64.8±16.4 ng for PS-1 filters, 53.4±2.9 ng for dry deposition filters, and 44.3±2.5 ng for soil. Average blank amounts for PS-1 PUFs, PS-1 filters, dry deposition filters, and soil were 3±2%, 9±12%, 26±12%, and 7±12% of the sample amounts for all analyzed PAHs, respectively.

Table 3.5 shows the average PCB amounts mostly detected in the blank matrices. PCB congeners from 44 to 209 were generally not detected in blanks (n=16). PCB-18 had the highest amount in blanks with an average of 0.93±0.20 ng for PUFs, 0.58±0.10 ng for PS-1 filters, 0.58±0.05 ng for dry deposition filters, and 0.48±0.04 ng for soil. Average blank amounts for PUFs, PS-1 filters, dry deposition filters, and soil were 1±2%, 5±9%, 9±14%, and 2±7% of the sample amounts for all analyzed PCBs, respectively.

Table 3.5 Average PCB amounts (ng, avg±SD) in blank matrices (n=4 for each).

PCBs	PS-1 PUF	PS-1 Filter	DD Filter	Soil
PCB-18	0.93±0.20	0.58±0.10	0.58±0.05	0.48±0.04
PCB-17	0.62±0.10	0.38±0.06	0.36±0.04	0.28±0.03
PCB-31	0.38±0.29	0.29±0.02	0.27±0.04	0.16±0.02
PCB-28	0.37±0.27	0.35±0.05	0.31±0.05	0.17±0.03
PCB-33	0.16±0.20	0.05±0.08	0.03±0.07	0.14±0.10
PCB-52	0.17±0.22	0.06±0.09	0.05±0.09	*nd*
PCB-49	0.39±0.08	0.15±0.12	0.03±0.06	*nd*
PCB-95	0.09±0.12	0.05±0.08	0.03±0.06	*nd*
PCB-101	0.13±0.12	0.09±0.09	0.03±0.05	*nd*
PCB-110	0.05±0.09	*nd*	*nd*	*nd*
PCB-149	0.02±0.05	*nd*	*nd*	*nd*

nd: Not detected.

Table 3.6 Average OCP amounts (ng, avg±SD) in blank matrices (n=4 for each).

OCPs	PS-1 PUF	PS-1 Filter	DD Filter	Soil
α-HCH	0.13±0.05	0.10±0.03	0.09±0.04	0.03±0.01
γ-HCH	0.17±0.07	0.18±0.02	0.19±0.06	0.07±0.02
CHLPYR	0.90±0.12	0.67±0.08	0.33±0.21	0.66±0.13
α-CHL	0.01±0.01	*nd*	*nd*	*nd*
γ-CHL	0.01±0.01	0.01±0.00	0.01±0.01	*nd*
t-NONA	0.01±0.01	0.01±0.00	0.01±0.01	*nd*
ESLF-I	0.54±0.24	0.33±0.11	0.18±0.09	0.05±0.01
ESLF-II	0.07±0.01	0.10±0.00	0.05±0.04	0.01±0.01
ESLF SUL	0.02±0.01	0.02±0.01	0.01±0.01	*nd*
p,p'-DDE	*na*	*na*	*na*	0.64±0.04

nd: Not detected, *na*: not analyzed.

The average amounts of OCP compounds mostly detected in blank matrices (n=16) are summarized in Table 3.6. Most OCPs were not detected in blanks. Chlorpyrifos had the highest amount found in blanks with an average of 0.90±0.12

ng for PUFs, 0.67±0.08 ng for PS-1 filters, 0.33±0.21 ng for dry deposition filters, and 0.66±0.13 ng for soil. Average blank amounts for PUFs, PS-1 filters, dry deposition filters, and soil were 4±7, 12±15, 16±19, and 7±13% of the sample amounts for all analyzed OCPs, respectively.

3.8.3 Detection Limits

Instrumental detection limits (IDL) were determined from linear extrapolation from the lowest standard in calibration curve using the area of a peak having a signal/noise ratio of 3. The quantifiable PAH and PCB amounts were approximately 0.15 and 0.10 pg for 1 µl injection, respectively. The quantifiable OCP amounts ranged between 0.02 (*c*-nonachlor)-0.35 pg (*p,p'*-DDT) for 1 µl injection. Instrumental detection limit was used for the compounds that were not detected in blanks.

Table 3.7 LODs (ng) for individual PAH compounds.

PAHs	PS-1 PUF	PS-1 Filter	DD Filter	Soil
ACT	21.6	17.3	9.7	11.2
FLN	47.0	37.4	20.0	20.3
PHE	173	114	62.1	51.7
ANT	2.7	2.1	1.1	1.3
CRB	3.0	*nc*	*nc*	0.58
FL	27.2	32.3	10.6	7.2
PY	29.7	24.1	8.7	5.3
BaA	*nc*	1.3	*nc*	0.21
CHR	13.9	5.9	5.2	1.3
BbF	*nc*	3.6	*nc*	*nc*
BkF	*nc*	2.6	*nc*	*nc*
BaP	*nc*	2.6	*nc*	*nc*

nc: Not calculated.

For the compounds detected in blanks, the limit of detection of the method (LOD, ng) was defined as the mean blank mass plus three standard deviations. LOD values for mostly detected PAHs, PCBs, and OCP compounds are presented in Table 3.7, 3.8, and 3.9 respectively. In general, the amounts of the studied compounds in the samples were substantially higher than LODs. Sample quantities exceeding the LOD

were quantified and blank-corrected by subtracting the mean blank amount from the sample amount for all samples.

Table 3.8 LODs (ng) for individual PCB congeners.

PCBs	PS-1 PUF	PS-1 Filter	DD Filter	Soil
PCB-18	1.5	0.86	0.71	0.61
PCB-17	0.92	0.55	0.48	0.36
PCB-31	1.2	0.36	0.39	0.22
PCB-28	1.2	0.51	0.46	0.25
PCB-33	0.75	0.30	0.23	0.43
PCB-52	0.83	0.31	0.32	*nc*
PCB-49	0.63	0.49	0.21	*nc*
PCB-95	0.44	0.28	0.21	*nc*
PCB-101	0.49	0.36	0.18	*nc*
PCB-110	0.31	*nc*	*nc*	*nc*
PCB-149	0.18	*nc*	*nc*	*nc*

nc: not calculated.

Table 3.9 LODs (ng) for OCP compounds.

OCPs	PS-1 PUF	PS-1 Filter	DD Filter	Soil
α-HCH	0.28	0.18	0.20	0.04
γ-HCH	0.39	0.25	0.36	0.13
CHLPYR	1.3	0.91	0.96	1.0
α-CHL	0.02	*nc*	*nc*	*nc*
γ-CHL	0.02	0.01	0.02	*nc*
t-NONA	0.02	0.01	0.02	*nc*
ESLF-I	1.3	0.65	0.46	0.09
ESLF-II	0.10	0.10	0.18	0.03
ESLF SUL	0.03	0.03	0.04	*nc*
p,p'-DDE	*nc*	*nc*	*nc*	0.77

nc: Not calculated.

3.8.4 Calibration Standards

The PAH calibration standard solution contained 16 PAHs, carbazole, and five deuterated PAHs (naphthalene-d_8, acenaphthene-d_{10}, phenanthrene-d_{10}, chrysene-d_{12}, and perylene-d_{12}) that were used to determine the analytical recoveries. Six levels of calibration standards (0.04, 0.4, 1.0, 4.0, 6.0, 10.0 μg ml^{-1} for PAHs, and deuterated PAHs at a fixed concentration of 8 μg ml^{-1}) were used to calibrate the GC/MS system.

The PCB calibration standard solution contained 41 PCB congeners and internal standard mix (PCB-14, -65, and -166). Five point calibration curves were used to calibrate the analytical system.

The OCP calibration standard solution contained a pesticide mix of 22 compounds, chlorpyrifos, and internal standard (BDE-77, 3,3´,4,4´-tetrabromodiphenyl ether). Five point calibration curves were used to calibrate the analytical system.

In every case, the r^2 of the calibration curve was ≥0.999. System performance was verified by the analysis of the mid-point calibration standard for every 12 h during the analysis period.

3.9 Data Analysis

3.9.1 Influence of Meteorological Parameters on Gas-Phase Compounds

Temperature has a strong influence on the volatilization rates of SOCs affecting their vapor pressures (Sofuoglu et al., 2004). As temperature rises, gas-phase air concentrations increase as a result of volatilization from the contaminated surfaces. The relationship between the air temperature and gas-phase partial pressure of SOCs in the air is described by the Clausius-Clapeyron (CC) equation:

$$\ln P = m \, (1 \, / \, T) + b \tag{3.1}$$

where P is the gas-phase partial pressure (atm) of the compound, T is the mean temperature (K), m is the slope, and b is the intercept of the curve. To apply the measurement data to CC equation, gas-phase ambient air concentrations were converted to partial pressures using the ideal gas law. The mean temperature was obtained by averaging the ambient air temperatures measured in 15 min intervals

over the each sampling period. CC slopes were obtained from a linear regression of ln P versus $1/T$.

Wind speed and direction are the other important atmospheric variables controlling gas-phase concentrations of SOCs in air. To assess the influence of wind speed and direction on gas-phase concentrations in air, a modified equation was obtained by inserting them into the CC equation (Sofuoglu et al., 2004; Brunciak et al., 2001a). This modified form of CC equation is:

$$\ln P = m_1 \, (1 \, / \, T) + \, m_2 \, U + m_3 \, \cos WD + b \qquad (3.2)$$

where U is the mean wind speed (m s^{-1}), WD is the predominant wind direction during the sampling period (deg), and m_1, m_2, m_3, and b are the multiple linear regression (MLR) parameters. Wind speed and cosine of wind directions in 15 min intervals were averaged over each sampling period.

3.9.2 Gas-Particle Partitioning

Two different sorption models have been used to describe the partitioning of SOCs between gas- and particle-phases, namely adsorption onto the aerosol surface and absorption into the organic phase of aerosols (Dachs & Eisenreich, 2000). Absorptive partitioning is believed to be the dominant mechanism when an organic fraction exists on the aerosol. The sub-cooled liquid vapor pressure (P_L) has been used as descriptor of sorption process for both adsorption and absorption (Lohmann, Harner, Thomas, & Jones, 2000). More recently, the octanol-air partition coefficient, K_{OA} has also been used as an alternative to vapor pressure for describing absorptive partitioning of SOCs between the atmosphere and organic phases (Dachs & Eisenreich, 2000; Harner & Bidleman, 1998).

3.9.1.1 Gas-Particle Partitioning Theory

It is common practice to describe the phase distribution using the dimensionless particle/gas partition coefficient, K_P' is:

$$K_P' = C_p / C_g \qquad (3.3)$$

The fraction of compound in particle-phase (ϕ) is calculated from measured the measured gas- (C_g, ng m^{-3}) and particle-phase (C_p, ng m^{-3}) concentrations using the following equation:

$$\phi = C_p / (C_g + C_p) \qquad (3.4)$$

Combining Eqs. (3.3) and (3.4), modified equation of ϕ is found as:

$$\phi = K_P' / (1 + K_P') \qquad (3.5)$$

When the total suspended particle concentration, C_{TSP} (μg m^{-3}) is known, it is further possible to calculate a particle/gas partition coefficient, K_P (m^3 μg^{-1}) as follows:

$$K_P = K_P' / C_{TSP} = (C_p / C_{TSP}) / C_g \qquad (3.6)$$

where (C_p/C_{TSP}) is the concentration on particles (C_p', ng μg^1) (Harner & Bidleman, 1998). Combining Eqs. (3.4) and (3.6), ϕ is also described as:

$$\phi = C_p' \, C_{TSP} / [C_g + (C_p' \, C_{TSP})] = K_P \, C_{TSP} / [1 + (K_p \, C_{TSP})] \qquad (3.7)$$

The extent of particle sorption is related to a chemical's volatility that is often expressed with the sub-cooled vapor pressure of the pure compound (P_L, Pa) or the octanol-air partition coefficient, K_{OA}. The Junge-Pankow model is the most common method for estimating adsorption of SOCs to aerosols as follows:

$$\phi = c\,\theta\,/\,[P_L + (c\,\theta)] \tag{3.8}$$

This model relates the fraction of chemical adsorbed to particles (ϕ) to the sub-cooled vapor pressure of the pure compound (P_L, Pa) and the particle surface area per unit volume of air (θ, cm^2 cm^{-3}). The parameter c (Pa cm) is related to the heat of desorption from the particle surface (Q_d, J mol^{-1}), the heat of vaporization from the liquid compound (Q_v, J mol^{-1}), and the moles of adsorption sites on the aerosol (N_s, mol cm^{-2}) (Falconer & Harner, 2000; Harner & Bidleman, 1998). The value of c is usually taken as 17.2 Pa cm. Values for the surface area parameter (θ, cm^2 cm^{-3}) are often assumed to be 1.1×10^{-5} for urban air, and 3.5×10^{-6} for rural air, and 4.2×10^{-7} for continental background air corresponding to an average TSP concentrations of 140, 86, and 13 µg m^{-3} at these sites, respectively (Bidleman & Harner, 2000).

K_P is also often correlated with P_L using the following equation:

$$\log K_P = m \log P_L + b \tag{3.9}$$

For equilibrium partitioning of a chemical between the gas- and particle-phases, the expected slope (*m*) of Eq. (3.9) is -1. Interpretation of the intercept term (*b*) depends on the assumed mechanism of particle-gas interaction. If compounds are adsorbed to active sites on the particle surface, *b* is related to the specific surface area of the particle and the excess heat of desorption of SOCs from the particle surface. If the mechanism is absorption into a liquid-like film on the aerosol, *b* depends on the fraction of organic matter in the particle (f_{OM}) and the activity coefficient of the compound in the organic film. Sampling artifacts, non-equilibrium conditions

between two phases or a lack of constancy in activities within a class of compounds may lead to values of $m \neq 1$ (Harner & Bidleman, 1998; Vardar et al., 2004).

3.9.1.2 Absorption Model

It has been proposed by Pankow that absorption of gas-phase compounds into an organic film coating the particle makes an important contribution to the overall particle-gas partitioning process. Pankow's expression for K_P ($m^3 \ \mu g^{-1}$) based on absorption is:

$$K_P = 10^{-6} \, R \, T \, f_{OM} / (M_{OM} \, \gamma_{OM} \, P_L) \qquad (3.10)$$

where f_{OM} is the fraction of the particle mass that consist of absorbing organic matter having molecular weight M_{OM} (g mol^{-1}) and activity coefficient, γ_{OM}, in the organic film (Bidleman, 1999).

3.9.1.3 K_{OA} Absorption Model

A logarithmic form of Eq. (3.10) is:

$$\log K_P = \log f_{OM} + \log [10^{-6} \, R \, T / (M_{OM} \, \gamma_{OM} \, P_L)] \qquad (3.11)$$

where the term $[10^{-6} \, R \, T / (M_{OM} \, \gamma_{OM} \, P_L)]$ is related to the partition coefficient of the compound between the organic matter and air. This suggests using the octanol-air partition coefficient, K_{OA}, as an alternative to vapor pressure when predominant distribution process is absorption.

The relationship of K_P to K_{OA} is:

$$K_P = K_{OA} f_{OM} (\gamma_{OCT}/\gamma_{OM}) (M_{OCT}/M_{OM})/ 10^{12} \rho_{OCT} \qquad (3.12)$$

where f_{OM} is the fraction of organic matter in the aerosol involved in partitioning, γ_{OCT} and γ_{OM} are the activity coefficients of the absorbing compound in octanol and aerosol organic matter, M_{OCT} and M_{OM} are the molecular weights of octanol (130 g mol^{-1}) and the organic matter, and ρ_{OCT} is the density of octanol (0.82 kg L^{-1}). With the assumptions that γ_{OCT}/γ_{OM} and $M_{OCT}/M_{OM}=1$, following equation is obtained:

$$\log K_P = \log K_{OA} + \log f_{OM} - 11.91 \qquad (3.13)$$

The K_{OA} absorption model (Eq. 3.13) can be used to predict values of K_P from knowledge of only K_{OA} and the organic fraction of the aerosol, f_{OM}, if it is further assumed that all of the aerosol organic matter is available to absorb gaseous compounds. A plot of $\log K_P$ vs. $\log K_{OA}$ has a theoretical slope of 1 for equilibrium partitioning. The intercept depends on the value of f_{OM} which determines the absorptive capacity of the aerosol (Falconer & Harner, 2000; Harner & Bidleman, 1998; Lohmann & Lammel, 2004). The fraction of particles (ϕ) is then calculated from K_P and TSP by Eq. (3.7).

Strong association of PAHs with soot particles in soot-water systems suggests that besides absorption, adsorption partitioning could also be an important sorption mechanism in the atmosphere. Therefore, the following equation for the overall gas-particle partition coefficient that accounts for both organic matter absorption and soot carbon adsorption was derived by Dachs & Eisenreich (2000):

$$K_P = [K_{OA} f_{OM} (\gamma_{OCT}/\gamma_{OM}) (M_{OCT}/M_{OM})/10^{12} \rho_{OCT}] + [(f_{EC}\, a_{EC})\, K_{SootAir}/10^{12}\, a_{AC}] \quad (3.14)$$

where f_{EC} is the fraction of elemental carbon in the aerosol, a_{EC} and a_{AC} (m^2 g^{-1}) are the specific surface areas of elemental carbon and activated carbon, respectively. $K_{SootAir}$ is the soot-air partition coefficient. Elemental carbon and octanol are the

surrogates for the soot carbon in adsorptive partitioning, and organic matter in absorptive partitioning, respectively.

Dachs, Ribes, Drooge, & Grimalt (2004) have suggested that the thermodynamics-based model recently reported by van Noort (2003) can be used to estimate $K_{SootAir}$ values for PAHs as a function of P_L (Pa) and a_{EC} (m^2 g^{-1}):

$$\log K_{SootAir} = -0.85 \log P_L + 8.94 - \log (998 / a_{EC}) \qquad (3.15)$$

The a_{EC} value (62.7 m^2 g^{-1}) was taken from a recent study by Jonker, & Koelmans (2002). It was assumed that $a_{EC}/a_{AC} = 1$, $f_{OM} = 1.5 f_{OC}$, and $f_{OC}/f_{EC} = 3$ where f_{OC} is the fraction of total organic carbon (Dachs & Eisenreich, 2000; Ribes, Van Drooge, Dachs, Gustafsson, & Grimalt, 2003).

Using models and measured values, gas-particle partitioning of PAHs, PCBs, and OCPs at the air sampling site was investigated. Organic matter (OM) contents of airborne particles were averaged as 40±10 and 28±6%, and average TSP concentrations were 95±61 and 199±143 μg m^{-3} for the summer and winter periods, respectively. In Junge-Pankow adsorption model (Eq. 3.8), the value of c was taken as 17.2 Pa cm. The surface area parameter (θ, cm^2 cm^{-3}) was assumed to be 1.1×10^{-5} for urban air corresponding to a TSP concentration of 140 μg m^{-3} (Bidleman & Harner, 2000). This value was scaled to seasonal TSP concentrations at the air sampling site and was adjusted to 1.1×10^{-5} (95/140) = 7.5×10^{-6} for the summer samples and 1.1×10^{-5} (199/140) = 1.6×10^{-5} for the winter samples.

3.9.2 Particle Dry Deposition Fluxes and Velocities

Using direct method, particle-phase dry deposition fluxes of SOCs (F_d, ng m^{-2} day^{-1}) were calculated by dividing the amount of compound deposited on unit area of the artificial surface per unit time of sampling as follows:

$$F_d = M_d / (A\ T_S) \tag{3.16}$$

where M_d is the particulate compound mass (ng), A is the total collection area of GFF sheets (m^2) and T_S is the sampling time (day).

Particle-phase dry deposition velocities (V_d, cm s^{-1}) were then calculated using the measured particle-phase dry deposition fluxes and atmospheric particle-phase concentrations (C_p, ng m^{-3}) of SOCs as:

$$V_d = F_d / C_p \tag{3.17}$$

3.9.3 Soil-Air Partitioning

Soil/air fugacity fractions of chemicals are used to indicate their equilibrium status in the soil-air system. Fugacity is a measure of chemical potential or partial pressure of a chemical in a particular medium that controls the transfer of chemicals between media (i.e. soil, air). Chemicals strive to establish an equal fugacity (equilibrium) in the soil-air system (Meijer et al., 2001). The equilibrium partitioning of a chemical between soil and air is defined by the dimensionless soil-air partition coefficient, K_{SA}':

$$K_{SA}' = C_S\ \rho_S / C_g \tag{3.18}$$

where C_S is the soil concentration (ng kg^{-1}, dry weight), ρ_S is the density of soil solids (kg m^{-3}), and C_g is the gas-phase air concentration (ng m^{-3}). If the system is not in equilibrium, the use of the term K_{SA}' is not correct and the values obtained from Eq. (3.18) are defined as soil-air quotients (Q_{SA}) (Meijer et al., 2003a).

Soil-air partition coefficient, K_{SA}, is dependent on temperature, humidity and the properties of the chemical and the soil (Meijer et al., 2003a). Sorption to the organic carbon fraction is the main mechanism of partitioning of persistent organic pollutants

to soil. The octanol-air partition coefficient (K_{OA}) is a key descriptor of chemical partitioning between the atmosphere and organic phases (Harner et al., 2000). Hippelein & McLachlan (1998) formulated a linear relationship that relates the K_{SA} to K_{OA} and to the organic carbon fraction of the soil as follows:

$$K_{SA} = 0.411 \, \rho_S \, \phi_{OC} \, K_{OA} \tag{3.19}$$

where ρ_S is the density of the soil solids (kg L^{-1}) and ϕ_{OC} is the fraction of organic carbon on a dry soil basis. The factor 0.411 improves the correlation between the K_{SA} and K_{OA} (Bidleman & Leone, 2004; Hippelein & McLachlan, 1998). Temperature dependent K_{OA} values can be measured directly for compounds of interest, but K_{SA} is soil-specific (Meijer et al., 2003a).

The net air-soil gas exchange flux is driven by the fugacity difference between air and surface soil (Jaarsveld, Van Pul, & De Leeuw, 1997). The instantaneous net flux (F_{net}, ng m^{-2} day^{-1}) is a function of K_{SA}, the concentration gradient and the overall mass transfer coefficient (MTC, cm s^{-1}) as follows:

$$F_{net} = \text{MTC} \, [C_g - (C_S \, \rho_S / K_{SA})] \tag{3.20}$$

In Eq. (3.20), first term (MTC C_g) indicates the gas flux towards the soil (deposition) and second term (MTC $[C_S \, \rho_S / K_{SA}]$) indicates the gas flux towards the air (volatilization).

The overall MTCs of gaseous pollutants can be predicted using the resistance model developed by analogy to electrical resistance (Jaarsveld et al., 1997). In this model, the atmosphere is considered to have three major resistances; aerodynamic (R_a), quasi-laminar boundary layer (R_b), and canopy (R_c). The overall MTC is the reciprocal of the overall resistance and can be expressed as:

$$\text{MTC} = 1 / (R_a + R_b + R_c) \qquad (3.21)$$

Aerodynamic resistance (R_a) accounts for turbulent diffusion transfer from the bulk atmosphere to the canopy. It depends on the wind speed, atmospheric stability, and surface roughness. The atmosphere is usually taken as unstable over the long sampling periods, thus the following equation for unstable atmosphere is used to calculate the aerodynamic resistance (Hicks, Baldocchi, Meyers, Hosker, & Matt, 1987):

$$R_a = 9 / (U_{10} \, \sigma_\theta^2) \qquad (3.22)$$

where U_{10} is the wind speed 10 m above the surface, and σ_θ is the standard deviation of the wind direction in radians.

Boundary layer resistance (R_b) is the resistance in the laminar sub-layer and depends on the molecular diffusion. It can be calculated from the following equation developed by Wesely & Hicks (1977):

$$R_b = [2 / (\kappa u^*)] \, [Sc / Pr]^{2/3} \qquad (3.23)$$

where Pr is Prandtl number of air (~0.72), Sc is the Schmidt number (v/D_A), v is the kinematic viscosity (cm^2 s^{-1}), D_A is the molecular diffusion coefficient of the contaminant in air (cm^2 s^{-1}), κ is the Karman's constant (~0.4), u^* is the friction velocity (cm s^{-1}). Canopy resistance (R_c) is not applicable to surface soils since it is associated with deposition to vegetated land.

The direction of the net gas exchange at soil-air interface is determined by the fugacity ratio. Concurrent air and soil concentrations are ideally used to assess the fugacity gradients of SOCs between the soil-air interface. A soil to air fugacity ratio $[(f_S/f_A)=(C_S \, \rho_S / K_{SA}) / C_g)]$ greater than 1 indicates that the soil is a source with net gas volatilization from soil to air, and a value less than 1 indicates the opposite that

the soil is a sink with net gas deposition from air to soil. For a system in equilibrium, f_S/f_A value is approximately equal to 1 (Cousins & Jones, 1998).

The fugacity ratios and soil-air gas exchange fluxes for PAH, PCB, and OCPs were calculated only at the air sampling site since both air (n=28) and soil (n=7) concentrations corresponding to the same sampling seasons were available. The average water and organic matter contents of soil samples (n=7) taken from the air sampling site were 7.2 and 8.8% (in dry sample), respectively (Table 3.2). It was assumed that the organic matter fraction is 1.5 times the organic carbon fraction and the density of soil solids was 2.0 g cm^{-3} for all calculations.

The uncertainty of the calculated f_S/f_A ratios and soil-air gas net exchange fluxes was assessed using a propagated error analysis. For each PAH, PCB, and OCP compounds, measurement errors in C_g, C_S, K_{SA} and MTC values were taken into account. The uncertainties of C_g, C_S, and K_{OA} (used to calculate K_{SA}) were assumed to be 15% (Harner & Bidleman, 1996; Meijer et al., 2003a) and uncertainty in the overall average MTC was assumed as 40% (Cetin & Odabasi, 2007).

CHAPTER FOUR
RESULTS AND DISCUSSION

This chapter presents the results of ambient air concentrations in gas- and particle-phases, influence of meteorological parameters on gas-phase concentrations, gas-particle partitioning, particulate dry deposition fluxes, settling velocities, soil concentrations, soil to air fugacity fractions, and gas exchange fluxes at the soil-air interface for the studied groups of compounds (i.e. PAHs, PCBs, OCPs). All results were compared with the values reported in the literature.

4.1 Polycyclic Aromatic Hydrocarbons (PAHs)

4.1.1 PAHs in Ambient Air

4.1.1.1 Ambient Air Concentrations of PAHs

Average atmospheric concentrations of individual PAHs measured in this study are presented in Table 4.1. Total (gas+particle) Σ_{15}-PAH (sum of 15 measured individual compounds) concentrations in the air ranged between 7.3-45 ng m^{-3} with an average of 25±8.8 ng m^{-3} in summer and between 10-72 ng m^{-3} with an average of 44±17 ng m^{-3} in winter (average±SD). Winter/summer concentration ratios for total PAH compounds ranged between 0.8 (acenaphthene)-6.6 (benz[a]anthracene). Higher PAH concentrations observed during winter were probably due to the increasing emissions from residential heating. Different ratios for individual compounds indicate that residential heating emissions create a different ambient PAH profile compared to summertime. Similar increases in winter PAH concentrations were recently reported (Bae et al., 2002; Gevao et al., 1998; Kiss et al., 2001; Odabasi, Cetin, & Sofuoglu, 2006a; Park et al., 2002b, 2001a; Schnelle-Kreis, Sklorz, Peters, Cyrys, & Zimmermann, 2005; Vardar et al., 2007).

Table 4.1 Atmospheric concentrations (ng m^{-3}) of individual PAHs measured at the air sampling site (1/2).

	Summer														
	Particle-Phase					Gas-Phase					Total (Gas+Particle)				
PAHs	Min.	Max.	Geometric Mean	Median	Avg±SD	Min.	Max.	Geometric Mean	Median	Avg±SD	Min.	Max.	Geometric Mean	Median	Avg±SD
ACT	0.05	0.1	0.07	0.06	0.07±0.03	0.9	2.0	1.5	1.6	1.5±0.3	0.07	2.0	1.2	1.5	1.5±0.5
FLN	0.08	0.4	0.2	0.2	0.2±0.1	1.2	6.1	3.6	4.0	3.8±1.2	1.2	6.2	3.7	4.2	4.0±1.3
PHE	0.3	0.8	0.5	0.5	0.5±0.1	5.0	22	12	13	13±4.0	0.5	23	10	13	12.4±5.3
ANT	0.02	0.07	0.03	0.03	0.04±0.01	0.08	1.5	0.3	0.2	0.5±0.4	0.1	1.0	0.3	0.2	0.5±0.4
CRB	0.01	0.06	0.02	0.02	0.02±0.01	0.06	0.5	0.2	0.2	0.3±0.2	0.07	0.6	0.2	0.2	0.3±0.2
FL	0.09	0.3	0.2	0.2	0.2±0.1	0.9	5.7	2.4	2.7	2.7±1.3	1.1	5.9	2.6	2.9	2.9±1.4
PY	0.09	0.3	0.2	0.2	0.2±0.1	0.7	3.4	1.6	1.5	1.8±0.7	0.9	3.6	1.8	1.8	2.0±0.7
BaA	0.04	0.2	0.1	0.1	0.1±0.03	0.01	0.08	0.03	0.02	0.03±0.02	0.06	0.2	0.1	0.1	0.1±0.05
CHR	0.2	0.6	0.3	0.3	0.4±0.1	0.2	0.5	0.3	0.3	0.3±0.1	0.4	1.1	0.7	0.7	0.7±0.2
BbF	0.1	0.5	0.2	0.2	0.2±0.1	0.01	0.05	0.02	0.02	0.02±0.01	0.1	0.5	0.2	0.2	0.3±0.1
BkF	0.08	0.3	0.2	0.2	0.2±0.05	0.01	0.02	0.01	0.01	0.01±0.004	0.08	0.3	0.2	0.2	0.2±0.05
BaP	0.05	0.2	0.1	0.1	0.1±0.03	0.002	0.007	0.004	0.004	0.004±0.001	0.06	0.2	0.1	0.1	0.1±0.03
IcdP	0.07	0.2	0.1	0.1	0.1±0.04	0.002	0.005	0.003	0.003	0.003±0.001	0.07	0.2	0.1	0.2	0.1±0.05
DahA	0.03	0.1	0.07	0.08	0.07±0.03	*nd*	*nd*	*nd*	*nd*	*nd*	0.03	0.1	0.07	0.08	0.07±0.03
BghiP	0.08	0.3	0.2	0.2	0.2±0.1	0.002	0.008	0.005	0.005	0.005±0.002	0.08	0.3	0.2	0.2	0.2±0.05
ΣPAHs	0.9	3.6	2.3	2.5	2.4±0.79	4.8	42	21	24	23±8.8	7.3	45	23	27	25±8.8

nd: Not detected.

Table 4.1 Atmospheric concentrations (ng m^{-3}) of individual PAHs measured at the air sampling site (2/2).

PAHs	Winter														
	Particle-Phase					Gas-Phase					Total (Gas+Particle)				
	Min.	Max.	Geometric Mean	Median	Avg±SD	Min.	Max.	Geometric Mean	Median	Avg±SD	Min.	Max.	Geometric Mean	Median	Avg±SD
ACT	0.02	0.07	0.03	0.02	0.03±0.02	0.3	1.8	1.1	1.3	1.2±0.4	0.3	1.8	1.1	1.3	1.2±0.4
FLN	0.06	0.1	0.07	0.07	0.08±0.01	1.3	7.5	4.7	5.3	5.2±1.8	1.3	7.6	4.8	5.4	5.2±1.9
PHE	0.4	0.9	0.7	0.7	0.7±0.1	4.6	31	15	17	17±6.7	4.6	31	16	17	17±7.1
ANT	0.01	0.1	0.08	0.1	0.09±0.04	0.2	3.3	1.1	1.3	1.4±0.8	0.2	3.4	1.2	1.4	1.5±0.8
CRB	0.001	0.05	0.01	0.02	0.02±0.02	0.04	0.6	0.2	0.1	0.2±0.1	0.04	0.6	0.2	0.1	0.2±0.2
FL	0.07	1.6	0.8	1.2	1.0±0.4	1.5	10	4.0	4.5	4.5±2.0	1.2	11	4.5	5.3	5.1±2.6
PY	0.07	1.6	0.8	1.1	1.0±0.4	0.9	9.8	2.8	2.9	3.3±2.2	1.0	11	3.7	4.1	4.3±2.5
BaA	0.05	1.6	0.7	0.8	0.8±0.4	0.004	0.1	0.04	0.05	0.05±0.04	0.1	1.6	0.7	0.9	0.9±0.4
CHR	0.2	6.1	1.9	2.3	2.5±1.6	0.2	1.2	0.4	0.4	0.5±0.3	0.5	7.2	2.4	2.6	3.0±1.9
BbF	0.1	3.7	1.0	1.1	1.3±0.9	0.003	0.02	0.009	0.009	0.01±0.01	0.02	3.7	0.7	1.1	1.2±0.9
BkF	0.1	2.2	0.8	0.9	1.0±0.6	0.002	0.01	0.01	0.01	0.01±0.002	0.004	2.2	0.6	0.9	1.0±0.6
BaP	0.06	1.5	0.6	0.6	0.7±0.4	0.001	0.003	0.001	0.002	0.002±0.001	0.06	1.5	0.6	0.6	0.7±0.4
IcdP	0.1	1.8	0.8	0.8	0.9±0.5	*nd*	*nd*	*nd*	*nd*	*nd*	0.1	1.8	0.8	0.8	0.9±0.5
DahA	0.02	0.9	0.2	0.3	0.3±0.2	*nd*	*nd*	*nd*	*nd*	*nd*	0.02	0.9	0.2	0.3	0.3±0.3
BghiP	0.1	2.4	0.9	0.9	1.1±0.6	0.001	0.005	0.002	0.001	0.002±0.002	0.1	2.4	0.9	0.9	1.1±0.6
ΣPAHs	0.9	20	9.2	11	11±5.3	9.3	53	30	34	33±12	10	72	40	47	44±17

nd: Not detected.

Atmospheric PAH concentrations from this study are within the range of previously reported values in Table 2.4 for the other urban and industrial sites through the world. Concentrations measured in this study were considerably lower than those reported by Demircioglu (2008) for urban sites in Izmir, by Tasdemir & Esen (2007a) for an urban/industrial site in Bursa, by Fang et al. (2004) for industrial and urban sites in Taiwan, by Possanzini et al. (2004) for urban Rome, and by Odabasi, Vardar, Sofuoglu, Tasdemir, & Holsen (1999b) for urban Chicago. However, measured PAH levels at the air sampling site in Aliaga were similar to those reported by Ohura et al. (2004) for industrial sites in Fuji and Shimizu, by Tsapakis & Stephanou (2005) for urban Heraklion, by Dachs et al. (2002) for urban/industrial Baltimore, and by Mandalakis et al. (2002) for urban Athens. In this study, the emissions from major industries may affect the air sampling site if the winds are from N and NE (Fig. 3.1). However, during the sampling programs, the prevailing winds were WNW and NW and probably therefore, relatively low concentrations were measured.
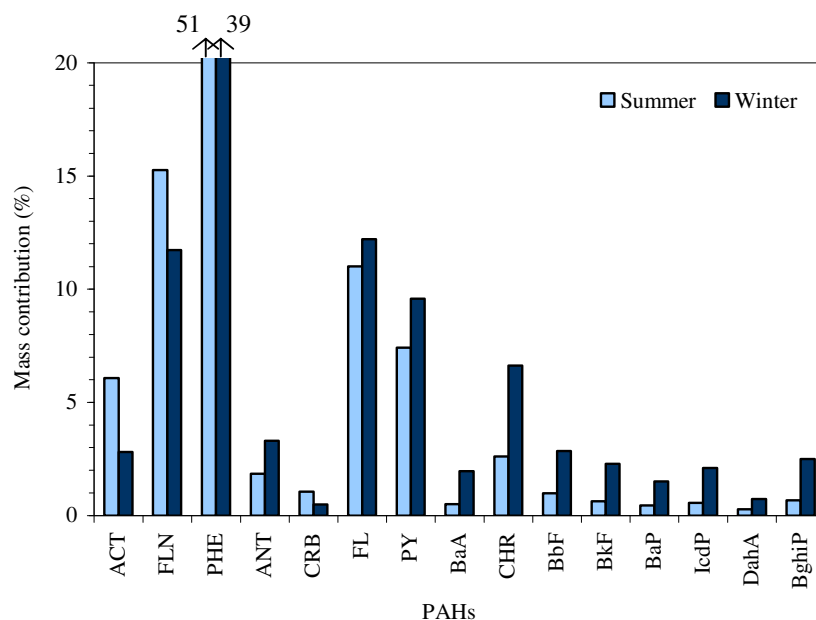

Figure 4.1 Contributions of individual PAHs to total PAH mass in air.

Fig. 4.1 shows the contribution of individual PAH compounds to total PAH mass in air. During both sampling campaigns, atmospheric Σ_{15}-PAHs concentrations were dominated by more volatile compounds existing predominantly in gas-phase. The results indicated that contribution of individual PAHs to total PAH mass in air generally decreased with increasing molecular weight of the compounds. Phenanthrene, fluorene, fluoranthene, and pyrene accounted for 51, 15, 11, and 7% of Σ_{15}-PAHs in summer, respectively while they were 39, 12, 12, and 10% of Σ_{15}-PAHs in winter. These contributions are similar to those reported by Gevao et al. (1998), Demircioglu (2008), Odabası et al. (1999b), and Possanzini et al. (2004).

PAH compounds with similar physical properties such as molecular weight, vapor pressure and solubility have similar distribution patterns in air samples. In this study, correlations between the gas- and particle-phase concentrations of 15 measured PAHs were analyzed and Pearson product correlation coefficients (r) were obtained. As a result, statistically significant correlation factors were only found between low molecular weight PAHs from acenaphthene to pyrene (r=0.50-0.98), and between high molecular weight PAHs from benz[a]anthracene to benzo[g,h,i]perylene (r=0.71-0.99). These findings are in parallel with the results previously reported by Odabasi et al. (1999b).

Average gas- and particle-phase distributions of individual PAHs for the summer and winter periods are illustrated in Fig. 4.2. The gas-phase percentage varied between not detectable (dibenz[a,h]anthracene in summer) up to 99% for the individual PAHs, and it decreased with increased molecular weight of the compounds as a result of their vapor pressures which control the gas-particle partitioning. As shown in Fig. 4.2, the 3-ring PAHs from acenaphthene to carbazole were associated primarily with gas-phase, while 5- to 6- ring ones from benz[b]flouranthene to benzo[g,h,i]perylene were associated primarily with particle-phase. However, the 4-ring PAHs were found to be partitioned between the gas and particle fractions. Partitioning between two phases of these medium volatility compounds was more sensitive to the ambient air temperature than compounds

having lower and higher volatility. These results are consistent with those reported previously by Dachs et al. (2002), Gevao et al. (1998), Odabasi et al. (1999a), Ohura et al. (2004), and Poor et al. (2004).
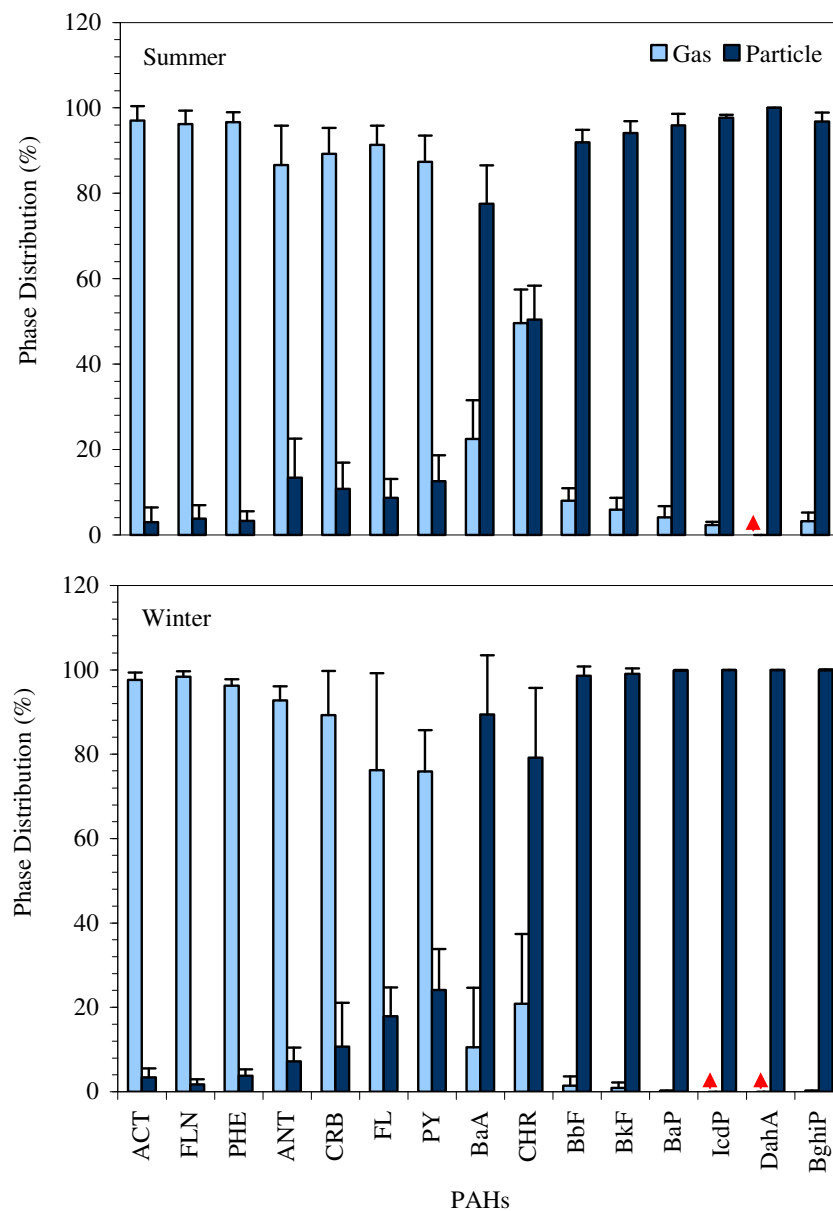

Figure 4.2 Average phase distributions of individual PAHs for the summer and winter periods. Error bars are 1 SD. (▲: Not detected).

Average gas-phase Σ_{15}-PAH concentrations were 23±8.8 and 33±12 ng m^{-3} in summer and winter, respectively while they were 2.4±0.8 and 11±5.3 ng m^{-3} for particle-phase. Gas-phase concentrations for summer and winter periods constituted 90 and 75% of total PAH mass in the air, respectively. Observed higher gas-phase percentage during summer may be due to increasing temperature which increases the volatilization rates of PAHs from the previously contaminated surfaces (Sofuoglu et al., 2001). This result is in parallel with the finding of Vardar et al. (2007) that reported gas-phase concentrations accounting for 89% and 66% of total PAH mass in air for summer and winter seasons, respectively. Sofuoglu et al. (2001) reported statistically more significant dependencies of volatile PAHs with ambient air temperatures compared to less volatile ones.

4.1.1.2 Influence of Meteorological Parameters on PAH Levels in Air

Eq. (3.2) was used to assess the effect of meteorological parameters on atmospheric total (gas+particle) concentrations of PAHs. Summary of the multiple linear regression (MLR) parameters for this equation are presented in Table 4.2.

Table 4.2 Summary of regression parameters for Eq. (3.2).

PAHs	m_1	m_2	m_3	r^2	n
ACT	0.01	-0.03	0.55[a]	0.26[b]	27
FLN	-0.13[a]	-0.37[a]	1.20[b]	0.48[a]	28
PHE	-0.37[a]	0.23	6.01[a]	0.47[a]	28
ANT	-0.06[a]	0.09[a]	0.61[a]	0.75[a]	28
CRB	0.007[b]	0.04[a]	0.22[a]	0.46[a]	28
FL	-0.15[a]	0.01	1.63[b]	0.47[a]	28
PY	-0.13[a]	0.34[a]	1.15[b]	0.64[a]	28
BaA	-0.05[a]	-0.001	0.05	0.80[a]	28
CHR	-0.14[a]	0.19[b]	0.16	0.66[a]	28
BbF	-0.07[a]	-0.07	0.04	0.58[a]	27
BkF	-0.05[a]	0.06[b]	0.13	0.77[a]	27
BaP	-0.04[a]	-0.05[b]	-0.09	0.67[a]	28
IcdP	-0.06[a]	0.006	-0.09	0.69[a]	28
DahA	-0.02[a]	0.04[a]	0.05	0.64[a]	28
BghiP	-0.06[a]	0.03	-0.04	0.68[a]	28

[a] $p<0.05$.

[b] $p<0.10$.

For the full dataset, temperature, wind speed, and wind direction together accounted for 26% (acenaphthene) to 80% (benzo[*a*]anthracene) of the variability in the atmospheric PAH concentrations (Table 4.2). The correlations and m_1 values were statistically significant for all PAHs ($p<0.05$-0.1) except for acenaphthene. Generally negative m_1 values were obtained for PAHs indicated that their concentrations increased with decreasing temperature. This was probably due to increased PAH emissions from combustion sources like residential heating with decreased air temperature. For most of the compounds, m_2 had positive values and they were statistically significant for 8 compounds indicating that advection was also a controlling parameter for the atmospheric PAHs. m_3 values were generally positive and statistically significant for 7 PAHs (acenaphthene through pyrene). Negative values point southerly directions for build-up of high concentrations while positive cosine values are associated with northerly winds. Different directions observed for individual PAHs may be due to their different sources affecting the sampling site.

MLR analysis was repeated for the two subsets of data (winter and summer samples). The results were similar for winter samples to those obtained from the full dataset. However, m_1 values were generally insignificant for the summer sampling period probably due to the observed narrow air temperature range (23.3-26.4ºC). Results of MLR analysis indicated that meteorological parameters have significant effect on the ambient PAH concentrations.

4.1.1.3 Gas-Particle Partitioning of PAHs

Atmospheric concentrations in gas- and particle-phases measured at the air sampling site were used to calculate the experimental gas-particle partition coefficient (K_P) values of PAHs (Eq. 3.6). Temperature dependent K_{OA} and P_L values for individual PAHs were calculated using the regression parameters recently reported by Odabasi et al. (2006a) and (2006b).

The plots of log K_P (experimental) vs. log P_L and log K_P (experimental) vs. log K_{OA} were derived for the whole number of sampling events and good correlations were found (r^2=0.82, m=-0.64, b=-4.1 for P_L and r^2=0.84, m=0.66, b=-8.5 for K_{OA}). For individual samples, r^2 values were between 0.83-0.97 for P_L and between 0.85-0.98 for K_{OA}. The regression parameters, m and b were -0.50 to -0.99, and -3.3 to -6.0 for P_L, respectively while the same parameters were 0.52 to 1.0 and -6.8 to -12.7 for K_{OA}. For some samples, the regression slopes of log K_P vs. log P_L and log K_P vs. log K_{OA} were different from the expected value of -1 and 1 (equilibrium), respectively. However, similar results were observed for PAHs in recent studies. Demircioglu (2008) correlated log K_P vs. log K_{OA} values of PAHs for all samples and found the regression parameters, m and b as 0.48 and -6.36 for suburban Izmir and 0.89 and -10.7 for urban Izmir. Regression parameters obtained at urban Izmir were similar to the ones obtained at the present study. The variation in slopes between suburban and urban sites was attributed to the different size distributions and sorbing properties of atmospheric particles measured for different sites (Demircioglu, 2008). Vardar et al. (2004) reported gas-particle partitioning results of PAHs for the lake and land samples in Chicago. They expected that the lake samples were closer to equilibrium than the land samples as they travel further from their source and had higher residence time in the atmosphere (aged particles). However, more shallow slopes for lake samples than the land samples were observed and this was attributed to non-exchangeability and differences in activity coefficients of PAHs. Lohmann et al. (2000) also reported the average slopes for PAHs in log Kp vs. log P_L (-0.8, -0.7) and log K_P vs. log K_{OA} (0.8, 0.7) correlations at the rural and urban/industrial sites, respectively. As a result of higher m values observed for rural site, they concluded that locally released PAHs need to equilibrate to the ambient temperature and background particles which can result more shallow slopes than 1 or -1.

Log-log plots of overall average K_P (experimental) vs. P_L and K_P (experimental) vs. K_{OA} values of PAHs (n=15) were illustrated in Fig. 4.3. Although two approaches are essentially equivalent, slightly higher r^2 value was observed in relationship with log K_P and log K_{OA}. Harner & Bidleman (1998) reported relatively higher slope for K_{OA} (0.83) than for P_L (-0.75) in log-log correlations of average K_P vs. P_L and K_P vs.

K_{OA} values of PAHs (n=4). As a result of observed good correlation between log K_P and log K_{OA}, they suggested that K_{OA} is a useful predictor for the partitioning of PAHs into aerosol organic matter.
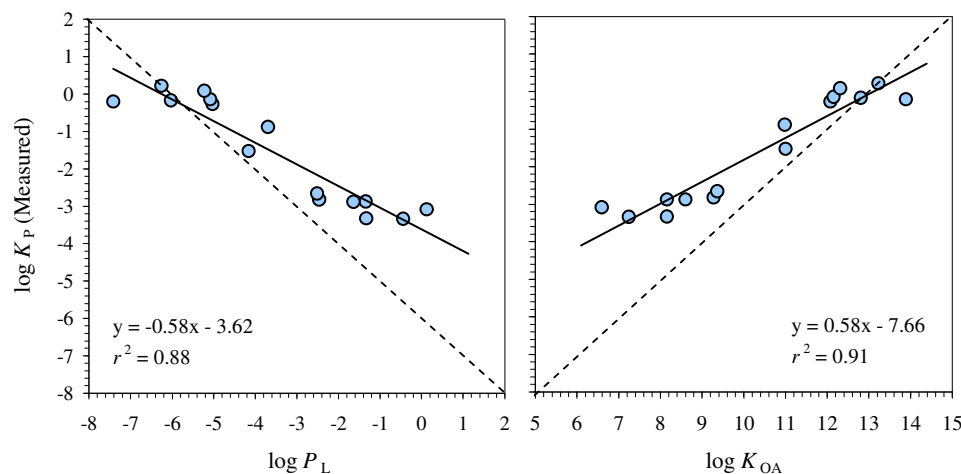
Figure 4.3 Plots of log K_P measured at the air sampling site vs. log P_L and log K_P vs. log K_{OA} for individual PAHs. The solid diagonal line represents a 1:1 relationship (equilibrium).

K_{OA} model (absorptive partitioning) and soot model (both absorptive and adsorptive partitioning) based K_P values for PAHs were determined using Eq. (3.13) and (3.14), respectively. For all sample events, the modeled results were compared with the measured values of K_P in Fig. 4.4. Although the agreement between the measured and modeled values was good (r^2=0.86, p<0.01), both models significantly predicted lower partition coefficients than those experimental values especially for 3-rings PAHs and higher partition coefficients for indeno[1,2,3-cd]pyrene and benzo[g,h,i]perylene. However, predictions for PAHs obtained by soot model were significantly better than those obtained by K_{OA} model. The range of measured/modeled K_P values was between 0.3±0.2-341±158 for K_{OA} model and between 0.2±0.1-109±51 (benzo[g,h,i]perylene-acenaphthene) for soot model. Their overall average ratios were 20±63 and 7±21, respectively. At a study conducted by Odabasi et al. (2006a) in urban Izmir, the ratios of measured/modeled partition coefficients varied from 1.1 (chrysene) to 15.5 (fluorene) for K_{OA} model, and from 0.6 (chrysene) to 4.5 (fluorene) for soot model. Better predictions of K_P values for

PAHs from soot model than those from K_{OA} model were also reported by Dachs & Eisenreich (2000), Demircioglu (2008), Lohmann & Lammel (2004) and Vardar et al. (2004). High K_P values for PAHs were related to the non-exchangeable fraction in soot particles by Dachs & Eisenreich (2000) and Harner & Bidleman (1998). They suggested that some of these PAHs may be extracted during analysis, and thus, non-exchangeable effect usually causes curvature in log-log plots of K_P vs. P_L or K_P vs. K_{OA}.
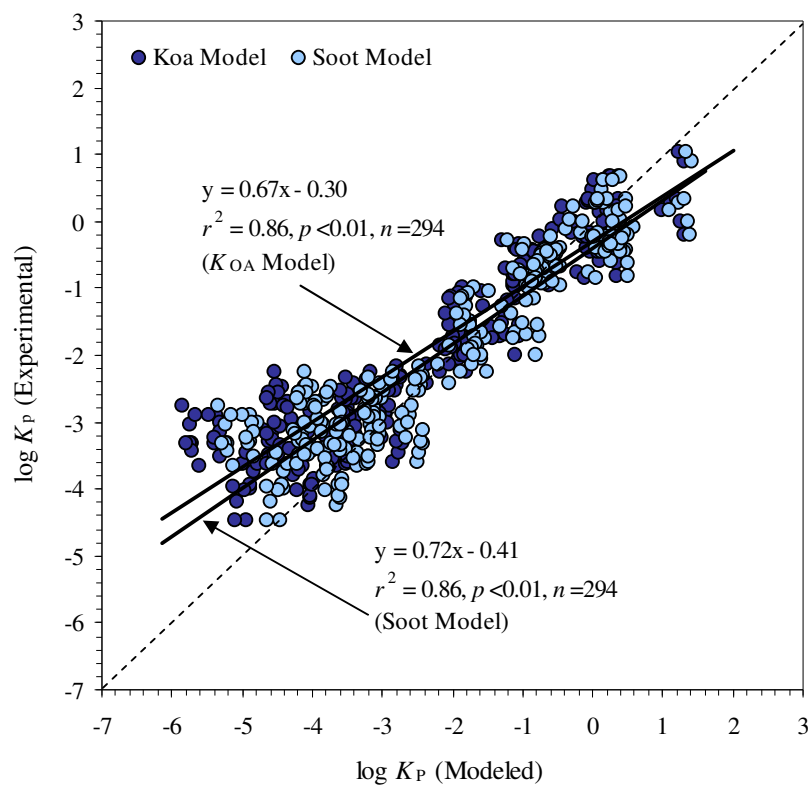
Figure 4.4 Comparison of the measured and predicted log K_P values by two partitioning models. The solid diagonal line represents a 1:1 relationship (equilibrium).

The fraction (ϕ) of individual PAHs in particle-phase was experimentally calculated using Eq. (3.4). Fig. 4.5 compares the average percent on particles (100×ϕ) as predicted by Junge-Pankow adsorption (Eq. 3.8) and K_{OA} absorption model (Eq. 3.7) with experimental values. The agreement between the measured and predicted phase distribution of PAHs was good. Experimental ϕ was also correlated

with the ones predicted by Junge-Pankow adsorption and K_{OA} absorption model for all data set, and statistically significant relationships were found (r^2=0.91, m=0.91, p<0.01, n=325, and r^2=0.95, m=0.93, p<0.01, n=294, respectively).
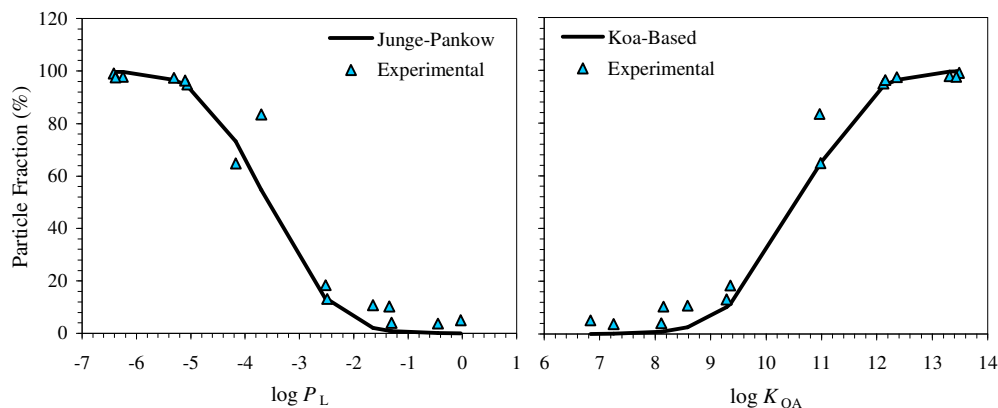
Figure 4.5 Comparison of measured particle fraction for PAHs with those obtained by Junge-Pankow adsorption and K_{OA} absorption model.

PAHs from acenaphthene through pyrene were predicted predominantly in gas-phase (ϕ<1% and <13%). Benz[a]anthracene and chrysene were found in both phases (ϕ=55-73%). But, PAHs from benzo[b]fluoranthene through benzo[g,h,i]perylene were mostly particulate (ϕ>94%). The same trend for PAHs was observed previously by Harner & Bidleman (1998) and Lohmann & Lammel (2004). However, experimental proportion of PAHs from acenaphthene to carbazole in particle-phase was higher than those predicted values. The ratio of measured/modeled ϕ values for these compounds was between 134 (acenaphthene)- 4.4 (phenanthrene) for Junge-Pankow adsorption model and between 118 (acenaphthene)- 4.2 (carbozole) for K_{AO} absorption model. Under-predicted ϕ values for the lower molecular weight PAHs were also reported by Lohmann & Lammel (2004). Particulate fraction values of PAHs from fluoranthene to benzo[g,h,i]perylene were generally good predicted using models. The range of measured/modeled ϕ ratio was between 0.9 (chrysene)-1.5 (benz[a]anthracene) and 1.0 (PAHs from chrysene to benzo[g,h,i]perylene)-1.6 (pyrene) for Junge-Pankow adsorption and K_{AO} absorption models, respectively. Generally, predictions using K_{OA} model were better than those obtained using Junge-

Pankow model. This result was supported by Kaupp & McLachlan (1999a) suggesting that absorption is the main mechanism for partitioning of SOCs to urban particulate matter.

4.1.2 Particle-Phase Dry Deposition Fluxes and Velocities of PAHs

Table 4.3 shows the particle-phase dry deposition fluxes (F_d) and deposition velocities (V_d) of individual PAH compounds measured with dry deposition plates. Eq. (3.16) was used to calculate particle fluxes of individual PAHs, and their average values ranged between 54±32 (dibenz[*a,h*]anthracene) to 3788±911 (phenanthrene) ng m^{-2} day^{-1} in summer and between 9.7±7.1 (carbazole) to 1784±285 (phenanthrene) ng m^{-2} day^{-1} in winter. Average particle Σ_{15}-PAHs fluxes measured in summer and winter were 5792±3516 and 2650±1829 ng m^{-2} day^{-1}, respectively. Unlike the ambient PAH concentrations, dry deposition fluxes were higher in summer than in winter. Due to the prevailing Mediterranean climate in this area, the soil is dry with a weaker vegetation cover in summer. Since large particles dominate the atmospheric dry deposition, higher summer fluxes can be attributed to larger particles from enhanced re-suspension of polluted soil particles and road dust.

Dry deposition fluxes of particle-phase PAHs measured in this study were within the range of previously reported values elsewhere in Table 2.7. The particle fluxes of PAHs measured by Tasdemir & Esen (2007b) for urban Bursa and by Franz et al. (1998) for rural Lake Michigan were relatively lower than the ones measured at the sampling site in Aliaga. However, fluxes reported for the suburban and urban sites in Izmir (Demircioglu, 2008), for urban Chicago (Bae et al., 2002; Odabasi et al., 1999a), and for the industrial, urban, and rural sites in Taiwan (Fang et al., 2004) were considerably higher than those reported values in this study.

Table 4.3 Particle-phase dry deposition fluxes (F_d) and deposition velocities (V_d) of individual PAHs measured at the air sampling site.

| | F_d (ng m^{-2} day^{-1}) | | | | | | | | | | V_d (cm s^{-1}) | | |
| | Summer | | | | | Winter | | | | | Overall | | |
PAHs	Min.	Max.	Geometric Mean	Median	Avg±SD	Min.	Max.	Geometric Mean	Median	Avg±SD	Geometric Mean	Median	Avg±SD
ACT	231	1676	597	612	703±412	236	244	240	240	240±4.0	11	13	12±2.7
FLN	478	4808	1509	1797	1801±1135	424	776	632	702	645±121	8.1	11	8.8±3.3
PHE	2023	5315	3664	3847	3788±911	1526	2182	1762	1644	1784±285	6.1	6.3	7.4±4.8
ANT	39	435	141	178	181±121	72	203	120	115	124±35	2.9	2.2	4.6±4.8
CRB	23	179	65	71	75±39	3.7	33	8.2	7.7	9.7±7.1	1.7	1.9	3.4±3.6
FL	206	775	430	448	459±157	223	883	370	323	403±186	1.0	0.8	1.8±2.2
PY	262	890	403	369	435±189	185	599	312	250	343±153	1.0	1.4	1.7±1.6
BaA	46	215	104	96	124±90.7	67	437	135	127	162±109	0.5	0.7	0.9±0.8
CHR	99	542	213	235	236±110	125	1655	445	408	563±435	0.5	0.5	0.6±0.4
BbF	64	199	117	128	123±38	50	547	157	136	195±137	0.3	0.4	0.4±0.3
BkF	44	335	99	106	114±70	36	310	110	110	131±78	0.4	0.3	0.5±0.5
BaP	35	404	76	80	97±90	29	271	86	88	105±71	0.4	0.3	0.6±0.7
IcdP	37	305	85	90	100±65	9.3	119	35	28	48±37	0.2	0.2	0.5±0.6
DahA	18	133	45	45	54±32	21	157	39	28	51±43	0.4	0.5	0.6±0.6
BghiP	44	762	108	112	153±180	31	361	110	103	137±98	0.3	0.3	0.6±0.9
ΣPAHs	502	10252	4003	7310	5792±3516	430	7294	2115	1995	2650±1829	0.7	0.7	1.9±3.2

Low molecular weight PAHs had a larger fraction in the dry deposition flux similar to their large contribution to the atmospheric concentrations (Table 4.3, Fig. 4.8). Phenanthrene, fluorene, acenaphthene, and fluoranthene accounted for 45, 21, 8, and 5% of Σ_{15}-PAH fluxes in summer, while phenanthrene, fluorene, chrysene, and fluoranthene accounted for 36, 13, 11, and 8% of Σ_{15}-PAH fluxes in winter, respectively.

Measured dry deposition fluxes were plotted against the atmospheric concentrations of particle-phase PAHs to investigate their relationship. All compounds analyzed and all samples collected in summer (n=175) and winter (n=159) sampling periods were included. The correlations between the fluxes and the concentrations were statistically significant for summer (r^2=0.23, p<0.01) and winter periods (r^2=0.49, p<0.01).

Particle-phase dry deposition velocities (V_d, cm s^{-1}) of PAHs were calculated using the dry deposition fluxes measured with dry deposition plates and atmospheric particle-phase concentrations, using Eq. (3.17). V_d values for PAHs ranged between 0.7±0.2 cm s^{-1} (benz[b]fluoranthene) and 12±2.7 cm s^{-1} (acenaphthene) with an overall average of 2.8±3.6 cm s^{-1} in summer, and between 0.07±0.04 cm s^{-1} (indeno[1,2,3-cd]pyrene) and 9.1±2.5 cm s^{-1} (fluorene) with an overall average of 0.8±2.2 cm s^{-1} in winter. The seasonal differences in deposition velocities are probably due to the variations of particle size distribution and the meteorological conditions (i.e. wind speed, ambient air temperature, and atmospheric stability).

The overall V_d values for the individual PAHs are presented in Table 4.3. The overall average V_d for Σ_{15}-PAHs was 1.9±3.2 cm s^{-1}. This value is higher than the ones typically assumed to calculate PAH dry deposition, however, it agrees well with the values determined using similar measurement techniques for dry deposition fluxes, as reported in Table 2.9. Using greased dry deposition plates, Franz et al. (1998) have reported that deposition velocities for the individual PAHs were between 0.4-2.1 and 1.0-3.7 cm s^{-1} in summer and winter in Chicago, respectively.

Odabasi et al. (1999a) calculated V_d values between 4.3-9.8 cm s^{-1} with an average of 6.7 cm s^{-1} in urban Chicago for a summer/fall period. Similarly, Vardar et al. (2002) have reported the mean overall dry deposition velocity of PAHs as 4.5 cm s^{-1} for winter period in Chicago. Demircioglu (2008) found the difference in deposition velocities of PAHs measured at suburban and urban sites of Izmir with an overall average of 1.5±2.4 and 1.0±2.3 cm s^{-1}, respectively. This was attributed to different size distributions of urban and suburban particles.
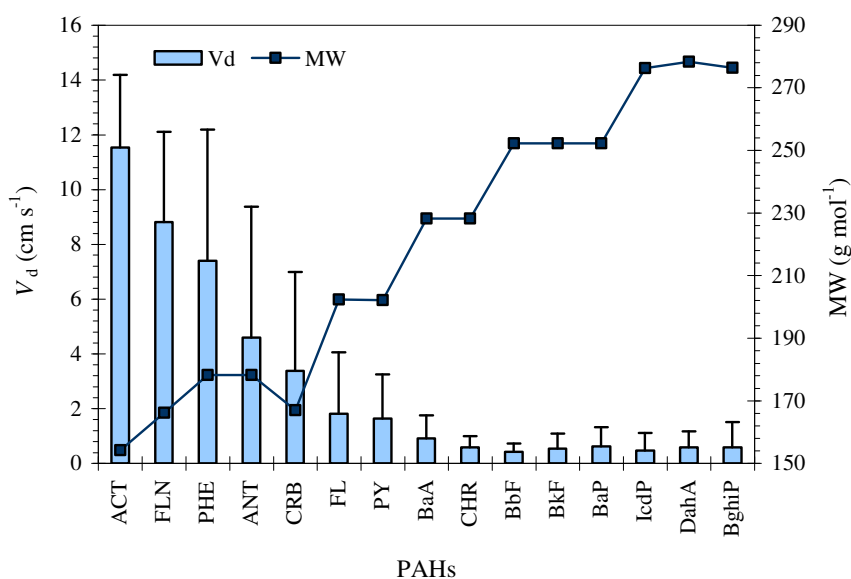
Figure 4.6 Overall average particulate dry deposition velocities of PAHs. Error bars are 1 SD.

Particle deposition velocity for individual PAHs generally decreased with increasing molecular weight (Fig. 4.6). The overall average V_d values for PAHs with molecular weights between 154-202 was 4.2±4.4 cm s^{-1} and for PAHs with molecular weights between 228-276 it was 0.6±0.7 cm s^{-1}. The overall dry deposition velocity for individual PAHs were well correlated with molecular weight (r^2=0.67, p<0.01). This decrease in deposition velocity with increasing molecular weight is supported by other experimental studies which have indicated that a greater fraction of the higher molecular weight PAHs are associated with fine particles relative to the lower molecular weight compounds (Allen et al., 1996; Kaupp & McLahlan, 1999b;

Kiss, Varga-Puchony, Rohrbacher, & Hlavay, 1998). A similar decrease in deposition velocity with increasing molecular weight was previously reported for PAHs (Demircioglu, 2008; Franz et al., 1998; Odabasi et al., 1999a; Shannigrahi, Fukushima, & Ozaki, 2005; Vardar et al., 2002).

4.1.3 PAHs in Soil

4.1.3.1 Soil Concentrations of PAHs

Table 4.4 shows the Σ_{15}-PAH levels in soils at the study area (n=48). Locations of the sampling points are illustrated in Fig. 3.2. Σ_{15}-PAH concentrations in soils ranged between 11 (rural site) and 4628 (industrial site) µg kg^{-1} (dry wt). They were within the range of previously reported values in Table 2.10. Soil Σ_{15}-PAH concentrations reported by Zhang et al. (2006) for the urban and rural sites in Hong Kong and Nadal et al. (2004) for the industrial, residential, and unpolluted sites in Spain were lower than the values obtained in this study while other investigations have reported similar or higher Σ_{15}-PAH values (Motelay-Massei et al., 2004).

Table 4.4 Σ_{15}-PAH concentrations (µg kg^{-1}, dry wt) in soils taken from the study area (n=48).

SN	Site	Σ_{15}-PAHs	SN	Site	Σ_{15}-PAHs	SN	Site	Σ_{15}-PAHs
1	1	197	17	18	97	33	39	69
2	2	24	18	19	158	34	42	880
3	3	26	19	20	1109	35	43	23
4	4	56	20	22	56	36	44	1368
5	5	11	21	23	34	37	45	53
6	6	87	22	24	243	38	46	318
7	7	102	23	25	4628	39	47	89
8	9	15	24	26	133	40	48	95
9	10	13	25	29	144	41	49	29
10	11	2059	26	30	188	42	50	54
11	12	42	27	32	49	43	53	94
12	13	295	28	33	94	44	54	38
13	14	26	29	34	212	45	55	38
14	15	40	30	35	248	46	58	2316
15	16	140	31	36	137	47	59	447
16	17	279	32	37	33	48	60	185

SN: Sample number.

Soil concentrations of individual PAHs were analyzed for all sampling points (*n*=48), and Pearson product correlation coefficients (*r*) were obtained. Statistically significant correlation factors between all individual PAHs (*r*=0.75-1.0) were found and this indicated that their concentrations in soils had similar distribution patterns between the sites.
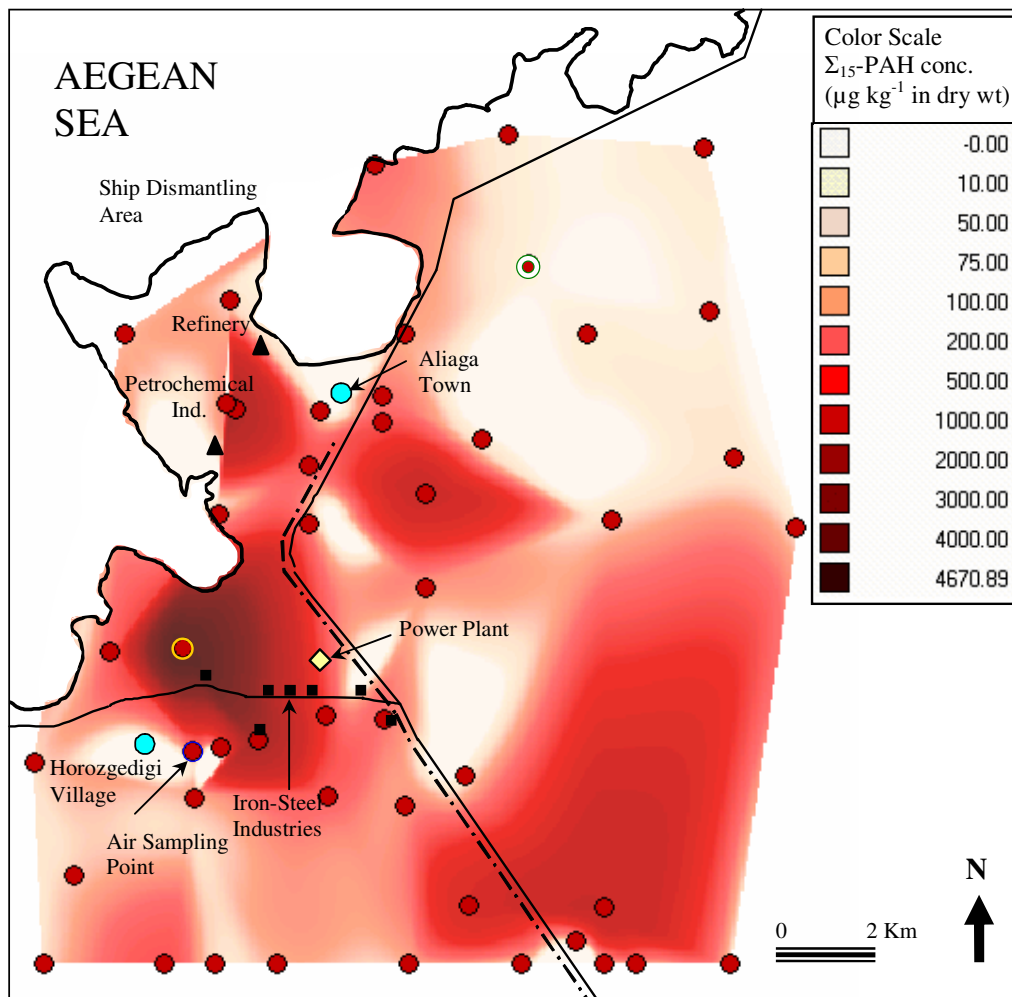
Figure 4.7 Spatial distribution of soil Σ_{15}-PAH concentrations in the study area (● : soil sampling points, ◐: residential areas, ◉: rural site, ○: industrial site).

Spatial distribution of Σ_{15}-PAH concentrations in soils (*n*=48) was mapped out by MapInfo Professional (Version 7.5) with Vertical Mapper (Version 3.0) (Fig. 4.7). The highest Σ_{15}-PAH concentrations were measured around the Aliaga town, steel

plants, the petroleum refinery, and the petrochemical plant indicating that these are the major PAH sources in the area.

The average PAH concentrations of the soil samples taken from the air sampling site (*n*=4 for summer and *n*=3 for winter) and the sites having maximum and minimum PAH concentrations are presented in Table 4.5. Seasonal PAH concentrations in soils were only measured at the air sampling site. Average soil Σ_{15}-PAH concentrations were 354±164 and 317±32 μg kg^{-1} (dry wt) in summer and winter, respectively. Results indicated that there were not large seasonal variations in soil concentrations of individual PAHs (summer/winter concentration ratio was between 0.75-1.4). The soil Σ_{15}-PAH concentrations at the air sampling site was relatively low than the ones at the industrial site. This site was not affected significantly by the major sources in the area. Thus, the relatively low atmospheric concentrations measured at the air sampling site can be attributed to its location and the prevailing wind direction.

Table 4.5 Individual PAH concentrations in soils (μg kg^{-1}, dry wt) at the air sampling site and at the sites having minimum (rural) and maximum (industrial) PAH levels in the study area.

	Air sampling Site (SN:29)										Rural Site (SN:5)	Industrial Site (SN:25)
	Summer (*n*=4)					Winter (*n*=3)						
PAHs	Min.	Max.	GM	M	Avg±SD	Min.	Max.	GM	M	Avg±SD		
ACT	1.3	2.1	1.8	2.0	1.9±0.4	1.2	4.1	2.0	1.6	2.3±1.6	*nd*	29
FLN	2.0	3.6	2.6	2.6	2.7±0.7	2.2	3.3	2.9	3.2	2.9±0.6	*nd*	60
PHE	14	38	25	28	27±10	27	30	29	28	29±1.5	1.2	648
ANT	1.9	5.6	3.8	4.4	4.1±1.7	4.1	4.5	4.4	4.5	4.4±0.3	0.07	130
CRB	0.2	0.9	0.5	0.7	0.6±0.3	0.5	1.0	0.6	0.5	0.7±0.3	0.3	29
FL	13	45	29	36	32±14	32	38	35	36	35±2.9	2.3	504
PY	11	45	28	35	32±15	31	35	32	31	32±2.1	1.5	507
BaA	8.0	35	21	26	24±12	18	21	20	21	20±1.4	0.4	316
CHR	18	85	50	65	58±30	44	56	48	46	49±6.4	1.9	652
BbF	14	48	30	36	34±15	23	32	28	30	29±4.6	0.9	361
BkF	11	27	18	19	19±6.8	15	23	19	19	19±4.3	0.6	226
BaP	10	27	15	14	16±7.3	20	22	22	22	22±1.2	0.4	288
IcdP	10	33	22	25	24±10	17	23	20	22	21±3.0	0.5	209
DahA	7.5	49	23	29	28±18	12	22	16	16	17±5.0	0.2	196
BghiP	13	77	40	52	49±28	28	45	35	34	35±9.0	0.7	475
Σ_{15}-PAHs	137	522	315	374	352±164	282	343	316	327	317±32	11	4628

SN: Site number, GM: Geometric Mean, M: Median, *nd*: Not detected.
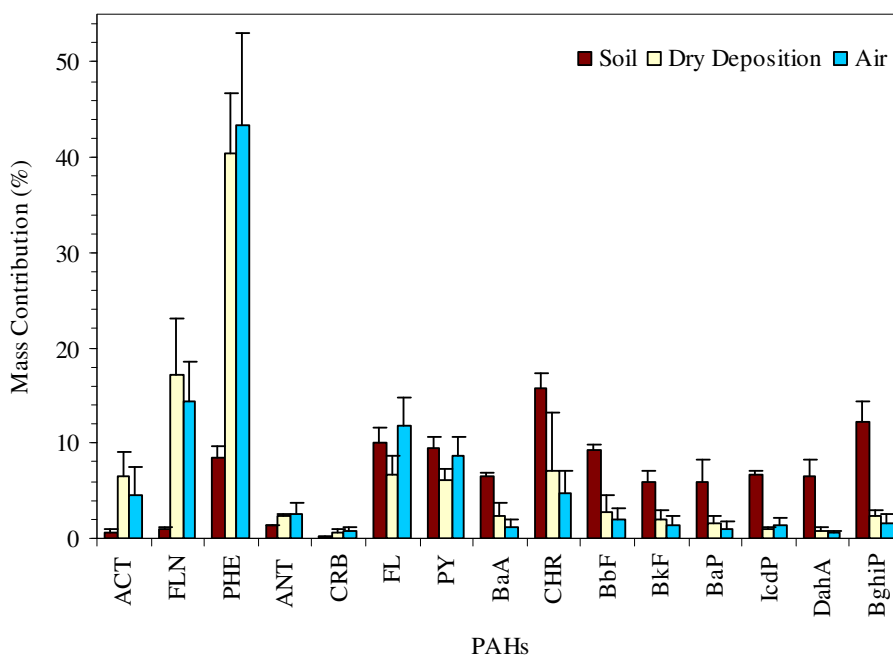
Figure 4.8 Overall averages PAH profiles in soil, dry deposition, and ambient air samples. Error bars are 1 SD.

Fig. 4.8 shows the overall average PAH profiles in soil (n=7), dry deposition (n=28), and ambient air (n=28) samples. Unlike the air samples, the PAH profile in soil was dominated by high molecular weight compounds. Chrysene, benzo[g,h,i]perylene, fluoranthene, and pyrene accounted for 16, 13, 10, and 9% of the Σ_{15}-PAHs, respectively. Since the sampling point is relatively close to the local sources, this can be explained by the 4-6-ring PAHs being deposited more easily close to the point sources than the lower molecular weight ones which are mainly in gaseous form and capable of long-range transport (Nadal et al., 2004). Although the Σ_{15}-PAH concentrations of ambient air were dominated by 3-ring PAHs, they accounted for only 11% of the total PAHs in soil. The difference in air and soil PAH profiles is also due to their different partitioning behaviors (i.e. low molecular weight compounds have relatively low soil-air partition coefficients). Volatilization from the previously polluted surfaces as a result of enhanced ambient air temperature and wind speed was suggested to be the dominant loss mechanism especially for the low molecular weight PAHs (Cousins, Beck, & Jones, 1999; Cousins & Jones, 1998). Soil PAH profiles were also variable for different sites, probably due to the sources

having different profiles affecting those sites. Variable distances from the sources may also have resulted in a change of PAH profiles during the transport.

4.1.3.2 Soil-Air Gas Exchange Fluxes of PAHs

The fugacity ratios (f_S/f_A) and soil-air gas exchange fluxes for PAHs were calculated at the air sampling site using the air ($n=28$) and soil concentrations ($n=7$) corresponding to the same sampling periods. K_{OA} values of the individual PAHs used for Eq. (3.19) were calculated as a function of temperature using the regression parameters recently reported by Odabasi et al. (2006a) and (2006b). Q_{SA} values were calculated using Eq. (3.18). A statistically significant correlation was found between log K_{OA} and log Q_{SA} values of all individual PAHs ($r^2=0.89$, $p<0.01$, $n=359$) indicating that the octanol is a good surrogate for soil organic matter (Fig. 4.9).
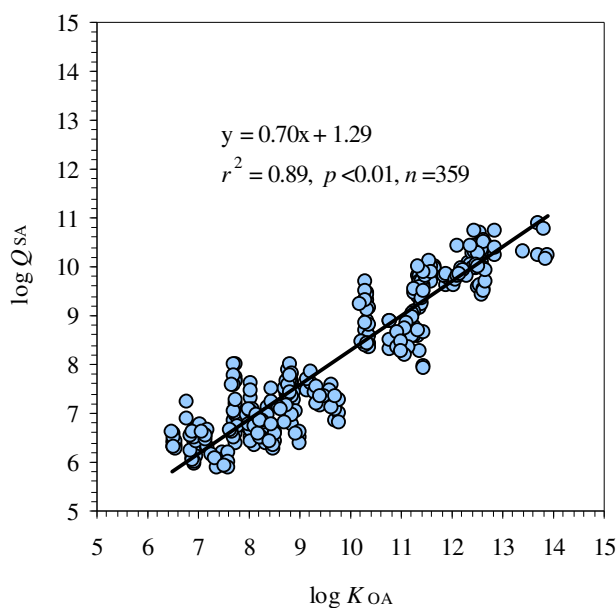
Figure 4.9 log K_{OA} vs. log Q_{SA} for all individual PAHs.

For a system in equilibrium, f_S/f_A value is approximately equal to 1 (Harner, Green, & Jones, 2000; Cousins & Jones, 1998). A propagation of the errors that are

associated with the calculation indicated that the equilibrium is represented by an f_S/f_A of 1.0±0.26 (i.e. a range of 0.74-1.26). Generally, the fugacity ratios of all compounds fell outside this uncertainty range and it can be concluded that for these compounds the soil and ambient air were not in equilibrium. For some samples (overall, 8% of the data set, n=360), the fugacity ratios especially for fluorene through pyrene were in the equilibrium range of 1.0±0.26.
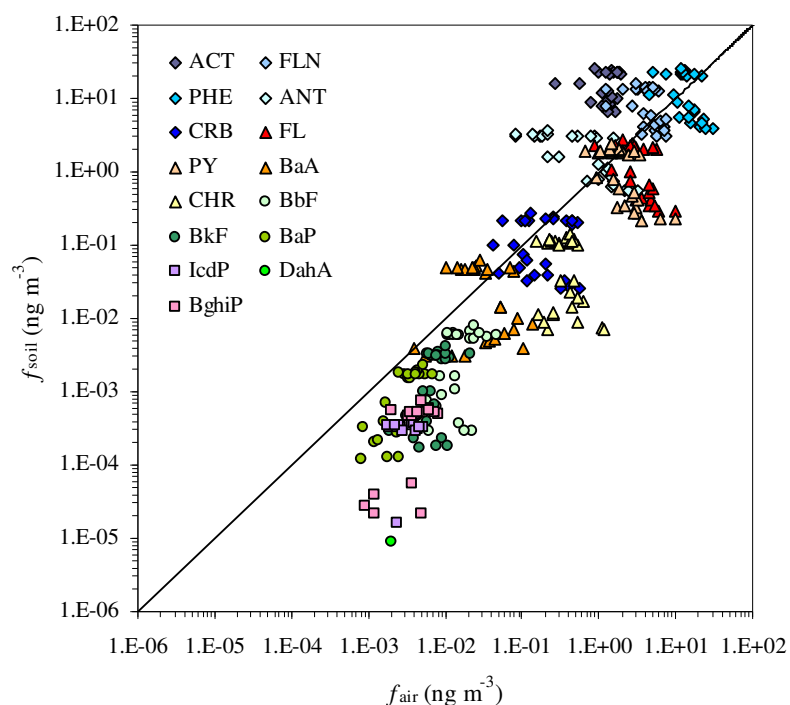
Figure 4.10 Relationship between the PAH fugacities (f) in air and soil.
The solid diagonal line represents a 1:1 relationship (equilibrium).

The relationship between the PAH fugacities in air and soil determined for both seasons is illustrated in Fig. 4.10. This figure indicated that the contaminated soil acted as a secondary source to the atmosphere for low molecular weight PAHs (acenaphthene-carbazole) for some samples. Similarly, Cousins & Jones (1998) have reported fugacity ratios greater than 1 for the low molecular weight PAHs. Soil-air partitioning of the medium volatility compounds (fluoranthene-benz[a]anthracene) was more sensitive to the seasonal air concentration and ambient air temperature

changes than the compounds having lower and higher volatility as indicated by their shift from volatilization to deposition from summer to winter. The heavier molecular weight ones (chrysene-benzo[g,h,i]perylene) with f_S/f_A values of <1 had a tendency to deposition. Once deposited, the heavier PAHs with high K_{SA} values tend to accumulate in soil for long periods. Thus, the soil acted as a sink for these compounds during both seasons (Fig. 4.10).
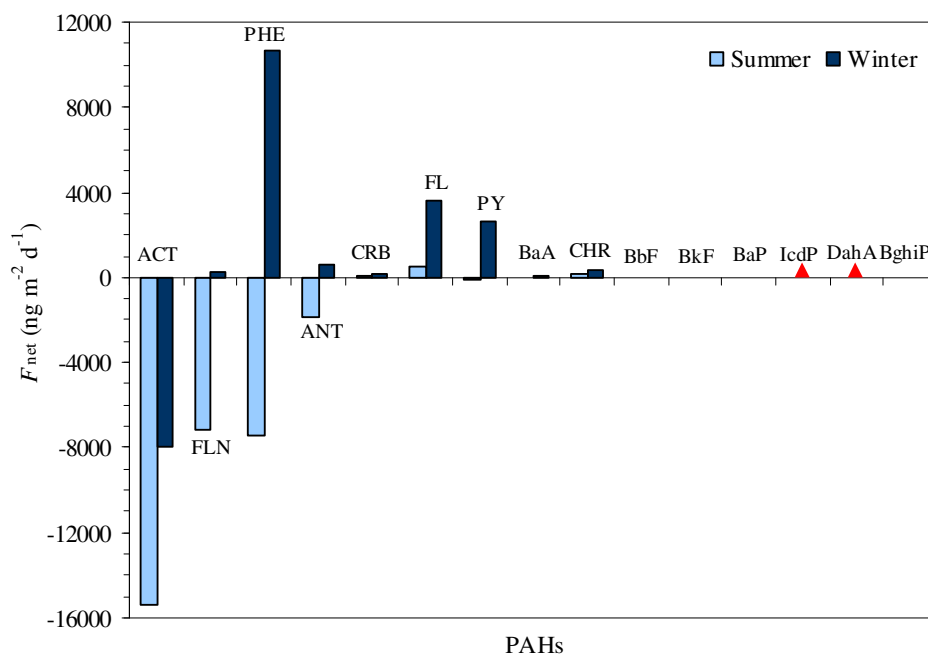
Figure 4.11 Calculated instantaneous soil-air net gas exchange fluxes (F_{net}) for two sampling periods. Negative values indicate net gas volatilization from the soil. (▲ : Not calculated).

For the samples that the soil and ambient air were not in equilibrium, the average estimated uncertainty in the soil-air net gas exchange fluxes (F_{net}) by error propagation ranged between ±43% (indeno[1,2,3-cd]pyrene, benzo[g,h,i]perylene) and ±57% (phenanthrene) with an overall average of ±50%. Relatively higher uncertainty values for some PAHs (especially low molecular weight ones) were probably due to their proximity to equilibrium.

Table 4.6 shows the calculated instantaneous soil-air net gas exchange fluxes (F_{net}) and MTCs for individual PAHs, using Eq. (3.20) and (3.21), respectively. Negative values indicate a net gas volatilization from soil to air and positive ones indicate a net gas deposition from air to soil. The ranges for the average net gas fluxes of PAH compounds were between 1.7±0.96 (benz[*a*]pyrene) and 15375±3690 ng m^{-2} day^{-1} (acenaphthene) in summer and between 1.1±0.73 (benz[*a*]pyrene) and 10647±8610 ng m^{-2} day^{-1} (phenanthrene) in winter. Low to medium molecular weight PAHs (acenaphthene-benz[*a*]anthracene) tended to volatilize in summer, but only acenaphthene had a tendency to volatilize in winter (Fig. 4.11). This result is consistent with the calculated soil/air fugacity ratios. Air temperature had a strong influence on the direction and magnitude of the gas-phase fluxes. For some PAHs (fluorine-benz[*a*]anthracene) a shift from volatilization to deposition was observed in winter. Generally, summertime gas exchange fluxes were higher than the wintertime ones, consistent with the measured higher gas-phase PAH concentrations in summer.

Table 4.6 Calculated MTCs (cm s^{-1}) and instantaneous soil-air net gas exchange fluxes (F_{net}, ng m^{-2} day^{-1}) of individual PAHs.

	Summer				Winter			
	MTC	F_{net}			MTC	F_{net}		
PAHs	Avg±SD	Min.	Max.	Avg±SD	Avg±SD	Min.	Max.	Avg±SD
ACT	0.86±0.22	-11313	-25105	-15375±3690	1.06±0.25	-3226	-17445	-7944±3882
FLN	0.84±0.22	-4777	-12512	-7162±2148	1.03±0.25	1276	-7402	220±4181
PHE	0.83±0.22	-3939	-17058	-7397±3604	1.02±0.25	5214	24215	10647±8610
ANT	0.83±0.22	-998	-2895	-1855±480	1.02±0.25	362	2100	628±1301
CRB	0.84±0.22	-62	264	50±155	1.03±0.25	20	455	146±168
FL	0.81±0.21	-362	2755	506±1332	1.00±0.24	477	11627	3578±2894
PY	0.81±0.21	-231	1223	-79±692	1.00±0.24	712	7427	2633±2025
BaA	0.78±0.21	-6.3	25	-11±15	0.96±0.24	2.6	97	38±28
CHR	0.78±0.21	62	309	168±83	0.96±0.24	131	1284	381±301
BbF	0.76±0.21	2.8	38	9.9±9.3	0.95±0.24	2.2	25	8.1±6.2
BkF	0.76±0.21	1.3	18	4.3±4.0	0.95±0.24	1.4	12	4.6±2.8
BaP	0.76±0.21	0.7	4.0	1.7±1.0	0.95±0.24	0.3	2.8	1.1±0.7
IcdP	0.75±0.20	0.7	5.0	2.0±1.1	0.93±0.24	*nc*	*nc*	*nc*
DahA	0.74±0.20	*nc*	*nc*	*nc*	0.92±0.24	*nc*	*nc*	*nc*
BghiP	0.75±0.20	0.7	7.8	2.9±1.7	0.94±0.24	0.7	4.3	1.9±1.5

nc: Not calculated.

Negative values indicate net gas volatilization from the soil.

Table 4.7 Annual fluxes (ng m^{-2} year^{-1}) and F_{SA}/F_{AS} ratios of PAH compounds.

PAHs	Wet Deposition[a]	Dry Deposition	Gas Absorption	Gas Volatilization	F_{SA}/F_{AS}
ACT	14,754	228,442	394,835	4,546,165	7.1
FLN	56,495	516,848	1,294,513	2,854,332	1.5
PHE	204,685	1,183,238	4,488,852	3,895,647	0.7
ANT	13,082	55,793	288,907	611,357	1.7
CRB	6,972	15,394	74,044	36,840	0.4
FL	43,000	156,869	1,178,097	330,852	0.2
PY	35,845	144,235	795,702	265,027	0.3
BaA	5,077	52,240	11,662	7,054	0.1
CHR	11,423	148,190	117,479	15,882	0.06
BbF	11,861	58,443	4,146	844	0.01
BkF	5,937	44,595	2,081	453	0.01
BaP	3,685	36,825	819	282	0.01
IcdP	6,564	27,023	803	73	0.002
DahA	2,813	19,110	*nc*	*nc*	*nc*
BghiP	5,689	52,838	1,056	94	0.002
ΣPAHs	427,882	2,740,082	8,652,998	12,564,902	

nd: Not calculated.
[a] Odabasi, 2007b.

Harner et al. (1995) have observed that the soil does not approach equilibrium with the air. This is because there is a significant non-diffusive transport from the air to the soil (e.g. wet and dry deposition) in addition to gas absorption onto the soil particles with only relatively slow emission into the air by volatilization. Table 4.7 shows the annual average fluxes of individual PAHs and the ratios of total fluxes representing soil to air (F_{SA}, i.e. gas volatilization) and air to soil (F_{AS}, i.e. gas absorption, dry and wet deposition) processes. Gas absorption and volatilization fluxes were calculated using Eq. (3.20). Wet deposition fluxes measured recently at a suburban site of Buca in Izmir during autumn 2005-spring 2006 (Odabasi, 2007b) were also used to estimate relative importance of different atmospheric processes. Additional mechanisms (e.g. reaction and leaching in soil) were ignored since it is not possible to estimate their magnitude and relative importance. All processes were comparable for Σ$_{15}$-PAHs but their input was dominated by gas absorption, especially for the low molecular weight PAHs. Gas absorption had a contribution of 73% to the atmospheric Σ$_{15}$-PAH inputs. Particle deposition was also significant mechanism for PAHs with a contribution of 23%. However, wet deposition accounted for only ~4%. The calculated F_{SA}/F_{AS} ratios of acenaphthene, florene, and

anthracene were above 1.0 suggesting that for these compounds, there was a net volatilization through the atmosphere. For the remaining PAHs, there was a net accumulation into the soil with F_{SA}/F_{AS} ratios less than 1.0 (Table 4.7).

4.2 Polychlorinated Biphenyls (PCBs)

4.2.1 PCBs in Ambient Air

4.2.1.1 Ambient Air Concentrations of PCBs

Total (gas+particle) Σ_{41}-PCB (sum of the 41 individual congeners) concentrations exhibited variability from 1024 to 7203 pg m^{-3} with an average of 3370±1617 pg m^{-3} in summer and from 288 to 2590 pg m^{-3} with an average of 1164±618 pg m^{-3} in winter (average±SD). Elevated ambient air concentrations during the summer months may be related to the increased volatilization rates of previously deposited PCBs on terrestrial surfaces. Observed seasonal cycling of PCB levels in air is supported by other recent studies that reporting similar observations (Cousins & Jones, 1998; Currado & Harrad, 2000; Hillery et al., 1997; Montone et al., 2003; Lee & Jones, 1999; Simcik et al., 1998; Stern et al. 1997; Yeo et al., 2003).

Σ_{41}-PCB concentrations from this study are relatively high in comparison with those previously reported values for other industrial and urban sites in Table 2.5. Cetin et al. (2007) reported similar total Σ_{36}-PCB concentrations of 3136±824 and 1371±642 pg m^{-3} at the same industrial site of Aliaga, and lower total Σ_{36}-PCB concentrations of 314±129 and 847±610 pg m^{-3} at urban Aliaga for summer and winter periods, respectively. For another urban site in Turkey, annual total Σ_{37}-PCB concentration of 492±189 pg m^{-3} on the average was measured by Cindoruk & Tasdemir (2006). Average total Σ_{50}-PCB concentration for summer-fall period was 1900±1700 pg m^{-3} at urban Chicago (Tasdemir et al., 2004a). Brunciak et al. (2001a) reported that the gas-phase average Σ_{83}-PCB concentrations in summer were 1180±420 pg m^{-3} at urban Baltimore and 550±220 pg m^{-3} at coastal Chesapeake

Bay. Average total Σ_{83}-PCB concentration at urban/industrial New Jersey was 1000 ± 820 pg m^{-3} (Brunciak et al., 2001b). Simcik et al. (1998) also reported Σ_{40}-PCB concentrations of 2971 and 303 pg m^{-3} in summer and winter periods for urban Chicago, respectively and 521 pg m^{-3} in summer for coastal Lake Michigan.

At the steel plants located close to the air sampling site, all kinds of scrap iron materials are stored, classified, cut into parts, and melted. PCBs may be present in the scrap, and emitted when the material is heated up during production or they may form as a result of thermal processes (Integrated Pollution Prevention and Control [IPPC], 2001). As a result, these industries may have a significant contribution to the PCB pollution in the study area. A recent study by Cetin et al. (2007) has also shown that these steel plants and polluted local soil significantly contribute to the particle-phase PCBs in the area. Relatively high PCB concentrations measured in this study were probably due to proximity of the sampling site to the steel plants as well as volatilization and re-suspension from the previously contaminated soils.

Table 4.8 shows the PCBs concentrations in air measured at this study. PCB congeners of 191, 205, and 208 were not detected at any of the ambient air samples (n=28). Total (gas+particle) PCB concentrations varied from 5.1 ± 3.6 (PCB-209) to 442 ± 210 pg m^{-3} (PCB-28) in summer and from 3.4 ± 2.7 (PCB-171) to 147 ± 75 pg m^{-3} (PCB-18) in winter. All PCBs except PCB-82, -194, and-206 had higher atmospheric concentrations in summer than in winter. Summer to winter ratios were between 0.9 (PCB-194) and 5.0 (PCB-17).

Table 4.8 Atmospheric concentrations (pg m^{-3}) of individual PCB congeners measured at the air sampling site (1/4).

| | Summer | | | | | | | | | | | | | | | |
| | Particle-Phase | | | | | Gas-Phase | | | | | Total (Gas+Particle) | | | | | |
PCB Congeners	Min.	Max.	Geometric Mean	Median	Avg±SD	Min.	Max.	Geometric Mean	Median	Avg±SD	Min.	Max.	Geometric Mean	Median	Avg±SD
18	2.3	19	5.5	6.3	6.6±4.5	42	888	276	328	367±251	45	897	283	333	374±252
17	1.6	20	4.7	4.5	6.1±5.2	41	1932	186	186	318±479	44	1941	196	189	324±480
31	4.1	20	7.6	7.6	8.4±4.2	62	1061	343	351	414±257	73	1072	355	364	423±257
28	3.8	18	8.4	8.8	9.1±3.8	63	792	373	404	433±210	74	806	385	416	442±210
33	4.8	23	8.7	8.5	9.4±4.5	57	627	244	263	289±158	65	637	255	270	298±159
52	3.6	17	6.3	6.3	6.9±3.5	55	392	208	224	227±84	62	336	216	232	234±84
49	3.5	16	5.9	5.5	6.8±4.1	38	309	158	169	174±69	44	317	165	178	181±70
44	2.3	8.4	4.1	3.9	4.4±2.1	46	198	89	97	95±39	46	202	92	100	99±39
74	2.7	4.8	3.4	3.2	3.5±0.8	37	96	62	64	64±14	37	99	63	66	65±15
70	1.9	13	4.2	3.9	4.8±2.9	41	165	95	101	99±28	47	171	100	109	104±29
95	1.7	5.3	2.4	2.2	2.6±1.0	40	152	71	77	76±31	45	155	73	80	78±31
101	1.2	16	3.0	3.0	3.9±3.8	35	139	92	101	96±26	39	142	95	103	100±27
99	1.1	5.4	1.8	1.7	2.0±1.1	12	46	30	32	32±8.2	14	47	32	33	33±8.5
87	2.7	2.8	2.8	2.8	2.8±0.1	26	52	36	37	37±7.2	26	55	36	37	37±7.7
110	1.7	5.2	3.4	3.9	3.6±1.2	26	92	55	59	57±16	31	96	59	63	61±16
82	*nd*	*nd*	*nd*	*nd*	*nd*	6.2	9.2	7.6	7.7	7.7±2.2	6.2	9.2	4.2	6.2	5.6±4.0
151	1.4	2.2	1.7	1.6	1.7±0.4	11	38	26	28	28±7.8	11	38	27	29	28±8.0
149	1.4	11	3.5	3.6	4.1±2.5	29	103	72	80	75±20	34	106	76	84	79±20
118	1.6	11	4.2	3.7	4.7±2.5	21	64	43	46	45±12	28	69	48	50	50±12
153	2.0	18	4.7	4.8	5.6±4.1	34	96	71	76	74±17	41	107	77	81	79±19
132	0.9	6.4	2.9	2.4	3.6±2.5	9.3	38	17	18	18±7.6	12	38	19	19	20±7.0
105	1.9	16	4.1	3.4	5.6±5.7	10	48	16	15	17±9.6	10	48	17	15	18±9.3

nd: Not detected.

Table 4.8 Atmospheric concentrations (pg m^{-3}) of individual PCB congeners measured at the air sampling site (2/4).

PCB Congeners	Summer														
	Particle-Phase					Gas-Phase					Total (Gas+Particle)				
	Min.	Max.	Geometric Mean	Median	Avg±SD	Min.	Max.	Geometric Mean	Median	Avg±SD	Min.	Max.	Geometric Mean	Median	Avg±SD
138	2.9	21	6.9	6.5	7.7±4.5	25	95	69	80	73±20	34	116	77	88	80±22
158	*nd*	*nd*	*nd*	*nd*	*nd*	6.5	48	9.8	8.5	12±12	6.5	48	10	8.5	12±12
187	1.3	3.6	2.7	3.0	2.8±0.7	17	35	25	27	26±6.6	18	36	27	27	27±6.6
183	1.4	2.6	2.1	2.5	2.1±0.6	8.6	19	14	15	14±3.7	9.4	21	14	15	15±4.0
128	*nd*	*nd*	*nd*	*nd*	*nd*	11	23	16	15	16±3.8	11	23	16	15	16±3.8
177	*nd*	*nd*	*nd*	*nd*	*nd*	6.5	15	12	12	12±2.6	6.5	15	12	12	12±2.6
171	*nd*	*nd*	*nd*	*nd*	*nd*	4.6	9.0	6.0	5.6	6.1±1.3	4.6	9.0	6.0	5.6	6.1±1.3
156	*nd*	*nd*	*nd*	*nd*	*nd*	4.1	10	7.6	8.0	7.8±2.0	4.1	10	7.6	8.0	7.8±2.0
180	3.0	8.4	5.8	5.5	6.1±1.8	13	52	33	32	35±11	21	59	40	38	41±11
191	*nd*	*nd*	*nd*	*nd*	*nd*	*nd*	*nd*	*nd*	*nd*	*nd*	*nd*	*nd*	*nd*	*nd*	*nd*
169	*nd*	*nd*	*nd*	*nd*	*nd*	8.8	17	12	13	13±3.2	10	17	13	13	13±2.8
170	2.5	7.4	4.8	5.0	5.0±1.7	11	25	18	17	19±4.5	11	29	18	19	19±7.0
199	*nd*	*nd*	*nd*	*nd*	*nd*	5.7	18	10	11	11±3.7	5.7	18	10	11	11.0±3.8
208	*nd*	*nd*	*nd*	*nd*	*nd*	*nd*	*nd*	*nd*	*nd*	*nd*	*nd*	*nd*	*nd*	*nd*	*nd*
195	*nd*	*nd*	*nd*	*nd*	*nd*	4.5	7.2	5.7	5.8	5.8±1.9	4.5	7.2	5.7	5.8	5.8±1.9
194	*nd*	*nd*	*nd*	*nd*	*nd*	5.5	12	8.4	8.6	8.7±2.8	5.5	12	8.4	8.6	8.7±2.8
205	*nd*	*nd*	*nd*	*nd*	*nd*	*nd*	*nd*	*nd*	*nd*	*nd*	*nd*	*nd*	*nd*	*nd*	*nd*
206	*nd*	*nd*	*nd*	*nd*	*nd*	*nd*	*nd*	*nd*	*nd*	*nd*	*nd*	*nd*	*nd*	*nd*	*nd*
209	1.7	5.1	2.9	3.4	3.4±2.5	3.5	10	6.0	6.8	6.8±4.6	3.5	10	4.2	4.3	5.1±3.6
∑PCBs	51	211	102	96	111±50	862	7041	2900	2833	3260±1618	1024	7203	3034	2982	3370±1617

nd: Not detected.

Table 4.8 Atmospheric concentrations (pg m^{-3}) of individual PCB congeners measured at the air sampling site (3/4).

| | Winter | | | | | | | | | | | | | | |
| | Particle-Phase | | | | | Gas-Phase | | | | | Total (Gas+Particle) | | | | |
PCB Congeners	Min.	Max.	Geometric Mean	Median	Avg±SD	Min.	Max.	Geometric Mean	Median	Avg±SD	Min.	Max.	Geometric Mean	Median	Avg±SD
18	1.9	13	4.2	4.1	5.0±3.3	16	268	113	144	142±74	18	279	119	147	147±75
17	1.0	8.9	2.5	2.3	3.1±2.3	8.9	117	53	68	64±32	11	123	56	70	68±33
31	1.4	14	4.6	3.9	5.4±3.4	19	137	83	102	97±44	21	195	88	105	102±47
28	1.3	14	5.1	5.4	6.0±3.4	25	182	89	102	101±45	26	196	94	107	108±48
33	3.2	15	6.5	5.9	7.0±3.1	20	165	74	85	84±38	24	180	81	90	91±40
52	1.8	14	4.4	3.7	5.2±3.4	22	154	72	85	84±43	25	162	77	87	89±45
49	1.7	9.4	3.6	3.4	4.0±2.3	15	87	47	56	52±22	18	97	51	57	56±23
44	1.3	15	3.9	3.7	5.2±4.4	15	91	41	44	47±23	15	102	44	53	51±25
74	1.4	7.1	3.0	3.0	3.6±2.2	7.6	37	19	21	21±9.8	1.4	43	17	20	22±13
70	2.5	18	5.1	3.9	6.2±4.7	12	76	35	40	40±22	12	94	38	42	45±25
95	1.2	15	2.8	1.8	3.8±3.9	10	73	29	33	37±24	9.6	85	31	34	40±27
101	1.8	26	4.1	3.0	6.1±7.1	12	83	29	31	37±26	13	94	33	34	43±31
99	1.2	11	2.5	1.9	3.3±3.0	5.3	31	11	12	14±9.5	5.8	37	13	12	16±12
87	4.0	20	9.8	11	11±6.6	7.1	35	14	13	17±11	6.7	48	16	13	20±16
110	2.2	36	6.3	4.0	9.8±11	9.2	57	22	22	28±19	9.2	82	27	23	36±27
82	1.3	6.3	3.0	3.5	3.5±2.0	1.8	8.1	4.0	3.9	4.5±2.1	1.8	14	4.7	4.1	5.7±3.8
151	1.1	13	2.2	1.5	3.4±4.1	2.6	16	6.0	6.5	7.4±4.6	2.6	29	7.0	6.5	9.3±7.5
149	1.7	46	5.3	4.1	8.7±12	6.3	41	18	19	22±13	8.5	86	23	22	30±22
118	1.1	41	5.7	4.6	9.9±12	6.6	38	15	14	18±12	9.0	68	21	15	27±21
153	1.0	78	7.3	6.1	14±20	6.7	36	16	15	19±11	11	112	25	24	33±28
132	1.3	19	3.4	2.8	4.8±5.0	2.9	13	5.9	4.8	7.0±4.1	3.4	30	8.8	7.5	11±7.9
105	1.9	21	5.8	4.8	8.1±6.9	2.6	13	5.8	6.4	6.6±3.5	2.6	31	8.2	7.2	11±9.3

nd: Not detected.

Table 4.8 Atmospheric concentrations (pg m^{-3}) of individual PCB congeners measured at the air sampling site (4/4).

| PCB Congeners | Winter | | | | | | | | | | | | | | |
| | Particle-Phase | | | | | Gas-Phase | | | | | Total (Gas+Particle) | | | | |
	Min.	Max.	Geometric Mean	Median	Avg±SD	Min.	Max.	Geometric Mean	Median	Avg±SD	Min.	Max.	Geometric Mean	Median	Avg±SD
138	4.8	111	15	13	24±30	5.9	41	16	17	20±12	9.1	143	29	26	41±37
158	4.6	10	6.1	5.4	6.4±2.5	1.2	5.1	2.6	2.8	2.9±1.4	1.2	14	3.3	2.8	4.7±4.2
187	0.9	23.2	3.1	2.7	4.6±6.0	1.7	8.1	3.7	3.7	4.0±1.8	1.7	29	6.4	6.4	8.0±6.6
183	1.2	14	2.5	2.3	3.4±3.8	1.3	4.9	2.2	2.2	2.4±1.0	1.3	17	3.8	4.4	4.8±3.9
128	6.9	14	9.9	9.7	10±3.8	3.1	6.2	4.3	4.3	4.5±1.6	3.1	14	6.5	6.6	7.4±4.1
177	2.0	16	3.7	2.7	5.0±5.2	1.4	5.0	2.4	2.3	2.6±1.1	1.4	19	4.2	4.4	5.6±4.8
171	0.7	7.6	1.9	1.9	2.8±2.8	1.2	2.1	1.6	1.6	1.6±0.4	1.4	8.8	2.8	2.7	3.4±2.7
156	4.3	8.9	5.6	5.1	5.8±2.2	1.7	2.7	2.1	2.2	2.2±0.7	1.7	8.9	4.0	4.3	4.6±2.5
180	1.7	73	8.3	7.7	13±18	2.4	14	3.7	3.5	4.3±3.1	2.4	76	12	12	17±18
191	nd	nd	nd	nd	nd	nd	nd	nd	nd	nd	nd	nd	nd	nd	nd
169	6.4	9.3	8.1	8.8	8.2±1.5	nd	nd	nd	nd	nd	6.4	9.3	8.1	8.8	8.2±1.5
170	1.9	43	7.0	6.8	9.9±11	1.7	6.9	3.1	3.1	3.7±2.5	1.7	43	7.1	7.4	10±11
199	4.9	18	7.8	5.3	9.4±7.5	2.1	2.3	2.2	2.2	2.2±0.1	2.1	18	6.2	6.2	8.2±6.9
208	nd	nd	nd	nd	nd	nd	nd	nd	nd	nd	nd	nd	nd	nd	nd
195	nd	nd	nd	nd	nd	nd	nd	nd	nd	nd	nd	nd	nd	nd	nd
194	5.6	19	8.4	7.0	9.6±6.2	nd	nd	nd	nd	nd	5.6	19	8.4	7.0	9.6±6.2
205	nd	nd	nd	nd	nd	nd	nd	nd	nd	nd	nd	nd	nd	nd	nd
206	7.2	12	9.2	9.3	9.4±2.3	nd	nd	nd	nd	nd	7.2	12	9.2	9.3	9.4±2.3
209	nd	nd	nd	nd	nd	nd	nd	nd	nd	nd	nd	nd	nd	nd	nd
∑PCBs	20	829	113	113	176±208	262	1775	865	1081	989±455	288	2590	994	1203	1164±618

nd: Not detected.

For both sampling periods, total PCB mass in air was dominated by lower chlorinated congeners. The tri-, tetra-, penta-CBs and the fractions of hexa-CBs through PCB-209 accounted for 55, 20, 11, and 14% of Σ_{41}-PCBs in summer, respectively. They were 44, 23, 17, and 16% in winter (Fig. 4.12). Seasonal variations of the congener profiles may be due to differences in the source profiles. Similar trends in the atmospheric mass contributions of PCB homologue groups were reported recently (Brunciak et al., 2001a and 2001b; Mandalakis & Stephanou, 2006; Montone et al., 2003; Yeo et al., 2003).
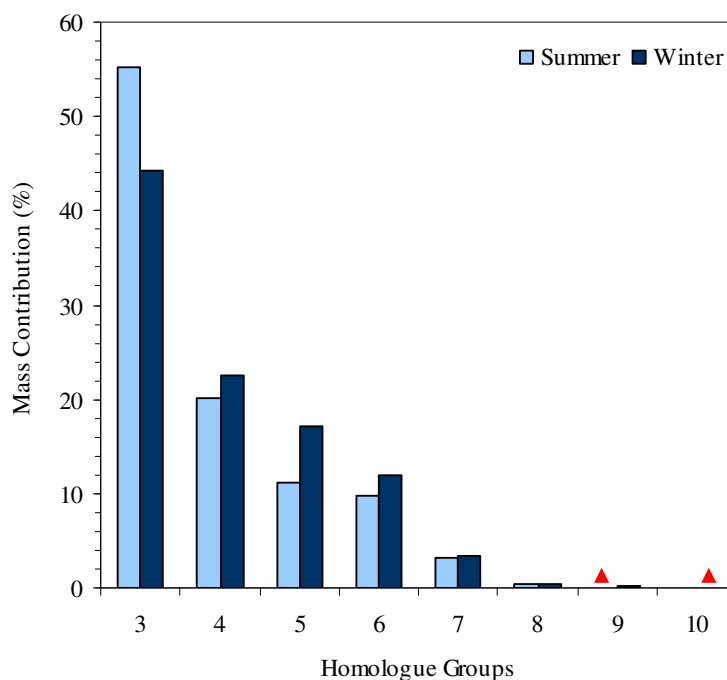

Figure 4.12 Contributions of PCB homologue groups to total PCB mass in air (▲ : Not detected).

Average gas- and particle-phase distributions of PCB homologue groups for the summer and winter sampling periods are illustrated in Fig. 4.13. Particle-phase percentage was higher during winter, especially for the heavier molecular weight PCBs. This might be due to the decrease in vapor pressures of the PCB congeners at lower temperatures. The average atmospheric concentrations of Σ_{41}-PCBs in gas-phase were 3260±1618 pg m^{-3} in summer and 989±455 pg m^{-3} in winter. For the

particle-phase, they were 111±50 and 176±208 pg m^{-3}, respectively (Table 2.8). Gas-phase concentrations constituted 96 and 79% of the total Σ_{41}-PCBs in air for the summer and winter periods, respectively. An increase in the gas-phase percentage of PCBs during summer months was also reported by Holsen, Noll, Liu, & Lee (1991), Mandalakis & Stephanou (2006), and Totten et al. (2004).
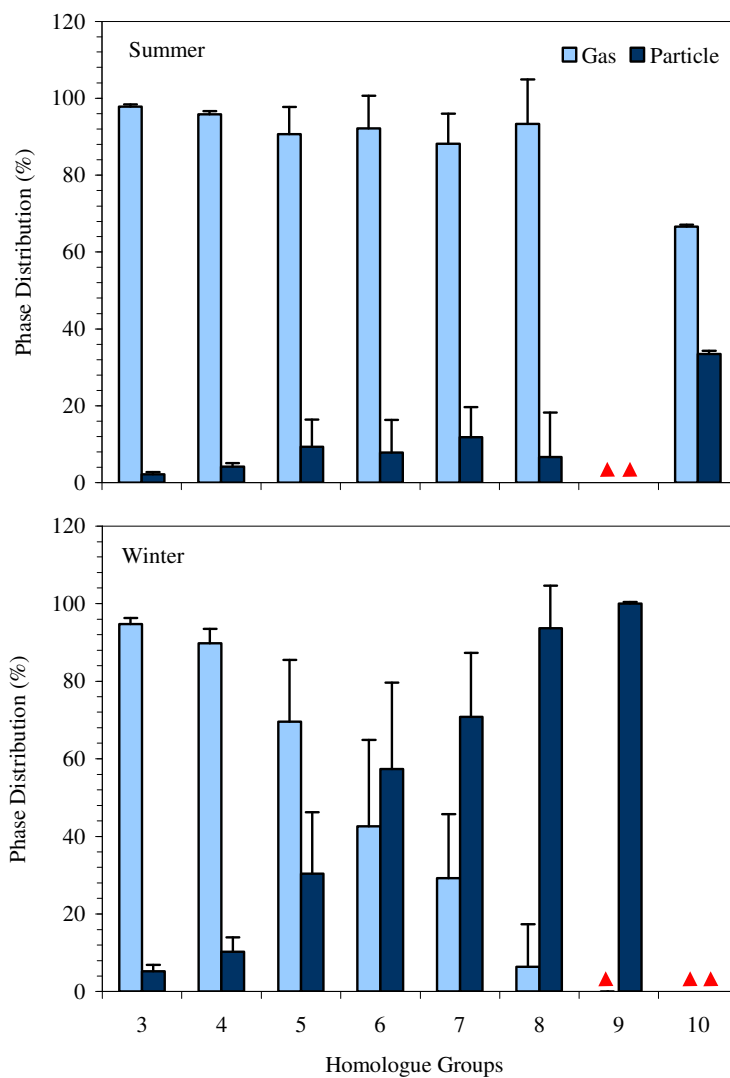

Figure 4.13 Average phase distributions of PCB homologue groups for both sampling periods. Error bars are 1 SD. (▲: Not detected).

4.2.1.2 Influence of Meteorological Parameters on PCB Levels in Air

The gas-phase ambient PCB concentrations depend on atmospheric variables such as wind speed, wind direction, and air temperature (Brunciak et al., 2001a). Eq. (3.1) was used to evaluate the relationship between the air temperature and the atmospheric concentrations of PCBs in gas-phase. For all of the studied PCB congeners, the temperature dependency of gas-phase concentrations was statistically significant ($p<0.05$-0.10) except PCB-82. The variation in temperature explained 4 to 91% (for PCB-82 and PCB-171, respectively) of the variability in gas-phase PCB concentrations. The regression slopes between -3252 (PCB-44) and -11044 (PCB-180) were relatively steep, and are consistent with those derived from other experimental studies (Brunciak et al., 2001b; Currado & Harrad, 2000; Mandalakis & Stephanou, 2006; Lee & Jones, 1999; Wania et al., 1998).

Table 4.9 Summary of regression parameters for Eq. (3.2).

PCBs	m_1	m_2	m_3	r^2	n	PCBs	m_1	m_2	m_3	r^2	n
18	-2116	-0.21[a]	0.67	0.34	28	149	-7407[a]	0.03	0.63[a]	0.56	28
17	-4150[b]	-0.20[a]	0.73	0.39	28	118	-5956[a]	0.06	0.56[b]	0.48	28
31	-5727[a]	-0.13[b]	0.84[a]	0.53	28	153	-8073[a]	0.04	0.63[a]	0.62	28
28	-6070[a]	-0.12	0.78[a]	0.56	28	132	-5339[a]	0.01	0.43	0.44	28
33	-4640[a]	-0.13[b]	0.63[b]	0.48	28	105	-5706[a]	0.05	0.43	0.47	27
52	-4526[a]	-0.07	0.72[a]	0.46	28	138	-7698[a]	0.02	0.54[b]	0.57	28
49	-5293[a]	-0.08	0.74[a]	0.55	28	158	-7500[a]	0.05	0.51	0.56	26
44	-3363[a]	-0.04	0.48[b]	0.37	28	187	-9541[a]	-0.04	0.78[a]	0.79	28
74	-6695[a]	0.03	0.83[a]	0.70	27	183	-8865[a]	-0.07	0.69[a]	0.83	28
70	-4957[a]	-0.001	0.65[a]	0.48	28	128	-7813[a]	-0.18	0.22	0.88	13
95	-4098[a]	-0.006	0.62[b]	0.32	28	177	-7108[a]	-0.09[a]	0.43[a]	0.86	24
101	-5842[a]	0.03	0.69[a]	0.45	28	171	-6852[a]	-0.02	-0.03	0.92	17
99	-5238[a]	0.04	0.57[b]	0.42	28	156	-7935[a]	-0.10	0.23	0.76	12
87	-5299[a]	0.06	0.56[a]	0.45	27	180	-10576[a]	-0.12[a]	0.62[a]	0.84	28
110	-4630[a]	0.03	0.56[b]	0.36	28	170	-6387[a]	-0.23[a]	0.62[a]	0.92	17
82	-3772	0.08	0.37	0.20	16	199	-9602[a]	-0.36	0.47	0.79	14
151	-7674[a]	0.02	0.78[a]	0.58	28						

[a] $p<0.05$.

[b] $p<0.10$.

Multiple linear regression (MLR) analysis was performed using Eq. (3.2) to investigate the effect of temperature, wind speed and direction on gas-phase atmospheric concentrations of individual PCBs. A summary of the MLR parameters is presented in Table 4.9. PCB congeners of 191, 169, 208, 195, 194, 205, 206 and 209 were detected in limited number of the samples. Therefore, MLR analysis results for these congeners were not reported. Temperature, wind speed and wind direction altogether accounted for 20 to 92% of the variability in gas-phase concentrations. Negative m_1 and m_2 values indicated that their gas-phase levels in air increased with temperature and decreased with wind speed, respectively. Relatively steep slopes (m_1) suggested that their ambient concentrations were influenced by short range or regional transport, and air-surface exchange from contaminated surfaces controlled the atmospheric levels in this area. Positive m_3 values showed that relatively higher gas-phase concentrations were observed when the wind was from northerly directions while the negative value points southerly directions. Based on statistically significant m_3 values, north of the sampling site might be an important source sector for most of the PCBs.

4.2.1.3 Gas-Particle Partitioning of PCBs

Partitioning between the gas- and particle-phases of PCBs in the air was assessed from models and measured values. Eq. (3.6) was performed to calculate the experimental partition coefficient (K_P) for PCBs measured at the air sampling site. Because the K_{OA} values as a function of temperature were not available for all PCBs, temperature dependent K_{OA} values of only 9 congeners (PCB-49, -95, -101, -105, -118, -138, -153, -171, and -180) were calculated using the regression parameters reported by Harner & Bidleman (1996). The K_{OA} values of PCB-82, -87, -99, and -128 at 20°C were taken from Chen et al. (2002), and the K_{OA} values of the remaining PCB congeners at 20°C were taken from Zhang et al. (1999). They were adjusted for temperature using the experimentally determined slopes of these 9 congeners. The adjustment was done based on the assumption of "similar compound" that was assessed using the chromatographic retention times of PCB congeners. Temperature

dependent P_L values for all of the studied PCBs were calculated using the regression parameters previously reported by Falconer & Bidleman (1994).

Plots of log K_P (experimental) vs. log P_L and log K_P (experimental) vs. log K_{OA} were derived for all samples and the resulting correlations were good (r^2=0.57 m=0.41, b=4.23 for P_L and r^2=0.60 m=0.41, b=6.97 for K_{OA}). For individual samples, r^2 values were between 0.22-0.97 for P_L and between 0.24-0.98 for K_{OA}. The regression parameters, m and b were -0.15 to -0.84, and -3.4 to -5.9 for P_L, respectively, while the same parameters were 0.15 to 0.82 and -4.4 to -11.2 for K_{OA}. Although good correlations were observed, regression slopes for P_L and K_{OA} were different from the expected value of -1 and 1 (equilibrium), respectively. Similar slope variations in log K_P vs. log P_L values of PCBs amongst samples were also observed by Tasdemir et al. (2004a) from the lake and land samples in Chicago, and this was attributed to the variations in ambient air concentrations and particulate characteristics (e.g. size, number of adsorption sites, water and OM content) during the sampling period. They found higher average slope for lake samples (-0.47±0.35) than for land samples (-0.34±0.22) due to aged particles carried over Lake Michigan. In the present study, measured atmospheric PCB concentrations fluctuated during the sampling periods probably due to proximity of sampling site to the Aliaga industrial region and meteorological variables (e.g. wind direction). The non-equilibrium conditions can also be considered as an important parameter for the shallow slopes for PCBs as a result of freshly emitted pollutions from the iron-steel plants located in the industrial region.

At a study conducted by Bidleman & Harner (2000), values of log K_P (experimental) were plotted against log P_L and log K_{OA} for PCBs, and three distinct lines for non-ortho (PCB-77, -126), mono-ortho (PCB-105, -118) and multi-ortho (PCB-49, -101, -138, -171) congeners were seen in the plot of log K_P vs. log P_L. Differences among the ortho-chlorine groups were largely resolved when K_{OA} was used as a fitting parameter. This indicated that partitioning of co-planar congeners from the air into octanol is enhanced compared to the non-planar ones. Fig. 4.14 shows the average values of log K_P plotted vs. log P_L and log K_{OA} for the studied

mono-ortho (co-planar) congeners (PCB-28, -31, -33, -70, -74, -105, and -118) and multi- ortho (non-planar) congeners. Resulting slopes and r^2 values in regression of log K_P vs. log K_{OA} and log K_P vs. log K_{OA} were almost same and no considerable difference was observed between non-planar and co-planar congeners in this study.
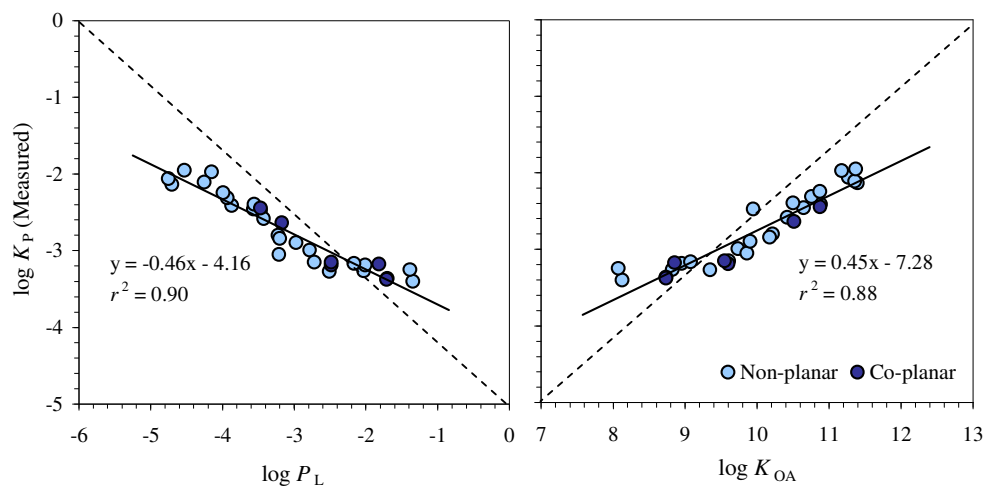

Figure 4.14 log-log plots of average K_P measured at the air sampling site vs. P_L and K_P vs. K_{OA} for PCB congeners. The solid diagonal line represents a 1:1 relationship (equilibrium).

Fig. 4.15 shows the log-log correlation between experimental and modeled K_P values. The overall agreement between the experimental and modeled partition coefficients was good (r^2=0.58, p<0.01). However, K_{OA} based model under-predicted the experimental K_P values especially for tri-CBs while over-predicted for hexa-CBs through PCB-209. The range of average measured/modeled K_P values for individual PCBs was from 0.10±0.05 (PCB-170) to 30±54 (PCB-17), and for all of the studied PCBs, overall average ratio was 3±15.
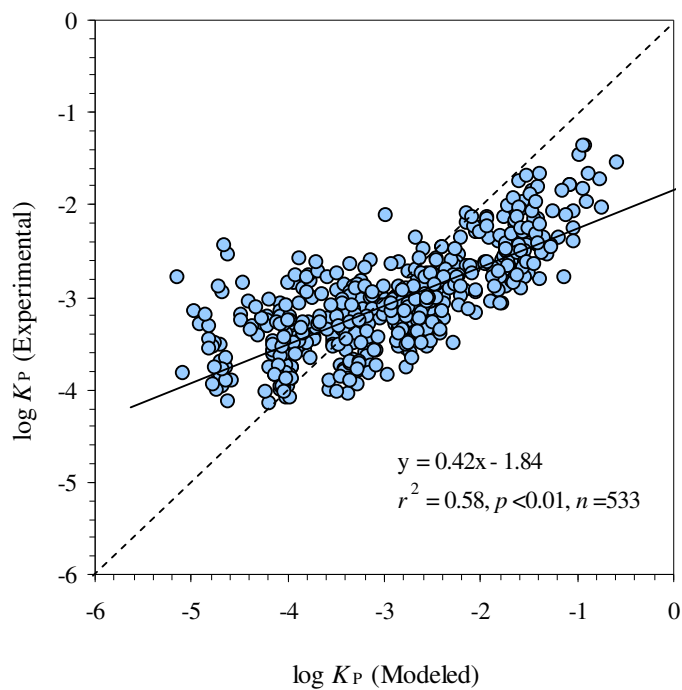
Figure 4.15 Correlation between the measured and predicted log K_P values of PCBs. The solid diagonal line represents a 1:1 relationship (equilibrium).
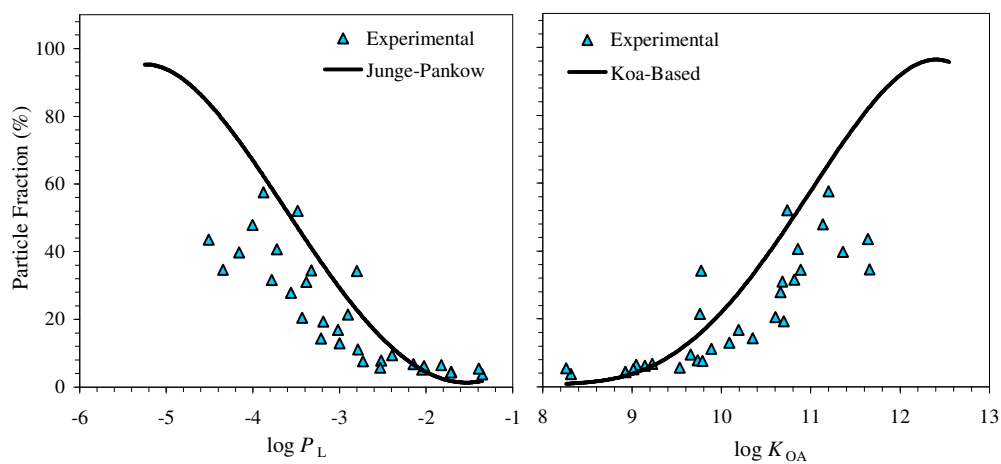

Figure 4.16 Comparison of measured particle fraction of PCBs with Junge-Pankow adsorption and K_{OA} absorption model.

The fraction (φ) of PCBs in particle-phase was experimentally calculated using Eq. (3.4). The comparison of the average measured particle fraction (100×φ) of PCB congeners with the ones predicted by Junge-Pankow adsorption (Eq. 3.8) and K_{OA} absorption model (Eq. 3.7) was illustrated in Fig. 4.16. These models were in a good agreement with experimental values. Experimental φ was correlated with the ones predicted by Junge-Pankow adsorption and K_{OA} absorption model for all data set and statistically significant relationships were found (r^2=0.72, p<0.01, n=590, and r^2=0.74, p<0.01, n=533, respectively).

The range for the average fraction of PCBs in particle-phase for the ones predicted by Junge-Pankow adsorption and by K_{OA} absorption model was between 1.1±1.1 (PCB-18)- 96±3.5 (PCB-206) and between 0.8±1.1 (PCB-17)- 97±2.1 (PCB-209), respectively. The tri- through penta-CBs were predicted predominantly in gas-phase (φ=1-53%), hexa- and hepta-CBs were partitioned between two phases (φ=27-83%), and octa-through PCB-209 were mostly particulate (φ=51-97%). However, PCB particulate fractions were under-estimated for low molecular weight PCBs and over-estimated for higher molecular weight ones. The range for the measured/modeled φ ratios was between 0.4±0.2 (PCB-149, -153, -170, -187) and 15±31 (PCB-17) for Junge-Pankow adsorption model and between 0.4±0.3 (PCB-170) and 25±39 (PCB-17) for K_{OA} absorption model. Their overall average ratios were 3±8 and 3±11, respectively. Similar results were observed for PCBs by Tasdemir et al. (2004a) and the overall average measured/modeled ratio of particulate fraction for all samples was reported to be 4. The difference between the measured and modeled φ values was attributed to assumed c and θ values that might not be constant for the sampling sites (Tasdemir et al., 2004a). This difference between the measured and modeled φ values was also related to the sampling artifact (blow-off) which results in loss of SOCs from filtered particulates (Harner & Bidleman, 1998).

4.2.2 Particle-Phase Dry Deposition Fluxes and Velocities of PCBs

Table 4.10 shows the average particle-phase dry deposition fluxes and velocities of individual PCBs. Eq. (3.16) was performed to calculate dry deposition fluxes. PCB congeners of 128, 156, 158, 169, 171, 177, 183, 191, 194, 195, 199, 205, 206, 208, and 209 were not detected at any of the dry deposition samples (n=28). The range for measured average particle-phase fluxes of individual PCBs was between 7.6±3.6 (PCB-99) and 50±27 (PCB-33) ng m^{-2} day^{-1} in summer and between 8.6±6.6 (PCB-151) and 42±34 (PCB-138) ng m^{-2} day^{-1} in winter (Table 4.10).

Table 4.10 Particle-phase dry deposition fluxes (F_d) and velocities (V_d) of PCB congeners.

	F_d (ng m^{-2} day^{-1})										V_d (cm s^{-1})		
	Summer					Winter					Overall		
PCBs	Min.	Max.	GM	M	Avg±SD	Min.	Max.	GM	M	Avg±SD	GM	M	Avg±SD
18	9.1	113	39	44	47±29	14	113	32	31	38±26	6.5	6.8	7.6±4.0
17	11	56	23	26	26±13	9.9	47	18	16	20±12	5.9	6.1	7.4±4.6
31	18	76	27	25	30±16	10	52	20	20	23±14	4.6	4.7	5.5±3.4
28	12	63	27	25	30±15	11	61	23	22	26±15	4.4	4.1	5.6±4.3
33	26	127	46	44	50±27	21	73	36	34	38±14	6.3	6.1	7.1±3.7
52	13	98	27	25	31±21	20	67	32	30	34±13	6.2	6.2	7.2±4.0
49	12	62	28	28	31±16	23	54	35	36	36±9.1	8.0	10	9.4±4.6
44	11	66	20	17	24±21	18	71	27	24	29±16	5.3	5.6	6.1±3.0
74	*nd*	*nd*	*nd*	*nd*	*nd*	18	44	24	20	26±12	9.4	9.7	9.7±3.5
70	8.2	13	10	10	10±1.9	12	68	21	19	25±18	3.8	4.2	4.5±2.4
95	8.8	14	11	11	11±2.0	6.9	53	14	13	17±12	5.2	4.5	5.7±2.7
101	6.6	23	9.2	8.9	9.9±4.7	6.8	76	19	18	24±19	4.5	4.5	5.1±2.4
99	4.6	14	7.1	6.8	7.6±3.6	4.4	33	10	9.0	12±8.0	4.6	4.4	5.1±2.6
87	*nd*	*nd*	*nd*	*nd*	*nd*	12	64	23	15	30±29	2.7	2.9	2.9±1.3
110	7.8	40	13	12	14±8.1	9.4	79	21	21	25±19	4.2	4.1	4.6±2.1
82	*nd*	*nd*	*nd*	*nd*	*nd*	15	18	16	16	16±2.7	*nc*	*nc*	*nc*
151	*nd*	*nd*	*nd*	*nd*	*nd*	4.7	23	7.3	5.5	8.6±6.6	3.7	4.2	4.0±1.6
149	6.9	20	12	12	13±3.9	6.3	74	19	18	24±20	3.9	4.4	4.3±1.7
118	7.6	26	15	16	16±5.9	5.4	73	18	18	22±18	3.6	3.4	4.0±1.9
153	8.1	37	15	15	16±7.3	7.2	100	20	18	28±28	3.4	3.6	3.9±2.0
132	7.0	17	11	11	12±4.6	9.1	28	16	15	17±8.2	3.4	3.1	3.9±2.4
105	7.6	11	9.0	9.0	9.0±1.3	14	29	21	24	22±7.5	2.3	2.4	2.4±0.7
138	27	43	32	31	33±7.2	15	133	34	30	42±34	2.9	2.6	3.4±2.0
187	*nd*	*nd*	*nd*	*nd*	*nd*	4.4	27	11	11	14±10	2.7	2.5	2.9±1.4
180	8.9	54	22	20	24±12	7.3	70	18	15	24±22	3.1	3.4	3.6±1.9
170	*nd*	*nd*	*nd*	*nd*	*nd*	14	40	23	27	27±19	1.1	1.1	1.1±0.1
∑PCBs	174	856	317	308	349±183	136	1593	405	393	469±328	4.5	4.6	5.5±3.5

nd: Not detected, *nc*: Not calculated, GM: Geometric mean, M: Median.

Like air samples, particle fluxes of Σ_{41}-PCBs dominated by low molecular weight PCBs. The tri-, tetra-, penta-CBs and the fractions of hexa-CBs through PCB-209 accounted for 52, 18, 12, and 18% of Σ_{41}-PCB fluxes in summer, respectively. The same homologue groups were 31, 24, 21 and 24% in winter (Fig. 4.19).

Average particulate dry deposition fluxes of Σ_{41}-PCBs in summer and winter periods were 349±183 and 469±328 ng m^{-2} day^{-1}, respectively (Table 10). Measured average particulate concentrations of Σ_{41}-PCBs in air were 1.6 times higher in winter than in summer (Table 4.8). Also, average total suspended particulate matter (TSP) concentrations measured in this study were higher in winter (199±137 μg m^{-3}) than in summer (95±58 μg m^{-3}) (Table 3.1). Thus, increased wintertime particulate fluxes of PCBs may be due to the increase in TSP concentrations and increased partitioning of PCBs to particle-phase at lower temperatures.

Particle deposition fluxes of PCBs at this study were higher than the previously reported values measured with similar techniques (Table 2.8). At a study conducted by Cindoruk & Tasdemir (2007b) at suburban Bursa, average particle flux of Σ_{29}-PCBs was reported as 46±41 ng m^{-2} day^{-1} using a water surface sampler. Tasdemir & Holsen (2005) and Tasdemir et al. (2004b) reported an average particle-phase Σ_{43}-PCB dry deposition flux of 240 and 190 ng m^{-2} day^{-1} for urban Chicago using a water surface sampler and deposition plates, respectively. Using deposition plates, Franz et al. (1998) also measured average $\Sigma44$-PCB dry deposition fluxes that were 210 ng m^{-2} day^{-1} at urban Chicago and 79 ng m^{-2} day^{-1} at rural Lake Michigan.

Particle-phase dry deposition velocities (V_d, cm s^{-1}) were calculated using the measured dry deposition fluxes (F_d, ng m^{-2} day^{-1}) and atmospheric particle-phase concentrations (C_p, pg m^{-3}), by Eq. (3.17). Average V_d values for the individual PCBs ranged from 2.1±0.5 (PCB-70) to 7.3±5.0 cm s^{-1} (PCB-49) in summer and from 1.1±0.1 (PCB-170, -171) to 11±3.2 cm s^{-1} (PCB-49) in winter. The average V_d values for Σ_{44}-PCBs were 5.0±3.0 and 5.9±3.8 cm s^{-1} for the summer and winter periods, respectively. The seasonal differences in deposition velocities are probably due to variations in the particle size distribution and the meteorological conditions

(i.e. wind speed, air temperature, and atmospheric stability). The deposition velocity increases with wind speed (Zhang, Gong, Padro, & Barrie, 2001). Thus, elevated wintertime deposition velocities measured in this study might be related to the average wind speed that was higher in winter (4.4 ± 2.5 m s^{-1}) than in summer (2.8 ± 1.1 m s^{-1}).

For both sampling periods, the correlation between the dry deposition fluxes and ambient particulate concentrations was statistically significant (for individual congeners r^2=0.25-0.89, overall r^2=0.33, p<0.01, n=430). The overall average V_d for Σ_{41}-PCBs was 5.5 ± 3.5 cm s^{-1} (Table 4.10). This value agrees well with the values determined using similar measurement techniques for dry deposition fluxes in other studies (Table 2.9). The overall average V_d value of 1.3 ± 1.9 cm s^{-1} was reported by Cindoruk & Tasdemir for urban Bursa. Tasdemir & Holsen (2005) and Tasdemir et al. (2004b) have reported overall average V_d values of 4.2 and 5.2 cm s^{-1} for urban Chicago, respectively. Franz et al. (1998) also calculated overall average V_d values as 4.4 cm s^{-1} in summer and 7.2 cm s^{-1} in winter for urban Chicago.
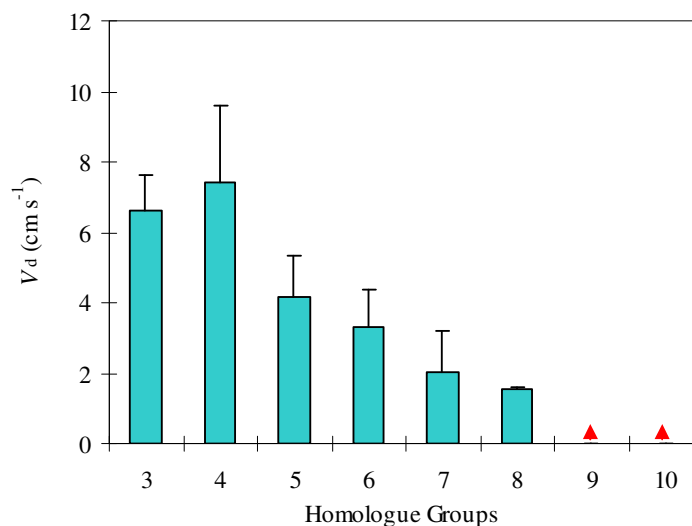

Figure 4.17 Overall average particle-phase dry deposition velocities (V_d) for PCB homologue groups. Error bars are 1 SD. (▲ : Not calculated).

Overall average dry deposition velocities of particulate PCB homologue groups are illustrated in Fig. 4.17. Dry deposition velocities of PCB congeners generally decreased with increasing molecular weight and chlorine content. A statistically significant correlation was found between the overall V_d values and molecular weights of PCB congeners (r^2=0.53, p<0.01, n=25). The overall average dry deposition velocities of tri-, tetra-, penta-, hexa-, and hepta-CBs were 6.6±1.0, 7.4±2.2, 4.3±1.2, 3.9±0.3, and 2.6±1.3 cm s^{-1}, respectively. Tasdemir & Holsen (2005) also found the highest V_d for tetra-CBs ranging between 3.6 and 7.8 cm s^{-1} for the homologue groups. This suggests that lower chlorinated PCBs have the higher deposition velocities probably due to their association with coarse particles in air.

4.2.3 PCBs in Soil

4.2.3.1 Soil Concentrations of PCBs

The soil Σ_{41}-PCB concentrations measured at 48 different points in the study area were highly variable, and varied from 0.2 (rural site, 10) to 805 (industrial site, 25) µg kg^{-1} (dry wt) (Table 4.11). They are within the range of previously reported values elsewhere in Table 2.11. At a study conducted by Cetin et al. (2007), Σ_{36}-PCB concentrations in soils were between 4.9 and 66 µg kg^{-1} (dry wt) for the suburban and industrial sites (n=6) in Aliaga, Izmir. A large variation in soil Σ_{69}-PCB concentrations ranging between 2.6-332 µg kg^{-1} (dry wt) has been found by Backe et al. (2004) for the 11 different urban, rural, and coastal sites in Sweden. Harner et al. (1995) have reported soil ΣPCB concentrations for four congeners (28, 52, 138, and 153) between 10-670 µg kg^{-1} (dry wt) at ten different sites in England.

To evaluate the effects of local sources contributing to the air pollution in Aliaga region, spatial distribution of Σ_{41}-PCB levels in soils (n=48) was mapped out by MapInfo Professional with Vertical Mapper (Fig. 4.18). The highest Σ_{41}-PCB concentrations were measured around the iron-steel plants, Aliaga town, ship dismantling area, refinery and petrochemicals complex suggesting that they are the

major PCB sources in the study area. This result was supported by another recent study conducted at the same site in Aliaga. Based on the results of factor analysis and chemical mass balance modeling, Cetin et al. (2007) concluded that the steel industry, fuel oil combustion or the vinyl chloride process in the petrochemical plant, and soil were significant PCB sources in Aliaga industrial site.

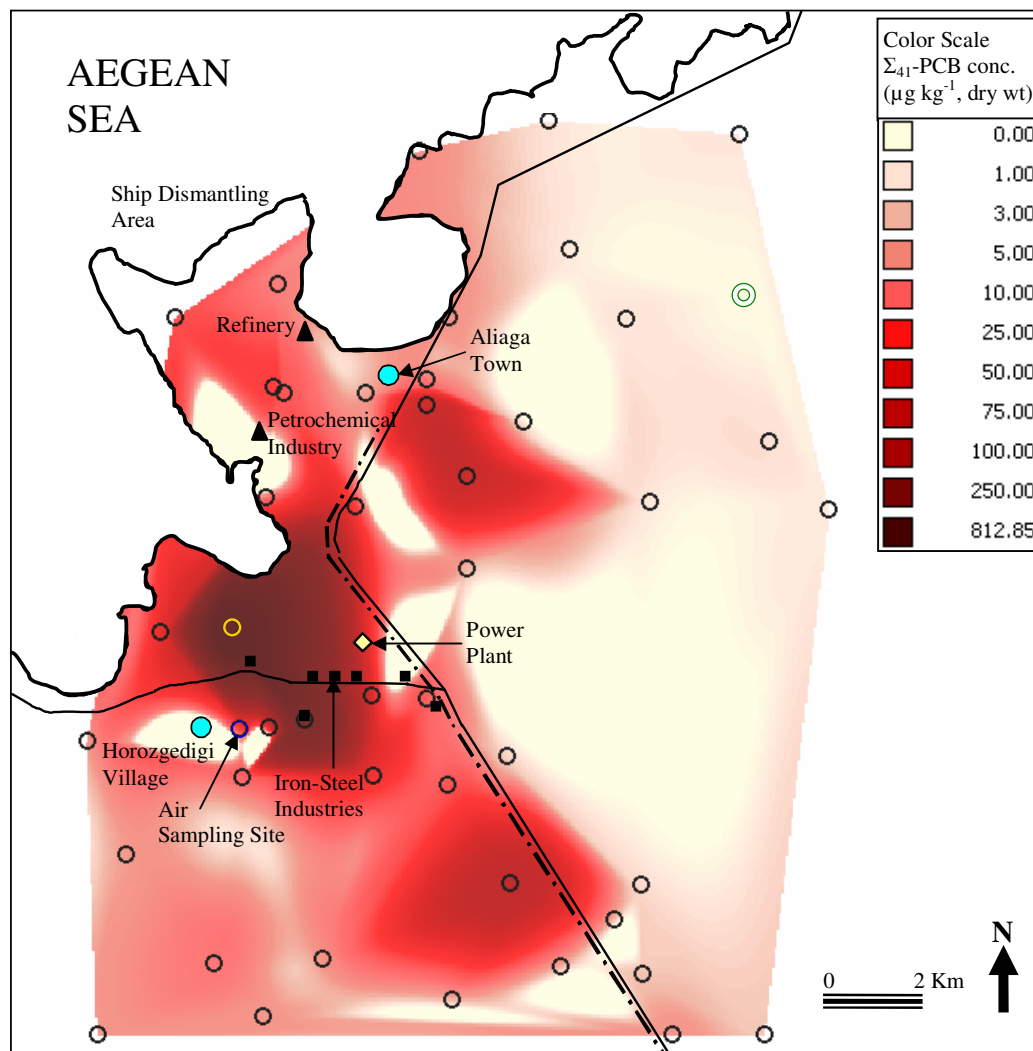Figure 4.18 Spatial distribution of soil Σ_{41}-PCB concentrations in the study area ($\circ$: soil sampling points, $\circ$: residential areas, $\circledcirc$: rural site, $\circ$: industrial site).

Fig. 4.7 and 4.18 demonstrated that Σ_{15}-PAHs and Σ_{41}-PCBs distributions in soils around the Aliaga study area were very similar to each other. A regression of Σ_{15}-

PAHs vs. Σ_{41}-PCBs concentrations in soils (n=48) showed good relationship (r^2=80, p<0.01) indicating that PAH and PCB distributions at the Aliaga study area are comparable, and thus, their soil levels may probably be influenced by the similar sources or meteorological parameters in the area.

Table 4.11 Σ_{41}-PCB concentrations ($\mu g\ kg^{-1}$, dry wt) in soils at the study area (n=48).

SN	Site	Σ_{41}-PCBs	SN	Site	Σ_{41}-PCBs
1	1	6.4	25	29	19
2	2	1.3	26	30	15
3	3	1.1	27	32	4.9
4	4	8.5	28	33	13
5	5	0.9	29	34	38
6	6	19	30	35	34
7	7	5.6	31	36	18
8	9	1.1	32	37	2.1
9	10	0.2	33	39	4.8
10	11	17	34	42	83
11	12	4.5	35	43	2.3
12	13	68	36	44	1.7
13	14	1.3	37	45	5.0
14	15	1.4	38	46	9.2
15	16	23	39	47	5.4
16	17	*nm*	40	48	2.4
17	18	10	41	49	3.0
18	19	26	42	50	5.2
19	20	71	43	53	5.6
20	22	1.0	44	54	2.8
21	23	0.9	45	55	2.6
22	24	42	46	58	464
23	25	805	47	59	56
24	26	3.3	48	60	9.4

nm: Not measured, SN: Sample number

Table 4.12 shows the PCB concentrations of homologue groups (the sum of all congeners at same homologue group) in soils taken from the air sampling site and from the sites having the minimum (in a rural site around Aliaga) and the maximum (in Aliaga industrial region) soil concentrations. The average soil Σ_{41}-PCB concentrations the air sampling site were 40±22 and 49±13 $\mu g\ kg^{-1}$ (dry wt) for the summer and winter sampling periods. Summer/winter ratio for the average soil concentration of individual PCBs ranged between 0.6 (PCB-44, -95, 82, -151, -149, -

132) and 2.3 (PCB-191). The overall average soil Σ_{41}-PCB concentration at the air sampling site (44±17 µg kg^{-1}, dry wt) was relatively low as compared to the highest soil concentration measured at the industrial site (805 µg kg^{-1}, dry wt). This can be attributed to its location with respect to the prevailing wind direction.

Table 4.12 Soil concentrations of PCB homologue groups (µg kg^{-1}, dry wt) at the air sampling site and at the sites having minimum (rural) and maximum (industrial) PCB levels in the study area.

Homologue Groups	Air Sampling Site (SN:29)										Rural Site (SN:10)	Industrial Site (SN:25)
	Summer ($n=4$)					Winter ($n=3$)						
	Min.	Max.	GM	M	Avg±SD	Min.	Max.	GM	M	Avg±SD		
Tri-CBs	2.0	5.3	3.2	3.2	3.4±1.4	2.5	5.1	3.7	3.9	3.9±1.3	0.09	133
Tetra-CBs	1.7	7.8	4.3	5.0	4.9±2.5	4.9	8.1	6.2	6.0	6.3±1.6	0.07	144
Penta-CBs	2.7	18	9.3	12	11±6.3	13	20	15	14	16±3.7	0.04	215
Hexa-CBs	2.7	20	10	14	13±7.2	14	22	17	15	17±4.3	0.03	234
Hepta-CBs	1.3	9.2	4.9	7.0	6.1±3.4	3.5	6.1	4.4	3.8	4.5±1.4	*nd*	69
Octa-CBs	0.3	2.0	1.1	1.7	1.4±0.8	0.8	1.5	1.0	0.9	1.1±0.3	*nd*	9.6
Nona-CBs	0.2	0.7	0.4	0.5	0.5±0.2	0.2	0.5	0.3	0.4	0.4±0.1	*nd*	1.0
PCB-209	0.1	0.2	0.1	0.1	0.1±0.05	0.06	0.07	0.07	0.1	0.07±0.004	*nd*	0.2
$\sum_{41}$-PCBs	11	63	34	44	40±22	41	63	48	42	49±13	0.2	805

nd: Not detected, SN: Site number, GM: Geometric mean, M: Median.

PCB homologue profiles in soil samples taken from the industrial site and air sampling site were similar (r^2=0.87, p<0.01) because both sampling points are relatively close to the steel plants. However, like the PCB profiles in ambient air samples at remote sites, the PCB profiles in rural soil were dominated by the lower chlorinated PCBs. A statistically significant correlation was found between the PCB homologue profiles for the air samples and rural soil (r^2=0.89, p<0.01). This suggested that the lower chlorinated PCBs are transported to relatively longer distances since they are found mainly in the gas-phase.

The overall average PCB homologue profiles in ambient air, dry deposition and soil samples are illustrated in Fig. 4.19. The tri-, tetra-, penta-, hexa-CBs, and the fractions of hepta-through PCB-209 accounted for 8, 13, 30, 33 and 16% of Σ_{41}-PCB concentration in soil taken from the air sampling site. Despite their large contribution in air samples, the tri- and tetra-CBs accounted for only a small part of the total PCB

mass in soil. The difference in air and soil PCB profiles may be due to their gas-particle distributions and their different partitioning behaviors (i.e. low molecular weight compounds have relatively low soil-air partition coefficients).
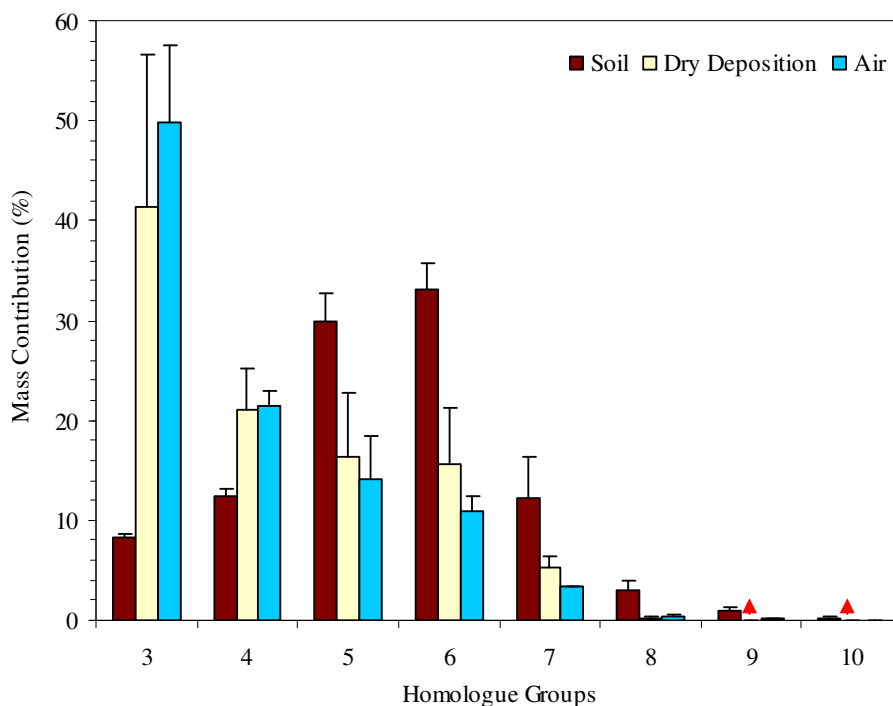
Figure 4.19 Overall average PCB homologue profiles in air, dry deposition, and soil samples. Error bars are 1 SD. (▲: Not detected).

4.2.3.2 Soil-Air Gas *Exchange Fluxes of PCBs*

The fugacity ratios and soil-air gas exchange fluxes were calculated at the air sampling site using the air (n=28) and soil PCB concentrations (n=7) corresponding to the same sampling periods. For all individual PCBs, Q_{SA} values were calculated using Eq. (3.18) and K_{OA} values used to calculate K_{SA} (Eq. 3.19) was taken from the literature (discussed above in Section 4.2.1.3). A statistically significant correlation was found between log K_{OA} and log Q_{SA} values of PCB congeners (r^2=0.71, p<0.01, n=844) indicating that the octanol is a good surrogate for soil organic matter (Fig.

4.20). Correlations between the log K_{OA} and log Q_{SA} values for non-planar and co-planar congeners (PCB-28, -31, -33, -70, -74, -105, -118, and -156 at mono-ortho position) were also determined separately. Both correlations were statistically significant, however the agreement between the log K_{OA} and log Q_{SA} values determined for co-planar congeners was relatively stronger (r^2=0.96, m=0.63, p<0.01, n=8) than those determined for non-planar ones (r^2=0.80, m=0.45, p<0.01, n=25). This was probably due to the enhanced partitioning of co-planar PCBs into the soil organic matter compared to non-planar ones.
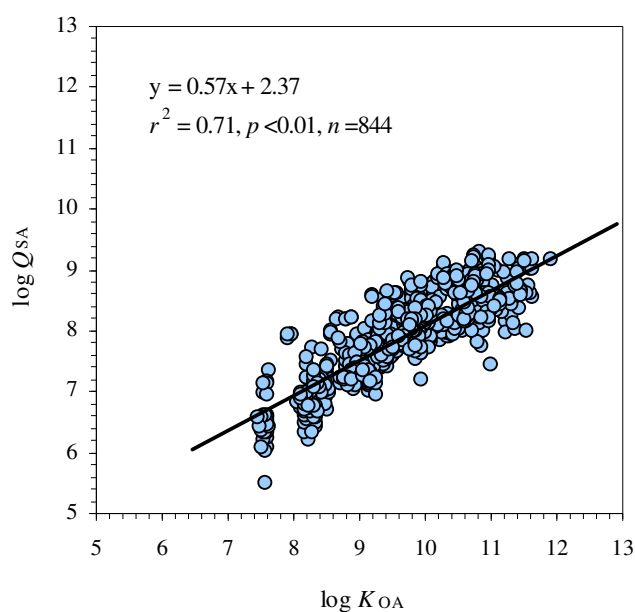
Figure 4.20 log K_{OA} vs. log Q_{SA} for all PCB congeners.

A propagation of the errors that are associated with the calculation indicated that the equilibrium is represented by an f_S/f_A of 1.0±0.26 (i.e. a range of 0.74-1.26). The fugacity ratios especially for the lower chlorinated congeners including PCB-17, 18, 44, 49, 52, 87, 95, and 110 were inside this uncertainty range for some samples (i.e. 32, 36, 43, 32, 46, 56, 43, and 32%, respectively). For all PCB congeners, 16% of the data set (n=847) fell inside this equilibrium range. For the rest, the soil and ambient air were not in equilibrium.

Fig. 4.21 shows the relationship between fugacity in air and soil for all congeners. Estimated f_S/f_A ratios showed that generally lighter congeners (tri- to penta-CBs) had a tendency to volatilize from the soil for some samples while the heavier ones (hexa- to deca-CBs) had a deposition tendency for all samples. Average fugacity ratios indicated volatilization for the congeners 17, 18, 52, and 82 in summer and 17, 18, 52, 95 in winter. For the rest, soil is a sink with net gas deposition. Cousins & Jones (1998) reported fugacity ratios slightly above one for PCB-28, -52, -101, -138, and -153 and lower than one for PCB-180. Backe et al. (2004) also reported fugacity ratios between 0.3 and 40 for PCB-28, -101, -138, -153 and -180.
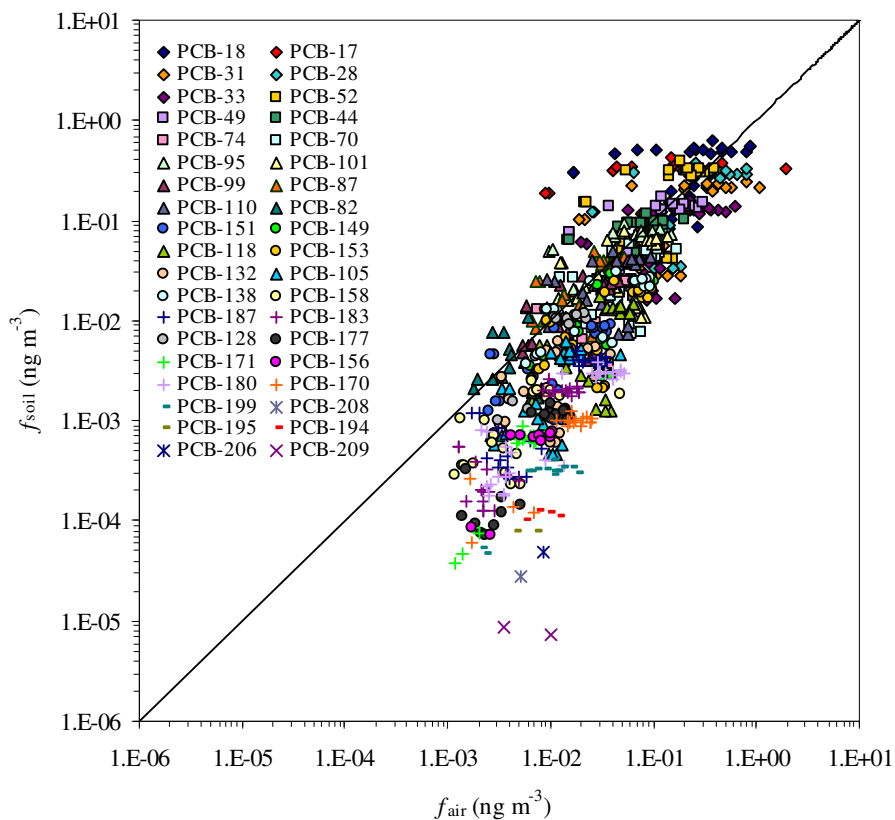

Figure 4.21 Relationship between the PCB fugacities (f) in air and soil. The solid diagonal line represents a 1:1 relationship (equilibrium).

For the samples that soil and ambient air were not in equilibrium, the average estimated uncertainty in the soil-air net gas exchange fluxes (F_{net}) by error propagation ranged between ±43% (PCB-156, -170, -171, -177, -194, -195, -199, -

206, -208, -209) and ±65% (PCB-17, -44, -87) with an overall average of ±52%. Relatively higher uncertainty values for some PCBs (especially lower chlorinated ones) were probably due to their proximity to equilibrium.

Table 4.13 shows the instantaneous soil-air net gas exchange fluxes (F_{net}) and MTCs for PCB congeners calculated using Eq. (3.20) and (3.21), respectively. Negative values indicate a net volatilization from soil to air and positive ones indicate a net deposition from air to soil. The ranges for the average net gas fluxes of PCB congeners were between -2.5±1.0 (PCB-82) and 148±176 ng m^{-2} day^{-1} (PCB-31) in summer and between 1.1±0.2 (PCB-171) and 44±51 ng m^{-2} day^{-1} (PCB-33) in winter. PCB congeners of 17, 18, 44, 52, 82, 87, and 95 tended to volatilize in summer but only PCB-17 and -18 had a tendency to volatilize in winter (Fig. 4.22). This result is consistent with the calculated soil/air fugacity ratios. Air temperature had a strong influence on the direction and magnitude of the gas-phase fluxes. For some PCB congeners, a shift from volatilization to deposition was observed in winter. Generally, summertime gas exchange fluxes were higher than the wintertime ones, consistent with the increased air concentrations of gas-phase PCB in summer.
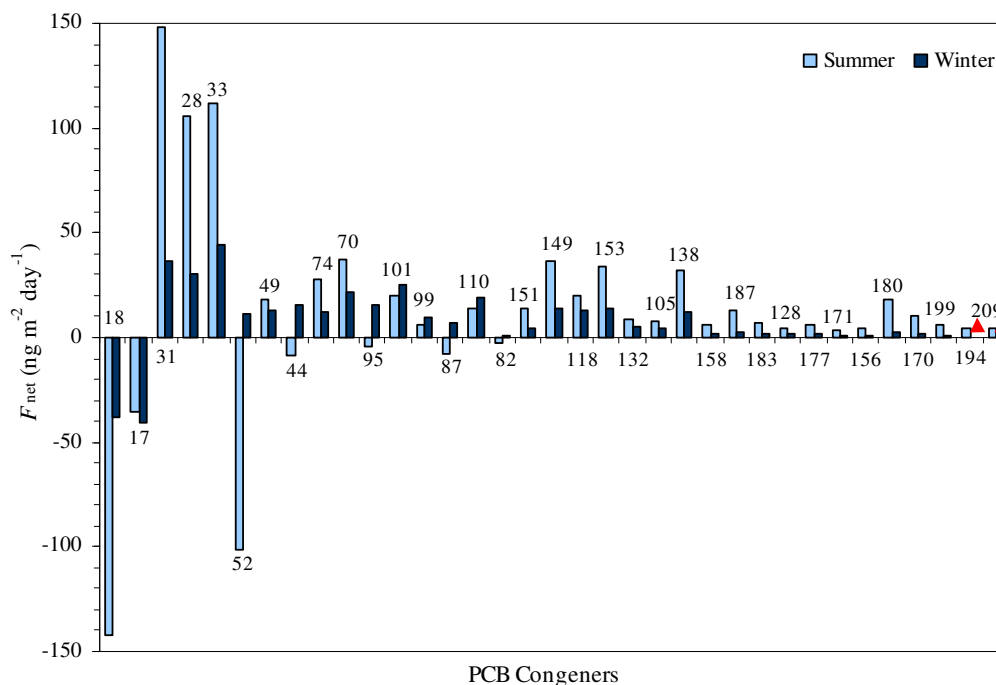

Figure 4.22 Net gas exchange fluxes (F_{net}) of PCBs between soil-air interface. (▲: Not detected).

Table 4.13 Calculated MTCs (cm s^{-1}) and instantaneous soil-air net gas exchange fluxes (F_{net}, ng m^{-2} day^{-1}) for PCB congeners.

PCB Congeners	Summer				Winter			
	MTC	F_{net}			MTC	F_{net}		
	Avg±SD	Min.	Max.	Avg±SD	Avg±SD	Min.	Max.	Avg±SD
18	0.78±0.21	-70	-383	-142±188	0.96±0.24	-35	-305	-38±189
17	0.78±0.21	-72	1094	-36±381	0.96±0.24	-12	-186	-41±84
31	0.78±0.21	49	580	148±176	0.96±0.24	22	179	36±64
28	0.78±0.21	-55	345	105±164	0.96±0.24	19	173	30±67
33	0.78±0.21	31	265	112±88	0.96±0.24	29	173	44±51
52	0.76±0.21	-50	-240	-102±61	0.94±0.24	-17	-135	11±106
49	0.76±0.21	-25	-96	18±61	0.94±0.24	10	77	13±44
44	0.76±0.21	-14	41	-8.7±29	0.94±0.24	7.8	84	15±43
74	0.76±0.21	11	47	28±8.8	0.94±0.24	-3.1	37	12±12
70	0.76±0.21	17	58	37±11	0.94±0.24	8.4	79	22±26
95	0.74±0.20	6.0	51	-4.2±27	0.93±0.24	-4.5	64	16±39
101	0.74±0.20	-12	48	20±20	0.93±0.24	9.8	68	25±37
99	0.74±0.20	-3.5	15	5.7±6.5	0.93±0.24	3.3	27	9.9±14
87	0.74±0.20	-5.7	-11	-8.1±2.5	0.93±0.24	-2.6	29	6.5±17
110	0.74±0.20	9.3	30	14±11	0.93±0.24	4.2	51	19±26
82	0.74±0.20	-1.8	-3.2	-2.5±1.0	0.93±0.24	-0.4	6.8	1.3±4.2
151	0.73±0.20	7.4	20	14±3.4	0.91±0.24	1.1	17	4.2±5.1
149	0.73±0.20	21	59	37±9.8	0.91±0.24	2.3	43	14±14
118	0.74±0.20	5.7	47	20±10	0.93±0.24	3.3	34	13±12
153	0.73±0.20	7.5	64	34±15	0.91±0.24	2.9	36	14±11
132	0.73±0.20	2.4	21	8.2±4.9	0.91±0.24	1.6	12	5.2±4.0
105	0.74±0.20	2.5	28	7.8±6.8	0.93±0.24	1.2	12	4.6±3.8
138	0.73±0.20	5.9	58	32±14	0.91±0.24	1.7	33	12±12
158	0.73±0.20	1.8	29	6.1±7.5	0.91±0.24	0.7	5.1	2.0±1.5
187	0.71±0.20	5.6	19	13±3.7	0.89±0.24	0.5	6.3	2.6±1.5
183	0.71±0.20	3.0	10	7.1±1.9	0.89±0.24	0.7	3.0	1.6±0.7
128	0.73±0.20	2.6	6.3	3.9±1.1	0.91±0.24	1.3	3.0	2.0±0.9
177	0.71±0.20	3.6	10	6.5±1.8	0.89±0.24	1.0	3.0	1.9±0.6
171	0.71±0.20	1.9	4.7	3.2±0.8	0.89±0.24	0.8	1.3	1.1±0.2
156	0.73±0.20	2.1	9.3	4.4±1.9	0.91±0.24	0.8	1.6	1.2±0.6
180	0.71±0.20	9.0	26	19±5.4	0.89±0.24	1.3	8.1	2.7±1.7
191	0.71±0.20	*nc*	*nc*	*nc*	0.89±0.24	*nc*	*nc*	*nc*
169	0.73±0.20	*nc*	*nc*	*nc*	0.91±0.24	*nc*	*nc*	*nc*
170	0.71±0.20	6.3	15	10±2.8	0.89±0.24	1.0	4.1	2.1±1.4
199	0.70±0.19	3.1	11	5.8±2.0	0.88±0.24	0.9	1.3	1.1±0.3
208	0.69±0.19	*nc*	*nc*	*nc*	0.87±0.23	*nc*	*nc*	*nc*
195	0.70±0.19	*nc*	*nc*	*nc*	0.88±0.24	*nc*	*nc*	*nc*
194	0.70±0.19	2.9	5.8	4.1±1.2	0.88±0.24	*nc*	*nc*	*nc*
205	0.70±0.19	*nc*	*nc*	*nc*	0.88±0.24	*nc*	*nc*	*nc*
206	0.69±0.19	*nc*	*nc*	*nc*	0.87±0.23	*nc*	*nc*	*nc*
209	0.68±0.19	1.5	6.6	4.0±3.6	0.86±0.23	*nc*	*nc*	*nc*

nc: Not calculated.

Negative values indicate net gas volatilization from the soil.

Table 4.14 Annual fluxes (ng m^{-2} year^{-1}) and F_{SA}/F_{AS} ratios of PCB congeners.

PCB Congeners	Wet Deposition[a]	Dry Deposition	Gas Absorption	Gas Volatilization	F_{SA}/F_{AS}
18	2,483	15,495	62,758	99,879	1.2
17	991	8,351	49,256	63,150	1.1
31	1,974	9,701	63,801	32,629	0.4
28	1,731	10,222	60,367	38,614	0.5
33	706	16,195	46,766	19,307	0.3
52	572	11,713	37,929	55,835	1.1
49	710	12,366	26,734	21,092	0.5
44	110	9,976	17,663	15,890	0.6
74	*nd*	9,365	11,171	3,916	0.2
70	198	7,682	18,026	7,384	0.3
95	245	5,554	14,839	12,512	0.6
101	303	6,224	19,972	11,901	0.5
99	91	3,818	6,863	4,174	0.4
87	593	11,086	6,373	5,329	0.3
110	255	7,107	12,921	7,046	0.4
82	5.9	6,018	1,595	1,374	0.2
151	54	3,150	4,303	1,169	0.2
149	295	6,547	12,191	3,194	0.2
118	120	7,099	8,090	1,945	0.1
153	84	8,151	11,709	2,748	0.1
132	2.3	5,247	3,213	719	0.08
105	*nd*	5,356	2,912	663	0.08
138	20	14,325	11,452	3,448	0.1
158	*nd*	*nd*	1,714	265	0.2
187	28	4,497	3,359	523	0.07
183	2.3	*nd*	1,844	261	0.1
128	*nd*	*nd*	3,011	1,780	0.6
177	*nd*	3,842	1,829	168	0.03
171	*nd*	*nd*	1,092	115	0.1
156	*nd*	*nd*	1,534	133	0.09
180	5.9	8,776	4,281	389	0.03
170	*nd*	9,821	3,210	173	0.01
199	*nd*	*nd*	1,921	59	0.03
194	*nd*	*nd*	1,504	20	0.01
209	*nd*	*nd*	1,472	1.6	0.001
ΣPCBs	11,577	227,682	537,678	417,804	

nd: Not detected.
[a] Odabasi, 2007b.

Table 4.14 shows the annual average fluxes of PCB congeners and the ratios of total fluxes representing soil to air (F_{SA}, i.e. gas volatilization) and air to soil (F_{AS}, i.e. gas absorption, dry and wet deposition) processes. Gas absorption and volatilization fluxes were calculated using Eq. (3.20). Wet deposition fluxes

measured recently at a suburban site of Buca in Izmir during autumn 2005-spring 2006 (Odabasi, 2007b) were also used to estimate relative importance of different atmospheric processes. All processes were comparable for Σ_{35}-PCBs but their input was dominated by gas absorption with a contribution of 69%. Dry deposition accounted for 29% of the atmospheric Σ_{35}-PCB inputs and was followed by wet deposition with a contribution of only 1%. The calculated ratios of PCB-17, -18, and -52 were slightly above 1.0 suggesting that for these congeners, soil and air may be approaching a steady state condition. For the remaining congeners, there was a net accumulation into the soil.

4.3 Organochlorine Pesticides (OCPs)

4.3.1 OCPs in Ambient Air

4.3.1.1 Ambient Air Concentrations of OCPs

Atmospheric pesticide concentrations measured at this study are summarized in Table 4.15. Dieldrin, endrin, endrin aldehyde, endrin ketone, and methoxychlor in the air samples (n=28) were under their detection limits for both sampling periods. For the rest, average total (gas+particle) concentrations ranged between 0.2±0.05 (*c*-nonachlor) and 2152±2974 pg m^{-3} (endosulfan-I) in summer, and between not detected (*nd*) (δ-HCH, *c*-nonachlor) and 121±160 pg m^{-3} (chlorpyrifos) in winter (average±SD).

Endosulfan-I had the highest average total concentration in summer, and was followed by endosulfan-II, and chlorpyrifos. In winter, major OCPs in air were chlorpyrifos, α-HCH, and endosulfan-I, respectively (Table 4.15). Measured high endosulfan and chlorpyrifos levels may probably due to their current uses in Turkey.

Table 4.15 Atmospheric concentrations (pg m^{-3}) of OCP compounds at the air sampling site (1/2).

| | Summer | | | | | | | | | | | | | | |
| | Particle-Phase | | | | | Gas-Phase | | | | | Total (Gas+Particle) | | | | |
OCPs	Min.	Max.	Geometric Mean	Median	Avg±SD	Min.	Max.	Geometric Mean	Median	Avg±SD	Min.	Max.	Geometric Mean	Median	Avg±SD
α-HCH	1.8	8.3	3.5	3.5	4.0±2.0	28	190	93	94	102±43	34	193	97	99	106±43
β-HCH	2.0	10	4.5	6.2	6.2±6.0	3.5	20	10	12	12±6.0	3.5	31	11	12	14±9.1
γ-HCH	1.4	8.0	3.7	3.6	4.2±2.1	21	76	42	41	44±16	26	82	46	44	49±16
δ-HCH	0.6	4.8	1.4	1.3	1.8±1.3	1.5	4.0	2.5	2.6	2.6±0.8	1.0	8.8	2.4	2.4	2.8±1.9
CHLPYR	2.8	17	6.3	6.8	7.1±3.7	16	689	80	75	135±178	21	706	89	80	143±181
HEP EPOX	0.2	3.9	1.0	1.0	1.3±1.1	2.2	10	4.6	4.6	5.0±2.3	2.2	13	5.4	5.9	6.0±3.0
α-CHL	0.1	0.4	0.2	0.2	0.2±0.1	1.3	5.7	2.7	3.0	2.9±1.3	1.3	6.2	2.8	3.0	3.0±1.4
γ-CHL	0.03	0.3	0.1	0.2	0.1±0.07	0.8	2.6	1.6	1.6	1.6±0.5	0.8	2.8	1.7	1.7	1.7±0.6
c-NONA	nd	nd	nd	nd	nd	0.1	0.2	0.2	0.2	0.2±0.05	0.1	0.2	0.2	0.2	0.2±0.05
t-NONA	0.03	0.1	0.05	0.04	0.05±0.04	0.7	2.1	1.2	1.2	1.3±0.4	0.7	2.1	1.2	1.2	1.3±0.4
ESLF-I	3.5	22	8.5	8.1	9.9±5.8	481	11704	1325	950	2142±2970	487	11726	1336	961	2152±2974
ESLF-II	5.5	109	19	13	29±31	66	1362	186	154	271±338	76	1422	213	201	300±351
ESLF SUL	1.6	12	3.4	3.1	4.2±3.1	4.8	60.9	10.0	9.3	13±14	6.4	73	14	14	17±16
p,p'-DDT	3.8	32	9.5	8.9	12±8.5	21	81	43	44	46±17	30	87	56	56	58±16
p,p'-DDD	1.0	5.1	2.6	2.6	2.8±1.1	6.9	26	16	17	17±5.3	10	27	19	20	19±4.7

nd: Not detected.

Table 4.15 Atmospheric concentrations (pg m^{-3}) of OCP compounds at the air sampling site (2/2).

| | Winter | | | | | | | | | | | | | | |
| | Particle-Phase | | | | | Gas-Phase | | | | | Total (Gas+Particle) | | | | |
OCPs	Min.	Max.	Geometric Mean	Median	Avg±SD	Min.	Max.	Geometric Mean	Median	Avg±SD	Min.	Max.	Geometric Mean	Median	Avg±SD
α-HCH	0.2	1.3	0.5	0.5	0.5±0.3	10	123	33	36	41±32	11	124	33	36	41±32
β-HCH	nd	nd	nd	nd	nd	4.3	21	8.4	8.2	9.4±5.2	4.3	21	8.4	8.2	9.4±5.2
γ-HCH	0.3	2.6	0.7	0.6	1.0±0.8	4.3	27	11	10	12±6.3	4.3	27	11	10	13±6.4
δ-HCH	nd	nd	nd	nd	nd	nd	nd	nd	nd	nd	nd	nd	nd	nd	nd
CHLPYR	1.9	457	21	9.3	86±137	3.6	170	22	22	42±54	11	481	53	39	121±160
HEP EPOX	0.3	2.9	0.6	0.3	1.1±1.4	0.4	5.6	1.3	1.2	1.6±1.3	0.4	8.4	1.6	1.3	2.2±2.2
α-CHL	0.04	0.09	0.07	0.08	0.07±0.03	0.3	1.0	0.5	0.5	0.6±0.2	0.3	1.0	0.5	0.5	0.6±0.2
γ-CHL	0.03	0.1	0.05	0.04	0.06±0.04	0.3	1.0	0.5	0.5	0.5±0.2	0.3	1.2	0.5	0.5	0.6±0.3
c-NONA	nd	nd	nd	nd	nd	nd	nd	nd	nd	nd	nd	nd	nd	nd	nd
t-NONA	nd	nd	nd	nd	nd	0.3	0.8	0.4	0.4	0.4±0.2	0.3	0.8	0.4	0.4	0.4±0.2
ESLF-I	1.0	12	2.7	2.5	4.0±4.0	4.7	36	17	17	19±9.3	4.7	38	19	18	21±11
ESLF-II	1.3	13	3.4	3.1	4.3±3.6	0.20	5.8	1.1	2.0	2.2±2.1	1.6	15	4.6	4.5	5.6±3.9
ESLF SUL	0.3	2.8	0.8	0.7	1.1±0.8	0.04	0.6	0.2	0.1	0.2±0.2	0.4	3.3	1.0	0.8	1.3±0.9
p,p'-DDT	1.4	13	4.4	4.5	5.1±3.0	2.7	18	5.3	5.2	6.2±4.1	4.9	21	11	11	11±4.6
p,p'-DDD	0.3	1.6	0.8	0.8	0.9±0.3	0.9	6.3	2.1	2.0	2.4±1.4	1.4	7.2	3.0	2.9	3.3±1.5

nd: Not detected.

Total (gas+particle) atmospheric concentrations of individual OCPs measured at this study were within the range of those previously reported values in Table 2.6. Atmospheric OCP levels that were found at a remote site in Germany (Wenzel et al., 2006), at the Arctic atmosphere (Hung et al., 2005), and at a rural/forested site in USA (Gioia et al., 2005) were lower than the obtained results. At a coastal/urban site of Izmir, Odabasi et al. (2008) reported generally higher atmospheric OCP concentrations in the summer and winter sampling periods, excepting *p,p'*-DDT, *p,p'*-DDD, and α, β, δ isomers of HCH which were measured higher at this study. Sofuoglu et al. (2004) also reported higher values of OCPs in spring at a suburban site of Izmir, except for endosulfan-I, endosulfan-II, *p,p'*-DDT and *p,p'*-DDD which were found higher in the summer sampling period of this study. Similarly, chlorpyrifos and endosulfan had the highest atmospheric concentrations among the OCPs measured in Izmir air (Odabasi et al., 2008; Sofuoglu et al., 2004).

γ-HCH released into the atmosphere both as lindane (pure γ-HCH) and as a component of technical HCH comprised of 60-70% α-HCH, 5-12% β-HCH, 10-15% γ-HCH, 6-10% δ-HCH, and other isomers (ATSDR, 2005). The uses of technical HCH and lindane have been banned for decades in Turkey (Acara et al., 2006). However, lindane is currently used in Europe (Lee et al., 2000; Wania et al., 1998). It was reported by Murayama et al. (2003) and Lee et al. (2000) that α- to γ-HCH ratio was close to 1 in areas where γ-HCH was used, and between 3-7 in areas where α-HCH was used or in remote areas. In this study, the average α- to γ-HCH ratio was 2.1±0.4 in summer and 3.1±0.9 in winter, indicating the effect of remote sources on the ambient HCH levels at the study site. Lower α- to γ-HCH ratio in summer may be related to the elevated atmospheric concentrations of γ-HCH during this period (Table 4.15). At the other studies performed in Izmir, relatively low average α- to γ-HCH ratios were found to be 1.1±0.3 for the coastal/urban site (Odabasi et al, 2008) and 1.2±0.5 for the suburban site (Sofuoglu et al., 2004). This may be due to higher atmospheric γ-HCH levels measured at coastal/urban and suburban sites in Izmir than those measured at the air sampling site in Aliaga (Table 2.6). Manz et al. (2001) reported that HCHs can be emitted by hazardous waste dumps, cable scrapping and incineration in smelting plants because of the previous usage of HCHs as an additive

in plasticizer production (e.g. in PVC sheathing of electric cables). At the iron-steel plants located in the Aliaga industrial region, all kinds of scrap iron materials are stored, classified, cut into parts, and melted. Therefore, relatively high α- to γ-HCH ratios in the air may also be due to high α-HCH levels at the air sampling site released from nearby iron-steel plants smelting of scrap materials contained PVC sheathed cables.

Technical endosulfan contains 70% of endosulfan-I and 30% of endosulfan-II. Endosulfan sulfate is their main degradation product (Hafner & Hites, 2003). Sofuoglu et al. (2004) reported the usage of endosulfan/chlorpyrifos ratio in Izmir area was 7.5. The average ratio of endosulfan-I and -II to chlorpyrifos in air was 23 ± 16 in summer and 1.0 ± 1.3 in winter. When endosulfan sulfate was included, seasonal ratios were almost not changed because of its little contribution (~3%) to Σendosulfan (endosulfan-I, -II, and endosulfan sulfate) mass in air for both seasons. Observed high Σendosulfans/chlorpyrifos ratio in summer can be attributed to the high regional and local applications of endosulfan during the summer months. Relatively low atmospheric Σendosulfans/chlorpyrifos ratio in winter may be due to different properties of these compounds (i.e. vapor pressure, octanol-air partition coefficient, and reactivity in the air) and their different seasonal uses for the agricultural purposes.

γ(*trans*)- to α(*cis*)-CHL ratio of ~1.2 in the technical chlordane and <1 in the Arctic atmosphere were reported by Hung et al. (2005). In Turkey, the use of chlordane was banned in 1979. The average ratio of atmospheric γ-/α-CHL at the air sampling site was found to be 0.7 ± 0.2 in summer and 1.0 ± 0.5 in winter suggesting that there was no fresh usage of chlordane-based pesticides in this area.

The correlations between the atmospheric total concentrations of related pesticides are illustrated in Fig. 4.23. Statistically significant correlation ($p<0.01$) was found between α- and γ-HCH isomers; γ-chlordane and other chlordane related compounds (heptachlorepoxide, α-chlordane, c-nonachlor, t-nonachlor); endosulfan-I

and other endosulfan related compounds (endosulfan-II, endosulfan sulfate); p,p'-DDT and p,p'-DDD in air samples (n=28). This indicates that the related OCPs in air are possibly affected by the same source and/or local processes in the ambient environment under the given meteorological conditions. However, there was a relatively weak correlation (p<0.05-0.10) between α-HCH and β, δ isomers. This might be because of their remote sources.

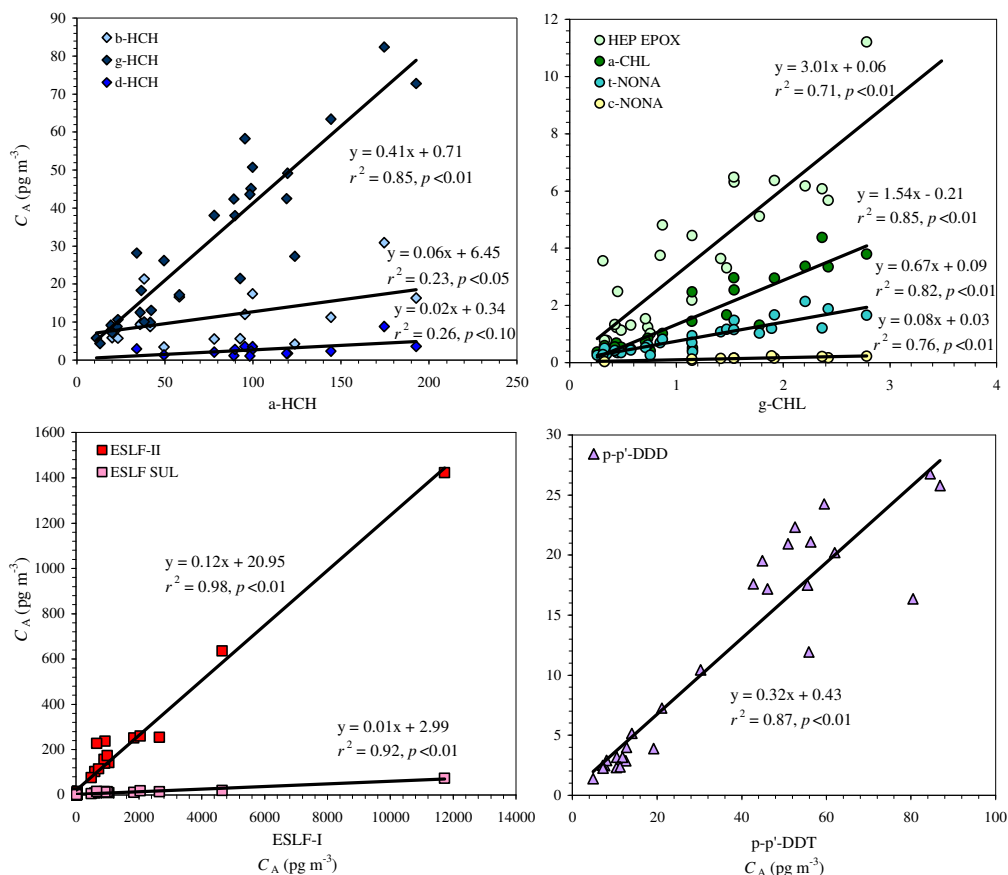
Figure 4.23 Correlations between the atmospheric total concentrations (C_A) of related pesticides.

Summertime average total concentrations for all of the studied OCPs in air were higher than the wintertime ones (Table 4.15). The summer/winter ratios were between 1.1 (chlorpyrifos) and 93 (endosulfan-I). Measured high atmospheric OCP levels in summer may be related to the enhanced local/regional applications of in-use pesticides and enhanced volatilization rates of the compounds during hot summer

months. Similar increases in atmospheric pesticide concentrations during summer were also reported by Cortes et al. (1999), Gioia et al. (2005), Halsall et al. (1998), Harrad & Mao (2004), Lee et al. (2000), Odabasi et al. (2008), and Sun et al. (2006).
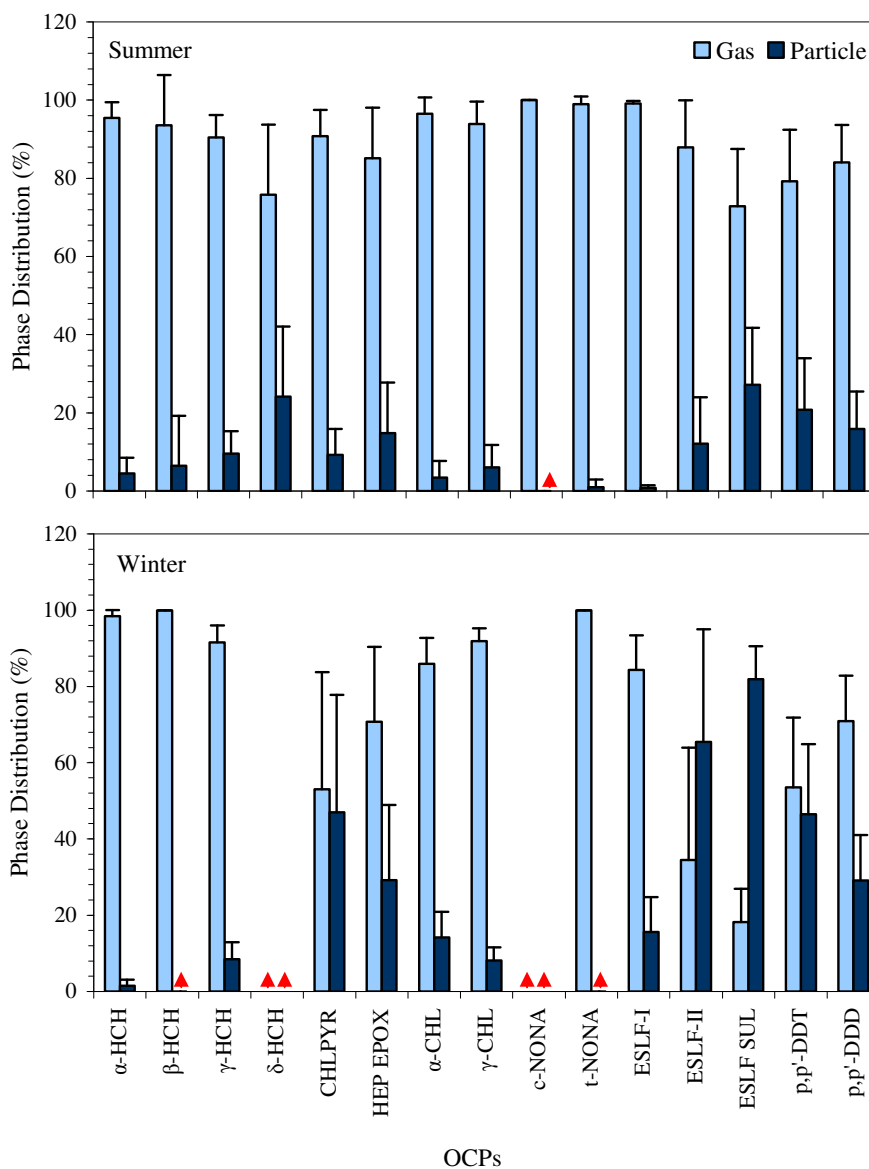

Figure 4.24 Average phase distributions of individual pesticides for the summer and winter periods. Error bars are 1 SD. (▲: Not detected).

Average OCP concentrations measured in particle-phase ranged between *nd* (*c*-nonachlor) and 29±31 pg m^{-3} (endosulfan-II) in summer, and between *nd* (*β*-HCH, *δ*-

HCH, *c*-nonachlor, *t*-nonachlor) and 86±137 pg m^{-3} (chlorpyrifos) in winter. For the gas-phase, they ranged between 0.2±0.05 (*c*-nonachlor) and 2142±2970 pg m^{-3} (endosulfan-I) in summer, and between *nd* (*δ*-HCH, *c*-nonachlor) and 42±54 pg m^{-3} (chlorpyrifos) in winter (Table 4.15). Generally, gas-phase percentages for individual pesticides were higher in summer than in winter, probably due to increased partitioning of compounds to gas-phase with temperature (Fig. 4.24).

4.3.1.2 Influence of Meteorological Parameters on OCP Levels in Air

The relationship between the air temperature and gas-phase partial pressure of individual pesticides in the air was evaluated using Eq. (3.1). The temperature dependency of gas-phase concentrations was statistically significant (*p*<0.01) for all of the studied pesticides except *β*-HCH, and changes in temperature accounted for 7 (*β*-HCH) to 94% (endosulfan-II) of the variability in gas-phase concentrations. The regression slopes between -1458 (*β*-HCH) and -32944 (endosulfan-II) were found to be rather steep and were consistent with those derived from other recent studies (Halsall et al., 1998; Harrad & Mao, 2004; Lee et al., 2000; Yeo et al., 2003). Among the studied pesticides, endosulfan-I, -II, and endosulfan sulfate had the highest slopes and r^2 values, supporting their seasonal variations in gas-phase concentrations. The slopes and r^2 values for *α*- and *γ*-HCH were found to be -5154, 0.39 and -6707, 0.61, respectively. This result is supported by Wania et al. (1998) indicating that gas-phase *γ*-HCH concentrations in air display stronger temperature dependencies than those of *α*-HCH and r^2 value of *γ*-HCH often exceeds 0.5.

Eq. (3.2) was performed to assess the influence of wind speed and wind direction on gas-phase OCP concentrations in air. Temperature, wind speed, and wind direction, altogether, accounted for 20 to 94% of the variability in the atmospheric concentrations of gas-phase OCPs (Table 4.16). Negative m_1 and m_2 values indicated that the gas-phase concentrations increased with temperature and decreased with wind speed, respectively. Steep slopes (m_1) suggested that the gas-phase concentrations were influenced by regional or short-range transport and by

volatilization from contaminated surfaces. Positive m_3 values are associated with northerly winds while negative values point southerly directions for relatively higher gas-phase concentrations. The low significance ($p > 0.10$) of the MLR analysis for m_1, m_2, m_3 parameters indicated the lack of correlation between the meteorological parameters and the gas-phase air concentrations of β-HCH. This indicates that its gas-phase concentrations might be transported from remote areas.

Table 4.16 Summary of regression parameters for Eq. (3.2).

OCPs	m_1	m_2	m_3	r^2	n
α-HCH	-3674[a]	-0.22[a]	0.60[a]	0.71	28
β-HCH	-1533	-0.07	0.73	0.20	18
γ-HCH	-6083[a]	-0.14[a]	0.69[a]	0.81	28
CHLPYR	-6416[a]	0.01	0.18	0.23	28
HEP EPOX	-7663[a]	0.09	0.44	0.59	28
α-CHL	-8558[a]	-0.05	0.21	0.86	26
γ-CHL	-5775[a]	-0.08[a]	0.47[a]	0.78	28
c-NONA	-22511[b]	0.22	-0.06	0.76	11
t-NONA	-5801[a]	-0.06[a]	0.06	0.85	28
ESLF-I	-24116[a]	0.09	0.73[b]	0.89	28
ESLF-II	-32458[a]	-0.10	0.20	0.94	22
ESLF SUL	-22751[a]	0.04	0.49	0.92	28
p,p'-DDT	-11016[a]	-0.05	0.22	0.88	28
p,p'-DDD	-10674[a]	-0.05	0.34	0.87	28

[a] $p < 0.05$.
[b] $p < 0.10$.

4.3.1.3 Gas-Particle Partitioning of OCPs

Temperature dependent K_{OA} values for individual pesticides were calculated using the regression parameters reported by Shoeib & Harner (2002). The parameters that were not available for chlorpyrifos, heptachlorepoxide, endosulfan-II, and endosufan sulfate were taken from Odabasi (2007a). P_L values for OCPs as a function of temperature were also calculated using the regression parameters given by Hlnckley, Bidleman, Foreman, & Tuschall (1990). The parameters that were not available for heptachlorepoxide and chlorpyrifos were taken from Odabasi (2007a).

The experimental K_P values for OCPs were determined using Eq. (3.6) and they were plotted against log P_L and log K_{OA}. For individual samples, r^2 values were between 0.03-0.72 for P_L and 0.07-0.62 for K_{OA}. Regression parameters, m and b, were -0.10 to -0.81 and -3.04 to -5.39 for P_L and 0.15 to 0.84 and -4.10 to -10.73 for K_{OA}, respectively. The variation in slopes indicated that atmospheric particles for different samples have different sorbing properties (Sofuoglu et al., 2004). Observed slopes and r^2 values in regression of log K_P vs. log K_{OA} and log K_P vs. log K_{OA} for OCPs were almost the same suggesting that both P_L and K_{OA} values can be used to describe the partitioning of OCPs between gas- and particle-phases. Figure 4.25 shows the plots of measured log K_P vs. log P_L and log K_P vs. log K_{OA} values of pesticides for all sample events. Statistically significant correlation was found for P_L (r^2=0.28, p<0.01, n=229) and for K_{OA} (r^2=0.28, p<0.01, n=230). However, the slopes of regression lines, -0.41 and 0.41, were different from the expected value of -1 and 1, respectively. Similarly, Sofuoglu et al. (2004) conducted a study on gas-particle partitioning of OCPs at suburban Izmir and found the regression slope of 0.46 in log K_P vs. log K_{OA} correlation for all samples.
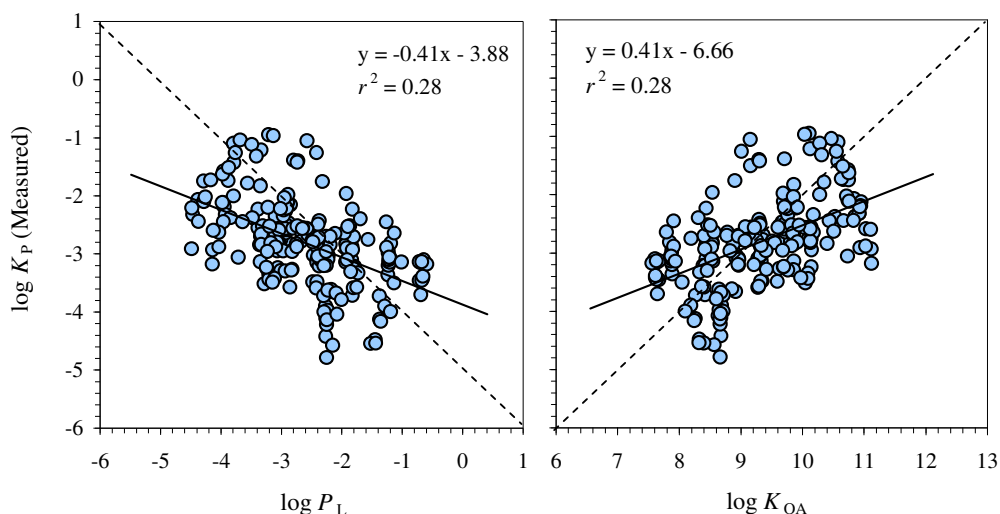

Figure 4.25 Plots of log K_P measured at the air sampling site vs. log P_L and log K_P vs. log K_{OA} for all samples. The solid diagonal line represents a 1:1 relationship (equilibrium).

Fig. 4.26 compares the experimentally determined (Eq. 3.6) and modeled (Eq. 3.13) log K_P values of OCPs for all samples. The relationship between the modeled and measured partition coefficients was good (r^2=0.27, p<0.01, n=230). However, the results indicated that K_{OA} based model under-predicts the experimental K_P values for α-HCH, γ-HCH, chlorpyrifos, heptachlorepoxide, endosulfan-II, and endosulfan sulfate while over-predicts for t-nonachlor and p,p'-DDD. Generally, predicted partition coefficients for endosulfan-I, p,p'-DDT, α-chlordane, and γ-chlordane were good. The range of average measured/modeled K_P values for individual pesticides was from 0.3±0.2 (p,p'-DDD) to 30±27 (γ-HCH), and for all OCP compounds, overall average ratio was 10±22.

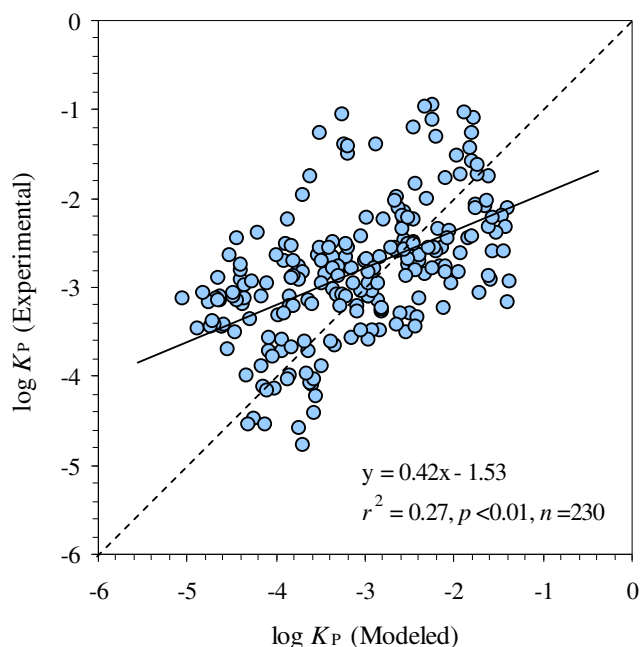Figure 4.26 Correlation between the measured and predicted log K_P values of OCPs. The solid diagonal line represents a 1:1 relationship (equilibrium).

The fraction (ϕ) of OCPs in particle-phase was calculated experimentally using Eq. (3.4). Fig. 4.27 compares the average measured particle fraction (100×ϕ) of pesticides with the ones predicted by Junge-Pankow adsorption (Eq. 3.8) and K_{OA}

absorption models (Eq. 3.7). Experimental ϕ values were correlated with the ones predicted by Junge-Pankow adsorption and K_{OA} absorption model for all data set, and statistically significant relationships were found (r^2=0.35, $p<0.01$, n=253, and r^2=0.34, $p<0.01$, n=230, respectively).
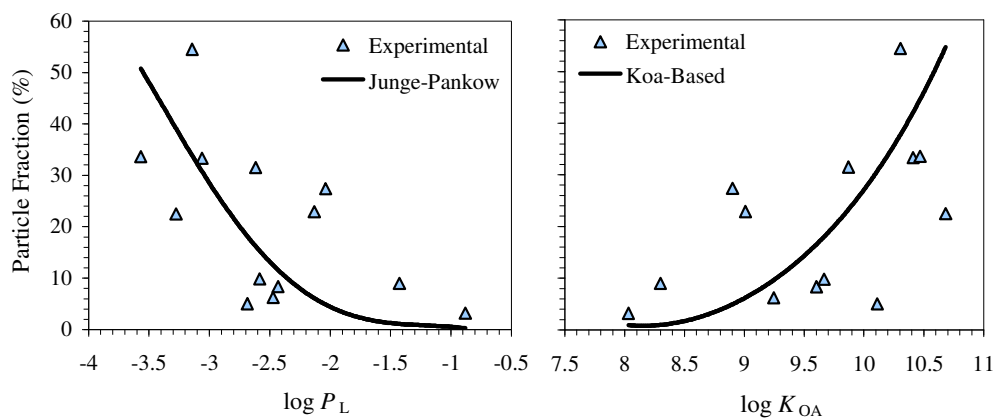

Figure 4.27 Comparison of measured particle fraction of OCPs with Junge-Pankow adsorption and K_{OA} absorption model.

Generally, all of the studied pesticides were mainly in gas-phase with a range of average predicted particulate fractions ($100 \times \phi$) between 0.33 (α-HCH) and 55% (p,p'-DDD). Although the relationship between the measured and predicted ϕ values was good, particulate fractions were predicted lower than their experimental results for α-HCH, γ-HCH, chlorpyrifos, heptachlorepoxide, γ-chlordane, endosulfan-II, and endosulfan sulfate. Good predictions were generally observed for α-chlordane, t-nonachlor, p,p'-DDT, and p,p'-DDD from Junge-Pankow adsorption model, and for α-chlordane, endosulfan-I, and p,p'-DDT from K_{OA} absorption model. The average ratio of measured/predicted ϕ values for individual OCPs ranged from 0.5±0.4 (endosulfan-I) to 44±61 (α-HCH) for Junge-Pankow model, and from 0.4±0.2 (t-nonachlor, p,p'-DDD) to 26±22 (γ-HCH) for K_{OA} model. For all of the studied OCPs, it was 10±25 and 7±13, respectively. Sofuoglu et al. (2004) used K_{OA} model to estimate the particulate percentages of OCPs at suburban Izmir and they reported good predictions for β-HCH, endosulfan-I, and p,p'-DDT, and under-predicted particulate percentages for α-HCH, γ-HCH, chlorpyrifos, and dieldrin.

4.3.2 Particle-Phase Dry Deposition Fluxes and Velocities of OCPs

Particle-phase OCP dry deposition fluxes (F_d, ng m^{-2} day^{-1}) were measured experimentally using dry deposition plates, and calculated using Eq. (3.16). The range for the average F_d values of individual pesticides was between 1.1±1.2 (t-nonachlor) and 503±455 ng m^{-2} day^{-1} (endosulfan-I) in summer and between 0.3±0.3 (t-nonachlor) and 110±157 ng m^{-2} day^{-1} (chlorpyrifos) in winter (Table 4.17). Generally, particle fluxes were higher in summer than in winter. Summer/winter ratios for the average F_d values of individual pesticides were between 0.4 (chlorpyrifos) and 32 (endosulfan-I). This result is consistent with particle-phase concentrations of OCPs (except chlorpyrifos) that were measured higher in summer than in winter (Table 4.15).

Table 4.17 Particle-phase dry deposition fluxes (F_d) and velocities (V_d) of individual OCPs.

OCPs	F_d (ng m^{-2} day^{-1})										V_d (cm s^{-1})		
	Summer					Winter					Overall		
	Min.	Max.	GM	M	Avg±SD	Min.	Max.	GM	M	Avg±SD	GM	M	Avg±SD
α-HCH	2.5	14	5.5	5.5	6.3±3.5	2.0	20	6.0	5.3	7.7±6.0	3.4	3.6	5.8±5.8
γ-HCH	3.8	29	8.2	7.6	9.7±6.9	4.1	16	6.2	5.3	6.9±3.9	3.8	5.1	4.8±3.1
CHLPYR	7.4	207	30	27	47±57	13	573	53	36	110±157	3.9	3.6	5.4±4.5
HEP EPOX	3.7	46	9.7	10	14±14	1.2	23	5.3	6.0	9.5±9.3	4.4	4.3	4.6±1.4
α-CHL	0.9	4.5	2.0	2.0	2.3±1.5	0.3	1.0	0.6	0.6	0.6±0.2	9.7	11	10±3.3
γ-CHL	0.1	11	0.8	0.7	1.7±3.3	0.1	1.5	0.6	0.5	0.7±0.5	6.1	6.7	8.1±5.3
t-NONA	0.4	2.8	0.8	0.6	1.1±1.2	0.1	0.5	0.3	0.3	0.3±0.3	11	11	11±5.1
ESLF-I	184	1715	375	265	503±455	4.5	38	12	9.1	16±13	6.7	6.7	8.2±5.3
ESLF-II	36	435	99	76	138±133	1.1	29	4.1	3.1	6.5±7.6	3.0	3.8	4.4±3.9
ESLF SUL	4.7	37	11	9.1	13±10	0.3	4.6	1.2	1.4	1.6±1.1	2.4	2.2	2.8±1.6
p,p'-DDT	9.7	210	19	16	31±52	4.1	164	14	11	23±41	2.7	2.5	3.3±2.5
p,p'-DDD	2.1	51	5.8	5.0	8.4±12	3.0	6.8	4.3	4.3	4.4±1.2	3.8	4.1	4.6±3.0
ΣOCPs											3.5	3.6	4.9±4.1

GM: Geometric mean, M: Median.

No previous measurement of particle-phase OCP dry deposition fluxes obtained with experimental techniques was available for comparison. However, there have been several studies on OCP dry deposition fluxes that were calculated using indirect method. At a coastal/urban site in Izmir, Odabasi et al. (2008) estimated particle fluxes of pesticides taking dry deposition velocities of OCPs that were determined

recently for urban and suburban sites in Izmir. They reported F_d values ranging between 0.6 (c-nonachlor) and 388 (chlorpyrifos) ng m^{-2} day^{-1}. Gioia et al. (2005) also assumed a deposition velocity of 0.5 cm s^{-1} to calculate F_d values of OCPs at the different sites in New Jersey. The calculated fluxes for Σchlordanes, ΣDDTs, endosulfan-I, -II, and endosulfan sulfate were 2.8, 1.5, 0.9, 1.8, and 0.7 ng m^{-2} day^{-1} for urban/industrial site; 1.8, 1.2, 0.2, 0.9, and 0.4 ng m^{-2} day^{-1} for suburban site; and 0.5, 0.3, 0.4, 0.9, and 0.6 ng m^{-2} day^{-1} for rural/forested site, respectively.

Currently used pesticides in Turkey, endosulfan and chlorpyrifos, had a large fraction in particle fluxes of OCPs at the air sampling site, like their large contributions to total OCP mass in air. Among the studied pesticides, endosulfan-I had the highest average deposition flux in summer and was followed by endosulfan-II and chlorpyrifos. In winter, they were chlorpyrifos, p,p'-DDT, and endosulfan-I, respectively. Similarly, Odabasi et al. (2008) reported the highest particle fluxes for in-use pesticides of chlorpyrifos and endosulfan in coastal/urban Izmir.

Particle-phase dry deposition velocities (V_d, cm s^{-1}) for individual pesticides were calculated using measured dry deposition fluxes and atmospheric particle-phase concentrations (Eq. 3.17). The range for the V_d values was between 2.3±1.4 ($α$-HCH) and 11±5.1 (t-nonachlor) cm s^{-1} in summer, and between 1.6±1.0 (endosulfan-II) and 13±4.7 ($α$-HCH) cm s^{-1} in winter. The overall average deposition velocities were 4.6±3.6 and 5.3±4.6 cm s^{-1} for the summer and winter sampling periods, respectively. The seasonal difference in V_d values may be due to different size distributions and meteorological variables observed for both seasons.

For both sampling periods, the correlation between the dry deposition fluxes and atmospheric particulate concentrations was statistically significant (r^2=0.73, p<0.01, n=112 for summer; r^2=0.88, p<0.01, n=98 for winter; and overall r^2=0.63, p<0.01, n=210). The overall average V_d values for individual pesticides varied from 2.8±1.6 (endosulfan sulfate) to 11±5.1 cm s^{-1} (t-nonachlor). This value was 4.9±4.1 cm s^{-1} for all of the studied pesticides (Table 4.17).

Particulate deposition velocities for other SOCs have been studied extensively. Reported overall average V_d values in Table 2.9 ranged between 0.4-6.7 cm s^{-1} for PAHs (Demircioglu, 2008; Esen et al., 2008; Tasdemir & Esen, 2007b; Vardar et al., 2002; Odabasi et al., 1999a; Franz et al., 1998) and between 0.7-7.2 cm s^{-1} for PCBs (Esen et al., 2008; Cindoruk & Tasdemir 2007b; Tasdemir & Holsen, 2005; Tasdemir et al., 2004b; Franz et al., 1998). Thus, the overall average V_d value in this study (4.9±4.1 cm s^{-1}) is consistent with those reported values for other SOCs.

4.3.3 OCPs in Soil

4.3.3.1 Soil Concentrations of OCPs

Among the collected sample matrices (i.e. soil, ambient air, dry deposition), *p,p′*-DDE was only analyzed for the soil samples taken from 48 different points in the study area. *γ*-HCH, *α*- CHL, *γ*-CHL, *t*-nonachlor, endosulfan-I, endosulfan-II, endosulfan sulfate, *p,p′*-DDT, *p,p′*-DDD, and *p,p′*-DDE were the most abundant compounds found in 100% of the soil samples (*n*=48), and they were followed by *α*-HCH (%98), *c*-nonachlor (%96), chlorpyrifos (%92), heptachlorepoxide (%77), *β*-HCH (%27), *δ*-HCH and dieldrin (%15), and endrin (%2). Endrin aldehyde, endrin ketone, and methoxychlor were under their detection limits (*n*=48).

Table 4.18 shows the related pesticide concentrations in soils (*n*=48) at the study area. These values are relatively high in comparison with those previously reported in Table 4.12. Soil concentrations of related pesticides showed a large variation between the sampling points, probably due to differences in pesticide application histories and dissipation rates. They ranged between 0.3-4157 µg kg^{-1} (dry wt) for ΣDDX, 0.09-26 µg kg^{-1} (dry wt) for Σendosulfans, 0.008-35 µg kg^{-1} (dry wt) for Σchlordanes, *nd*-6.8 µg kg^{-1} (dry wt) for chlorpyrifos and 0.007-2.3 µg kg^{-1} (dry wt) for ΣHCHs (Table 4.18). The highest levels in soils were generally found for ΣDDX, in agreement with the recent studies (Bidleman & Leone, 2004; Meijer et al., 2003a; Harner et al., 1999). The formulation of technical DDT mainly contains 65-80% of

p,p'-DDT. p,p'-DDD and p,p'-DDE are impurities in technical DDT as well as its degradation products. Because of their extremely low water solubility and their high organic carbon partition coefficients (K_{OC}), DDT and its metabolites are essentially immobile in soil, becoming strongly absorbed onto the surface layer of soils (UNEP, 2006). In Turkey, the use of DDT was restricted in 1978, and then, it was prohibited in 1985 (Acara et al., 2006). Therefore, high ΣDDX concentrations in soils may probably due to their persistence in soil as a result of their heavy historical usage in the study area, assuming that illegal usage has really been stopped.

Related pesticide concentrations in soils taken from the study area (n=48) were correlated between each other, and statistically significant relationships (p<0.01) were found between the α-HCH and other HCHs (r^2=0.73 for β-HCH, 0.59 for γ-HCH); γ-CHL and other chlordane related compounds (r^2=1.0, 0.90, 0.82, and 0.54 for α-CHL, c-nonachlor, t-nonachlor, and heptachlorepoxide, respectively); p,p'-DDT and other DDT related compounds of p,p'-DDD and p,p'-DDE (r^2=0.99 for each). The results indicated that their soil concentrations in the study area were affected by similar factors such as local ongoing or regional sources and meteorological parameters. However, there was a weak correlation between α-HCH and δ-HCH (r^2=0.39, p>0.10), probably because of their remote sources. Correlations between endosulfan-I and other endosulfans were comparable (r^2=0.15, p<0.01 for endosulfan-II, r^2=0.10, p<0.05 for endosulfan sulfate). This can be attributed to different application histories of endosulfan between the sites and variation in their transportation/degradation rates in soils.

The α- to γ-HCH ratio in soils ranged between 0.2 (urban site-13) and 2.9 (industrial site-58). At the air sampling site, overall average α- to γ-HCH ratio in soil and air was found as 1.0±0.2 and 2.6±0.8, respectively. Different ratios obtained at the air and soil matrices at the air sampling site might be due to differences in degradation rates and partitioning behaviors of these compounds.

Table 4.18 Soil concentrations of related pesticides (ng kg^{-1}, dry wt) at the study area (*n*=48).

SN	Sites	ΣHCHs	CHLPRF	ΣChlordanes	ΣESLFs	ΣDDX	DIELD and END	SN	Sites	ΣHCHs	CHLPRF	ΣChlordanes	ΣESLFs	ΣDDX	DIELD and END
1	1	26	*nd*	89	298	1075	*nd*	25	29	67	302	227	124	53226	*nd*
2	2	15	23	18	276	997	*nd*	26	30	34	77	161	466	6272	617
3	3	28	13	24	140	837	*nd*	27	32	211	79	16	181	2258	*nd*
4	4	23	35	16	157	297	*nd*	28	33	231	212	11	159	1598	*nd*
5	5	22	*nd*	1040	18054	257784	*nd*	29	34	454	4245	155	222	232099	*nd*
6	6	20	18	16	252	432	*nd*	30	35	154	392	95	1196	107399	*nd*
7	7	128	864	86	382	1115	*nd*	31	36	26	161	33	443	35300	*nd*
8	9	6.9	14	11	388	414	*nd*	32	37	19	45	31	231	7464	*nd*
9	10	12	10	9.7	89	272	*nd*	33	39	111	648	49	397	1441	*nd*
10	11	74	299	63	123	573	*nd*	34	42	24	*nd*	23	119	2275	*nd*
11	12	29	53	21	232	332	*nd*	35	43	9.2	*nd*	111	152	2583	*nd*
12	13	149	409	322	574	88671	*nd*	36	44	179	33	22322	134	4156822	1069
13	14	21	65	35	140	1265	116	37	45	23	28	25	1182	709	*nd*
14	15	75	431	70	274	618	*nd*	38	46	608	750	3079	25762	217685	2092
15	16	61	94.2	185	217	677	*nd*	39	47	17	37	23	634	2279	*nd*
16	17	47	197	27	360	1786	*nd*	40	48	24	75	274	509	16227	*nd*
17	18	62	34	61	276	1743	*nd*	41	49	9.5	19	7.9	142	510	*nd*
18	19	106	573	35	175	903	*nd*	42	50	14	13	38	387	1830	*nd*
19	20	75	1696	28	187	5937	*nd*	43	53	25	456	216	1058	93619	*nd*
20	22	13	28	214	223	17759	*nd*	44	54	18	33	25	2285	1415	*nd*
21	23	29	42	782	86	4136	*nd*	45	55	132	30	48	296	11247	35
22	24	154	668	69	328	4551	*nd*	46	58	2291	6811	120	760	5032	*nd*
23	25	1731	671	265	258	6632	*nd*	47	59	370	226	1444	495	103668	3966
24	26	1080	235	34898	3567	115512	92013	48	60	69	243	75	1718	5027	*nd*

nd: Not detected, SN: Sample number, ΣHCHs: Sum of the *α*, *β*, *γ*, and *δ* isomers of HCH, ΣChlordanes: Sum of HEP EPOX, *α*- and *γ*-CHL, *c*- and *t*-NONA, ΣESLFs: Sum of ESLF-I, -II, and ESLF SUL, ΣDDX: Sum of *p,p′*-DDT, -DDD, and DDE.

Spatial distribution of related pesticide levels in soils (*n*=48) at Aliaga study area was mapped out by MapInfo Professional with Vertical Mapper which is a GIS (geographic information system) mapping software. The maps (Fig. 4.28-4.32) showed that Aliaga soils are a potential source for regional recycling of pesticides in the study area and are likely to contribute to ambient air concentrations of these compounds.
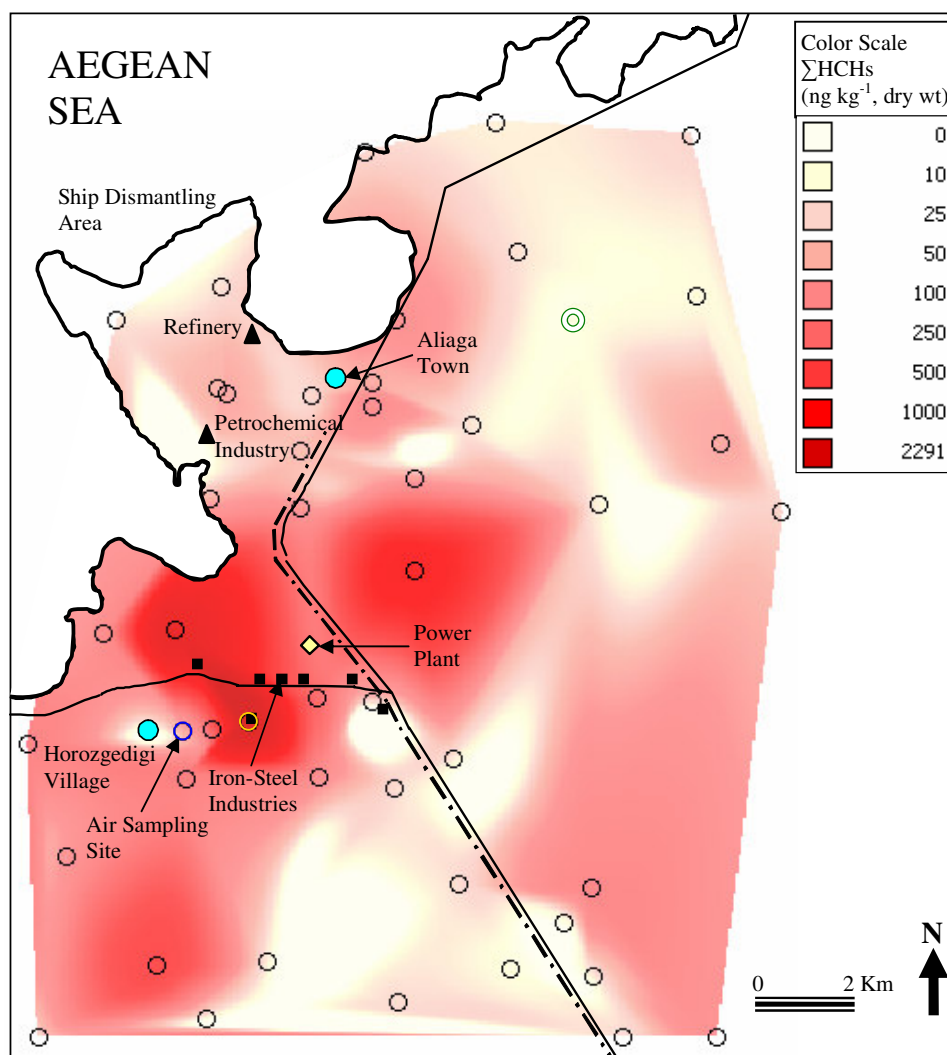

Figure 4.28 Spatial distribution map of ΣHCH levels in soils (n=48). (○: soil sampling points, ○: industrial site, ◎: rural site).

Spatial distribution map of ΣHCH levels in soils (*n*=48) are illustrated in Fig. 4.28. The highest soil concentrations for ΣHCHs were measured around the iron-steel plants in Aliaga industrial region (sites 25, 34, 58) and agricultural/rural areas (sites 24, 26, 46) suggesting that they are the major HCH sources in the study area (Table 4.18). Manz et al. (2001) reported that besides their agricultural uses, HCHs can also be emitted by hazardous waste dumps, cable scrapping, and incineration in smelting plants because of the previous usage of HCHs as an additive in plasticizer production (e.g. in PVC sheathing of electric cables). At the iron-steel plants located close to the air sampling site, all kinds of scrap iron materials are stored, classified, cut into parts, and melted. Therefore, high HCH levels in soils collected at the industrial region may be due to the emissions from iron-steel plants processing scrap materials with PVC sheathed cables. The overall average ΣHCH concentration (0.3±0.1 μg kg^{-1}, dry wt) in soils taken from the air sampling site (*n*=7) was relatively low in comparison with the highest soil concentration (2.3 μg kg^{-1}, dry wt) measured at the industrial site (site 58). This can be attributed to its location with respect to the prevailing wind direction.

Fig. 4.29 showed that the highest chlorpyrifos concentrations in soils were measured around the industrial region (sites 25, 34, 58), rural/agricultural areas (sites 24, 39, and 46), and Aliaga town (sites 7, 20) (Table 4.18). In Aliaga study area, chlorpyrifos is currently used for the different kinds of crop production such as corn, barley, oats, vineyard, and olive grove (MARA, 2008). Therefore, high chlorpyrifos levels at these sites may be because of its agricultural applications. The overall average chlorpyrifos level in soils (*n*=7) at the air sampling site (0.1±0.09 μg kg^{-1}, dry wt) was relatively low in comparison with the highest level (6.8 μg kg^{-1}, dry wt) measured at the industrial site (site 58). The highest chlorpyrifos level at the industrial site may be related to nearby agricultural areas.
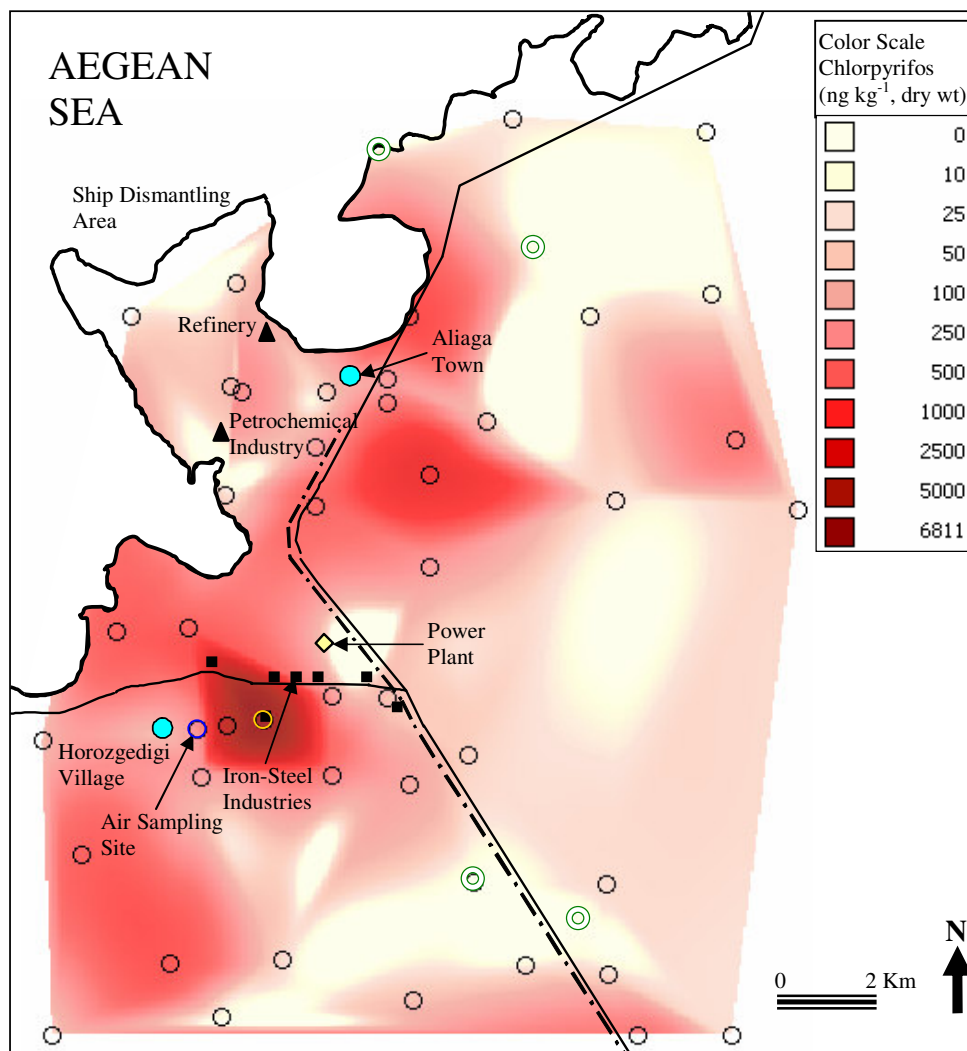
Figure 4.29 Spatial distribution map of chlorpyrifos levels in soils (n=48) (○: soil sampling points, ○: industrial site, ◎: rural site).

Fig. 4.30 shows the spatial distribution of Σendosulfan levels in soils (*n*=48) at the study area. The highest endosulfan concentrations in soils were measured at the rural/agricultural sites (sites 5, 26, 35, 45, 46, 53, 54) and Aliaga town (site 60). Endosulfan is currently used for the vegetable production in the study area (MARA, 2008). Thus, high soil concentrations of Σendosulfans can be attributed to its current applications at these sites. The overall average Σendosulfan level in soils (*n*=7) at the air sampling site (0.3±0.1 μg kg^{-1}, dry wt) was relatively low as compared with the highest soil level at the rural/agricultural site (site 46) (26 μg kg^{-1}, dry wt).
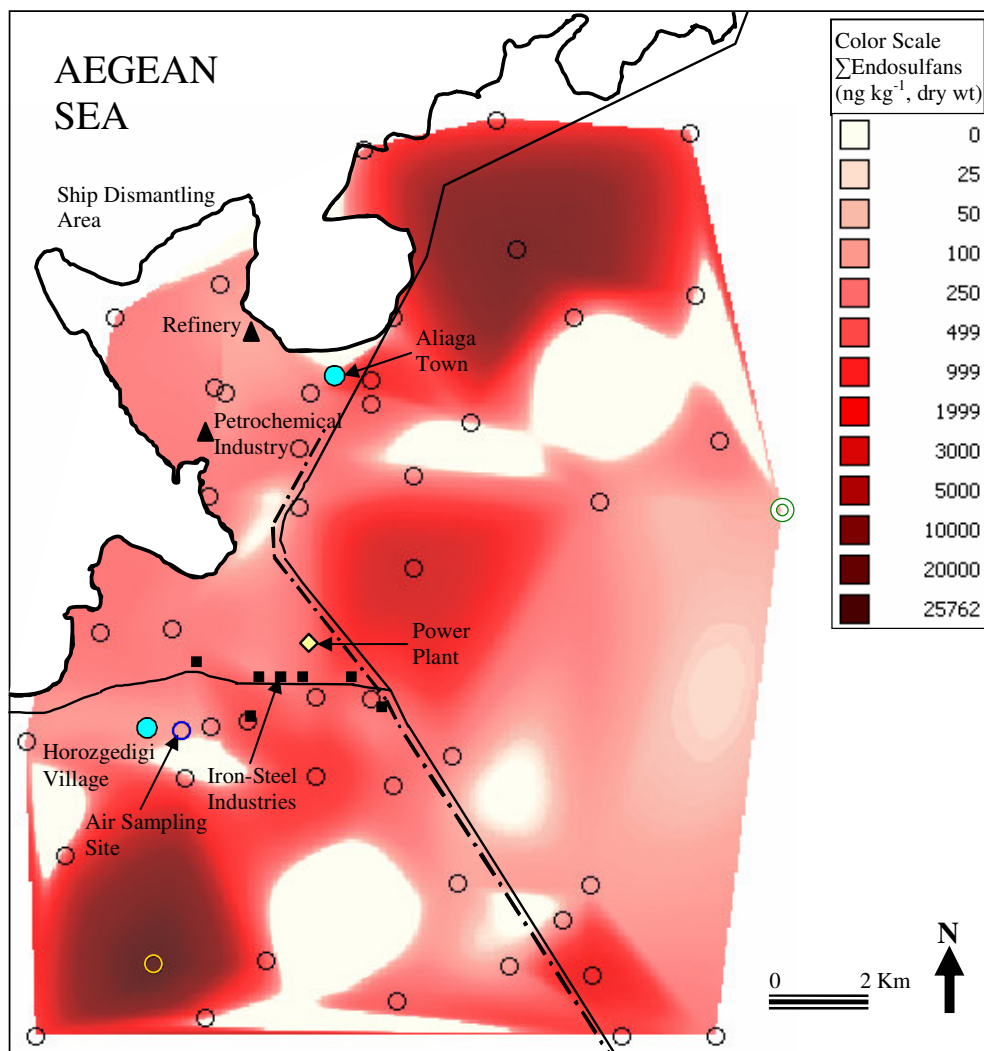
Figure 4.30 Spatial distribution map of Σendosulfan levels in soils (n=48) (○ : soil sampling points, ○ : agricultural site, ◎ : rural site).

Fig. 4.31 showed that the highest soil levels of Σchlordanes were measured at the rural/agricultural areas (sites 5, 26, 44, 46) and around the industrial region (site 59). This may probably due to their historical usage at the study area. The overall average Σchlordane concentration in soils (n=7) collected at the air sampling site was 0.4±0.2 µg kg^{-1} (dry wt). The highest soil concentration of 35 µg kg^{-1} (dry wt) was observed at the rural/agricultural site (site 26).
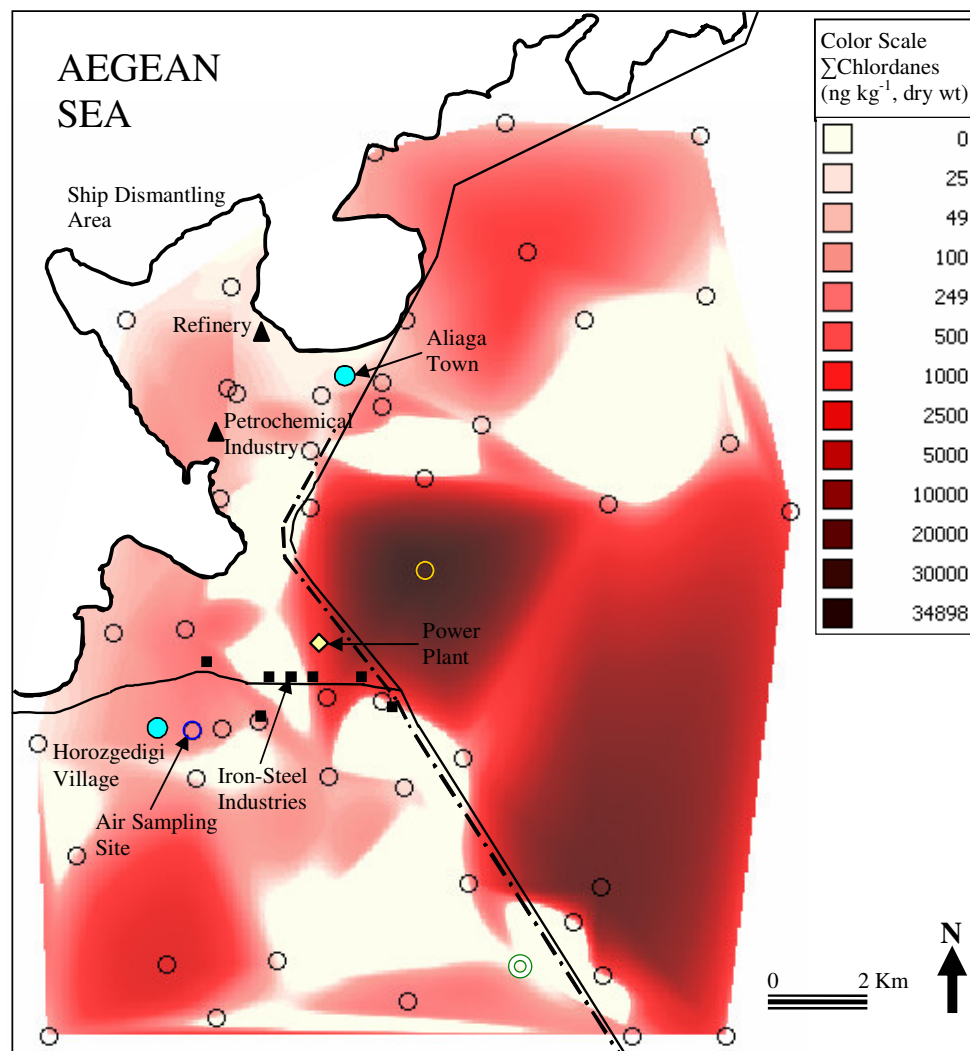
Figure 4.31 Spatial distribution map of Σchlordane levels in soils (n=48) (○ : soil sampling points, ○ : agricultural site, ◎ : rural site).

Fig. 4.32 showed that Aliaga soil were highly polluted with DDT related compounds, especially at the rural/agricultural areas (sites 5, 22, 26, 35, 36, 37, 44, 46, 48, 53, 55), around the industrial region (sites 25, 30, 32, 34, 58, 59), at the air sampling site (site 29), around the petrochemical complex (site 18) and Aliaga town (site 13, 20, 60). This suggests that they are the major p,p'-DDT, p,p'-DDD, and p,p'-DDE sources in the study area. The highest soil concentration of ΣDDX (4157 µg kg^{-1}, dry wt) was measured at the rural/agricultural area (site 44), probably due to their historical usage and persistence in Aliaga soil.
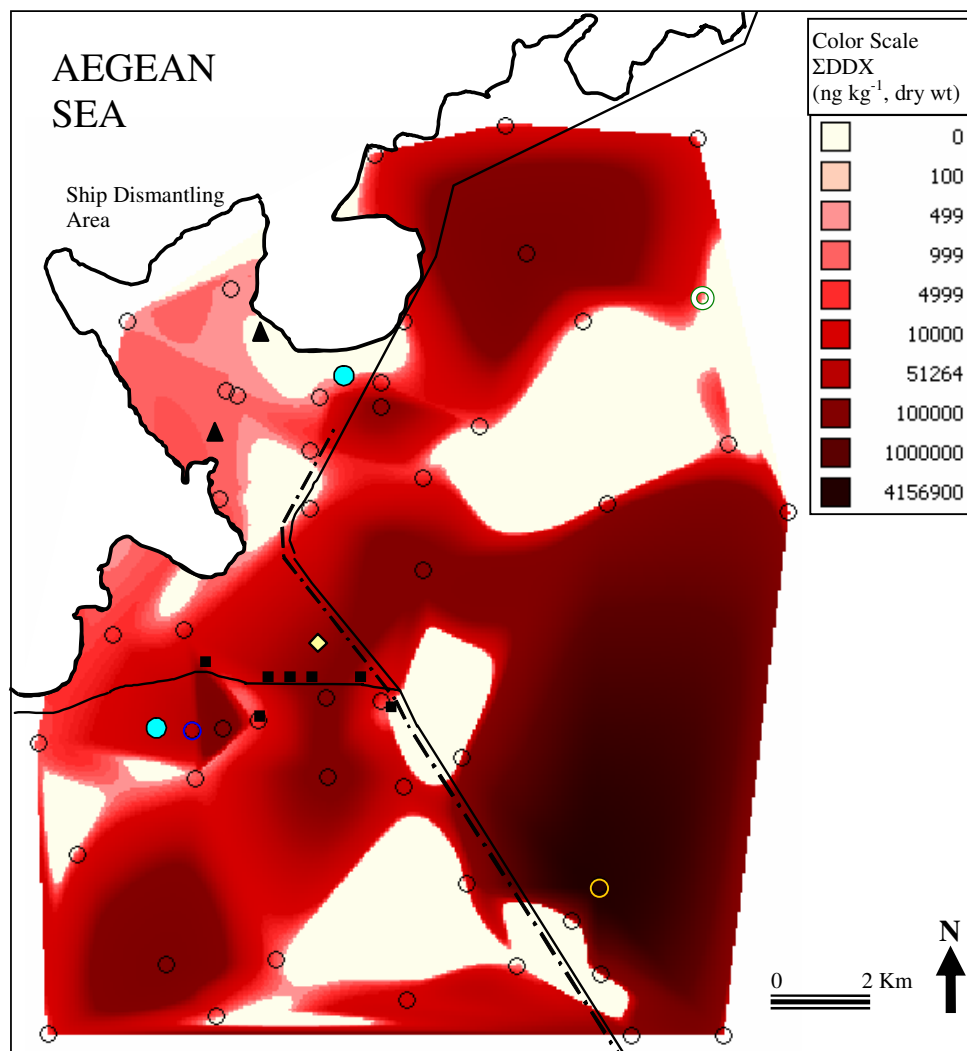
Figure 4.32 Spatial distribution map of ΣDDX levels in soils (n=48) (○: soil sampling points, ○: agricultural site, ◎: rural site, ●: residential areas, ◇: power plant, ■: iron-steal industries, ▲: refinery and petrochemical industry, ○: air sampling site).

The average soil concentrations of individual pesticides at the air sampling site are presented in Table 4.19. p,p'-DDT had the highest soil concentrations for both sampling periods. p,p'-DDT was followed by p,p'-DDD and endosulfan-I in summer, and by p,p'-DDD and β-HCH in winter. Summer/winter ratio for the average OCP concentrations in soils varied from 0.3 (δ-HCH) and 2.1 (endosulfan-II).

Table 4.19 Individual OCP concentrations in soils (ng kg^{-1}, dry wt) at the air sampling site (SN: 29).

OCPs	Summer (*n*=4)					Winter (*n*=3)				
	Min.	Max.	GM	Median	Avg±SD	Min.	Max.	GM	Median	Avg±SD
α-HCH	20	43	32	37	34±9.8	52	94	65	56	68±23
β-HCH	31	155	94	123	107±47	150	258	191	178	196±56
γ-HCH	30	48	35	33	35±7.4	58	86	68	64	69±15
δ-HCH	6.7	14	9.5	9.4	9.9±3.5	26	38	33	35	33±6.0
CHLPYR	38	76	59	67	61±15	80	315	131	90	162±133
HEP EPOX	60	77	68	65	68±7.3	35	68	46	41	48±18
α-CHL	4.5	121	39	81	63±47	78	130	106	116	108±27
γ-CHL	3.8	115	34	67	55±44	65	104	83	84	84±20
c-NONA	1.7	48	20	44	33±22	46	63	55	57	56±8.6
t-NONA	12	163	64	142	100±75	139	191	168	178	169±27
ESLF-I	27	225	96	96	119±75	52	118	72	62	77±36
ESLF-II	16	125	60	69	72±40	24	52	32	26	34±16
ESLF SUL	57	144	75	60	80±37	122	244	163	145	171±65
p,p'-DDT	710	19738	5744	13059	10071±8202	8828	10473	9555	9435	9579±832
p,p'-DDD	50	2279	521	1310	1062±942	754	832	801	819	802±42

GM: Geometric mean.

Although endosulfan and chlorpyrifos had the highest atmospheric concentrations at the air sampling site, they were only a small part of total pesticide mass in soil. However, on the contrary their low atmospheric levels, DDT related compounds had the highest soil concentrations. The difference between air and soil OCP profiles may be because of gas-particle distributions, different partitioning and degradation behaviors of the compounds in air and soil matrices.

4.3.3.2 Soil-Air Gas *Exchange Fluxes of OCPs*

The fugacity ratios and soil-air gas exchange fluxes of OCPs were calculated at the air sampling site using air (*n*=28) and soil (*n*=7) concentrations representing the same sampling season. K_{OA} values for individual OCPs as a function of temperature were calculated using the regression parameters given by Shoeib & Harner (2002). The parameters that were not available for chlorpyrifos, heptachlorepoxide, endosulfan-II, and endosufan sulfate were taken from Odabasi (2007a). The log K_{OA} and log Q_{SA} values of all OCPs correlated well (r^2=0.64, p<0.01, *n*=367) indicating that the octanol is a good surrogate for soil organic matter (Fig. 4.33).
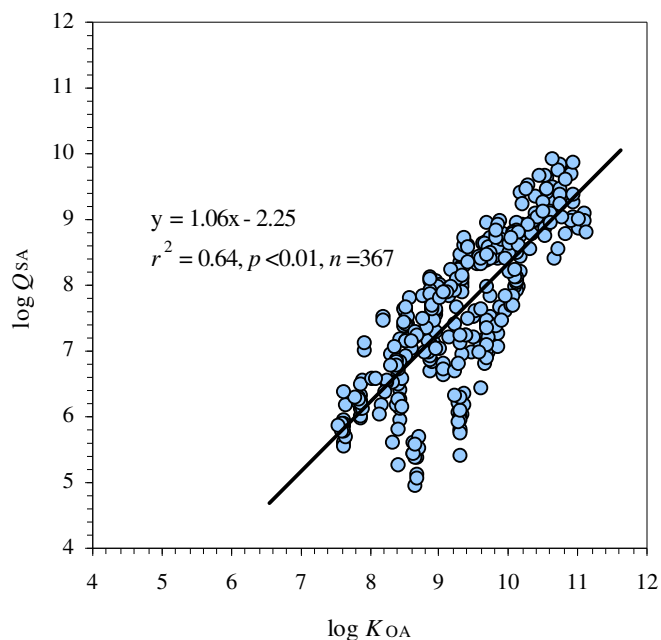
$y = 1.06x - 2.25$

$r^2 = 0.64, p < 0.01, n = 367$

Figure 4.33 log K_{OA} vs. log Q_{SA} for all OCP compounds.

A propagation of the errors associated with the calculation of f_S/f_A indicated that the equilibrium is represented by 1.0±0.26 (i.e. within a range of 0.74-1.26). The f_S/f_A ratios especially for *p,p*-DDT, *γ*-HCH, *t*-nonachlor, *γ*-CHL, and *α*-CHL were inside this uncertainty range constituting 25, 29, 39, 43, and 50% of the samples (*n*=26 for *α*-CHL, *n*=28 for the rest), respectively. For all individual pesticides, 19% of the fugacity ratio data set (*n*=366) fell inside this range, thus referring to equilibrium. For the rest, soil and adjacent air were not in equilibrium.

Relationship between the air and soil fugacity values of individual OCPs are illustrated in Fig. 4. 34. HCHs, chlorpyrifos, endosulfan-I, endosulfan-II and *p,p'*-DDD with f_S/f_A ratios <1 were mainly deposited from the atmosphere to the soil. Therefore, the soil acted as a sink for these compounds. However, all chlordane related OCPs (i.e. heptachlorepoxide, *α*-CHL, *γ*-CHL, *c*-nonachlor, *t*-nonachlor), endosulfan sulfate, and *p,p'*-DDT with fugacity ratios >1 were mainly volatilized during both seasons (Fig. 4.34) and the contaminated soil acted a secondary source to the atmosphere for these pesticides. Bidleman & Leone (2004) reported average

fugacity ratios representing near equilibrium for α-CHL, γ-CHL, t-nonachlor, and dieldrin, and net volatilization for γ-HCH, and p,p'-DDT.
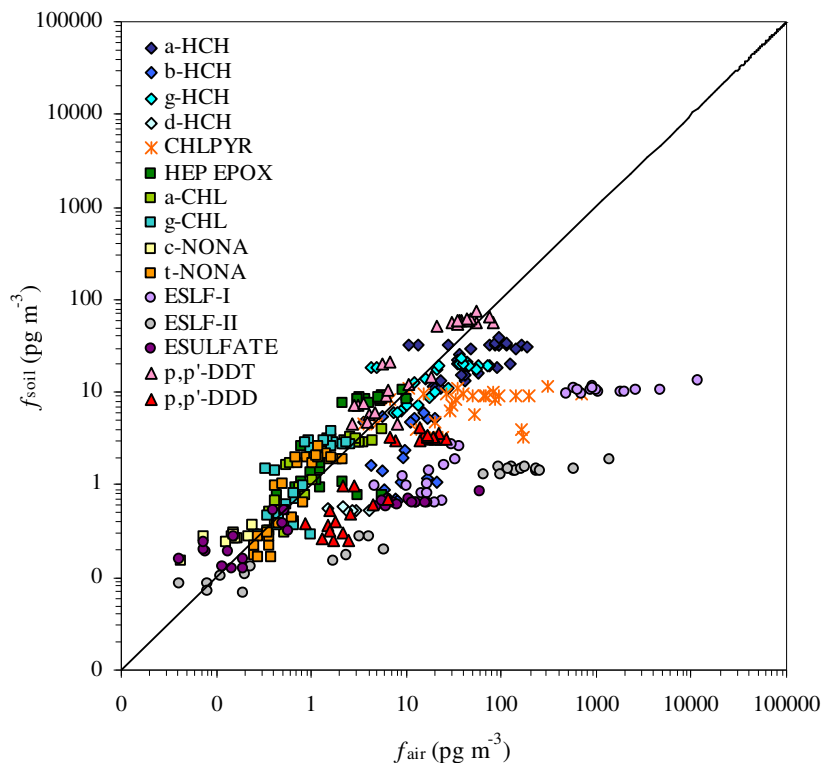
Figure 4.34 Relationship between the OCP fugacities (f) in air and soil. The solid diagonal line represents a 1:1 relationship (equilibrium).

For the samples that the soil and ambient air were not in equilibrium (1.0±0.26), the average estimated uncertainty in the net gas fluxes by error propagation ranged between ±43 (endosulfan-I) and ±67% (α-CHL and p,p'-DDT) with an overall average of ±53% (n=297). Relatively higher uncertainty values estimated for some OCPs were probably due to their proximity to equilibrium.

The calculated instantaneous soil-air net gas exchange fluxes and MTCs for OCPs are presented in Table 4.20. Negative values indicate a net volatilization from soil to air and positive ones indicate a net deposition from air to soil. The average net gas fluxes for individual pesticides ranged from -0.07±0.02 (c-nonachlor) to

1287 ± 1506 ng m^{-2} day^{-1} (endosulfan-I) in summer and from -0.03 ± 0.1 (endosulfan sulfate) to 42 ± 62 ng m^{-2} day^{-1} (chlorpyrifos) in winter. All chlordane related compounds and *p,p'*-DDT tended to volatilize in summer, and in winter, pesticides tending to volatilize were *α*-CHL, *γ*-CHL, t-nonachlor, endosulfan sulfate, and *p,p'*-DDT. This result is consistent with the calculated f_S/f_A ratios. In winter period, a shift from volatilization to deposition was observed for heptachlorepoxide while this observation was in contrast for endosulfan sulfate. Magnitudes of the gas fluxes in summer were higher than in winter as the atmospheric concentrations of OCPs in gas-phase.

Table 4.20 Calculated MTCs (cm s^{-1}) and instantaneous soil-air net gas exchange fluxes (F_{net}, ng m^{-2} day^{-1}) for OCP compounds.

	Summer				Winter			
	MTCs	F_{net}			MTCs	F_{net}		
OCPs	Avg±SD	Min.	Max.	Avg±SD	Avg±SD	Min	Max	Avg±SD
α-HCH	0.78±0.21	12	145	52±38	0.96±0.24	5.3	52	15±21
β-HCH	0.78±0.21	-0.9	16	5.9±5.8	0.96±0.24	1.3	17	6.6±4.5
γ-HCH	0.78±0.21	6.7	61	20±16	0.96±0.24	3.0	-14	0.6±9.1
δ-HCH	0.78±0.21	0.5	3.7	1.6±1.1	0.96±0.24	*nc*	*nc*	*nc*
CHLPYR	0.74±0.20	5.6	310	71±84	0.92±0.24	-0.7	175	42±62
HEP EPOX	0.72±0.20	-1.3	-4.9	-2.6±1.0	0.91±0.24	-0.2	5.4	0.3±1.8
α-CHL	0.71±0.20	-0.3	1.0	-0.2±0.8	0.89±0.24	-0.1	-1.1	-0.3±0.6
γ-CHL	0.71±0.20	-0.2	-1.8	-0.8±0.4	0.89±0.24	-0.07	-1.1	-0.2±0.8
c-NONA	0.75±0.20	-0.05	-0.1	-0.07±0.02	0.93±0.24	*nc*	*nc*	*nc*
t-NONA	0.75±0.20	-0.3	-1.2	-0.6±0.2	0.93±0.24	0.07	-0.5	-0.06±0.3
ESLF-I	0.77±0.21	328	5560	1287±1506	0.95±0.24	2.7	32	15±9.0
ESLF-II	0.77±0.21	45	647	165±173	0.95±0.24	-0.05	3.8	1.4±1.6
ESLF SUL	0.76±0.21	2.7	28	7.3±6.5	0.95±0.24	-0.05	0.2	-0.03±0.1
p,p'-DDT	0.71±0.20	-8.3	-27	-12±10	0.89±0.24	-1.2	-14	-3.9±5.6
p,p'-DDD	0.72±0.20	3.2	14	8.0±3.3	0.90±0.24	0.4	3.2	1.4±0.8

nc: Not calculated.

Negative values indicate net gas volatilization from soil to air.

Table 4.21 shows the annual average fluxes of individual pesticides and the ratios of total fluxes representing soil to air (F_{SA}, including gas volatilization) and air to soil (F_{AS}, including gas absorption, dry and wet deposition) mechanisms. Gas absorption and volatilization fluxes were calculated using Eq. (3.20). Wet deposition fluxes measured recently at a suburban site of Buca in Izmir during autumn 2005-spring 2006 were taken from Odabasi (2007b) to estimate relative importance of

different processes. Additional mechanisms (e.g. reaction and leaching in soil) were ignored since it is not possible to estimate their magnitude and relative importance. Comparison of the estimated particle and gas deposition fluxes (wet and dry) indicated that these mechanisms might be significant inputs of OCPs to the soil surfaces in the study area. However, gas absorption for α, δ, γ isomers of HCH, endosulfan-I and-II and dry deposition for β-HCH, chlorpyrifos, heptachlorepoxide, α-CHL, endosulfan sulfate, p,p'-DDT, and -DDD were dominating. The contribution of wet deposition was important especially for chlorpyrifos and chlordane related OCPs. The calculated F_{SA}/F_{AS} ratios suggested that there was a net accumulation into the soil for all pesticides. At Guzelyali Port in Izmir Bay, Odabasi et al. (2008) conducted a study to determine the relative contributions of different atmospheric mechanisms to the pollutant inventory of the Bay water column and they reported similar results for OCPs.

Table 4.21 Annual fluxes (ng m^{-2} year^{-1}) and F_{SA}/F_{AS} ratios of individual pesticides.

OCPs	Wet Deposition[a]	Dry Deposition	Gas Absorption	Gas Volatilization	F_{SA}/F_{AS}
α-HCH	351	2,536	18,471	6,600	0.3
β-HCH	nd	3,258	3,017	685	0.1
γ-HCH	408	3,116	8,622	4,195	0.3
δ-HCH	nd	nd	707	135	0.2
CHLPYR	18,885	29,639	23,090	1,866	0.03
HEP EPOX	2,998	4,458	711	1,129	0.1
α-CHL	361	477	366	460	0.4
γ-CHL	463	462	299	531	0.4
c-NONA	89	nd	32	61	0.5
t-NONA	335	308	188	328	0.4
ESLF-I	820	105,208	239,150	1,475	0.004
ESLF-II	632	27,335	37,120	234	0.004
ESLF SUL	348	2,747	1,681	121	0.03
p,p'-DDT	477	9,847	5,578	8,603	0.5
p,p'-DDD	nd	2,404	2,161	441	0.1

nd: Not detected.
[a] Odabasi, 2007b.

CHAPTER FIVE
CONCLUSIONS AND SUGGESTIONS

5.1 Conclusions

Atmospheric concentrations, particle fluxes, and the magnitude and direction of soil-air gas exchange were investigated for the studied groups of compounds (i.e. PAHs, PCBs, and OCPs) to determine the relative importance of the mechanisms for their movement between the air and soil at the air sampling site. Additionally, SOCs concentrations in soils taken from the 48 different points in the study area were measured and their spatial distributions that can be related to the local sources were mapped out using a GIS mapping software of MapInfo with Vertical Mapper.

Atmospheric total (particulate+gas) Σ_{15}-PAH concentrations were 25±8.8 and 44±17 ng m^{-3} (average±SD) in summer and winter, respectively. Winter/summer individual total PAH concentration ratios ranged between 0.8 (acenaphthene) and 6.6 (benz[a]anthracene) indicating that wintertime concentrations were affected by residential heating emissions. The more volatile PAHs existing predominantly in gas-phase (i.e. phenanthrene, fluorene, fluoranthene, and pyrene) were the most abundant compounds for both seasons. Gas-phase concentrations for the summer and winter periods constituted 90 and 75% of total Σ_{15}-PAHs in air, respectively.

Atmospheric total Σ_{41}-PCBs concentrations were higher in summer (3370±1617 pg m^{-3}) than in winter (1164±618 pg m^{-3}), probably due to increased volatilization at higher temperatures. Summer/winter ratios of individual PCBs were between 0.9 (PCB-194) and 5 (PCB-17). For both sampling periods, lower chlorinated congeners (i.e. tri-, tetra-, penta-CBs) dominated total PCB mass in air. Particle-phase percentage was higher during winter, especially for the heavier congeners as a result of the decrease in vapor pressures of PCBs at lower temperatures. Similar to PAHs, higher gas-phase percentage for atmospheric total Σ_{41}-PCBs was observed in summer (96%) than in winter (79%).

Dieldrin, endrin, endrin aldehyde, endrin ketone, and methoxychlor in all samples were under their detection limits. Among the studied OCPs, endosulfan-I had the highest atmospheric level in summer, followed by endosulfan-II and chlorpyrifos. In winter, they were chlorpyrifos, α-HCH, and endosulfan-I. Summertime total OCP concentrations (0.2 ± 0.05 to 2152 ± 2974 pg m^{-3}) (range, average$\pm$SD) were higher than the wintertime ones (*nd* to 121 ± 160 pg m^{-3}) with summer/winter ratios between 1.1 (chlorpyrifos) and 93 (endosulfan-I). This is probably due to the increased local/regional applications of in-use pesticides (endosulfan, chlorpyrifos) and increased volatilization rates of the OCPs during this season.

Particulate fluxes (ng m^{-2} day^{-1}, average$\pm$SD) for Σ_{15}-PAHs were higher in summer (5792 ± 3516) than in winter (2650 ± 1829). For the individual OCPs, they varied from 1.1 ± 1.2 (*t*- nonachlor) to 503 ± 455 (endosulfan-I) in summer and from 0.3 ± 0.3 (*t*- nonachlor) to 110 ± 157 (chlorpyrifos) in winter. Generally PAH and OCP fluxes were higher in summer than in winter, probably due to large particles from enhanced re-suspension of polluted soils and road dust under warm, dry and windy summer conditions in the area. However, higher particulate fluxes for Σ_{41}-PCBs were measured in winter (469 ± 328) than in summer (349 ± 183). Measured average atmospheric concentrations of particle-phase Σ_{41}-PCBs were 1.6 times higher in winter than in summer. Thus, increased wintertime fluxes for PCBs may be related to the increased partitioning of PCBs to particle-phase at lower temperatures. Calculated overall average particle deposition velocities for PAHs, PCBs, and OCPs were 2.9 ± 3.5, 5.5 ± 3.5, and 4.9 ± 4.1 cm s^{-1}, respectively. They agree with the previously reported values for SOCs.

Soil concentrations of PAHs, PCBs, and OCPs showed a large variation between the sampling points (*n*=48). This can be explained by differences in dissipation rates of compounds, soil properties and other environmental conditions such as proximity to sources of pollutants, land use, and the wind direction. The soil concentrations (μg kg^{-1}, dry wt) ranged between 11 (rural site) and 4628 (industrial site) for Σ_{15}-PAHs, and between 0.2 (rural site) and 805 (industrial site) for Σ_{41}-PCBs. Soil concentrations of Σ_{15}-PAHs and Σ_{41}-PCBs at the industrial site were 421 and 2516

times higher than those measured at the rural sites, respectively. This indicates that Aliaga industrial region with many iron-steel plants is an important source especially for PCBs. High PAH and PCB levels were also measured around the petroleum refinery, petrochemical plant, ship dismantling area, and Aliaga town. Thus, these sites are the major PAH and PCB sources in the area. The overall average soil concentrations at the air sampling site were relatively low (337±119 and 44±17 μg kg^{-1}, dry wt for Σ_{15}-PAHs and Σ_{41}-PCBs, respectively) as compared to the highest soil concentrations at the industrial site. This can be attributed to its location with respect to the prevailing wind direction.

A comparison of atmospheric PAH concentrations with the literature values showed that PAH levels at the air sampling site are in the lower range of the previously reported values for the other industrial and urban sites. The emissions from major industries may affect the air sampling site if the winds are from N and NE. But during the sampling programs, the prevailing winds were WNW and NW and it might be why relatively low concentrations were measured. However, comparatively high PCB levels measured at this site suggest that ambient PCB levels are likely to be influenced by the nearby industrial region.

Endrin aldehyde, endrin ketone, and methoxychlor were under their detection limits in soils taken from 48 different points in the study area. The range of soil concentration (μg kg^{-1}, dry wt) was between 0.06-1533 for ΣDDX, 0.09-26 for Σendosulfans, 0.01-35 for Σchlordanes, nd-6.8 for chlorpyrifos and 0.01-2.3 for ΣHCHs. The highest pesticide levels in soils (n=48) were generally found for ΣDDX, probably due to their persistence as a result of heavy historical usage in the study area, assuming that illegal usage does not take place. Spatial distribution map of ΣDDX also shows that Aliaga soil was highly polluted by DDT related compounds, especially at the rural/agricultural areas; around the industrial region, the petrochemical complex and Aliaga town. The highest level for ΣHCHs was measured at the industrial site. The emissions from iron-steel smelters using scrap iron including PVC sheathed cables may be the reason of high ΣHCHs levels at this site. For endosulfan, the highest levels were measured at the rural/agricultural sites

and Aliaga town while other in-use pesticide of chlorpyrifos was measured at high levels around the industrial region. The rural/agricultural areas and the industrial region are also likely to have been contaminated with Σchlordane and are sources of pollution in the area.

Calculated fugacity ratios and net gas fluxes at the soil-air interface indicated that low molecular weight PAHs (acenaphthene-benz[a]anthracene) tended to volatilize in summer, but only acenaphthene tended to volatilize in winter. Similar results were found for PCBs. The contaminated soil was a secondary source to the air for lighter PCBs and a sink for heavier ones. PCB congeners of 17, 18, 44, 52, 82, 87, and 95 tended to volatilize in summer, but only PCB-17 and -18 had a tendency to volatilize in winter. All processes affecting atmospheric inputs of Σ_{15}-PAHs and Σ_{35}-PCBs were comparable importance, but their inputs were dominated by gas absorption with a contribution of 73% and 69%, respectively. Dry particle deposition accounted for 23% and 29%. The contribution of wet deposition was only ~4% and 1% of the total atmospheric inputs of Σ_{15}-PAHs and Σ_{35}-PCBs, respectively.

Calculated fugacity ratios and net gas fluxes for OCPs showed that all chlordane related compounds and p,p'-DDT tended to volatilize in summer, and in winter, OCPs tending to volatilize were α-CHL, γ-CHL, t-nonachlor, endosulfan sulfate, and p,p'-DDT. All mechanisms were comparable for pesticides. However, gas absorption for α, δ, γ isomers of HCH, endosulfan-I and -II and dry deposition for β-HCH, chlorpyrifos, heptachlorepoxide, α-CHL, endosulfan sulfate, p,p'-DDT, and -DDD were the dominant mechanisms. The contribution of wet deposition was important especially for chlorpyrifos and chlordane related OCPs.

The calculated F_{SA}/F_{AS} ratios of acenaphthene, florene, and anthracene were above 1.0 suggesting that for these compounds, there was a net volatilization through the atmosphere. However, the ratios of PCB-17, -18, and -52 were slightly above 1.0 suggesting that for these congeners, soil and air may be reaching a steady state condition. For the rest (all OCPs and the remaining PAHs, and PCBs), there was net accumulation into the soil as the F_{SA}/F_{AS} ratios were less than 1.0.

5.2 Suggestions

Possible artifacts during the ambient air and dry deposition sampling including adsorption of the gaseous fraction by the filter material itself should be further investigated and quantified for SOCs.

Wet deposition fluxes were taken from Odabasi (2007b) to estimate the relative importance of different processes, and additional mechanisms (e.g. reaction and leaching in soil) were ignored. Comparison of the estimated particle and gas fluxes (wet and dry) showed that these mechanisms might make significant inputs of SOCs to the soil surfaces in the study area. Therefore, a more comprehensive study including wet deposition fluxes should be carried out at this site.

Soil-air gas exchange fluxes were only determined at the sampling site since both ambient air and soil samples representing the same sampling period were available for this site. To enrich the data and compare the results, additional studies can be carried out at the different sites (e.g. rural, urban, and remote sites) in the study area.

Ambient air and soil data suggested that the Aliaga industrial region, petrochemical complex, petroleum refinery, and ship dismantling areas are potential PAH and PCB sources in the study area. Therefore, further ambient air, soil, water, and dry/wet deposition sampling should be performed around these sites to determine the contributions of individual local sources. The degree of contributions of the iron-steel plants on the measured high levels of PCBs, PAHs, and some OCPs (such as HCHs and chlordanes) around the industrial site should be investigated.

To identify the origin of PAHs, PCBs and OCPs in ambient air and soil, their distribution patterns or the ratios of certain species in individual source emissions can be employed. Ambient air and soil concentrations measured at the present study should be further evaluated together with source data for this aim.

REFERENCES

Acara, A., Balli, B., Yeniova, M., Aksu, P., Duzgun, M., & Dagli, S., (2006). *Türkiye'nin kalici organik kirletici maddelere (pop'ler) ilişkin Stockholm özleşmesi için taslak ulusal uygulama plani, UNIDO-POP'ler projesi.* Proje No. GF/TUR/03/008. From, http://www.cevreorman.gov.tr/belgeler3/nip_plan.doc.

Agency for Toxic Substances and Disease Registry (ATSDR). (2007). *Toxicological profile for heptachlor and heptachlor epoxide.* U.S. Department of Health and Human Services, Public Health Service. Retrieved November 2007, from http://www.atsdr.cdc.gov/toxprofiles/tp12.pdf.

Agency for Toxic Substances and Disease Registry (ATSDR). (2005). *Toxicological profile for alpha-, beta-, gamma-, and delta-hexachlorocyclohexane.* U.S. Department of Health and Human Services, Public Health Service. Retrieved August 2005, from http://www.atsdr.cdc.gov/toxprofiles/tp43.pdf.

Agency for Toxic Substances and Disease Registry (ATSDR). (2002a). *Toxicological profile for DDT, DDE, and DDD.* U.S. Department of Health and Human Services, Public Health Service. Retrieved September 2002, from http://www.atsdr.cdc.gov/toxprofiles/tp35.pdf.

Agency for Toxic Substances and Disease Registry (ATSDR). (2002b). *Toxicological profile for aldrin/dieldrin.* U.S. Department of Health and Human Services, Public Health Service. Retrieved September 2002, from http://www.atsdr.cdc.gov/toxprofiles/tp1.pdf.

Agency for Toxic Substances and Disease Registry (ATSDR). (2002c). *Toxicological profile for methoxychlor.* U.S. Department of Health and Human Services, Public Health Service. Retrieved September 2002, from http://www.atsdr.cdc.gov/toxprofiles/tp47.pdf.

Agency for Toxic Substances and Disease Registry (ATSDR). (2000a). *Toxicological profile for polychlorinated biphenyls (PCBs).* U.S. Department of Health and Human Services, Public Health Service. Retrieved November 2000, from http://www.atsdr.cdc.gov/toxprofiles/tp17.html.

Agency for Toxic Substances and Disease Registry (ATSDR). (2000b). *Toxicological profile for endosulfan.* U.S. Department of Health and Human Services, Public Health Service. Retrieved September 2000, from http://www.atsdr.cdc.gov/toxprofiles/tp41.pdf.

Agency for Toxic Substances and Disease Registry (ATSDR). (1997). *Toxicological profile for chlorpyrifos.* U.S. Department of Health and Human Services, Public Health Service. Retrieved September 1997, from http://www.atsdr.cdc.gov/toxprofiles/tp84.pdf.

Agency for Toxic Substances and Disease Registry (ATSDR). (1996). *Toxicological profile for endrin.* U.S. Department of Health and Human Services, Public Health Service. Retrieved August 1996, from www.atsdr.cdc.gov/toxprofiles/tp89.pdf.

Agency for Toxic Substances and Disease Registry (ATSDR). (1995). *Toxicological profile for polycyclic aromatic hydrocarbons (PAHs).* U.S. Department of Health and Human Services, Public Health Service. Retrieved August 1995, from http://www.atsdr.cdc.gov/toxprofiles/tp69.pdf.

Agency for Toxic Substances and Disease Registry (ATSDR). (1994). *Toxicological profile for chlordane.* U.S. Department of Health and Human Services, Public Health Service. Retrieved May 1994, from www.atsdr.cdc.gov/toxprofiles/tp31.pdf.

Alegria, H., Bidleman, T.F., & Figueroa, M.S. (2006). Organochlorine pesticides in the ambient air of Chiapas, Mexico. *Environmental Pollution*, 140, 483-491.

Allen, J. O., Dookeran, N. M., Smith, K. A., Sarofim, A. D., Taghizadeh, K., & Lafleur, A. L. (1996). Measurement of polycyclic aromatic hydrocarbons

associated with size-segregated atmospheric aerosols in Massachusetts. *Environmental Science and Technology*, 30, 1023-1031.

Asman, W.A.H., Felding, G., Kudsk, P., Larsen, J., Mathiassen, S., & Spliid, N.H. (2001). Pesticides in air and in precipitation and effects on plant communities. Pesticides Research No. 57. *Danish Environmental Protection Agency*.

Bae, S.Y., Yi, S.M., & Kim, Y.P. (2002). Temporal and spatial variations of the particle size distribution of PAHs and their dry deposition fluxes in Korea. *Atmospheric Environment,* 36, 5491-5500.

Backe, C., Cousins, I.T., & Larsson, P. (2004). PCB in soils and estimated soil-air exchange fluxes of selected PCB congeners in the south of Sweden. *Environmental Pollution*, 128, 59-72.

Backe, C., Larsson, P., & Okla, L. (2000). Polychlorinated biphenyls in the air of southern Sweden - spatial and temporal variation. *Atmospheric Environment*, 34 (9), 1481-1486.

Bamford, H.A., Poster, D.L., Huie, R.E., & Baker, J.E. (2002). Using extrathermodynamic relationships to model the temperature dependence of Henry's law constants of 209 PCB congeners. *Environmental Science and Technology*, 36, 4395-4402.

Bamford, H.A., Poster, D.L., & Baker, J.E. (2000). Henry's law constants of polychlorinated biphenyls and their variation with temperature. *Journal of Engineering Data*, 45, 1069-1074.

Bidleman, T.F., & Leone, A.D. (2004). Soil-air exchange of organochlorine pesticides in the Southern United States. *Environmental Pollution*, 128, 49-57.

Bidleman, T.F., & Harner, T. (2000). *Sorption to aerosols*. Part II, Chapter 10. Handbook of Property Estimation Methods for Chemicals: Environmental and Health Sciences. Edited by Boethling, R.S. and Mackay, D. Boca Raton: CRC Press LLC, 2000.

Bidleman, T.F. (1999). Atmospheric transport and air-surface exchange of pesticides. *Water, Air and Soil Pollution*, 115, 115-166.

Breivik, K., Sweetman, A., Pacyna, J.M., & Jones, K.C. (2007). Towards a global historical emission inventory for selected PCB congeners-A mass balance approach-3. An update. *Science of the Total Environment*, 377, 296-307.

Breivik, K., Sweetman, A., Pacnya, J.M., & Jones, K.C. (2002a). Towards a global historical inventory for selected PCB congeners –a mass balance approach 1.global production and consumption. *The science of the Total Environment*, 290, 181-198.

Breivik, K., Sweetman, A., Pacnya, J.M., & Jones, K.C. (2002b). Towards a global historical inventory for selected PCB congeners –a mass balance approach 2. emissions. *The science of the Total Environment*, 290, 199-224.

Brunciak, P.A., Dachs, J., Franz, T.P., Gigliotti, C.L., Nelson, E.D., Turpin, B.J., & Eisenreich, S.J. (2001a). Polychlorinated biphenyls and particulate organic/elemental carbon in the atmosphere of Chesapeake Bay, USA. *Atmospheric Environment*, 35, 5663-5677.

Brunciak, P.A., Dachs, J., Gigliotti, C.L., Nelson, E.D., & Eisenreich, S.J. (2001b). Atmospheric polychlorinated biphenyl concentrations and apparent degradation in coastal New Jersey. *Atmospheric Environment*, 35, 3325-3339.

Cetin, B., & Odabasi, M. (2007). Particle-phase dry deposition and air-soil gas exchange of polybrominated diphenyl ethers (PBDEs) in Izmir, Turkey. *Environmental Science and Technology*, 41, 4986-4992."

Cetin, B., Yatkin, S., Bayram, A., & Odabasi, M. (2007). Ambient concentrations and source apportionment of PCBs and trace elements around an industrial area in Izmir, Turkey. *Chemosphere*, 69, 1267-1277.

Cetin, B., Ozer, S., Sofuoglu, A., & Odabasi, M. (2006). Determination of Henry's law constants of organochlorine pesticides in deionized and saline water as a function of temperature. *Atmospheric Environment*, 40, 4538-4546.

Chen, J., Xue, X., Schramm, K.W., Quan, X., Yang, F., & Kettrup, A. (2002). Quantitative structure-property relationship for octanol-air partition coefficients of polychlorinated biphenyls. *Chemosphere*, 48, 535-544.

Cindoruk, S.S., & Tasdemir, Y. (2007a). Characterization of gas/particle concentrations and partitioning of polychlorinated biphenyls (PCBs) measured in an urban site of Turkey. *Environmental Pollution*, 148, 325-333.

Cindoruk, S.S., & Tasdemir, Y. (2007b). Deposition of atmospheric particulate PCBs in suburban site of Turkey. *Atmospheric Research*, 85, 300–309.

Cindoruk, S.S., Esen, F., & Tasdemir, Y. (2007). Concentration and gas/particle partitioning of polychlorinated biphenyls (PCBs) at an industrial site at Bursa, Turkey. *Atmospheric Research*, 85, 338–350.

Cindoruk, S.S., & Tasdemir, Y. (2006). Characterization of gas/particle concentrations and partitioning of polychlorinated biphenyls (PCBs) measured in an urban site of Turkey. *Environmental Pollution*, 148, 325-333.

Cortes, D.R., Hoff, R.M., Brice, K.A., & Hites, R.A. (1999). Evidence of current pesticide use from temporal and clausius-clapeyron plots: a case study from the integrated atmospheric deposition network. *Environmental Science and Technology*, 33, 2145-2150.

Cousins I.T., Beck, A.J., & Jones, K.C. (1999). A review of the process involved in the exchange of semi-volatile organic compounds (SVOC) across the air-soil interface. *The Science of the Total Environment*, 228, 5-24.

Cousins I.T., & Jones, K.C. (1998). Air-soil exchange of semi-volatile organic compounds (SOCs) in the UK. *Environmental Pollution*, 102, 105-118.

Cousins I.T., McLachlan, M.S., & Jones, K.C. (1998). Lack of an aging effect on the soil-air partitioning of polychlorinated biphenyls. *Environmental Science and Technology*, 32, 2734-2740.

Cousins, I.T., Kreibich, H., Hudson, L.E., Lead, W.A., & Jones, K.C. (1997). PAHs in soils: contemporary UK data and evidence for potential contamination problems caused by exposure of samples to laboratory air. *The Science of the Total Environment*, 203, 141-156.

Currado, G.M., & Harrad, S. (2000). Factors influencing atmospheric concentrations of polychlorinated biphenyls in Birmingham, U.K. *Environmental Science and Technology*, 34, 78-82.

Dabestani, R., & Ivanov, I.N. (1999). A compilation of physical, spectroscopic and photophysical properties of polycyclic aromatic hydrocarbons. *Photochemistry and Photobiology*, 70(1), 10-34.

Dachs, J., Ribes, S., Drooge, B. V., & Grimalt, J. (2004). Response to the comment on "Influence of soot carbon on the soil-air partitioning of polycyclic aromatic hydrocarbons". *Environmental Science and Technology*, 38, 1624-1625.

Dachs, J., Glenn IV, T.R., Gigliotti, C.L., Brunciak, P., Totten, L.A., Nelson, E.D., Franz, T.P., & Eisenreich, S.J. (2002). Processes driving the short-term variability of PAHs in the Baltimore and northern Chesapeake Bay atmosphere, USA. *Atmospheric Environment*, 36, 2281-2295.

Dachs, J., & Eisenreich, S.J. (2000). Adsorption onto aerosol soot carbon dominates gas-particle partitioning of polycyclic aromatic hydrocarbons. *Environmental Science and Technology*, 34, 3690-3697.

Daly, G.L., Lei, Y.D., Teixeira, C., Muir, D.C.G., Castillo, L.E., Jantunen, L.M.M., & Wania, F. (2007). Organochlorine pesticides in the soils and atmosphere of Costa Rica. *Environmental Science and Technology*, 41, 1124-1130.

Demircioglu, E. (2008). *An investigation on atmospheric polycyclic aromatic hydrocarbons (PAHs) in Izmir*. PhD Thesis. Dokuz Eylul University, Izmir, Turkey.

Eaton, A.D., Clesceri, L.S., Rice, E.W., & Greenberg, A.E. (2005). *Standard Methods for the Examination of Water and Wastewater*. 21st ed., Centennial Edition, American Public Health Association (APHA), American Water Works Association (AWWA), Water Environment Federation (WEF).

Esen, F., Tasdemir, Y., & Vardar, N. (2008). Atmospheric concentrations of PAHs, their possible sources and gas-to-particle partitioning at a residential site of Bursa, Turkey. *Atmospheric Research*, 88, 243-255.

EPI Suite V3.20 Software. (2007). *The estimation program interface (EPI) developed by U.S. Environmental Protection Agency*. Retrieved September 2007, from http://www.epa.gov/opptintr/exposure/pubs/episuitedl.htm.

Falconer, R.L., & Harner, T. (2000). Comparison of the octanol-air partition coefficient and liquid-phase vapor pressure as descriptors for particle/gas

partitioning using laboratory and field data for PCBs and PCNs. *Atmospheric Environment*, 34, 4043-4046.

Falconer, R.L., & Bidleman, T.F. (1994). Vapor pressures and predicted particle/gas distributions of polychlorinated biphenyl congeners as a functions of temperature and ortho-chlorine substitution. *Atmospheric Environment*, 28 (3), 547-554.

Fang, G.C., Chang, K.F, Lu, C., & Bai, H. (2004). Estimation of PAHs dry deposition and BaP toxic equivalency factors (TEFs) study at urban, Industry Park and rural sampling sites in central Taiwan, Taichung. *Chemosphere*, 55, 787-796.

Franz, T.P., Eisenreich, S.J., & Holsen, T.M. (1998). Dry deposition of particulate polychlorinated biphenyls and polycyclic aromatic hydrocarbons to Lake Michigan. *Environmental Science and Technology*, 32, 3681-3688.

Gevao, B., Hamilton-Taylor, J., & Jones K.C. (1998). Polychlorinated biphenyl and polycyclic aromatic hydrocarbon deposition to and exchange at the air-water interface of Esthwaite Water, a small lake in Cumbria, UK. *Environmental Pollution*, 102, 63-75.

Gioa, R., Offenberg, F.H., Gigliotti, C.L., Totten, L.A., Du, S., & Eisenreich, S.J. (2005). Atmospheric concentrations and deposition of organochlorine pesticides in the US Mid-Atlantic region. *Atmospheric Environment*, 39, 2309-2322.

Golomb, D., Barry, E., Fisher, G., Varanusupakul, P., Koleda, M., & Rooney, T. (2001). Atmospheric deposition of polycyclic aromatic hydrocarbons near New England coastal waters. *Atmospheric Environment*, 35, 6245-6258.

Hafner, W.D., & Hites, R.D. (2003). Potential sources of pesticides, PCBs, and PAHs to the atmosphere of Great Lakes. *Environmental Science and Technology*, 37, 3764-3773.

Halsall, C.J., Sweetman, A.J., Barrie, L.A., & Jones, K.C. (2001). Modelling the behaviour of PAHs during atmospheric transport from the UK to the Arctic. *Atmospheric Environment*, 35, 255-267.

Halsall, C.J., Bailey, R., Stern, G.A., Barrie, L.A., Fellin, P., Muir, D.C.G., Rosenberg, B., Rovinsky, F.Ya., & Pastukhov, B. (1998). Multi-year observations of organochlorine pesticides in the Arctic atmosphere. *Environmental Pollution*, 102, 51-62.

Harner, T., Green, N.J.L., & Jones, K.C. (2000). Measurements of octanol-air partition coefficients for PCDD/Fs: a tool in assessing air-soil equilibrium status. *Environmental Science and Technology*, 34, 3109-3114.

Harner, T., Wideman, J.L., Jantunen, L.M.M., Bidleman, T.F., & Parkhurst, W.J. (1999). Residues of organochlorine pesticides in Alabama soils. *Environmental Pollution*, 106, 323-332.

Harner, T., & Bidleman, T.F. (1998). Octanol-air partition coefficient for describing particle/gas partitioning of aromatic compounds in urban air. *Environmental Science and Technology*, 32, 1494-1502.

Harner, T., & Bidleman, T.F. (1996). Measurements of octanol-air partition coefficients for polychlorinated biphenyls. *Journal of Chemical and Engineering*, Data 41, 895-899.

Harner, T., Mackay, D., Jones, K.C. (1995). Model of the long-term exchange of PCBs between soil and the atmosphere in the southern U.K. *Environmental Science and Technology*, 29, 1200-1209.

Harrad, S., & Mao, H. (2004). Atmospheric PCBs and organochlorine pesticides in Birmingham, UK: concentrations, sources, temporal and seasonal trends. *Atmospheric Environment*, 38, 1437-1445.

Hicks, B.B., Baldocchi, D.D., Meyers, T.P., Hosker Jr., R.P., Matt, D.R. (1987). A preliminary multiple resistance routine for deriving dry deposition velocities from measured quantities. *Water, Air and Soil Pollution*, 36, 311-330.

Hillery, B.R., Basu, I., Sweet, C.W., & Hites, R.A. (1997). Temporal and spatial trends in a long-term study of gas-phase PCB concentrations near the Great lakes. *Environmental Science and Technology*, 31, 1811-1816.

Hippelein, M., & McLachlan, M.S. (2000). Soil/air partitioning of semivolatile organic compounds. 2. Influence of temperature and relative humidity, *Environmental Science and Technology*, 34, 3521-3526.

Hippelein, M., & Mclachlan, M.S. (1998). Soil/air partitioning of semivolatile organic compounds. 1. Method development and influence of physical-chemical properties. *Environmental Science and Technology*, 32, 310-316.

Hlnckley, D.A., Bldleman, T.F., Foreman, W.T., & Tuschall, J.R. (1990). Determination of vapor pressures for nonpolar and semipolar organic compounds from gas chromatographic retention data. *Journal of Chemical and Engineering Data*, 35, 232-237.

Holsen, T.M., Noll, K.E., Liu, S.P., & Lee, W.J. (1991). Dry deposition of polychlorinated biphenyls in urban areas. *Environmental Science and Technology*, 25, 1075-1081.

Hung, H., Blanchard, P., Halsall, C.J., Bidleman, T.F., Stern, G.A., Fellin, P., Muir, D.C.G., Barrie, L.A., Jantunen, L.M., Helm, P.A., Ma, J., & Konoplev, A. (2005). Temporal and spatial variables of atmospheric polychlorinated biphenyls (PCBs), organochlorine (OC) pesticides and polycyclic aromatic hydrocarbons (PAHs) in the Canadian Arctic: Results from a decade of monitoring. *Science of the Total Environment*, 342, 119-144.

IPPC (European Commission, Integrated Pollution Prevention and Control). (2001). *Best Available Techniques Reference Document on the Production of Iron and Steel.* Retrieved December 2001, from http://eippcb.jrc.es/pages/FActivities.htm.

Jaarsveld, J.A., Van Pul, W.A.J., & De Leeuw, F.A.A.M. (1997). Modelling, transport and deposition of organic pollutants in the European Region. *Atmospheric Environment*, 31, 1011-1024.

Jabusch, T.M., & Swackhamer, D.L. (2005). Partitioning of polychlorinated biphenyls in octanol/water, triolein/water, and membrane/water systems. *Chemosphere*, 60, 1270-1278.

Jantunen, L.M.M., Bidleman, T.F., Harner, T., & Parkhurst, W.J. (2000). Toxaphene, chlordane, and other organochlorine pesticides in Alabama air. *Environmental Science and Technology*, 34, 5097-5105.

Jonker, M.T.O., & Koelmans, A.A. (2002). Sorption of polycyclic aromatic hydrocarbons and polychlorinated biphenyls to soot and soot-like materials in the aqueous environment: mechanistic considerations. *Environmental Science and Technology, 36*, 3725-3734.

Kaupp, H., & McLahlan, M. S. (1999a). Gas/particle partitioning of PCDD/Fs, PCBs, PCNs and PAHs. *Chemosphere*, 38 (14), 3411-3421.

Kaupp, H., & McLahlan, M. S. (1999b). Atmospheric particle size distributions of polychlorinated dibenzo-p-dioxins and dibenzofurans (PCDD/Fs) and polycyclic aromatic hydrocarbons (PAHs) and their implications for wet and dry deposition. *Atmospheric Environment*, 33, 85-95.

Kiss, G., Varga-Puchony, Z., Tolnai, B., Varga, B., Gelencser, A., Krivacsy, Z., & Hlavay, J. (2001). The seasonal changes in the concentration of polycyclic

aromatic hydrocarbons in precipitation and aerosol near Lake Balaton, Hungary. *Environmental Pollution*, 114, 55-61.

Kiss, G., Varga-Puchony, Z., Rohrbacher, G., & Hlavay, J. (1998). Distribution of polycyclic aromatic hydrocarbons on atmospheric particles of different sizes. *Atmospheric Research*, 46, 253-261.

Krauss, M. & Wilcke, W. (2003). Polychlorinated naphthalenes in urban soils: analysis, concentrations, and relation to other persistent organic pollutants. *Environmental Pollution*, 122, 75-89.

Kurt-Karakus, P.B., Bidleman, T.F., Staebler, R.M., & Jones, K.C. (2006). Measurement of DDT fluxes from a historically treated soil in Canada. *Environmental Science and Technology*, 40, 4578-4585.

Lee, R.G.M., Burnett, V., Harner, T., & Jones, K.C. (2000). Short-term temperature-dependent air-surface exchange and atmospheric concentrations of polychlorinated naphthalenes and organochlorine pesticides. *Environmental Science and Technology*, 34, 393-398.

Lee, R.G.M., & Jones, K.C. (1999). The influence of meteorology and air masses on daily atmospheric PCB and PAH concentrations at a UK location. *Environmental Science and Technology*, 33, 705-712.

Lohmann, R., & Lammel, G. (2004). Adsorptive and absorptive contributions to the gas-particle partitioning of polycyclic aromatic hydrocarbons: state of knowledge and recommended parameterization for modeling. *Environmental Science and Technology*, 38 (14), 3793-3803.

Lohmann, R., Harner, T., Thomas, G.O., & Jones, K.C. (2000). A comparative study of the gas-particle partitioning of PCDD/Fs, PCBs, and PAHs. *Environmental Science and Technology*, 34, 4943-4951.

Mandalakis, M., & Stephanou, E.G. (2006). Atmospheric concentration characteristics and gas-particle partitioning of PCBs in a rural area of eastern Germany. *Environmental Pollution*, 147, 211-221.

Mandalakis, M., Tsapakis, M., Tsoga, A., & Stephanou, E.G. (2002). Gas-particle concentrations and distribution of aliphatic hydrocarbons, PAHs, PCBs and PCDD/Fs in the atmosphere of Athens (Greece). *Atmospheric Environment*, 36, 4023-4035.

Manz, M., Wenzel, K.D., Dietze, U., & Schuurmann, G. (2001). Persistent organic pollutants in agricultural soils of central Germany. *The Science of the Total Environment*, 277, 187-198.

Ministry of Agriculture and Rural Affairs (MARA). (2008). *Working Reports for the years between 2005-2007*. Republic of Turkey, Ministry of Agriculture and Rural Affairs, Provincial Directorate of Aliaga/Izmir.

Ministry of Agriculture and Rural Affairs (MARA). (2007). *Statistical report for 2006*. Republic of Turkey, Ministry of Agriculture and Rural Affairs, Provincial Directorate of Izmir.

Meijer, S.N., Shoeib, M., Jantunen, L.M.M., Jones, K.C., & Harner, T. (2003a). Air-soil exchange of organochlorine pesticides in agricultural soils. 1. Field measurements using a novel in situ sampling device. *Environmental Science and Technology*, 37, 1292-1299.

Meijer, S.N., Shoeib, M., Jones, K.C., & Harner, T. (2003b). Air-soil exchange of organochlorine pesticides in agricultural soils. 2. Laboratory measurements of the soil-air partition coefficients. *Environmental Science and Technology*, 37, 1300-1305.

Meijer, S.N., Harner, T., Helm, P.A., Halsall, C.J., Johnston, A.E., & Jones, K.C. (2001). Polychlorinated naphthalenes in U.K. soils: Time trends, markers of source, and equilibrium status. *Environmental Science and Technology*, 35, 4205-4213.

Miller, T.L. (1996). *Extension toxicology network pesticide information profiles (EXTOXNET)*. Retrieved June 1996, from http://extoxnet.orst.edu/pips/ghindex.html.

Montone, R.C., Taniguchi, S., & Weber, R.R. (2003). PCBs in the atmosphere of King George Island, Antarctica. *The Science of the Total Environment*, 308, 167-173.

Motelay-Massei, A., Ollivon, D., Garban, B., Teil, M.J., Blanchard, M., & Chevreuil, M. (2004). Distribution and spatial trends of PAHs and PCBs in soils in the Seine River basin, France. *Chemosphere*, 55, 555-565.

Murayama, H., Takase, Y., Mitobe, H., Mukai, H., Ohzeki, T., Shimizu, K., & Kitayama, Y. (2003). Seasonal change of persistence organic pollutant concentrations in air at the Nigata area, Japan. *Chemosphere*, 52, 683-694.

Nadal, M., Schuhmacher, M., & Domingo, J.L. (2004). Levels of PAHs in soil and vegetation samples from Tarragona County Spain. *Environmental Pollution*, 132, 1-11.

Nagpal, N.K. (1993). *Ambient water quality criteria for polycyclic aromatic hydrocarbons (PAHs)*. Ministry of Environment, Lands and Parks, Province of British Columbia, Technical Appendix, Water Quality Branch, Water Management Division. Retrieved February 1993, from http://www.env.gov.bc.ca/wat/wq/BCguidelines/pahs.

Nagpal, N.K. (1992). *Water quality criteria for polychlorinated biphenyls (PCBs).* Ministry of Environment, Lands and Parks, Province of British Columbia, Technical Appendix, Water Quality Branch, Water Management Division. Retrieved January 1992, from

http://www.env.gov.bc.ca/wat/wq/BCguidelines/pcbs.

National Library of Medicine (NLM). (2008a). *Specialized Information Services (SIS), Toxnet, ChemIDplus Advanced.* Retrieved April 10, 2008, from http://chem.sis.nlm.nih.gov/chemidplus.

National Library of Medicine (NLM). (2008b). *Specialized Information Services (SIS), Toxnet, Hazardous Substance Data Bank (HSDB).* Retrieved April 10, 2008, from http://toxnet.nlm.nih.gov.

Odabasi, M., Cetin, B., Demircioglu, E., & Sofuoglu, A. (2008). Air–water exchange of polychlorinated biphenyls (PCBs) and organochlorine pesticides (OCPs) at a coastal site in Izmir Bay, Turkey. *Marine Chemistry*, 109, 115–129.

Odabasi, M. (2007a). OCPs. Department of Environmental Engineering, Dokuz Eylul University, Izmir, Turkey. Unpublished results.

Odabasi, M. (2007b). Wet deposition. Department of Environmental Engineering, Dokuz Eylul University, Izmir, Turkey. Unpublished results.

Odabasi, M., Cetin E., & Sofuoglu A. (2006a). Determination of octanol-air partition coefficients and supercooled liquid vapor pressures of PAHs as a function of temperature: Application to gas/particle partitioning in an urban atmosphere. *Atmospheric Environment*, 40, 6615-6625.

Odabasi, M., Cetin, B., & Sofuoglu, A. (2006b). Henry's law constant, octanol-air partition coefficient and supercooled liquid vapor pressure of carbazole as a

function of temperature: Application to gas/particle partitioning in the atmosphere. *Chemosphere*, 62, 1087-1096.

Odabasi, M., Sofuoglu A., Vardar N., Tasdemir Y., & Holsen T.M. (1999a). Measurement of dry deposition and air-water exchange of polycyclic aromatic hydrocarbons with the water surface sampler. *Environmental Science and Technology*, 33, 426-434.

Odabasi, M., Vardar N., Sofuoglu A., Tasdemir Y., & Holsen T.M. (1999b). Polycyclic aromatic hydrocarbons (PAHs) in Chicago air. *The Science of the Total Environment*, 227, 57-67.

Odabasi, M. (1998). *The measurement of PAH dry deposition and air-water exchange with the water surface sampler.* Ph.D. Thesis, Illinois Institute of Technology, Chicago.

Ohura, T., Amagai, T., Fusaya, M., & Matsushita, H. (2004). Spatial distributions and profiles of atmospheric polycyclic aromatic hydrocarbons in two industrial cities in Japan. *Environmental Science and Technology*, 38, 49-55.

Oregon Department of Environmental Quality (DEQ) & U.S. Environmental Protection Agency (U.S. EPA). (2005). Portland Harbor joint source control strategy. Final-December, 2005. .http://www.deq.state.or.us/nwr/PortlandHarbor.

Padmanabhan, J., Partasarathi, R., Subramanian, V., & Chattaraj, P.K. (2006). QSPR models for polychlorinated biphenyls: n-Octanol/water partition coefficient. *Bioorganic and Medicinal Chemistry*, 14, 1021-1028.

Park, J.S., Wade, T.L., & Sweet, S.T. (2002a). Atmospheric deposition of PAHs, PCBs and organochlorine pesticides to Corpus Christi Bay, Texas. *Atmospheric Environment*, 36, 1707–1720.

Park, S.S., Kim, Y.J., & Kang, C.H. (2002b). Atmospheric polycyclic aromatic hydrocarbons in Seoul, Korea. *Atmospheric Environment*, 36, 2917-2924.

Park, J.S., Wade, T.L., & Sweet, S.T. (2001a). Atmospheric distribution of polycyclic aromatic hydrocarbons and deposition to Galveston Bay, Texas, USA. *Atmospheric Environment*, 35, 3241-3249.

Park, J.S., Wade, T.L., & Sweet, S.T. (2001b). Atmospheric deposition of organochlorine contaminants to Galveston Bay, Texas. *Atmospheric Environment*, 35, 3315-3324.

Park, J.S. (2000). *Atmospheric deposition of PAHs, PCBs, and pesticides to the south Texas bays, Galveston Bay and Corpus Christy Bay*. Ph.D. Dissertation. Texas A & M University, College Station, TX, USA.

Poor, N., Tremblay, R., Kay, H., Bhethanabotla, V., Swartz, E., Luther, M., Campbell, S. (2004). Atmospheric concentrations and dry deposition rates of polycyclic aromatic hydrocarbons (PAHs) for Tempa Bay, Florida, USA. *Atmospheric Environment*, 38, 6005-6015.

Possanzini, M., Di Palo, V., Gigliucci, P., Sciano, M.C.T., & Cecinato, A. (2004). Determination of phase-distributed PAH in Rome ambient air by denuder/GC-MS method. *Atmospheric Environment*, 38, 1727-1734.

Rissato, S.R., Galhiane, M.S., Ximenes, V.F., Andrade, R.M.B., Talamoni, J.L.B., Libanio, M., Almeida, M.V., Apon, B.M., & Cavalari, A.A. (2006). Organochlorine pesticides and polychlorinated biphenyls in soil and water samples in the Northeastern part of Sao Paulo State, Brazil. *Chemosphere*, 65, 1949-1958.

Regional Water Quality Control Plant (RWQCP). (1997). *Organochlorine pesticides source identification*. Palo Alto Regional Water Quality Control Plant. EIP Associates. October 28, 1997.

Ribes, S., Van Drooge, B., Dachs, J., Gustafsson, Q., & Grimalt, J. O. (2003). Influence of soot carbon on the soil-air partitioning of polycyclic aromatic hydrocarbons. *Environmental Science and Technology, 37*, 2675-2680.

Ruzickova, P., Klanova, J., Cupr, P., Lammel, G., & Holoubek, I. (2008). An assessment of air soil exchange of polychlorinated biphenyls and organochlorine pesticides across Central and Southern Europe. *Environmental Science and Technology*, 42, 179-185.

Sahzuvar, L., Helm, P.A., Jantunen, L.M:, Bidleman, T.F. (2003). Henry's law constants for α-, β-, γ-hexachlorocyclohexanes (HCH) as a function of temperature and revised estimates of gas exchange in Arctic region. *Atmospheric Environment*, 37, 983-992.

Schnelle-Kreis, J, Sklorz, M., Peters, A., Cyrys, J., & Zimmermann, R. (2005). Analysis of particle associated semi-volatile aromatic and aliphatic hydrocarbons in urban particulate matter on a daily basis. *Atmospheric Environment*, 39, 7702-7714.

Scholtz, M.T., & Bidleman, T.F. (2006). Modelling of the long term fate of pesticide residues in agricultural soils and their surface exchange with the atmosphere: Part 1 Model description and evaluation. *Science of the Total Environment*, 368, 823-838.

Shannigrahi, A.S., Fukushima, T., & Ozaki, N. (2005). Comparison of different methods for measuring dry deposition fluxes of particulate matter and polycyclic aromatic hydrocarbons (PAHs) in the ambient air. *Atmospheric Environment*, 39, 653-662.

Shoeib, M., & Harner, T. (2002). Using measured octanol-air partition coefficients to explain environmental partitioning of organochlorine pesticides. *Environmental Toxicology and Chemistry*, 21 (5), 984-990.

Simcik, M.F., Franz, T.P., Zhang, H., & Eisenreich, S.T. (1998). Gas-particle partitioning of PCBs and PAHs in the Chicago urban and adjacent coastal atmosphere: states of equilibrium. *Environmental Science and Technology*, 32, 251-257.

Sofuoglu, A., Cetin, E., Bozacioglu, S.S., Sener, G.D., & Odabasi, M. (2004). Short-term variation in ambient concentrations and gas-particle partitioning of organochlorine pesticides in Izmir, Turkey. *Atmospheric Environment*, 38, 4483-4493.

Sofuoglu A., Odabasi, M., Tasdemir Y., Khalili, N.R., & Holsen T.M. (2001). Temperature dependence of gas-phase polycyclic aromatic hydrocarbon and organochlorine pesticide concentrations in Chicago air. *Atmospheric Environment*, 35, 6503-6510.

Spectrum (2003a). *Chemical fact sheet for acenaphthene*. Retrieved 2003, from http://www.speclab.com/compound/c83329.htm.

Spectrum (2003b). *Chemical fact sheet for anthracene*. Retrieved 2003, from http://www.speclab.com/compound/c120127.htm.

Spectrum (2003c). *Chemical fact sheet for fluoranthene*. Retrieved 2003, from http://www.speclab.com/compound/c206440.htm.

Spectrum (2003d). *Chemical fact sheet for fluorene*. Retrieved 2003, from http://www.speclab.com/compound/c86737.htm.

Spectrum (2003e). *Chemical fact sheet for naphthalene*. Retrieved 2003, from http://www.speclab.com/compound/c91203.htm.

Spectrum (2003f). *Chemical fact sheet for phenanthrene*. Retrieved 2003, from http://www.speclab.com/compound/c85018.htm.

Stern, G.A., Halsall, C.J., Barrie, L.A., Muir, D.C.G., Fellin, P., Rosenberg, B., Rovinsky, F.Y., Kononov, E.Y., & Pastuhov, B. (1997). Polychlorinated biphenyls in Arctic air. 1. Temporal and spatial trends: 1992-1994. *Environmental Science and Technology*, 31, 3619-3628.

Sun, P., Blanchard, P., Brice, K., & Hites, R.A. (2006). Atmospheric organochlorine pesticide concentrations near the Great Lakes: Temporal and spatial trends. *Environmental Science and Technology*, 40 (21), 6587-6593.

Tasdemir, Y., & Esen, F. (2007a). Urban air PAHs: Concentrations, temporal changes and gas/particle partitioning at a traffic site in Turkey. *Atmospheric Research*, 84, 1–12.

Tasdemir, Y., & Esen, F. (2007b). Dry deposition fluxes and deposition velocities of PAHs at an urban site in Turkey. *Atmospheric Environment*, 41, 1288–1301.

Tasdemir, Y., & Holsen, T.M. (2005). Measurement of particulate phase dry deposition fluxes of polychlorinated biphenyls (PCBs) with a water surface sampler. Atmospheric Environment, 39, 1845-1854.

Tasdemir, Y., Vardar, N., Odabasi, M., & Holsen, T.M. (2004a). Concentrations and gas/particle partitioning of PCBs in Chicago. *Environmental Pollution*, 131, 35-44.

Tasdemir, Y., Odabasi, M., Vardar, N., Sofuoglu, A., Murphy, T.J., & Holsen, T.M. (2004b). Dry deposition fluxes and velocities of polychlorinated biphenyls (PCBs) associated with particles. *Atmospheric Environment*, 38, 2447-2456.

Temime-Roussel, B., Monad, A., Massiani, C., & Wortham, H. (2004). Evaluation of a denuder tubes for atmospheric PAH partitioning studies- 1: evaluation of the trapping efficiency of gaseous PAHs. *Atmospheric Environment*, 38, 1913-1924.

Terzi, E., & Samara, C., (2004). Gas-particle partitioning of polycyclic aromatic hydrocarbons in urban, adjacent coastal, and continental background sites of western Greece. *Environmental Science and Technology*, 38, 4973-4978.

Toxic Organic Compounds in the Environment (TOCOEN). (2007). Persistent, Bioaccumulative and Toxic Chemicals in Central and Eastern European Countries, State of the Art Report. TOCOEN report no: 150a. Retrieved May 2000, from
http://www.recetox.muni.cz/res/file/reporty/tocoen-report-150a-id431.pdf.

Totten, L.A., Gigliotti, C.L., Vanry, D.A., Offenberg, J.H., Nelson, E.D., Dachs, J., Reinfelder, J.R., & Eisenreich, S.J. (2004). Atmospheric concentrations deposition of polychlorinated biphenyls to the Hudson River estuary. *Environmental Science and Technology*, 38, 2568-2573.

Tsapakis, M., & Stephanou, E.G. (2005). Occurrence of gaseous and particle polycyclic aromatic hydrocarbons in the urban atmosphere: study of sources and ambient temperature effect on the gas/particle concentration and distribution. *Environmental Pollution*, 133, 147-156.

Tsapakis, M. & Stephanou, E.G. (2003). Collection of gas and particle semi-volatile organic compounds: use of an oxidant denuder to minimize polycyclic aromatic hydrocarbons degradation during high-volume air sampling. *Atmospheric Environment*, 37, 4935-4944.

United Nations Environment Programme (UNEP). (2006). *Draft technical guidelines for environmentally sound management of wastes consisting of, containing or contaminated with 1,1,1-trichloro-2,2-bis(4-chlorophenyl)ethane (DDT)*. UNEP/CHW/OEWG/5/INF/9/Rev.1. Retrieved March 2006, from http://www.basel.int/meetings/oewg/oewg5/docs/i09r1e.doc.

United Nations Environmental Program (UNEP) Chemicals. (2002). *Regionally based assessment of persistent toxic substances*. Mediterranean regional report. Retrieved December 2002, from http://www.chem.unep.ch/Pts/regreports/Mediterranean.pdf.

United Nations Environment Programme (UNEP). (1999a). *Inventory of information sources on chemicals, persistent organic pollutants*. Retrieved November 1999, from http://www.chem.unep.ch/pops/pdf/invsrce/inventpopscomb.pdf.

United Nations Environment Programme (UNEP). (1999b). *Guidelines for the identification of PCBs and materials containing PCBs*. Prepared by UNEP chemicals. First issue. Retrieved August 1999, from http://www.chem.unep.ch/pops/pdf/PCBident/pcbid1.pdf.

U.S. Environmental protection Agency (U.S. EPA) & Oregon Department of Environmental Quality [DEQ]. (2005). *Portland harbor joint source control strategy*. Final Report. Retrieved December 2005, from http://yosemite.epa.gov/R10/CLEANUP.NSF/6d62f9a16e249d7888256db4005fa293/31ae45c9c90a674988256e470062ced9/$FILE/Final%20PH%20JSCS_December%202005%20with%20Appendices%20compacted.pdf.

U.S. Environmental Protection Agency (U.S. EPA). (2002a). *The foundation for global action on persistent organic pollutants: A United States perspective*. EPA/600/P-01/003F, NCEA-I-1200. Retrieved March 2002, from http://www.epa.gov/NCEA/pdfs/pops/POPsa.pdf.

U.S. Environmental Protection Agency (U.S. EPA) (2002b). *Columbia River basin fish contaminant survey*. Region 10. Volume I, Appendix C, Toxicity Profiles. Retrieved January 2002, from http://yosemite.epa.gov/r10/oea.nsf/af6d4571f3e2b1698825650f0071180a/17210 25f37881ac788256c59007e2ac1/$FILE/V1_App_C.pdf.

U.S. Environmental Protection Agency (U.S. EPA). (1997). *Toxicological review of chlordane (technical) (Cas No. 12789-03-6)*. In support of summary information on the integrated risk information system (IRIS). Retrieved December 1997, from http://www.epa.gov/iris/toxreviews/0142-tr.pdf.

U.S. Environmental Protection Agency (U.S. EPA). (1996). PCBs: *Cancer Dose-Response Assessment and Application to Environmental Mixtures*. EPA/600/P–96/001F. Retrieved September 1996, from http://www.epa.gov/pcb/pubs/pcb.pdf.

U.S. Environmental Protection Agency (U.S. EPA). (1986). *Ambient water quality criteria for Chlorpyrifos*. EPA 440/5-86-005. Retrieved September 1986, from http://www.epa.gov/waterscience/criteria/library/ambientwqc/chlorpyrifos86.pdf.

U.S. Environmental Protection Agency (U.S. EPA). (1980a). *Ambient water quality criteria for hexachlorocyclohexane*. EPA 440/5-80-054. Retrieved October 1980, from http://www.epa.gov/waterscience/criteria/library/ambientwqc/hexachlorocyclohex a80.pdf.

U.S. Environmental Protection Agency (U.S. EPA). (1980b). *Ambient water quality criteria for endosulfan*. EPA 440/5-80-046. Retrieved October 1980, from http://www.epa.gov/waterscience/criteria/library/ambientwqc/endosulfan80.pdf.

U.S. Environmental Protection Agency (U.S. EPA). (1980c). *Ambient water quality criteria for endrin*. EPA 440/5-80-047. Retrieved October 1980, from http://www.epa.gov/waterscience/criteria/library/ambientwqc/endrin80.pdf.

Vallack, H.W., Bakker, D.J., Brandt, I., Lunden, E.B., Brouwer, A., Bull, K.R., Gough, C., Guardans, R., Holeubek, I., Jansson, B., Koch, R., Kuylenstierna, J., Lecloux, A., Mackay, D., McCutcheon, P., Mocarelli, P., & Taalman, R.D.F. (1998). Controlling persistent organic pollutants- what next? *Environmental Toxicology and Pharmacology*, 6, 143-175.

van Noort, P.C.M. (2003). A thermodynamics-based estimation model for adsorption of organic compounds by carbonaceous materials in environmental sorbents. *Environmental Toxicology and Chemistry, 22*, 1179-1188.

Vardar, N., Esen, F., & Tasdemir, Y. (2007). Seasonal concentrations and partitioning of PAHs in a suburban site of Bursa, Turkey. *Environmental Pollution*, Article in press.

Vardar, N., Tasdemir, Y., Odabası, M., & Noll, K.E. (2004). Characterization of atmospheric concentrations and partitioning of PAHs in the Chicago atmosphere. *Science of the Total Environment*, 327, 163-174.

Vardar, N., Odabasi, M., & Holsen, T.M. (2002). Particulate dry deposition and overall deposition velocities of polycyclic aromatic hydrocarbons. *Journal of Environmental Engineering*, 128, 269-274.

Virtual Computational Chemistry Laboratory (VCCL). (2007). *ALOGPS 2.1 program*. Retrieved 2007, from http://146.107.217.178/lab/alogps/start.html.

Wania, F., Haugen, J.E., Lei, Y.D., & Mackay, D. (1998). Temperature dependence of atmospheric concentrations of semivolatile organic compounds. *Environmental Science and Technology*, 32, 1013-1021.

Wenzel, K.D., Hubert, A., Weissflog, L., Kuhne, R., Popp, P., Kindler, A., Schuurmann, G. (2006). Influence of different sources on atmospheric organochlorine patterns in Germany. *Atmospheric Environment*, 40, 943-957.

Wenzel, K.D., Manz, M., Hubert, A., & Shuurmann, G. (2002). Fate of POPs (DDX, HCHs, PCBs) in upper soil layers of pine forest. *The Science of the Total Environment*, 286, 143-154.

Wesely, M.L., & Hicks, B.B. (1977). Some factors that affect the deposition rates of sulfur dioxide and similar gases on vegetation. *APCA Journal*, 27, 1110-1116.

World Health Organization (WHO). (2005) *The WHO recommended classification of pesticides by hazard and guidelines to classification 2004*. International Programme on Chemical Safety (IPCS). ISBN 92 4 154663 8. Retrieved April 2005, from http://www.inchem.org/documents/pds/pdsother/class.pdf.

World Health Organization (WHO). (2000). *Air quality guidelines for Europe*. 2nd edition. WHO Regional Office for Europe, Copenhagen, Denmark. WHO Regional Publications, European Series, No. 91. ISBN 92 890 1358 3. Retrieved 2000, from http://www.euro.who.int/document/e71922.pdf.

World Health Organization (WHO). (1979). *International programme on chemical safety. Environmental health criteria 9. DDT and its derivatives*. ISBN 9241540699. From http://www.inchem.org/documents/ehc/ehc/ehc009.htm.

Yeo, H.G., Choi, M., Chun, M.Y., & Sunwoo, Y. (2003). Concentration distribution of polychlorinated biphenyls and organochlorine pesticides and their relationship with temperature in rural air of Korea. *Atmospheric Environment*, 37, 3831-3839.

Zhang, H.B., Luo, Y.M., Wong, M.H., Zhao, Q.G., & Zhang, G.L. (2007). Concentrations and possible sources of polychlorinated biphenyls in the soils of Hong Kong. *Geoderma*, 138, 244-251.

Zhang, H.B., Luo, Y.M., Wong, M.H., Zhao, Q.G., & Zhang, G.L. (2006). Distributions and concentrations of PAHs in Hong Kong soils. *Environmental Pollution*, 141, 107-114.

Zhang, L., Gong, S., Padro, J., & Barrie, L. (2001). A size-segregated particle dry deposition scheme for an atmospheric aerosol module. *Atmospheric Environment*, 35, 549-560.

Zhang, X., Schramm, K.W., Henkelmann, B., Klimn, C., Kaune, A., Kettrup, A., & Lu, P. (1999). A method to estimate the octanol-air partition coefficient of semivolatile organic compounds. *Analytical Chemistry*, 71, 3834-3838.

Zhou, W., Zhai, Z., Wang, Z., & Wang, L. (2005). Estimation of n-octanol/water partition coefficients (K_{OW}) of all PCB congeners by density functional theory. *Journal of Molecular Structure: THEOCHEM*, 755, 137-145.

APPENDIX

LIST OF SYMBOLS

A	Total collection area of GFF sheets
a_{EC}	Specific surface areas of elemental carbon
a_{AC}	Specific surface areas of activated carbon
b	Intercept of the curve
C_A	Atmospheric total concentrations of the compound
C_g	Gas-phase air concentration of the compound
C_p	Particle-phase air concentration of the compound
C_S	Soil concentration of the compound
C_{OM}	Concentration of organic matter content of TSP
C_{TSP}	Concentration of TSP
D_A	Molecular diffusion coefficient of the compound in air
F_d	Particle-phase dry deposition fluxes
F_{net}	The net soil-air gas exchange flux
F_{AS}	Total fluxes representing air to soil
F_{SA}	Total fluxes representing soil to air
f_A	Fugacity in air
f_{EC}	Fraction of elemental carbon in the aerosol
f_{OC}	Fraction of total organic carbon
f_{OM}	Fraction of organic matter in the particle
f_S	Fugacity in soil
H	Henry's law constant
K_{OA}	Octanol-air partition coefficient
K_{OC}	Organic carbon partition coefficient
K_{OW}	Octanol-water partition coefficient
K_P'	Dimensionless particle/gas partition coefficient
K_P	Particle/gas partition coefficient
$K_{SootAir}$	Soot-air partition coefficient
K_{SA}'	Dimensionless soil-air partition coefficient

K_{SA}	Soil-air partition coefficient
m	Regression slope
M_d	Particulate compound mass
M_{OCT}	Molecular weight of the organic matter
M_{OM}	Molecular weight of octanol
P	Gas-phase partial pressure of the compound
P_L	Sub-cooled liquid vapor pressure
Pr	Prandtl number of air
Q_{SA}	Soil-air quotients
R_a	Aerodynamic resistance
R_b	Boundary layer resistance
R_c	Canopy resistance
Sc	Schmidt number
S_W	Solubility in water
T	Air temperature
T_B	Boiling point
T_M	Melting point
T_S	Sampling time
U	Wind speed
U_{10}	Wind speed 10 m above the surface
u^*	Friction velocity
ν	Kinematic viscosity
V_d	Particle-phase dry deposition velocities
ϕ	Fraction of compound in particle-phase
θ	Particle surface area per unit volume of air
γ_{OCT}	Activity coefficient in octanol
γ_{OM}	Activity coefficient in aerosol organic matter
ρ_{OCT}	Density of octanol
ρ_S	Density of soil solids
ϕ_{OC}	Fraction of organic carbon on a dry soil basis
σ_θ	Standard deviation of the wind direction
κ	Karman's constant